A Thesis Submitted for the Degree of Doctor of Philosophy at

Harper Adams University

Louise Wright

The use of low energy 680nm LASER alone or in combination with photosynthetic electron transport chain inhibitors in the management of weeds

Submitted for the degree of Doctor of Philosophy

Submission Date: 06/05/2020

CORRECTIONS SUBMISSION DATE: 22/07/2021

Acknowledgements

Abstract

This thesis outlines the evidence detailing the potential of the use of low energy LASER energy, in particular, LASER diodes emitting 680nm light as a novel approach in the management of weeds in agriculture. The data presented quantifies the changes in plant cellular biochemistry upon use of the 680nm LASER alone or in combination with selected photosystem II inhibitors and for comparison, a herbicide of an alternative mode of action. Changes in the state of photosystem II are quantified, as is plant membrane stability quantified by percentage relative conductivity measurements and reactive oxygen species production and the biochemical response to this. One main focus of the thesis is the OJIP parameter reading outputs. This includes the commonly used Fv.Fm ration and a range of other parameters which are less commonly used but form detailed evidence of the changes in photosystem II upon application of the 680nm LASER and herbicide treatment.
The culmination of linking the aforementioned measurement areas provides a clear image of the plant responses to treatment which can form a basis on which to design further studies and decisions as to the suitability of LASER energy in the management of weeds can be made.

Glossary

%RC	Percentage relative conductivity
Abs.RC	Absorbance of light by the reaction centres
AI	Active ingredient
ATP	Adenosine triphosphate
BSA	Bovine serum albumin
CA	Chenopodium album
CAL	Calaris herbicide
Chl	Chlorophyll
CO2	Carbon dioxide
CZ	Central zone
DIoRC	Dissipation of light by the reaction centres
EL	Electrolyte leakage
ETC	Electron transport chain
EToRC	Quantification of the electron transport rate
Fv.Fm	Ratio quantifying the functional state of PSII
HAU	Harper Adams University
HW	Hot water
IR	Infra red energy
LASER	Light amplification by stimulated emission of radiation
LD	LASER diode
lha^{-1}	litres per hectare
LHCI	Light harvesting complex I
LHCII	Light harvesting complex II
MOA	Mode of action
NBT	Nitro-blue tetrazolium chloride
NEV	Nevada herbicide
OEC	Oxygen evolving complex
OJIP	O-J, J-I and I-P phases of photosynthesis
PAR	Photosynthetically active radiation
Pheo	Pheophytin
PSI	Photosystem I
PSII	Photosystem II
PZ	Peripheral zone
RC	Reaction centre
REoRC	Quantification of light received by PSI
ROS	Reactive oxygen species
SA	Sinapis arvensis
SAM	Shoot apical meristem
SEM	Scanning electron microscope
SF	Sencorex Flow herbicide
SOD	Superoxide dismutase
TRoRC	Trapping capability by the reaction centres
UK	United Kingdom

Table of Contents

Table contents

Chapter 4 - Plant responses post 680nm LASER treatment

Chapter 5 - plant responses post 680nm LASER and herbicide treatment

Chapter 1

Literature Review

1.1.   The economic impact of weeds in agriculture

Farming in the United Kingdom (UK), in 2019 accounted for the use of 72% of land, equating to 17.5 million hectares (DEFRA, 2019). The total area of cropped land increased between 2018 and 2019 by 0.6% (DEFRA, 2014). This translated to a forecast of total income in 2019 from farming in the UK of £5.38 billion (DEFRA, 2014). Being such a considerable aspect of the UK economy, farming practises and the yield gained from crops grown needs to be protected as factors affecting yield have a knock on effect on the profitability of farming. Factors likely to affect yield include weeds, pest and diseases along with genetic traits, such as the ability of the crop to resist lodging, which can reduce yield by up to 75% at ear emergence in wheat (HGCA, 2005a) and the ability to produce tillers (HGCA, 2005b). External factors affecting yield, which are largely environmental factors include climatic, edaphic, biotic and physiographic (Bunting, 1982, Hall, 1982, Van Ittersum, 1997).

Weeds, pest and disease pressures are three main contributors to loss of yield in agricultural crops. Quantifying yield losses globally is complicated due to the vast array of factors affecting crop production, including climate, weed, pest and disease type and type of crop grown in different areas (Savary et al., 2019). Specifically, wheat crop losses in North West Europe can reach 24.9% even with plant protection products, without which, losses could be far higher (Savary et al., 2019)

In this study, the management of weeds in agricultural crops will be the main focus. Whilst crop loss according to pest and pathogens is available (Savary et al., 2019), data detailing yield losses as a result of weed pressure is less abundant. Both Hay (1974) and Avery (2006) state that weeds have been a limiting factors in the yield of crops since the advent of farming. Weeds are responsible for an average minimum yield loss of 13.2% per year on a global scale, (Oerke, 1999) translating to over $1.4 trillion annually in 2020 (CPI Inflation Calculator, 2020). Oerke (2006) later revised this yield loss estimation to be 34% on average globally, indicating that weed control is a growing problem. Putting this into context, (Berca, 2004) stated that weeds are 'eating the food' of more than 1 billion of Earth's inhabitants. With widespread and diverse herbicide resistance, this figure is likely to be far greater today.

Weeds are defined, in anthropocentric terms by agriculturists, as certain groups of plants that are considered native or introduced alien species that has a perceived negative ecological or economic effect on agricultural or natural systems (Booth, 2003). Weeds make up 1% of plant species globally but have the ability to affect crop yield worldwide and cause issues outside of agriculture, for example, affecting the integrity of buildings (Celesti-Grapow, 2004). The successful germination and growth patterns result in attention of the grower being diverted from the main crop to the management of weeds, and the economic sink nature of weeds means they are capable of impinging on profit margins considerably through the need of extra labour, herbicide costs and direct damage to crops through competition of resources including light and nutrients.

1.2.   Current weed control measures

Herbicides are a very cost and time effective method of limiting the competitive effects of weed plants on the crop. More recently, public perception may have been a contributing factor to the rise of environmental concerns surrounding herbicide use including water pollution, and the onset of herbicide resistance of some weed plants and lack of time and cost effective cultural controls has intensified the need for alternative weed control methods.

Non chemical methods of weed control have been researched extensively. Hoeing and harrowing are the main alternative methods in arable crops but these techniques can mobilise weed seeds further up the soil profile where they are able to germinate and emerge (Heisel et al., 2001). The aim is a stale seedbed for these types of control. Some recent research has been focused on the use of thermal control methods including flaming and hot water application (HW). HW application has been used in parks, school grounds, greenhouses and more relevant to this research, in agricultural fields (Astatkie et al., 2007). HW is applied directly to weeds and with the absence of a flame, is unlikely to cause a fire. HW can also be applied in varying weather conditions including wind or rain with little drift, runoff or loss of efficacy (Riley, 1995) allowing application throughout the year. However, the effectiveness of HW application largely depends on the weed species and growth stage (Kolberg and Wiles, 2002). This observation is supported by Astatkie et al. (2007) who looked at the effectiveness of applications of infra-red radiation application (IR), HW and flaming techniques alongside the practical considerations of applying these treatments from a machine mounted on a tractor. This group found that only 0-48% of older weeds (>8 leaves) were killed with HW, a percentage which is lower than IR application at all machine

velocities (between 1.5 and 2.5 kmh^{-1}) and flaming. Other studies have found that HW was as effective as Glyphosate at the 4-6 leaf stages in Chenopodium album but only at the seeding stage of redroot pigweed (Kolberg and Wiles, 2002). However, (Rifai et al., 2002) stated that an additional application of HW was needed for the treatment to be as effective as a herbicidal application. Despite HW application being more effective than weeding by hand (Sirvydas et al., 2004), unavoidable caveats to this method include the need for large amounts of hot water and steam and repeated applications. Kolberg and Wiles (2002) found that they used 3200kg of water per ha for a single dose but needed to refill the tank more than 3 times to cover 1ha, whereas other methods including using IR avoid tank refilling and can be applied accurately thus reducing the likelihood of damaging the crop (Bond and Grundy, 2001, Lague, 2001).

When using IR as a weed control method, more ground can be covered in one run but more time is needed for the IR appliances to become hot enough to become effective compared to HW and can be less effective than flaming (Parish, 1990, Lague, 2001). The effectiveness the IR approach can be increased by angling the heated elements so that the weeds in question can be targeted accurately with high energy density.

The flaming technique was first applied on a large scale in the United States of America (USA) in the 1940s in crops including cotton, maize and blueberries (Lague, 2001). This method was generally applied pre-crop emergence followed by mechanical inter- and intra-row weeding (Melander and Rasmussen, 2001) and has also been used post-emergence of the crop in heat tolerant crops including maize and onions (Ascard, 1989). Flames can reach up to 1000°C and are applied for 0.1s at least resulting in killing plants by cellular rupture leading to tissue desiccation (Lague, 2001, Parish, 1990). Flaming was usually carried out pre-crop emergence as young weed seedlings are more sensitive to high temperatures, specifically the hypocotyl near the soil surface and shoot apices being susceptible to damage by heat (Sutcliffe, 1977). The success of this method largely depends on the weed species being targeted. For example, the organisation of leaf sheaths, petioles and surrounding leaves may present a large enough barrier to heat, allowing continued growth of the plant from the shoot apical meristem (SAM). Therefore, older plants are not as susceptible to this treatment, a statement supported by Kolberg and Wiles (2002) who found that when using flaming, older redroot pigweed was harder to kill than older lambsquarters. Crop plants and especially those with shallow root systems (Bond and Grundy, 2001) are also likely to be damaged with this treatment and so targeting weeds at later growth stages adds complexity to a method which is not equipped to allow for added complications.

Flaming does have advantages. For example, it can be carried out on wet soils and does not bring buried weed seeds to the surface. Pests and pathogens may also be killed, but conversely, beneficial insects may also be inadvertently targeted. The main reason this technique fell out of favour in the late 1970s was due to the availability of herbicides and the high cost of petroleum (Kepner, 1978). Flame weeding has not been commercialised more recently due to the extra time needed for application than for herbicides (Leroux, 2001) and the high energy requirements.

It is evident that tailoring of applications to weed species and growth stage may prove to be effective in weed control. Using visual recognition technology which is more readily available today compared to when the above studies were run could mitigate against some of the caveats outlined. For example, targeting weeds at early growth stages has been shown to be important (Astatkie et al., 2007, Hansson and Ascard, 2002, Kolberg and Wiles, 2002, Rifai et al., 2002) and present day technology has the ability to identify subtle plant characteristics.

HW, IR and flaming applications have the major downside of a large carbon footprint and the high likelihood of damage to crop plants. In addition, these methods are not selective with respect to non-target organisms. Therefore, an accurate method of treatment which is also considered a 'greener' approach is needed.

Cultural weed management practices include collecting weed seeds during harvest after emission from the combine harvester before the weed seeds can reach the soil surface. This can be achieved in a number of ways including bale-direct systems where a baler is towed behind the combine harvester, and a chaff lining inside the combine harvester which funnels debris containing weed seeds into a smaller vestibule (Walsh et al., 2018). There are challenges and limitations in this approach. Weeds which qualify for this technique are those which retain seeds until harvest and have limited seed shatter. Further, weed height should be no less that the minimum height above the ground the combine harvester is able to cut at, circa 15cm. Plants including wild oat and cleavers have proved to be susceptible to this treatment (Tidemann et al., 2017).

Precision agriculture using highly technical equipment able to map low yielding areas or sections of crop needed herbicide treatment. Despite the potential of large economic gain, the uptake of precision farming has been slower than expected and is mostly suited to high value and horticultural crops (Fernandez-Quintanilla et al., 2018). However, the equipment to fully employ precision farming is costly and training is required, so growers often rely on external companies to carry out mapping.

Bacteria have also been used to manage weed growth as biological control agents. Bacteria have great potential as weed control agents due to the rapid growth of the bioherbicide produced (Johnson et al., 1996, Li et al., 2014) simple propagation protocols (Li et al., 2014) and ease and success of genetic manipulation (Johnson et al., 1996). Fungal species have also been trialed in weed control but will less success than with bacterial methods. More successful treatments include BioMal, a formulation of *Colletotrichum gloeosporioides* f.sp. *malvae*, used in the management of round leaf mallow (*Malva pusilla*) (Mortensen, 1988). Viruses have also been considered in weed management practices as bio herbicides but many viruses have been deemed to be inappropriate for specific biological control due to their genetic variability and lack of host specificity (Kazinczi et al., 2006). This approach is more suited to management of invasive species in broader ecosystems rather than specifically managed areas such as intensive farming cropping systems (Harding and Raizada, 2015). However, some viruses have proven to be adept weed control agents, for example Tobacco Mild Green Mosaic Tobamovirus has been used in the management of tropical soda apple (*Solanum viarum*) in Florida (Diaz et al., 2014, Ferrell et al., 2008)and *Araujia* Mosaic Virus for control of moth plant (*Araujia hortorum*) in New Zealand (Elliott et al., 2009)

1.3. Weed management using herbicides

Herbicides have provided a revolutionary and efficient method of weed control over the last 70 years (Heap, 2020) and herbicides remain the primary weed control method in global conventional agriculture (Beckie et al., 2019). There are 25 groups of herbicides with modes of action targeting a wide range of plant processes, some of which include lipid and amino acid biosynthesis, photosynthesis, pigment biosynthesis and plant growth regulation (HRAC, 2020b). However, as with most modern technologies, herbicides are not future proof and weeds are able to develop resistance to active ingredients. As of March 2020, five hundred and twelve unique cases of herbicide resistance have been reported globally (Heap, 2020).

Resistance can arise from gene mutations which give rise to resistant plants in a population, even before the use of a chemical treatment. These plants are able to reproduce and pass on resistance genes until a population of plants remains where herbicides have no effect. The first documented case of herbicide resistance surfaced in 1968, recorded as triazine resistant *Senecio vulgaris* (Ryan, 1970). Interestingly, herbicide resistance has experienced a changing demographic, where up until the 1990s, resistance was a growing problem in developed countries which were affluent and could afford large quantities of herbicide and would use them liberally (Heap, 2014, Heap, 2008). More recently, it is developing countries

experiencing the brunt of the resistance surge as prices of herbicides drop and these countries become more economically independent and are able to move away from weed management practices such as hand roging.

To confound the increasing herbicide resistance crisis, the pace of new herbicides being added to the market place has slowed dramatically. Between 1950 and 1980, approximately 23 new herbicides covering a range of HRAC groups were introduced (Heap, 2009). Only one new herbicide with a novel site of action has not been developed and released on to the commercial market for more than 30 years (Beckie et al., 2019). A more recent discovery was a lipid biosynthesis inhibition mode of action (Campe et al., 2018), relieving some pressure on the market. Herbicide development is costly. The whole process from discovery to commercialisation costs in the region on $300 million and regulations and policies have developed to be a challenge (Peters and Strek, 2018). In addition, the time line from discovery to commercialisation often exceeds 10 years.

In light of such challenges, especially herbicide resistance and the new active ingredient shortage, increasing importance is placed on preserving the herbicides still available to farmers and growers. Therefore, finding non-chemical and novel approaches to weed management is vital to maintain and even increase crop yield.

1.4.   LASER technology

The term LASER is an acronym for light amplification by stimulated emission of radiation (Gould, 1959). LASER light sources are different to other light sources by the way that light emission is coherent, characterized by a constant phase difference at the same frequency and waveform (Gould, 1959). Such spatial coherence allows spot sizes of LASER beams to be defined and altered allowing for precise applications including LASER cutting (Balykin and Sidorov, 1987). The power output of LASERs is also a variable which can be changed to fit the application demand. Spatial coherence also results in LASER beams remaining parallel and narrow over large distances, also termed collimation. (Li et al., 2018). A collimated beam does not go outside its parallel constrains and so the spot size at the source and over a distance is consistent with limited diffraction, also referred to as a Gaussian beam (Shirai et al., 2003). In addition, LASERs are also able to emit only one wavelength of light if desired if the temperature of the source if controlled. This ability to emit a desired wavelength forms the reason for the use of LASER diode light sources in this study.

One common problem of the thermal control methods described earlier, is the difficulty in performing intra-row weeding. This coupled with the extensive and unselective application of heat which has potential to damage crops, high labour costs and high carbon footprint (Astatkie et al., 2007, Raffaelli et al., 2011) are reasons why herbicides are still the primary method of weed control worldwide. A selective, low energy, precise method of weed control may be the answer to weed control. Research presented in this thesis explored if these demands can be fulfilled in the form of 680nm LASER energy.

To date, only a handful of papers concentrating on weed control through LASER technology have been published. LASERs have been used to cut stems of weed plants (Bayramian, 1993, Heisel et al., 2002, Heisel et al., 2001) but effectiveness of this depends on the stem thickness. The cutting action of a carbon dioxide (CO_2) LASER is caused by heating of water in the plant cells resulting in explosive boiling (Langerholc, 1979) and it is this action of boiling cellular water which has been the focus of LASER studies to kill plants. In the study conducted by Heisel et al. (2002), the LASER cut through the stem and the dry weight of the treated plants was reduced, but was only feasible beneath the apical meristem.

Jones (1996) showed that the growth of dicotyledonous and monocotyledonous weeds could be slowed compared to that growth rate of the crop by cutting the weeds with LASERs at ground level, usually killing dicotyledonous weeds. Grass weeds very often recovered from this treatment, whereas broadleaved weeds seldom did. This could be due to the shoot apical meristem being located below the soil surface in grasses whereas the SAM is located in multiple areal parts of the plant in broadleaf weeds. Cutting weeds is advantageous compared to harrowing or hoeing for example, as less energy may be required; machinery is not dragged through the soil and soil is not physically moved. It has been shown that when weeds including *Chenopodium album* L. and *Echinochloa crus-galli* L. are cut 2cm above the soil surface, weed dry matter produced by the plant thereafter is reduced by 94-98% compared to untreated plants 20 days post treatment (Nawroth, 1996). This is unsurprising due to the location of the shoot apical meristem in broadleaves, as mentioned. CO_2 LASERs were used by Heisel et al. (2001) to cut *Chenopodium album*, *Sinapis arvensis* and *Lolium perenne*, a different mechanism to the LASER diode used in this current research.

LASERs have been used to cut the stems of weeds and cutting below the meristem was found to be most effective (Heisel et al., 2001). Heisel et al. (2001) found, rather unsurprisingly, that the median effective dose (ED_{50}) increased with growth stage; more energy is needed to kill a larger, more mature plant. The ED_{50} of late growth stage *S.arvensis* was 5.2 J mm^{-1}. This equates to less than 50% of the maximum dose used in

this current study. The grass weed, *Lolium perenne* could be cut more easily. This was likely to be due to the thinner leaves of the grass weeds compared to the thicker stems of the broadleaved weeds. When *Sinapis arvensis* and *Chenopodium album* were cut below the shoot apical meristem (SAM), a lower dose was needed compared to cutting above the SAM and *Chenopodium album* demonstrated the ability to regrow when cut above the SAM. An obvious caveat to this research is that this team only measured stem thickness of 10 plants per species, growth stage and height. Had more plant species with varying stem thicknesses have been measured, a more accurate assessment could have been made. Having said this, the fact that more energy is needed to cut a thicker, more mature stem is expected.

However, whilst good control rates were achieved using LASERs to cut through weed stems, there are downsides. As soil surfaces in the field are uneven making horizontal LASER cuts in the field unrealistic and inadvertent cutting of crop plants is probable. Therefore, in trial by Heisel et al. (2001), pots were tilted by 15 degrees. In the laboratory setting this is easily achieved, but practicalities such as these make cutting weed stems difficult in the field setting and so other target sites including the shoot apical meristem (SAM), which would require 'top down application' of LASER energy appear more feasible.

There are further downfalls to using this technique in the field setting. For example, CO_2 LASERs cannot be switched on and off quickly (Heisel et al., 2001), unlike the diode LASERs used in this current study. Therefore, there would be a high likelihood of damaging the crop plant when using a mobile LASER. This also means that more energy is being consumed without any weed control effects, resulting in a higher unnecessary carbon footprint. This method relies heavily on sophisticated detection systems and computer vision so LASER energy can be targeted to weeds. In certain crops, detecting the stem may prove difficult for some weed species, for example, black grass in wheat or barley. Further to this, detection systems usually provide top down views of the plants (Sogaard, 2005, Sokefeld, 2000, Mathiassen et al., 2006) and not stem characteristics.

Mathiassen et al. (2006) used top-down views of the weed species including *Stellaria media, Tripleurospermum inodorum* and *Brassica napus* to target the apical meristems, aiming to damage plant tissue and reducing if not preventing new growth. This team found that the 5W LASER had a greater effect on the weeds, killing more at a lower energy level compared to the 90W LASER. The 5W LASER had a wavelength of 532nm with a spot diameter of either 0.6 and 2.5mm² and the 90W LASER a wavelength of 810nm with a spot diameter of either 1.1 or 4.5mm². The mortality of *S.media* was not affected by the spot diameter setting when using the 5W LASER. The small spot diameter was more lethal than the large spot

when using the 90W LASER due to the greater intensity beam which was able to penetrate the petioles protecting the meristem of *S.media*. *T.inodorum* suffered increased mortality with both LASERs when spot size was increased. The results showed that *S.media* and *T.inodorum* were more susceptible to treatment than *B.napus*, possibly due to the closed structure surrounding the meristem of *B.napus*, thus concealing it from LASER treatment. Further to this it is not possible to compare spot diameter effects on *B.napus*. This is due to the dose required to achieve the desired effect in 90% of the treated samples (ED_{90}) being only estimated for the larger of the spot sizes for each LASER. There is debate in the field surrounding the effectiveness of spot size and in this study, no overall relationship was found between wavelength, spot size and plant species. The differences in plant physiology are likely to be the main factor rather. In this study by Mathiassen et al. (2006), the results suggest that there is a better absorption of the 532nm wavelength compared to the 810nm wavelength. This seems to be a point of confusion in the field as Woltjen et al. (2008) state that a high absorption value translates into high surface absorption and less energy penetration further into the meristem, whereas lower absorption values leads to greater volume absorption. According to Woltjen et al. (2008), a low absorption and high transmission of energy is crucial for a high ED_{90}. As stated earlier practical aspects of using a CO_2 LASER are more complex (Heisel et al., 2001) than when using a LASER diode and should be considered.

The LASER beam in this study was delivered through a thin 1000um fibre to an optical hand piece with a standard focus length of 11mm, 20mm and 30mm and the hand piece was held at these distances from the plant tissue (to ensure focus) and aimed at the apical meristem. This is a difference to the LASER equipment used in this current research as the LASER is fixed at a set position and cannot be altered easily.

1.5. Meristem physiology

The shoot apical meristem (SAM) contains a small group of pluripotent stem cells. These are cells, which can give rise to all cell types of the plant architecture, which generate daughter cells which form the main aerial mass of the plant. After extensive research focusing on molecular interactions controlling the maintenance and function of this region (Barton, 2010, Veit, 2004), it is now accepted to view the SAM as an organ in its own right.

Chlorophyll fluorescence (detailed on page 31-40), a technique used to assess the working state of photosystem two (PSII) is made possible as light absorbed by chlorophyll can (i)

drive photochemistry; (ii) be re-emitted as heat; or (iii) be re-emitted as light (fluorescence) (Hubbart et al., 2013). The SAM is not photosynthetically active and does not contain any chlorophyll. This heterotrophic status is confirmed when the cells of the meristem are viewed under a transmission electron microscope, revealing proplastids with limited lamella structure.

This said, the meristem is crucial in the development and growth of aerial parts of the plant including leaves, flowers, branches and internodes (Perales and Reddy, 2012). The SAM can be divided into three zones; (i) the central zone (CZ) composed of slowly dividing stem cells (Barton, 2010); (ii) the peripheral zone (PZ) which surrounds the CZ where cells divide at a faster rate compared to the CZ; and (iii) the rib meristem (RM) which is located beneath the CZ (Perales and Reddy, 2012).

With this in mind, it is important to look at the penetration depth of LASER energy when employing top down LASER treatment as in Mathiassen et al. (2006). According to (Sahlhof and Sonnenburg, 2000), the penetration depth of a CO_2 LASER beam is less than 0.1mm (100μm), and for this reason, effects of the LASER are usually only limited to the upper epidermis. In many plants the SAM is protected by young leaves and leaf primordia, the latter of which can be up to 1000μm thick. Therefore, LASER energy would be required to penetrate this plant tissue before contacting the meristem, subsequently damaging stem cells in the CZ to prevent growth.

Exposing the meristem is possible in the laboratory setting, however, targeting weeds with LASERs in the field with the hope of targeting the meristem is made more complex. For example, exposing the meristem is tedious in the laboratory with correct tools; this expectation is impractical in the field setting. Targeting the SAM location is possible with current technology aided by sophisticated visualising techniques but a method needs to be developed to affect the meristem in terms of LASER energy absorption through plant tissue.

As stated on page 23, meristematic tissue is not photosynthetically active and extensive work has been conducted where the SAM has been targeted in order to physically damage the organ. Work in this study will focus on the use of LASER energy of 680nm and the use of photosynthetic electron transport inhibitors (detailed in section 1.12) with a view to inhibit photosynthesis. As a result, the SAM is not a focus of this study, the leaves are.

1.6.   Excess light absorption/photoinhibition

Photosystems absorb large amounts of light and funnel this into adenosine triphosphate (ATP) production. The requirement for light energy can be detrimental to the integrity of the plants' machinery. The energy carried by a single photon causes a large energy disruption to the system, which under normal conditions can be handled efficiently and without damage to the photosynthetic machinery. Under certain stressful conditions, this energy is not dealt with efficiently and this can lead to the production of damaging biochemical species if not dissipated. The odds of PSII being damaged by light energy under normal growing conditions are approximately one in one million (Anderson et al., 1998), demonstrating the highly efficient processes of the photosynthetic repair mechanisms rather than the chemical robustness of PSII itself (Melis, 1999, Tikkanen et al., 2014) as detailed below.

Under light intensities exceeding the processing and repair capabilities of the plant, the photosynthetic activity of PSII begins to decline (Murata et al., 2007a). This is termed photoinhibition and light intensities leading to photoinhibition vary according to plant species (Aro et al., 1993, Havaux et al., 2005, Inoue et al., 2011, Murata et al., 2007a, Takahashi and Murata, 2008) and is an unavoidable caveat for photosynthetic organisms (Anderson and Chow, 2002). The seriousness of photoinhibition depends on the balance of damage to PSII and the efficiency of the repair mechanisms. The extent of photodamage can be determined by removing the repair process mechanisms by supplying the plant with protein synthesis inhibitors including chloramphenicol (Murata et al., 2007a). From tests including the chloramphenicol plant treatment, it is now argued that the previous scheme for photoinhibition is incorrect and a new scheme now exists. The first photoinhibition scheme described the production of ROS from reduction of Q_A subsequently attacking the integrity of PSII directly (Vass et al., 1992). A study conducted by Nishiyama et al. (2004) later disproved this theory when it was found that the rate of photodamage was not related to the abundance of ROS. Further, the production of H_2O_2 either through triggering an increase in intracellular H_2O_2 or inactivating gene responsible for the scavenging of H_2O_2 inhibited the repair of PSII but had no damaging effect on PSII directly (Nishiyama et al., 2001).

The findings detailed above lead to a proposal for a new, two step mechanism of photoinhibition. The initial stage is damage to the oxygen evolving complex (OEC) which is a water-oxidizing enzyme involved in the photo-oxidation of water during the light reactions of photosynthesis (Murata et al., 2007a). The second step is the inactivation of the photochemical RC of PSII due to inhibition of RC repair pathways (Ohnishi et al., 2005).

There are additional environmental factors which can contribute to the plants' susceptibility to photoinhibition and include high air temperatures and salt stress (Long et al., 1994, Murata et al., 2007b). Heat stress inactivates the oxygen-evolving complex in PSII directly and salt stress suppresses the synthesis of the D1 protein *de novo* along with the synthesis of almost all other proteins, some of which are needed in the PSII repair pathways (Murata et al., 2007b). Due to the sessile nature of plants, highly sophisticated protection and defence mechanisms have developed in plants to mitigate against this frequently unavoidable scenario.

To protect the integrity of PSII, the cyclic electron flow (CEF) has evolved to be a robust method of preventing photo damage to the PSII RC P680. When the P680 RC becomes excited by incident light the result is P680$^+$. This species is one of the most oxidising species known in biological systems (Dall'Osto et al., 2012). With P680 in the excited form, P680+, the formation of ROS and free radicals is abundant due to the oxidising nature of P680+. ROS including $^1O_2$ can be generated through high light exposure as by-products of photosynthesis (Knox and Dodge, 1985, Zolla and Rinalducci, 2002). The production of ROS do not generally pose a threat to the integrity of the plant cell as scavenging enzymes such as superoxide dismutase and ascorbate peroxidase 'mop-up' ROS as do antioxidants including β-carotene and α-tocopherol (Asada, 1999, Havaux et al., 2005). However, when the intensity of light absorbed is greater than the capacity of the scavenging systems to 'mop-up' dangerous chemical species, the outcome can be oxidative stress (Asada, 1999) which can inhibit the cellular repair mechanisms (Murata et al., 2007b).

Photosystem I seems to be less prone to photo damage compared to photosystem II presumably due to the longer excited state lifetime of PSII (Caffarri et al., 2014) but PSI can suffer from photodamage under stress conditions that prevent electron flow in the thylakoids (Scheller and Haldrup, 2005, Sonoike, 2011).

The cyclic electron flow (CEF) has been shown to be important for activation of thermal energy dissipation (qE) through the generation of a ΔpH gradient across the thylakoid membrane (Takahashi and Badger, 2011, Takahashi et al., 2009) as it is thought that this ΔpH gradient aids photo protective mechanisms. Thermal energy dissipation prevents inhibition of the repair of damaged PSII and limits PSII photodamage (Takahashi et al., 2009). It is clear that the CEF is crucial in the mechanism for the repair of PSII. Therefore, if the CEF is stopped using herbicides such as electron transport chain inhibitors including Calaris® and Sencorex Flow®, then the repair to damaged PSII machinery cannot be triggered. Electron transport chain inhibitors including Calaris® and Sencorex Flow® are used in this study and their modes of action discussed in detail on page 42-44.

The aim of this study is to use both 680nm LASER energy and electron transport chain (ETC) inhibitors to overload PSII. With the ETC inhibiting herbicides preventing the CEF, damage cannot be repaired and ROS production is more likely. The 680nm LASER will act as a high light intensity source and with the 680nm wavelength, it is hypothesised that this light will be absorbed very well by P680. P680 is so called due to its ability to absorb light at the 680nm wavelength. The difference between photoinhibition and PSII overload is subtle; photoinhibition occurs with light of the visible range, whereas PSII overload concentrates on the PSII RC P680 where a high 680nm light intensity is applied. This study will culminate in the application of 680nm light in conjunction with ETC inhibitors in order to force PSII to close down enabling control of weed growth.

1.7. Expectations after LASER treatment

1.7.1. Free radicals and reactive oxygen species

Reactive oxygen species (ROS) are produced in all aerobic life form and their production is considered unavoidable (Halliwell, 2006). ROS including superoxide ($O_2^{\bullet-}$) and hydroperoxyl ($HO_2^{\bullet-}$) as well as non-radical ROS including hydrogen peroxide (H_2O_2) and singlet oxygen ($^1O_2$) play a crucial role in normal processes inside cells acting as signalling molecules (Foyer and Noctor, 2005, Pitzschke et al., 2006). ROS and non-ROS signalling can occur during the initiation of gene transcription and at low concentrations can induce defence genes, adaptive responses including growth and development processes (Foreman et al., 2003, Foyer and Noctor, 2005) and the modification of transcription factors (Apel and Hirt, 2004a). In addition, stress responses may be triggered through ROS production by influencing the expression of several genes in highly selective processes (Laloi et al., 2004, Neill et al., 2002). ROS can be produced under other stressful conditions for example, drought, salinity, high light intensity and mechanical damage (Hideg et al., 2011) but also through normal cellular processes including electron transfer reactions as in photosynthesis (Sharma and Dubey, 2005).

ROS in high concentration can result in detrimental outcomes for cellular components and overall integrity. For example, ROS are known to cause direct damage to proteins including those in the photosynthetic ETC (Krieger-Liszkay et al., 2008a, Vass and Cser, 2009, Vass et al., 2007) and to the repair system proteins which are activated after damage (Allakhverdiev and Murata, 2004, Nishiyama et al., 2005, Shibata et al., 2006, Nishiyama et al., 2004, Nishiyama et al., 2001). Therefore, effective systems have evolved to manage

ROS using highly efficient antioxidant enzymes including superoxide dismutase (SOD) and catalase as well as non-enzymatic protection including the quenching activities of β-carotene (Telfer, 2014), tocopherol (Kruk et al., 2005) and plastoquinone (Kruk and Trebst, 2008, Yadav et al., 2010).

It is generally accepted that as the concentration of ROS pools in organelles increases due to stress, the systems to counteract these are also upregulated in order to minimise any negative consequences (Baker and Orlandi, 1995, Barba-Espin et al., 2010, Gechev et al., 2002, Hafez et al., 2012). Sharma and Dubey (2005) observed that in twenty day old rice seedlings experiencing mild drought stress, SOD activity increased by 71-78% in roots and 56-90% increased activity in shoots compared to unstressed seedlings. This coincided with a significant increase in $O_2^{\cdot-}$ production in roots and shoots of rice plants. Similarly, rice seedlings experiencing arsenite treatment also induced oxidative stress, with a concomitant increase in the levels of both enzymatic and non-enzymatic antioxidants (Mishra et al., 2011). Conversely, in a 2013 review, Choudhury et al. (2013) alluded to the diminution of antioxidants under abiotic stress, including drought, high salinity and wounding, adding that ROS in high concentrations can directly damage antioxidants if completely overloaded. In addition, Dat et al. (1998) found that decline in the activity of ascorbate-glutathione enzymes in drought conditions could be down to significantly enhanced levels of ROS, which, when interacting with the enzyme could oxidise it and could lead to it inactivation. This study did not analyse SOD, and therefore, it is unwise to apply this to all antioxidant enzymes.

Supplying plants with a wavelength of light that is readily absorbed by the PSII reaction centre P680 has the potential to generate ROS. It is hypothesised that a light source of 680nm will be readily absorbed by the P680 RC due to the affinity of the Chlorophyll a special pair within the P680 RC to absorb at this wavelength (Ishikita et al., 2006). Thus, there is a high likelihood of supplying the Chlorophyll a special pair with a satiable and overloading amount of 680nm light, the result of which could lead to ROS production. The theoretical mechanism for ROS production, especially production of singlet oxygen due to 680nm light overload is as follows. The excited states of the chlorophyll molecules residing in the LHCs, inner antenna and also the RC of which P680 is included have excited states which can last up to a few nanoseconds (Krieger-Liszkay, 2005). This length of time is long enough to allow the conversion of energy from excited chlorophyll into an electrochemical potential through charge separation. In this study, the aim is to provide P680 with an excess of useable energy. In reality, if energy supplied to P680 is not used, the spins of the excited electrons can become perturbed resulting in the production of triplet state chlorophyll (Fufezan et al., 2002a, Hideg et al., 2007). This species has a life time of ~3ns and can react with $3O_2$ to produce the highly volatile singlet oxygen providing there are no effective

quenchers in the surrounding vicinity (Krieger-Liszkay, 2005). There are two β-carotene molecules present in the reaction centre of P680 which function as singlet oxygen quenchers and due to the distance of these being too great from P680, are unable to quench excited state chlorophyll (Loll et al., 2005, Umena et al., 2011).

As stated, the production of singlet oxygen is highly likely should the 680nm light be absorbed efficiently by the P680 RC. Due to the short life time of singlet oxygen (0.5-1.0μs in plants (Laloi and Havaux, 2015)), assays to quantify singlet oxygen is difficult without highly specialised tools, not present in HAU. Therefore, as detailed on page 50, the effect of singlet oxygen will be quantified by the levels of lipid peroxidation of cell membranes through a measurement of conductivity.

Superoxide can be generated due to stress in plant cells. However, this study aims to pin point the effects of the 680nm incident LASER light on PSII specifically. Superoxide is produced at PSII under stressful conditions, but more so at PSI (Asada, 1999, Asada, 2006, Rizhsky et al., 2003, Scheller and Haldrup, 2005). The water-water cycle is an effective generator of superoxide on the reducing side of PSI, the aim of which is to dissipate excess light by increasing the rate of electron transport (Asada, 1999, Asada, 2006, Rizhsky et al., 2003). It is possible that with an increased absorption of 680nm, excess energy would be funnelled through to PSI resulting in superoxide production via the water-water cycle in order to clear the backlog of excess absorbed light. SOD unit analysis could therefore provide an insight as to the fate of incident 680mn light if it is passed on from the PSII P680 RC to Pheo and so on, thus affecting the photosynthetic ETC outside of PSII. Greater SOD production could suggest the 680nm light is failing to overload and shutdown PSII and in fact having the opposite effect of promoting electron transport on to PSI. It will be interesting to assess SOD levels with and without photosynthetic ETC inhibiting herbicide treatment to determine the robustness of this mechanism.

1.7.2.   Protein damage and photosynthetic protein damage

There is evidence in the field that ROS target protein repair processes rather than causing direct protein damage.   For example, ROS may not damage PSII directly, but cause detrimental effects to the photosynthetic mechanism by inhibiting PSII repair processes (Allakhverdiev and Murata, 2004, Nishiyama et al., 2005, Shibata et al., 2006, Nishiyama et al., 2004, Nishiyama et al., 2001). Nishiyama et al. (2004) found that when molecular oxygen, the precursor for singlet oxygen was removed from cells, the rate of photodamage was unaltered, suggesting this ROS targets the repair processes instead of photosynthetic

proteins allowing photosynthesis to continue to a point. Okada et al. (2011) supported this as when the gene for the $^1O_2$ scavenger α-tocopherol was altered, the rate of photodamage was unaffected but the rate of PSII repair decelerated quantified by the rate of oxygen evolution in the presence of 0.5mM 2,6-Dimethoxybenzoquinone, showing that it is likely that ROS target repair processes. This could be a powerful method to assess the rate of repair after 680nm LASER treatment.

ROS can inhibit repair through the suppression of protein synthesis. The D1 protein is a crucial component in the PSII complex. Even in a normal, unstressed plant, D1 turnover is ongoing (Miyao et al., 1995, Okada et al., 1996). The turnover process starts with the degradation of the now non-functioning protein, de novo synthesis of the precursor, insertion of the new D1 protein and then maturation through carboxy-terminal processing of the D1 protein before reactivation of the OEC (Aro et al., 2005, Huesgen et al., 2009, Mulo et al., 2008, Nixon et al., 2010). Analysing individual stages of this process allows monitoring of the turnover of D1 in order to reveal information about the repair dynamics of PSII. This probing method has been analysed in cyanobacteria where it was found that de novo synthesis of the D1 protein in these organisms was suppressed when the intracellular levels of H_2O_2 and $^1O_2$ were elevated as well as the synthesis of many other proteins (Allakhverdiev and Murata, 2004, Nishiyama et al., 2004, Nishiyama et al., 2001). This suggests that ROS may target the machinery necessary to synthesis proteins *de novo*. In addition, the gene coding for D1, *psbA*2 is specifically inactivated by H_2O_2 and $^1O_2$ and further investigation into this indicated that elongation step in the translation of *psbA*2 mRNA is likely to be targeted (Nishiyama et al., 2004, Nishiyama et al., 2001). The *de novo* synthesis of D1 *in planta* may differ from cyanobacteria marginally, but comparisons could be drawn from both systems as both are photosynthetic organisms. Further, the evidence suggesting ROS can inhibit the *de novo* protein synthesis of the D1 protein is likely to mean that the *de novo* synthesis of other photosynthetic proteins is also affected which could cause a steep decline in photosynthetic capability.

In later experiments in this project, Florasulam will be applied to plants along with 680nm LASER energy. Florasulam inhibits plant amino acid synthesis. It will be interesting to see if there is a relationship between administering Florasulam and 680nm LASER energy as inhibition of amino acid synthesis could in turn inhibit de novo protein synthesis. If ROS damage arises from an excess of 680nm light, normal photosynthetic processes could be jeopardised. This could highlighted by a decline in the chlorophyll fluorescence parameter, FvFm as detailed on page 36.

1.7.3.   Loss of cell membrane integrity

Along with the direct and indirect damage to photosystem II caused by ROS, cellular integrity at the phospholipid bilayer is also jeopardised through lipid peroxidation. This response can be measured by electrolyte leakage quantified by the level of conductivity (µS) to assess the tolerance of a plant towards stress (Bajji et al., 2002, Lee et al., 2002, Fan et al., 2015). Lipid peroxidation can be caused by stress including waterlogging (Shabala, 2011), high temperatures (Liu and Huang, 2000) and low temperatures where electrolyte leakage (EL) levels were shown to significantly increase (Fan et al., 2015).

There are many types of ROS produced in plant stress responses including superoxide but only singlet oxygen and free radicals are sufficiently reactive to oxidize polyunsaturated fatty acids directly (Mueller et al., 2006). It is hypothesised that singlet oxygen will be the predominant ROS formed after 680nm LASER and herbicide treatment, alone or in conjunction. Damage to membranes occurs in close proximity to the site of singlet oxygen production, partially due to its short life time of 0.5-1µs (Li et al., 2012, Telfer, 2014) thus often escaping scavenging by cellular antioxidants. Whilst other ROS do have an influence in lipid peroxidation, singlet oxygen was shown to be a major ROS species involved in photo-oxidative lipid oxidation and damage in *Arabidopsis thaliana* (Triantaphylides et al., 2008). It is generally accepted that singlet oxygen molecules and other ROS react directly with double bonds of fatty acids by abstracting a hydrogen atom to produce allylic hydroperoxides initiating a chain reaction of lipid peroxidation (Chan et al., 2012). During the lipid peroxidation cascade, membrane lipids are oxidized producing LOOH (Girotti, 1998) and in turn be converted into fatty acid peroxyl which participate in lipid fragmentation products, lipid peroxidation propagation and the production of singlet oxygen (Miyamoto et al., 2007).
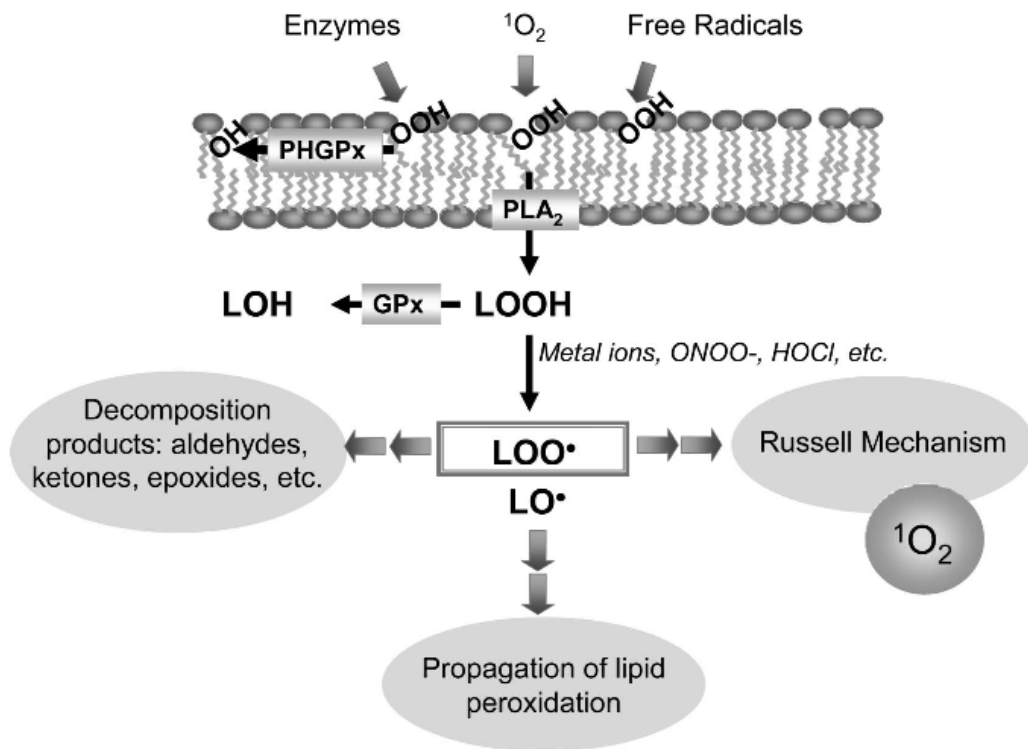
Figure 1 schematic to depict the generation and fate of lipid hydroperoxides in membranes. Phospholipid glutathione peroxidase (PHGPx) can reduce phospholipid hydroperoxides producing LOOH. These hydroperoxides be scavenged by glutathione peroxidases (GPx) or decomposed generating fatty acid peroxyl (LOO.) alone or together with alcoxyl radicals (LO.) that can participate in further reactions. Figure from (Miyamoto et al., 2007)

Though % relative conductivity has provided meaningful results in many studies, care should be taken when analysing data as sample preparation could lead to elevated results. For example, in the study conducted by Iakimova and Woltering (2018), wounded plants had greater EL levels with concurrent increase in ROS production. ROS production could lead to a knock on lipid peroxidation effect, thus confounding the issue.

1.8.   Chlorophyll fluorescence

1.8.1.   Introduction

Recent developments in technology have led to the use of chlorophyll fluorescence meters to assess OJIP parameters. OJIP represents the O-J, J-I and I-P transient phases of photosynthesis (Kupper et al., 2019) and are detailed in the diagram below. The OJIP transient phases translate in to powerful parameters which can give an insight into processes at specific check points in the photosynthetic pathway.

Measuring various photosynthetic parameters using chlorophyll fluorescence dates back to the 1930s (Papageorgiou and Govindjee, 2004), however the speed and ease of chlorophyll fluorescence has moved forward to the small, hand held devices used in this study capable of measuring *in vivo* stress (Maxwell and Johnson, 2000). Chlorophyll fluorescence is an incredibly informative tool when analysing photosynthesis as it directly relates to the rate of energy flow via the ETC. As with most scientific protocols, this chlorophyll fluorescence is not without caveats. For example, any factors affecting the metabolism of the plant can influence OJIP parameters even if such factors do not directly affect photosynthesis, including disease and pest infestation (Barbagallo et al., 2003)
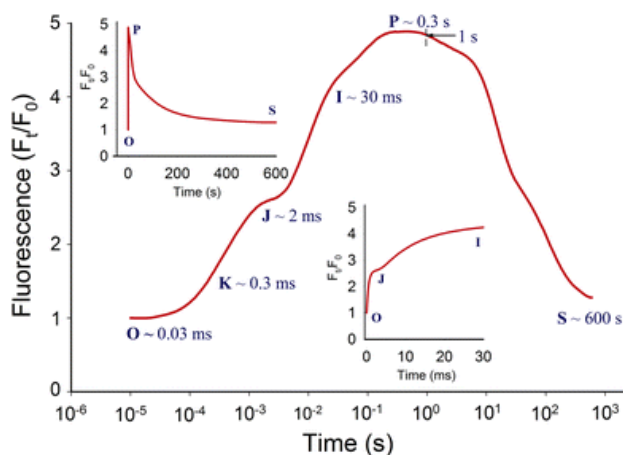
Figure 2 A Chlorophyll a polyphasic fluorescence curve in plants (main plot). The transient is plotted on a logarithmic time scale from 10 μs to 600 s. The same curve is plotted in regular time scale (top left). The initial part of OJIP transient (0–30 ms) is plotted on regular time scale (lower right). The O, K, J, I P and S refer to the selected time points used by the JIP-test for the determination of structural and functional parameters and denote the fluorescence intensity F_o (at 30 μs); the fluorescence intensity F_K (at 300 μs); the fluorescence intensities F_J (at 2 ms) and F_I (at 30 ms); the maximal fluorescence

intensity, $F_P = F_M$ (at time denoted as t_{FM}). Usually, for analysis of fluorescence transient, the record is limited to 1 s, creating typical OJIP-polyphasic fluorescence rise (Kalaji et al., 2016)

Across this study, OJIP parameters were measured immediately before herbicide application and every 24 hours after treatment using a Photon Systems Instruments FluorPen FP100, Czech Republic until the plant leaves became too damaged to take reliable measurements. This section will outline the principles of chlorophyll fluorescence and how data can be applied to the outcomes of this project.

1.8.2.   PSII antenna complex

Photosynthetically active radiation (PAR) ranges from 400-700nm. There are a range of photosynthetic pigments, chlorophyll included, housed mainly in the light harvesting antenna complexes (LHC) located in the thylakoid membranes which are responsible for trapping light from the PAR range. An antenna complex is made up of various pigment molecules namely chlorophylls and carotenoids and connected by proteins (Fig 4).

There are two forms of chlorophyll, *a* and *b*. The former is present in all photosynthetically active organisms which product oxygen (Kalaji et al., 2011, Kalaji et al., 2016, Maxwell and Johnson, 2000). Chlorophyll *b* is 30% less abundant than chlorophyll *a* in plant leaves and is found in plants and chlorophytes (Kume et al., 2018, Xu et al., 2001). Chlorophyll *a* which is more of a focus than chlorophyll *b* in this study is composed of a porphyrin ring where 4 nitrogen atoms coordinate a central magnesium ion. It is the alternating pattern of single and double bonds and rings including porphyrin which allow light absorption. The phytol chain of chlorophyll does not play a role in light absorption but anchors the chlorophyll into the thylakoid membrane. The peak absorption of chlorophyll a is between 420 and 660nm and chlorophyll b, 435 and 642nm. It is therefore the role of the other photosynthetic pigments including carotenoids to make use of the PAR wavelengths which are not absorbed by chlorophyll. There are three types of carotenoids with absorption peaks ranging from 420 to 480nm. Carotenoids not only absorb light but have a vital role in protecting chloroplast lipids against photo-oxidation by removing excess energy from excited chlorophyll molecules by thermally deactivating them (Braslavsky and Holzwarth, 2012). This interception inhibits the production of singlet oxygen which can lead to lipid peroxidation (page 30).
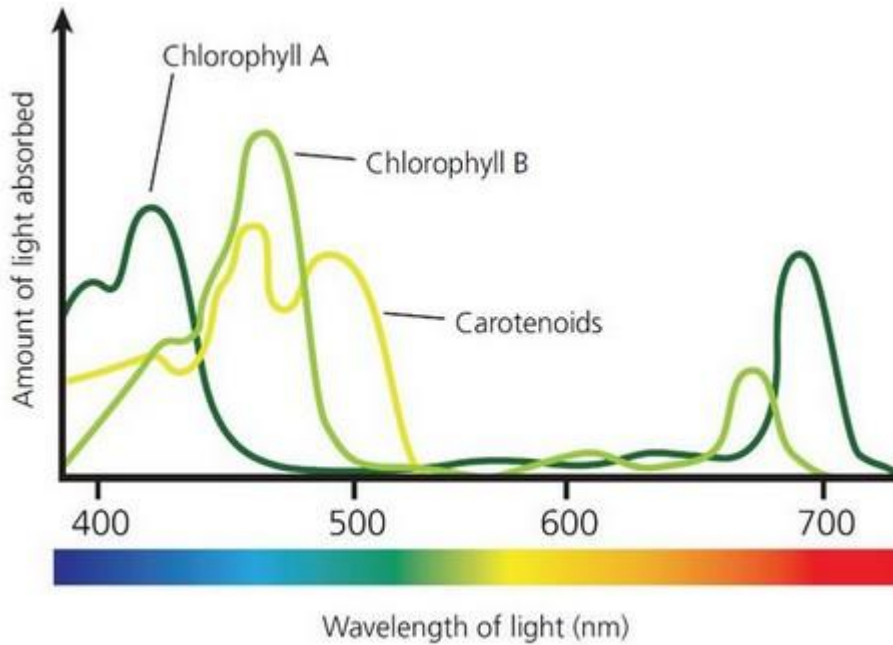
Figure 3 The absorption spectra of chlorophyll and carotenoids

When a chlorophyll molecule or another photosynthetic pigment in an antenna complex absorbs a photon, the energy profile of the molecule is raised to the excited state. From the point of photon absorption in the LHC, a series of electron transfers take place resulting in energy migration from the antenna complex to the chlorophyll *a* special dimer P680 (so called due to its peak absorption being 680nm) in the RC of PSII. Subsequently, P680 loses an electron to the intermediary acceptor, pheophytin (Pheo) also located in PSII to form P680+ and Pheo-. From here, the reduced Pheo then transfers the electron onto plastoquinone QA. This pathway can be depicted by the following scheme:

P680+ Pheo- QA → P680+ Pheo QA-
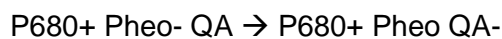
P680 is the last point of call for energy processing in PSII before the electron transport chain commences and P680 kick-starts electron transport due to its highly oxidising nature. Therefore, measurements of certain biochemical activities at P680 can provide an insight into processes before this point. This is important in this project as supplying 680nm light or treating with herbicides (or both) could influence factors downstream of P680, i.e., electron transport rate.
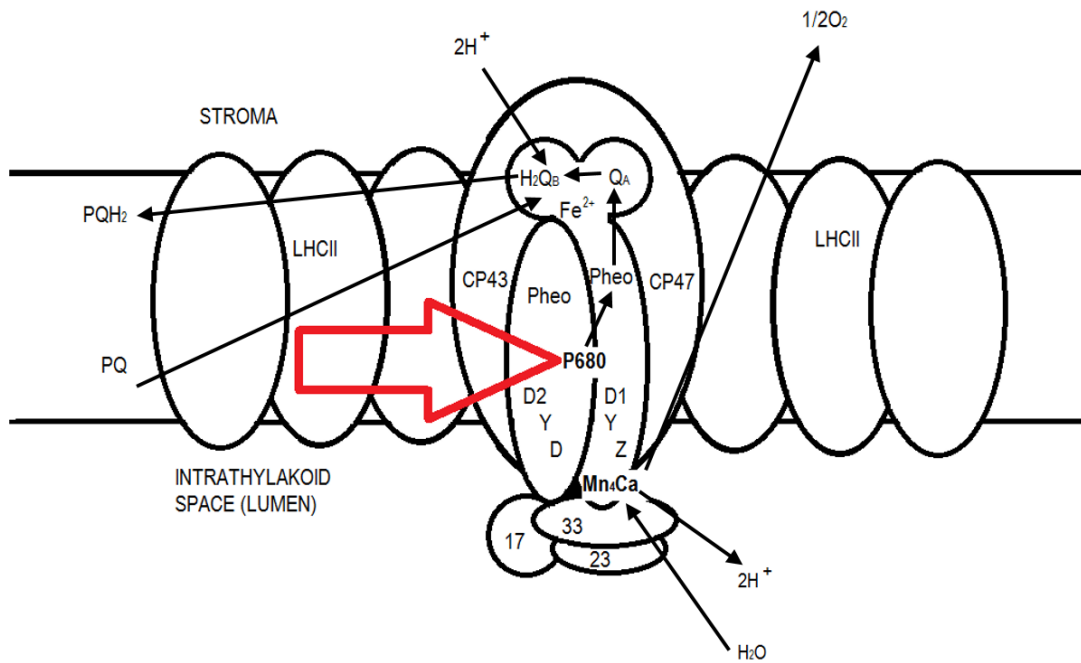
Figure 4 Schematic representation of photosystem II.
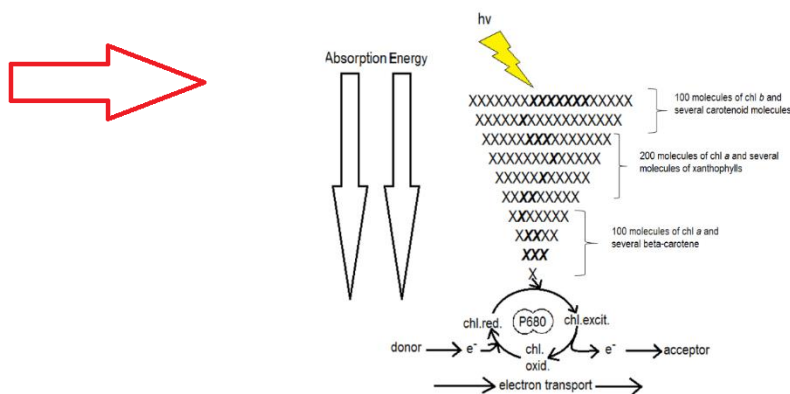
Figure 5 Schematic representation of the process taking place during the area marked by the red arrow in Figure 4.

1.8.3.   Dark adaptation

In order to gain reliable OJIP data, the leaf sample must be dark adapted using the Fluropen leaf clips. These leaf clips also ensure that the leaf sample area remains in complete darkness between the administering of saturating light pulses by the Fluorpen. Dark adaptation is necessary in order to inactivate a select group of enzymes which could, if active lead to repair of the photosynthetic machinery. In other words, the aim is to keep the

leaf in the damaged state so that stress can be measured. Any light pollution on the leaf sample could trigger repair processes, thus yielding misleading data. The inactivation of enzymes includes Rubisco (Streusand and Portis, 1987) which is involved in carbon fixation, phosphoribulokinase (calvin cycle catalysis), fructose 1,6-bisphosphate (glycolysis catalysis), sedoheptulose 1,7-bisphosphate (calvin cycle) (Buchanan, 1984), ATP synthase (ATP production) (Stumpp et al., 1999) and ferredoxin-NADP+ reductase (FNR) (photosynthesis) (Carrillo et al., 1981). These enzymes are light activated and become inactive during dark adaptation. The half time of the inactivation of rubisco is around 3 minutes (Eichelmann et al., 2005), however, the dark adaptation time is largely dictated by the inactivation of FNR and to add further complexity, this inactivation half-life time is also dependent on species. For example, Pinus spp, a C3 plant, the same class as *S.arvensis* and *C.album* needs to be dark adapted for at least 60 minutes for the full inactivation of FNR (Schansker et al., 2006). FNR must be completely inactive to gain reliable results as this enzyme has a critical role in the photosynthetic electron transport pathway and if this pathway is allowed to run, repair of proteins in the chain can commence. Activation of these critical enzymes must be triggered before steady state photosynthesis commences in order to get accurate fluorescence readings (Papageorgiou and Govindjee, 2011). Therefore, in order to cover any doubt as to the length of time for dark adaptation, 60 minutes is a satisfactory period so that reliable data can be gathered.

1.9.   Parameters measured

OJIP analysis will be a major tool in determining whether PSII has become overloaded by the 680nm LASER light used alone or in combination with ETC inhibitors. The term 'overload' in this thesis focuses on the special chlorophyll *a* pair of the P680 RC and not PSII in general.

A total of five OJIP parameters were measured across this study. Often in studies analysing photosynthesis, the FvFm is the only parameter used. However, the additional parameters measured in this study give more detailed information about the workings of the photosystems and detail regarding different stages of the process than when using FvFm alone (Force et al., 2003). Whilst FvFm gives an overview of the working state of PSII, the other four parameters (pages 36-41) are all interconnected and provide a powerful and quantifiable description of the energy fluxes within PSII.

1.9.1.   Fv/Fm (TRo/ABS)

FvFm fundamentally is a probability ratio; the likelihood of an absorbed photon being trapped by the PSII RC leading to Q_A reduction. FvFm is used frequently in photosynthesis related research as it is fast and simple to measure. For example, it has a very clearly established range of accepted values in which plants are deemed to be working normally without stress factors hindering photosynthesis. This range lies between 0.79 and 0.83 and anything below suggests the plant is experiencing photosynthetic stress and Q_A is not reduced.

FvFm is often used to support the diagnosis of photoinhibition (Burritt and Mackenzie, 2003, Kato et al., 2002) from excessive incident light. The field is opening up to the idea that the importance of FvFm could be over-relied upon as this parameter only gives a general overview and shows the narrowest range of change (Force et al., 2003); other OJIP parameters delve deeper into more specific energy transfer phases including EToRC and Abs.RC and are much more sensitive to change. Even though the FvFm parameter is a simple measurement where a value below 0.79 suggests photosynthetic decline, the underlying reasons for the lower value are not always so simple.

Firstly, leaf optics can affect the absorption and reflectance of light and so changing the Fm and Fo values. Fo and Fm values form the basis of the FvFm ratio. Leaf optics might be altered by stress including drought (Babar et al., 2006) or specifically in this case, herbicide treatment. It is also likely that the reflectance and absorbance spectra from leaves of differing plant species can vary, therefore, care should be taken when comparing FvFm values between plant species. In addition, as discussed in Chapter 3, certain doses of 680nm LASER energy can damage the surface of the leaf thus altering surface optics. These doses have been omitted from the study.

Secondly, it is widely accepted in the field that low FvFm values correlate to a reduction in the rate of photosynthesis. This is only partly true; if FvFm values are lower, this can only be taken to mean a decline in photosynthetic performance is ongoing if values correlate with the maximum quantum yield of photosynthetic exchange of CO_2 or O_2. Under high light intensity, it is possible to have a decline in FvFm value but no detriment to the photosynthetic performance (Demmig-Adams and Adams, 2006).

Nevertheless, FvFm is one OJIP parameter which will be used as a tool to identify changes in the state of photosynthesis in treated plants. Due to some doubt in the field as to the suitability of FvFm to correctly identify subtle photosynthetic changes in response to treatments, four other OJIP parameters will be used as tools in conjunction with FvFm to

determine which treatments (herbicide alone, 680nm LASER alone and 680nm LASER in conjunction with herbicide) are more effective when overloading PSII.

1.9.2. Abs.RC

Abs.RC denotes the total number of photons absorbed by chlorophylls in reaction centres divided by the total number of RCs which remain in an active state (Force et al., 2003) or to simplify, the absorbed photon flux per RC.   The Abs.RC value is highly influenced by the number of inactive or active RCs. This parameter is a good indication of how capable the plant antenna complexes are at regulating the amount of light reaching the RC. For example, Force et al. (2003) found a decline in the Abs.RC value in *Pisum* thylakoids (less light absorbed) when illuminated compared to *Monstera* leaves, suggesting that the *Pisum* thylakoids contain a more advanced regulatory mechanism which prevents excess light reaching the RC, which can be highly detrimental to the photosynthetic machinery (Aro et al., 1993, Inoue et al., 2011, Powles, 1984)(– as excited P680+ is highly oxidising and a potentially dangerous molecule). In this study where only 680nm light is incident, it is hoped that the P680 RC will absorb well at this wavelength. Abs.RC could therefore give a good indication as to the amount of 680nm light absorbed at varying LASER doses.

1.9.3. TRoRC

TRoRC denotes the maximum trapping rate of the PSII RC ultimately leading onto the reduction of Q_A (Ceusters et al., 2019, Fan et al., 2015). Alternatively speaking, a high TRoRC shows that the RC is happily absorbing energy from the antenna complex and beginning to channel the absorbed energy onto the photosynthetic ETC. As with the link between Abs.RC and DIoRC, the addition of TRoRC into this already powerful relationship further exposes the finer workings of the PSII antenna complex and P680 RC, especially when comparing TRoRC and EToRC (see pages 36-41). A plant sample in good physiological health and under no light stress would have a high Abs.RC, high TRoRC and low DIoRC. This shows that a high amount of the available energy is being used and not dissipated (DIoRC). A stressed plant experiencing high light intensities could show higher Abs.RC, low electron trapping TRoRC and thus a very high dissipation level (DIoRC).

1.9.4.   EToRC

EToRC quantifies the electron transport flux from reduced Q_A to Q_B per active PSII RC (Ceusters et al., 2019, Fan et al., 2015). This point is the commencement of the photosynthetic electron transport chain. Once the electron has been passed to Q_A, the parameter EToRC holds no information for downstream processes beyond this point and is the last point of call regarding gathering information detailing flux in PSII. Downstream flux states, particularly in PSI could be quantified by the use of REoRC which quantifies the electron flux reducing the PSI acceptor side per RC (Ceusters et al., 2019, Fan et al., 2015).

The parameter EToRC is an excellent descriptor of the conclusion of process taking place in the PSII zone. EToRC values in the range of 0.7-0.85 are typical for unstressed plants, whereas values in the region of 0.3 – 0.1 and even into minus figures highlight severe stress conditions in the plant. Highly disrupted EToRC values suggests dysfunction in the P680 RC (Force et al., 2003). When using herbicides which disrupt the ETC, including Calaris® and Sencorex Flow® low EToRC values compared to untreated plants would be expected.

1.9.5.   DIoRC

DIoRC refers to the effective energy dissipation of an active RC. Alternatively DIoRC can mean the ratio of total dissipation to the amount of active RCs due to the high dissipation of the inactive RCs (Ceusters et al., 2019, Fan et al., 2015, Force et al., 2003). Dissipation in this situation refers to the method of removing absorbed energy either through heat loss, energy transfer to other systems or fluorescence (Strasser et al., 2010). Incident photon levels which are in too high a quantity for the RC to trap are dissipated via non photochemical methods including heat. Alone, the DIoRC parameter reveals very little except for reliable quantification of heat dissipation but it is the relationship with EToRC which can reveal deleterious effects including photoinhibition. For example, Force et al. (2003) illuminated plants including *Monstera deliciosa, Philodendron selloum* and *Pisum sativum* and analysed closely the relationship between DIoRC and EToRC parameters to highlight photoinhibition. For example, an increase in dissipation (DIoRC) coupled with a decline in the electron transport probability EToRC indicated photoinhibition.

Energy dissipation is a protective mechanism. It would be highly detrimental to the plant to pass all of the energy absorbed by the antenna complexes onto the RC as downstream ROS production is likely. Therefore, some plants for example in the Force et al. (2003) study may have developed protective mechanisms where less energy is absorbed by the antenna complex and passed onto the RC (lower Abs.RC).

1.10. How these five OJIP parameters might be affected by LASER and herbicide treatment

The FvFm parameter, which as stated above shows the narrowest range of change when photosynthetic systems are perturbed. With 680nm LASER and herbicide treatment applied (individually or in conjunction), the FvFm values would be expected to drop below the value range that indicates the plant is in normal working order. With Calaris® and Sencorex Flow® application, a reduction in the FvFm value can be predicted with confidence as photosynthetic ETC inhibitors will cause electron flow to decline. This is highly likely to result in ROS production leading to overall plant stress. The mode of action of Nevada® is different to Calaris® and Sencorex Flow® and contains different active ingredients. As fluroxpyr and florasulam (AI of Nevada®) do not target photosynthetic systems directly, the FvFm value could decline, but may take longer to do so compared to plants treated with Calaris® and Sencorex Flow®.

680nm LASER treatment is hypothesised to overload the P680 RC causing stress due to ROS production at the chl *a* special pair. This could cause a transient decline in FvFm values as it is possible that the plant could recover from 680nm LASER treatment. In reality, there is a chance that 680nm LASER treatment alone could promote electron transport due to the specific application of 680nm light to the P680 RC. With the 680nm LASER and herbicide application in conjunction, it is very likely that FvFm values will reduce, but currently it is not clear whether this is due to the overriding chemical action of the herbicides of if the 680nm LASER treatment will contribute to FvFm decline.

The DIoRC parameter could provide a more detailed insight than FvFm into the effects 680nm LASER treatment or herbicide treatment has on the plant. Higher values of DIoRC could suggest more energy is absorbed by the antenna complexes (higher Abs.RC values) and ultimately passed onto the P680 RC. If the energy arrives at the P680 RC and is in quantities which exceed the damage mitigation capabilities of the cell, it is then likely to be released in order to ROS production. Alternatively, 680nm light might be absorbed by the antenna complex and effectively used by P680 as this is the optimum wavelength for absorption by the special pair of chl *a* in the P680 RC. Light energy efficiently trapped at the P680 RC be funnelled into the ETC, resulting in lower DIoRC values, and greater EToRC values.

The Abs.RC parameter is integral in understanding the effects of the 680nm LASER and herbicide treatment. Pigments including carotenoids in the antenna complexes of PSII regulate the quantity of light being passed on to downstream components and ultimately the

P680 RC. It is also possible that as the optimal wavelength of light for maximal absorption at P680 is 680nm, more 680nm light energy is funnelled down to P680 than ideally should be compared to the PAR spectrum. It is worth remembering that in this study, 680nm LASER is the only light treatment and photoinhibition refers to the damaging high light intensity from the PAR spectrum. In this study the aim is to specifically target P680 and overload the chl *a* molecules. Thus, as 680nm is so specific, the Abs.RC readings could be greater than plants exposed to PAR.

Other factors could affect Abs.RC values, including herbicide treatment i.e., treatment with Calaris®, a carotenoid biosynthesis inhibitor could increase absorption at the P680 RC due to the lack of carotenoids regulating the light intensity reaching the P680 RC.

Abs.RC is a parameter which is more powerful and telling when coupled with DIoRC. If excess light is absorbed by the antenna complex, it is likely that more energy will be dissipated via non-photochemical methods, i.e., heat and fluorescence.   Alternatively, as the light source of 680nm is specific to the P680 RC, the light may be used more efficiently. Adding ETC inhibiting herbicides may increase DIoRC values due to a block on the movement of electrons through the ETC from Q_A to Q_B.

TRoRC values in this study could be influenced by a number of factors associated with 680nm LASER and herbicide treatments. Calaris® contains 70g/litre of mesotrione, the mode of action *in planta* is the inhibition of carotenoid biosynthesis (for a detailed explanation of each herbicide used in this study, see pages 43 to 45). A reduced abundance of carotenoids, particularly in the antenna complex of PSII could lead to lower absorption of 680nm photons resulting in a lower quantity of light available to be trapped. There are some considerations to take into account regarding this last statement. One consideration would be surrounding the initial absorption of 680nm light as eluded to above. Carotenoids are vital in absorbing certain wavelengths of light in regions of the PAR spectrum where absorption by chlorophyll is not possible. The main target of the 680nm LASER light is the P680 RC, which as stated absorbs 680nm light highly effectively. With this in mind, it is possible that the carotenoids in the LHC are redundant when absorbing 680nm light and so light is still as effectively trapped in the presence of mesotrione as without. Carotenoids do have a role in making the light absorbed 'safe' for the downstream photosynthetic components but the exact consequences of carotenoid biosynthesis inhibition are largely unknown. In addition, the application of 680nm LASER energy will supply proportionally more 680nm light than found naturally in the PAR spectrum. It is possible that the case of more light available to the special pair Chl *a*, the more absorbed and trapped.

Therefore, it will be interesting to see the relationship between Abs.RC and TRoRC and if these two parameters when used together can go towards finding an explanation.

The EToRC parameter is yet another component which can aid understanding into the complex PSII energy transfer system. Coupled with the use of the previously mentioned parameters, EToRC is final parameter which can give a more complete description of the effects of the 680nm LASER and herbicide treatment. It would be unsurprising to see reduced EToRC levels after Calaris® and Sencorex Flow® treatment due to the ETC inhibiting activity of these herbicides. With Spitfire treatment, a drop in EToRC values would be unlikely as the mode of action of Nevada® does not directly target the ETC.

680nm LASER treatment may increase EToRC values, contrary to the aim of this project. This is because as already stated above, 680nm light is highly specific to P680 RC absorption, and therefore, more light available to be funnelled into the ETC if not dissipated. Alternatively, administering 680nm LASER energy could overload the P680 RC leading to closure of the RC and inhibition of the ETC. It will be interesting to see the effects of herbicide and 680nm LASER energy combined, and as previously stated to see if the herbicide overshadows the effects of the LASER or if the dual action if an effective way to overload the P680 RC.

One of the aims of this study is to determine if PSII can be overloaded using 680nm laser energy. As mentioned on page 23, the term 'overload' in this thesis focuses on the special chlorophyll *a* pair of the P680 RC and not PSII in general. The PSII antenna complex is highly efficient at filtering out light of too great an intensity thus protecting P680. P680 as Figure 4 shows is the final RC before passing electrons onto pheophytin, Q_A and then Q_B. Too much energy in the P680 RC increases the likelihood of over exciting Chl *a* and producing ROS which are highly detrimental to the integrity of the plant (see page 26) (Apel and Hirt, 2004b, Asada, 2006, Gao et al., 2008, Mattila et al., 2015, Van Breusegem and Dat, 2006). It is hoped that, as the LASER diode emits a wavelength of 680nm, the energy might bypass the antennas defences composed of carotenoids and xanthophylls (see page 26) and overexcite Chl *a* and cause P680 to shut down. Therefore, the term 'overload' refers to supplying P680 with excess energy, whereas 'photoinhibition' refers to inflicting stress on PSII in general including antenna pigments and complexes.

1.11.   Plants used in this study

The two plants used in this study are *Sinapis arvensis* and *Chenopodium album*. These plants were chosen because of their ease of germination and growth, both have large true leaf sizes and troublesome nature in agriculture.

The size of the true leaf is important due to the method of assessing the effects caused by the 680nm LASER and herbicide doses. This is especially important for OJIP measurements due to the size of the leaf clip aperture, 0.5cm diameter. For OJIP readings to be taken, it is crucial that the clip aperture diameter is within the boundary of the leaf. Any area of the aperture where there is no leaf covering, the readings will be unusable. It is for this reason why monocotyledonous weeds and dicotyledonous weeds with small leaf sizes including *Galium aparine* (cleavers) have not been used.

Sinapis arvensis and *Chenopodium album* cause significant trouble in agriculture. *Sinapis arvensis* is a close relative of oilseed rape (OSR) (*Brassica napus*) and so targeting *Sinapis arvensis* within an OSR crop without deleterious effects on the cash crop can be challenging. In addition, *Sinapis arvensis* seed closely resembles OSR seed leading to contamination of harvested seed, increasing the linolenic and erucic acid levels in extracted oil (Warwick et al., 2000). There can be 500-5000 seeds produced per plant (Guyot, 1962) able to lie dormant for 60 years or more (Mulligan and Bailey, 1975)There have been numerous reports of *Sinapis arvensis* resistance to ALS inhibitors (B/2) and photosystem II inhibitors (C1/5) globally since 1993 with once case of resistance to two sites of action reported in Turkey in 2008 (Heap, 2020).

Chenopodium album a rapidly growing and competitive plants and is able to produce approximately 500 - 20,000 seeds per plant depending on the competition of the crop and weed density (Guyot, 1962). To add to the issue, seed viability can be up to 40 years (Williams, 1963, Toole, 1946)Therefore creating a stale seed bed where *Chenopodium album* seeds are present in the soil profile can take many years. Resistance to photosystem II inhibitors (C1/5) is widespread on a global scale with resistance to atrazine, metribuzin, and simazine reported in Chenopodium album in 1975 in the United States of America (Heap, 2020).

With an abundance of report of herbicide resistance in these species, it is important to develop other methods of management of these plants which do not so heavily rely on herbicide control. Further, the development of a method of control which improves the efficacy of the herbicide leading to a slower and less frequent onset of herbicide resistance would be highly beneficial where so few new active ingredients are being brought to market.

1.12.   Herbicides used in this study

Weaknesses in the photosynthetic electron transport chain can be exploited using herbicides including Calaris® and Sencorex Flow®. Calaris® and Sencorex Flow® are able to inhibit photosystem II (PSII) therefore reducing the quantum turnover of the protein complex. Calaris® and Sencorex Flow® were used in this study along with a third herbicide, Nevada®, which has a different mode of action to Calaris® and Sencorex Flow® (see table 1(Chapter 2))

As in Chapter 2, the Fluorpen was used to measure the parameters Abs.RC, DIoRC, TRoRC, EToRC and FvFm. For a detailed description of each parameter see pages 36 to 38.

The aim of the research detailed in this thesis was to study the biochemical behaviour of two plant species, *Sinapis arvensis* and *Chenopodium album* in response to treatment with Calaris®, Sencorex Flow® and Nevada®. It is important to assess the responses of the plants using a herbicide with a mode of action other than PSII inhibition to determine the effect of the 680nm LASER energy on plants in conjunction with a chemical focusing on other biochemical processes. It may be possible that a more detrimental effect on the plants is achieved when two completely different biochemical lines of attack are used; in this case with the use of Nevada®, the hypothesised PSII overload using the 680nm LASER and protein biosynthesis inhibition.

Using the data gathered from this study, it could be possible to locate gaps in photosynthetic integrity and exploit these gaps to increase weed control efficacy.

1.12.1.   Mode of action of Calaris®

Calaris® is composed of 70g/L mesotrione (HRAC group F2) and 330 g/L terbuthylazine, members of the triketone and triazine chemical families, respectively. The triazine family of herbicides, of which terbuthylazine (HRAC group C1) is a member of, binds to the plastoquinone (PQ) –binding site on the D1 protein. This is found in the reaction centre of PSII. The result of this is electron transfer inhibition between Q_A to Q_B (Arntzen et al., 1981, Blyden and Gray, 1986, Ort et al., 1983), stopping CO_2 fixation and leading to a shortage in $NADP^+$ and ATP needed for plant growth and cellular repair. The inability of the system to reoxidize Q_A promotes the production of excited or triplet state chlorophyll leading to the formation and accumulation of singlet and triplet state chlorophyll and singlet oxygen, which

as stated on pages 29-30 can initiate a chain reaction of lipid peroxidation. As a result, the scavenging carotenoids can become overwhelmed and are unable to mop up this oxidising energy (Hess, 2000). Lipids and proteins are attacked and oxidized, resulting in loss of chlorophyll (and carotenoids) and in leaky membranes causing rapid cellular disintegration (Ayala et al., 2014, Bhattacharjee, 2005).

Mesotrione, (HRAC group F2) the second active ingredient of Calaris® is absorbed by the roots and translocated to the leaves. Mesotrione binds to and inhibits the activity of 4-hydroxyphenyl-pyruvate-dioxygenase (HPPD). The downstream product of HPPD is homogentisate (HGA) which in plants, is a precursor in tocochromanols and prenylquinone (including plastoquinone (PQ)) biosynthesis. Tocochromanols including tocopherols and tocotrienols have strong antioxidant activity. The inhibition of HPPD is hugely detrimental to the plant leading to bleaching caused by reduced pigment biosynthesis and perturbed chloroplast development. In addition, due to the inhibition of carotenoid and a-tocopherol biosynthesis (Kopsell et al., 2009), degradation of the D1 protein is allowed through ROS attack (Armel et al., 2005) as the protective effect of the ROS (and triplet chlorophyll) scavenging activity of a-tocopherol is no longer present. Further, the mixture of these two active ingredients (F2 and C1) allows for more effective D1 inhibition by PSII inhibitors, in this case terbuthylazine (Trebst et al., 2002, Armel et al., 2005). This reduced scavenging activity results in further disruption of carotenoid biosynthesis, the interference of intact chlorophyll and lipid peroxidation leading to membrane leakage (Hess, 2000).

1.12.2.   Mode of action of Sencorex Flow®

The active ingredient of Sencorex Flow® is 600g/L metribuzin (HRAC group C1) which is systemic with contact and residual activity. As with Calaris®, Sencorex Flow® is a photosystem II inhibitor and works in much the same was as terbuthylazine in Calaris®.

1.12.3.   Mode of action of Nevada®

Nevada® contains two active ingredients, 100g ae/L fluroxpyr (HRAC group O) and 5g/L florasulam (HRAC group B). Fluroxpyr, a synthetic auxin. Cell walls are composed of glucan-based cellulose microfibrils bound in a hydrated matrix made of pectins, hemicelluloses, structural proteins and proteoglycans (Burton et al., 2010, Cosgrove, 2005). The role of auxins, or in the case of fluroxpyr a synthetic auxin is the stimulation of cell wall

elongation and loosening (Cosgrove, 2016). Auxins are able to enter the plant nucleus and switch on the genes responsible for the synthesis and regulation of proton pump activity leading to apoplast acidification (Perrot-Rechenmann, 2010). In this H^+ rich environment, cell wall loosening enzymes namely expansins are activated and break the bonds between wall components causing wall enlargement. In turn, this activates calcium channels resulting in growth cessation (Majda and Robert, 2018). The final step of this chain is a loss in turgor pressure due to leaky walls prohibiting the plant to regulate the production of different cell sizes and shapes necessary for plant viability (Kroeger et al., 2011, Wei and Lintilhac, 2007).

Florasulam (group B) is an acetohydroxy acid synthase (AHAS) inhibitor. This enzyme is crucial for the biosynthesis of isoleucine, leucine and valine. Therefore, these two active ingredients work together in a highly effective way, resulting in a very efficient herbicide. Fluroxpyr weakens the cell wall of plants and florasulam stops important amino acid biosynthesis which are needed in cell walls (Burton et al., 2010). Further to this, fluroxpyr triggers rapid growth which cannot be sustained due to the mode of action of florasulam, likely causing a huge stress response.

Chapter 2

Materials and Methods

2.1   Growing *Chenopodium album* and *Sinapis arvensis*

Chenopodium album and *Sinapis arvensis* seeds were sown uniformly in a seed tray containing John Innes Number 2 compost. The growth lamps in the glasshouse were illuminated for 16 hours per day, only automatically switching off when full, uninterrupted natural sunlight was available. The temperature was set at 15°C during daytime and 5°C during night-time. Grow lamps were sourced from Sylvania, (Newhaven, East Sussex, UK), high pressure sodium, E40 fitting, 400W, (230V, 2050K) and 128.000 Phyto-Lm (product code, SHP-TS GROLUX). PAR levels in the glass house were not measured but the lamps used emit high photo-active radiation up to 1180μmol/s.   Humidity ranged from 62% to 91% with a mean of 83.3%. Seeds were purchased from herbiseed.com and replenished when stocks depleted. Eighty seedlings of each species were sown randomly in seed trays of 23cm X 27cm and 6cm depth. At the stage of cotyledon emergence, the plants were transplanted from the seed tray and grown in the same size seed tray aforementioned in a 3x3 formation. Trays were laid out on the glasshouse bench in a randomised complete block design from the commencement to end of the trial once the final OJIP parameter measurements had been taken. Plants were grown to 2 true leaf stage and only trays containing plants of very similar growth development and health were used in the upcoming trials. Any plants which has been infested with pests or displayed evidence of disease infection were not used. From sowing to use in the trial, the plants were watered daily to field capacity and closely monitored for wilting and other stress symptoms.

2.2   Leaf thickness

Leaf thickness of *Chenopodium album* and *Sinapis arvensis* plants was measured using a micrometer (Mitutoyo MDC-25SX, Japan). Plants were grown in the glasshouse under the same conditions and to the same stage as plants treated with herbicide and/or 680nm LASER as in future studies. *Chenopodium album* leaves were significantly thicker than *Sinapis arvensis* leaves ($P < 0.001$, T-Test) (mean 0.2862mm *Chenopodium album* and mean 0.2088mm *Sinapis arvensis*). However, as stated in section 6, the measurements are standardised to percentage relative conductivity therefore mitigating against the possible difference in leaf thickness and water content.

2.3   Herbicide application

Herbicides were administered to plants using the automated pot sprayer located in the main glass house at Harper Adams University. Doses were calculated to include the field rate according to the herbicide in use and a serial dilution was carried out to gain five doses containing the herbicide mixed with water (1.0lha^{-1}, 0.5lha^{-1}, 0.25lha^{-1}, 0.125lha^{-1}, 0.0625lha^{-1}, 0.0lha^{-1} (control)). The field rate of the specific herbicides is the rate commercial growers are likely to use. This represents the maximum concentration of chemical legally permitted and is dependent on the active ingredient in the product. Lower doses were used in this study to assess if the same outcome of PSII overload could be achievable compared to the maximum permitted dose. The control dose, was water. The control plants were sprayed with water first and then the lowest chemical dose was sprayed on allocated plants with the strongest dose of 1.0lha^{-1} being sprayed last to avoid any contamination which would increase the treated dose. The highest dose was 1.0lha^{-1} for Calaris®, Sencorex Flow® and Nevada®.

Plants to be treated were watered in the morning at 9am prior to spraying and were sprayed at 2:30pm where possible to maintain consistency and for any residual water on the plant leaves to evaporate. Plant were sprayed using the pot sprayer in the HAU main glasshouse, with a flat fan nozzle and a pressure of 2 bar and a traveling velocity of 6km/h. Once sprayed, the trays of plants were arranged in the pre-determined randomised complete block design used during growth in a bay in the glasshouse and with sufficient distance between trays to avoid plants in neighbouring trays from touching. Plants were not watered between spraying and experimental data gathering or 680nm LASER treatment.

2.4   680nm LASER specification

The term LASER is an acronym of Light Amplification by Stimulated Emission of Radiation. In this study, a LASER diode (LD) able to consistently emit light at the wavelength of 680nm was used. The reason behind the use of 680nm light is detailed on page 23.

In an ideal LASER set up, the light beam would be a parallel column and showing no deviation Figure 7). In this instance, due to technical limitations and difficulty sourcing a 680nm light source, a multimode LD was used to provide the necessary light source.   A multimode device was needed in order to achieve the necessary level of power from the LD. This technical limitation adds complexity when collimating the beam. A visual representation
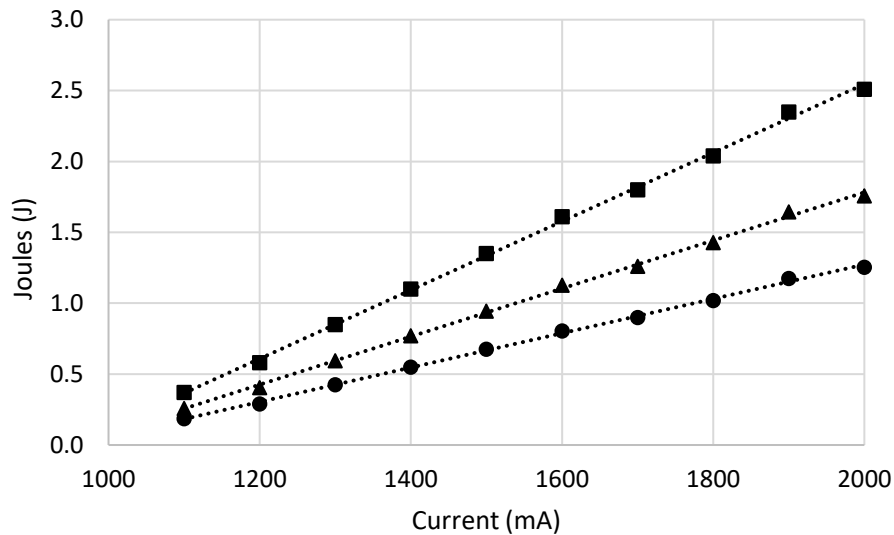
Figure 6: 5s dwell time,●; 7s dwell time,▲; 10s dwell time,■.

Current mA vs Joules (J) to show the range of doses administered to plants with varying 680nm LASER dwell times at a distance of 32cm from the point of contact on the plant leaf to the 680nm LASER diode.

of this is shown in Figure 8. The outcome of this set up is a non-parallel column where incident light from the LD disperses on contact with the lens. This would only cause experimental issues if the plants were treated at different distances to the source. The multimode model yields a spot size of 300μm at a distance of 32cm from the point of contact on the leaves to the 680nm LASER diode.

Using multimode LDs (in order to gain sufficient power) results in temperature sensitivity in the emission wavelength, meaning the temperature of the LD must be kept constant to avoid deviation from 680nm. Any small deviation from 680nm could lead to erroneous results through not having the desired biochemical effect on PSII as temperature influences the thermal population distributions in the valence and conduction band. Typically there is an increase of ≈ 0.3 nm per 1 K temperature rise. Therefore the temperature of the LD will be thermally controlled and set at 20˚C. The beam size emitted from the 680nm LD was 300μm diameter, the area of which is 544 times smaller than the area of the leaf clip aperture.

Figure 8 presents the range of 680nm LASER doses administered to plants and shows the relationship between current (mA) and Joules (J). Figure 6 also shows the consistent range of 680nm LASER doses administered, only with a larger increment of Joules (J) between dwell times of 10s and 7s compared to between 5s and 7s dwell times due to technical limitations of the 680nm LASER. The temperature emitted by the 680nm LASER was not recorded but was kept constant throughout all treatments using a temperature controller.

Therefore, heat emitted by the LASER on the plant surface was consistent throughout treatments.
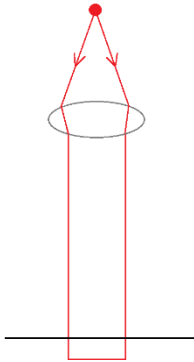
Figure 7 Schematic of an ideal parallel column of light
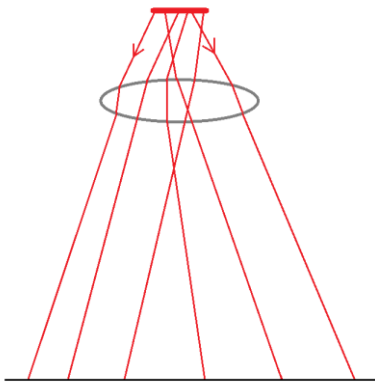
Figure 8 Schematic representation of the multimode model 680nm LASER system used in this study

2.5   680nm LASER application

When measuring the effects of the 680nm LASER on OJIP parameter data, 680nm LASER energy was administered to plants through the open leaf clip aperture to ensure the correct region of leaf was being assessed. Plants were situated in growing trays and trays were placed on the base of the 680nm LASER unit a distance of 32cm from the LASER diode. As plants are not uniform in height, measures were taken to control the distance of the treated leaf from the 680nm LASER using a platform on which the leaf and leaf clip was placed during treatment to ensure uniformity across the study. Leaves were treated once but up to

two leaves per plant were treated when the number of leaves available to be used to record OJIP readings was limited.

When administering 680nm LASER energy for percentage relative conductivity and SOD studies, leaf excisions were placed on the same platform as with the OJIP study method to maintain consistency across the study to enable comparisons between treatment effects.

2.6   OJIP analysis

OJIP analysis was carried out with the FP100 FluorPen, (Photosystems Instruments, Prague, Czech Republic).

Prior to the measurement of OJIP parameters, plants were dark adapted for 60 minutes using the leaf clips. When placing clips on the leaves for dark adaptation, care was taken to avoid physical damage to the leaf which could have affected leaf viability or optical changes to the leaf surface thus rendering the OJIP parameter readings unusable.

The FluorPen was set to record OJIP parameters only and each reading took approximately 13 seconds. Once a series of readings had been recorded, the data was transferred to Excel spreadsheets to aid analysis in statistical software.

2.7   Percentage relative conductivity analysis

Damage to the cell membrane after herbicide, 680nm LASER and combined treatment was determined by measuring the percentage relative conductivity of leaf samples. The method to quantify percentage relative conductivity was carried out according to DaCosta et al. (2004) with minor modifications. For herbicide treated samples, four $1cm^2$ leaf samples were excised using a sterilised scalpel blade and were rinsed with distilled water three times post-treatment (with herbicide and or 680nm LASER) and immersed in 20ml distilled water in 25ml plastic tubes under room temperature (21°C) for 18 hours. Plant samples to be 680nm LASER treated were excised prior to LASER application and placed a predetermined distance from the 680nm LASER diode. Care was taken to avoid the leaf samples drying out in the 680nm LASER unit.

The initial conductivity ($C_{initial}$) of the solution was read with a conductivity meter (Jenway 4510, Bibby Scientific Ltd, Staffordshire, UK) after the leaf samples had been in distilled

water for 18 hours. Leaves were then autoclaved (Vario 2228, Dixon's Ltd, Essex, UK) at 121°C for 15 minutes to achieve total cellular ablation and release of cellular contents. Final conductivity (C_{final}) was measured when the solution had cooled to room temperature. The relative conductivity was estimated as a percentage according to the formula: ($C_{initial}$ / C_{final}) x 100. The plastic tubes were able to withstand the pressure and temperatures in the autoclave and remain intact.

2.8   Superoxide dismutase level analysis

2.8.1 Methodological background

Superoxide dismutase (SOD) is an umbrella term used to describe a collection on metalloproteins which are able to catalyse the dismutation reaction of two superoxide free radicals into molecular oxygen and H_2O_2 (Alscher et al., 2002, Beauchamp and Fridovich, 1971, Constantine et al., 1977, Fridovich, 1986, Fridovich, 1997, Giannopolitis and Ries, 1976, Giannopolitis and Ries, 1977). In plants, three forms of the enzyme exist, as classified by the metal ion located in the active site of the enzyme, either copper or zinc, manganese or iron (Kanematsu and Asada, 1990, Smith and Doolittle, 1992). SODs are often described as the first line of defense against potential damage inflicted upon cellular components by superoxide (Alscher et al., 2002).

Superoxide can be indirectly quantified using SOD activity as a secondary probe (Banowetz et al., 2004, Beauchamp and Fridovich, 1971). 5-nitroblue tetrazolium chloride (NBT), a yellow compound is reduced to blue monoformazan by the superoxide radical.

SOD activity is quantified via the competitive inhibition of NBT reduction by the superoxide radical and the colour change measured using a spectrophotometer at a wavelength of 560nm. High greater absorbance indicates less SOD present.

2.8.2 Extraction of SOD

Extraction of SOD was carried out according to Constantine et al. (1977), Beauchamp and Fridovich (1971) and Elavarthi and Martin (2010) with minor modifications.

Treated samples were taken out of the ice box and an area with 1cm diameter with the treated plant material in the centre of this area excised. Each excised portion was immediately placed in a pre-cooled Eppendorf tube after excision and placed in ice in order to keep time not on ice to a minimum. This was repeated for every treated area and then

those which received the same herbicide/680nm LASER treatment were pooled and thoroughly ground in a pre-cooled mortar and pestle until no fibrous residue was visible.

Of this ground plant material, 0.15g was taken and placed in a pre-cooled Eppendorf tube and stored on ice until the pre-cooled at 4°C buffer was added. The extraction buffer consisted of 100ml 0.1mM EDTA (pH7.8) and 100ml PBS pH7.8 mixed thoroughly using a shaker board. 1.5ml of the buffer was added to the Eppendorf containing the ground plant material. The material was fully re-suspended and then centrifuged at 15000g for 10 minutes in a centrifuge (Sigma, Germany, 114 model, manufactured in 2005, 14800r.p.m maximum) and 0.5ml of the supernatant removed and stored on ice. The pellet was re-suspended again and centrifuged at 15000g for a further 10 minutes and 0.5ml supernatant removed, supernatants combined and stored on ice.

This was repeated for all treated samples including control (non-treated) samples.

2.8.3 SOD assay protocol

The assay protocol for SOD standard curve production and SOD determination in samples was carried out according to Beauchamp and Fridovich (1971) and Constantine et al. (1977). The reaction mixture was as described in Tables 1 and 2 (Chapter 2).

The reaction mixture consisting of each ingredient excluding the riboflavin was made in a 25ml sample tube. The reaction mixture excluding the NBT was made in another 25ml sample tube. The reaction mix excluding NBT would form the background control, the value of which would be subtracted from the sample and standard readings. All reagents were stored at 4°C when not in use.

A standard curve was formed by diluting SOD from bovine liver, lyophilized powder, ≥1500 units/mg protein from Sigma-Aldrich, UK, and serial diluted to form a range of 1:100 to 1:10000000. Treated plants samples were also serially diluted from 1:100 to 1:10000000. The dilution of treated plant sample which gave an absorbance at 560nm in the linear part of the standard curve would be used to assess SOD units/ml.

There were 6 replicates of each treated plant sample dilution on the 96 well plate, along with the same internal standard concentrations used for the standard curve, background controls and negative controls, containing all of the reaction mix excluding SOD. The reaction mix was made fresh at the start of each assay. Edge effects of the 96 well plate were minimised by adding buffer to the outer wells and only having valued samples within this boundary.

Each sample and standards had been stored in the freezer at -20°C and only removed before being used in the assay. Once the whole sample had returned to liquid phase, 100ml was taken for the serial dilution and was then immediately returned to -20°C conditions. The riboflavin, which was kept in the dark at all times using aluminium foil wrapped around the container, was added last to the reaction mixture. The plate was placed at a distance of 30cm under a fluorescent lamp in an incubator (Panasonic MIR-154-PE) set at 20°C for 6 minutes. After 6 minutes, the wells were mixed to remove precipitation and then returned to the incubator for another 6 minutes.

After the incubation period, the plate was transferred to the plate reader (Optima Fluostar plate reader, BMG Labtech) set at 560nm with shaking to take place every cycle. The plate was read for 1 cycle.

2.8.4 Bradford assay protocol

In order to express SOD as SOD units /mg total protein, a Bradford assay was carried out to assess protein levels extracted from the samples. The dilution of the sample used was within the linear range of the standard curve (Figure 9) using Bovine serum albumin (BSA) as a standard as in Bradford (1976). This process gives the units of SOD per mg of total protein present.

The assay was carried out according to Bradford (1976). Coomassie Brilliant Blue G250 (Sigma Aldrich, 98%) was dissolved in 50ml of ethanol (95%) in an aluminium-covered beaker to exclude light. This was stirred for 1 hour using a magnetic stirrer. After 1 hour, the mixture was poured into a 1000ml flask covered in aluminium foil and 100ml phosphoric acid 85% (w/v) added. This was made up to 1000ml using distilled water.

Prior to use, the necessary amount in order to complete the standard curve or sample assay was filtered using Whatman Number 1 filter paper. The filtrate was kept in the dark. To produce the standard curve, BSA was used as a standard and a serial dilution was carried out to get a range of protein values (see Figure 9). 20μl of each standard was used per microplate well (96 wells) when constructing the standard curve and 20μl of each sample was also used in each well when running the Bradford assay. Each well had a maximum capacity of 300μl.

200μl of filtered reagent was used in each well when running the standard curve and sample assay. The plate reader (Optima Fluostar plate reader, BMG Labtech) was set at 595nm for 1 cycle.
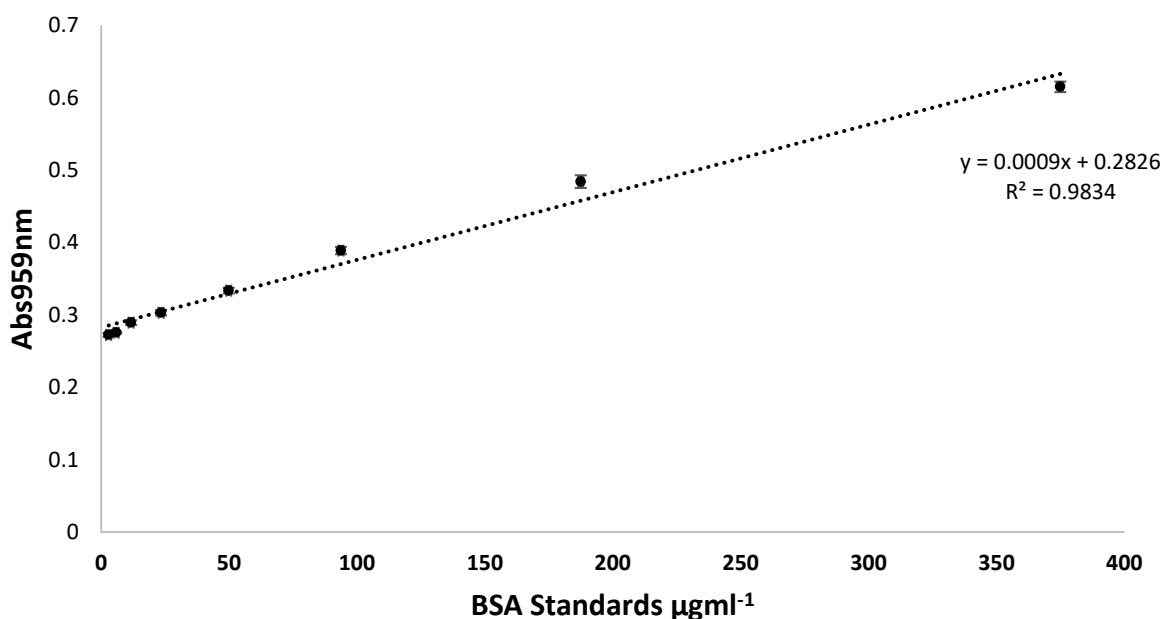
Figure 9 Bradford assay standard curve. Trend line denotes line of best fit, error bars denote ± standard error of the mean (SEM), n=18

There were 7 replicates of each treated plant sample in each microplate along with internal standards. Edge effects were negated by filling outside wells with distilled water.

The reaction mixture for the SOD standard curve (and sample assays) was as follows (Tables 1 and 2):

Table 1 Reaction mixture composition for SOD assay			
Substance	g/25ml	Concentration of Components in Reaction Mixture	µl Per 300µl well
1mM NBT	0.0220	33µM	5.0
L-Methionine	0.1863	10mM	15.0
EDTA	0.0930	0.66mM	10.0
Riboflavin	0.0019	0.0033mM	2.5
PBS buffer	*	See table 5	117.5

*One tablet was dissolved in 100ml distilled water and the pH adjusted to pH7.8. See table 2 for individual component breakdown.

Table 2 – Breakdown of individual PBS components	
Component	Molarity (mol)
Sodium chloride	0.137
Potassium chloride	0.003
Disodium hydrogen phosphate	0.008
Potassium dihydrogen phosphate	0.0015

The standard curve was constructed using a serial dilution of SOD enzyme which was ordered from Sigma Aldrich. The SOD was from bovine erythrocytes (catalogue number S7571) and stored at -20°C with a specific activity of ≥3000 units/mg protein.

2.9   Statistical analysis

Statistical analyses were conducted using GenStat 18th Edition, VSNi, Hemel Hempstead, UK. Statistical tests included one and two sample T-Tests, one-way analysis of variance (ANOVA), factorial ANOVA, linear regression and Tukey's test for 95% confidence intervals. The statistical software 'R' (R Foundation for Statistical Computing) was used to form the paired correlations test and Kruskal tests.

Chapter 3

Biological stress indication after Calaris®, Sencorex Flow® and Nevada® treatment in *Sinapis arvensis* and *Chenopodium album* plants

3.1 Objective

The objective of this chapter was to determine which dose of herbicide to use later in the study when combined with the 680nm LASER. The overall aim of this research was to use a low dose of herbicide in combination with a low energy LASER to control weed growth. Therefore, this chapter aims to find the lowest dose of the herbicides used which ultimately kills the treated plant, but still with assessable and quantifiable room for method improvement for when the 680nm LASER is used in conjunction; these treatments should combine and not be mutually exclusive.

3.2 Abstract

Three herbicides containing different groups of active ingredients were applied to *Chenopodium album* and *Sinapis arvensis* at a range of doses. Calaris® and Sencorex Flow® caused inhibition of photosystem II (PSII) highlighted by the decline in electron transport rate, quantified by the OJIP parameter EToRC. Nevada® which does not contain and PSII inhibitors failed to effect PSII negatively. Percentage relative conductivity (%RC) increased in both plant species with increasing dose of Calaris® and Sencorex Flow® with increasing time post treatment, but %RC was resistant to change post Nevada® treatment. Calaris® and Nevada® treated *Chenopodium album* samples contained the greatest level of SOD units per mg total protein, with Sencorex Flow® treated *Chenopodium album* SOD levels showing little deviation to the control (0.0lha^{-1}). Calaris® treatment produced the greatest SOD units per mg total protein in *Sinapis arvensis* samples.

The results of this study will aid comparison between 680nm LASER treatment data and herbicide+680nm LASER treatment combined in order to determine if the addition of 680nm LASER energy proves detrimental to the integrity of PSII as hypothesised.

3.3   Background

Herbicides are an important weed management method globally. The pressures to develop alternative weed control approaches is heightening with the increasing and widespread resistance to herbicides (Heap, 2020) and consumer demand for herbicide free produce (OCA, 2020)

Three herbicides have been used in this study. Two of the herbicides, Calaris® and Sencorex Flow® are photosystem II (PSII) electron transport chain (ETC) inhibitors. Calaris® is composed of 70g/L mesotrione, a HPPD inhibitor (HRAC group F2) and 330 g/L terbuthylazine, a PSII ETC inhibitor (HRAC group C1) (HRAC, 2020a). The active ingredient of Sencorex Flow® is 600g/L metribuzin, a PSII ETC inhibitor (HRAC group C1) (HRAC, 2020a).Nevada® contains two active ingredients, 100g ae/L fluroxpyr, a synthetic auxin (HRAC group O) and 5g/L florasulam, a acetohydroxy acid synthase (AHAS) inhibitor (HRAC group B) (HRAC, 2020b) Details of the mode of action (MOA) of these herbicide can be seen on pages 43-45 or Table 3.

The aim of the study detailed in this chapter is to find an optimal experimental herbicide dose for each herbicide and plant species used (*Chenopodium album* and *Sinapis arvensis*) on which the wider study can be built. Once an optimal herbicide dose has been found which inflicts detrimental effects on PSII, the 680nm LASER (detailed in Chapter 4) can be applied in order to assess the effects both treatments have on the workings of the ETC. In addition, the work in this chapter aimed to detail an optimal day for the addition of 680nm LASER treatment post herbicide treatment. Beyond day 4 post herbicide treatment in both *C.album* and *S,arvensis*, the plants became too damaged to take OJIP readings. Taking OJIP readings every 24 hours post treatment provided clear intervals where data gathered showed clear changes in OJIP values. More frequent gathering of data would have given little additional benefit as the decline in OJIP values was consistent and steady. Further, for the benefit of the interpretation of results and the reader of this project, smaller intervals could have made the project more complicated to understand.

Whilst Nevada® is not a PSII ETC inhibitor, Nevada® treatment could provide useful information regarding its effects on biochemical processes within PSII and enable comparisons to be drawn between the three herbicides of different modes of action. Nevada® contains two active ingredients of two different classes to provide two different MOA, not related to photosynthesis or specifically PSII inhibition. In addition, the MOA of Nevada® is not related to the MOA of the 680nm LASER and so inhibiting weed growth is

targeted from two different lines of attack. Nevada® is readily available on a commercial scale as are Calaris® and Sencorex Flow®.

This chapter analyses the biochemical implications of herbicide treatment focusing on the impact on the PSII reaction centre (RC) P680. In depth analysis of OJIP parameters, leaf conductivity readings and superoxide dismutase (SOD) assays will lead to a decision on the optimal dose of herbicide for the remainder of the study.

Table 3 Record of the composition, mode of action, chemical family, activity group and formulation of Calaris®, Sencorex Flow® and Nevada®

Herbicide	Calaris®	Sencorex Flow®	Nevada®
Composition	Mesotrione: 70 g/l Terbuthylazine: 330 g/l	Metribuzin: 600g/l	Fluroxypyr: 100 g/l Florasulam: 5 g/l
Mode of action	Mesotrione: Bleaching: inhibition of 4-hydroxyphenyl-pyruvate-dioxygenase Terbuthylazine: Inhibits PSII - binds to the plastoquinone (PQ) –binding site on the D1 protein	Inhibits PSII - binds to the plastoquinone (PQ) –binding site on the D1 protein	Fluroxypyr: foliar uptake causing auxin-type response Florasulam: Inhibits plant amino acid synthesis - acetohydroxyacid synthase AHAS
Chemical family	Triketone Triazine	Triazinone	Pyridine compound Triazolopyrimidine
Activity Group	Group F2 (Mesotrione) + Group C1 (Terbuthylazine)	Group C1	Group O (Fluroxypyr) + Group B (Florasulam)
Formulation	Suspension Concentrate	Suspension Concentrate	Suspension Emulsion

3.4   OJIP results

In order to present a quantified overview of the changes in energy flux at different stages of light processing by PSII, OJIP parameters, Fv.Fm, Abs.RC, TRoRC, EToRC and DIoRC (OJIP parameters defined in the literature review chapter, page 36-38) were measured before herbicide treatment and every 24 hours post treatment to provide a detailed insight into the chemical effects on PSII post treatment. The effects of lower herbicide doses were analysed to assess effectiveness; the main aim of the project is to use a low dose of herbicide along with low energy LASERs to combine to form a powerful weed control method. This provided evidence for the effects on PSII for a range of herbicide doses in both *Chenopodium album* and *Sinapis arvensis* plants.

3.4.1 OJIP analysis for Calaris®-treated *Sinapis arvensis*
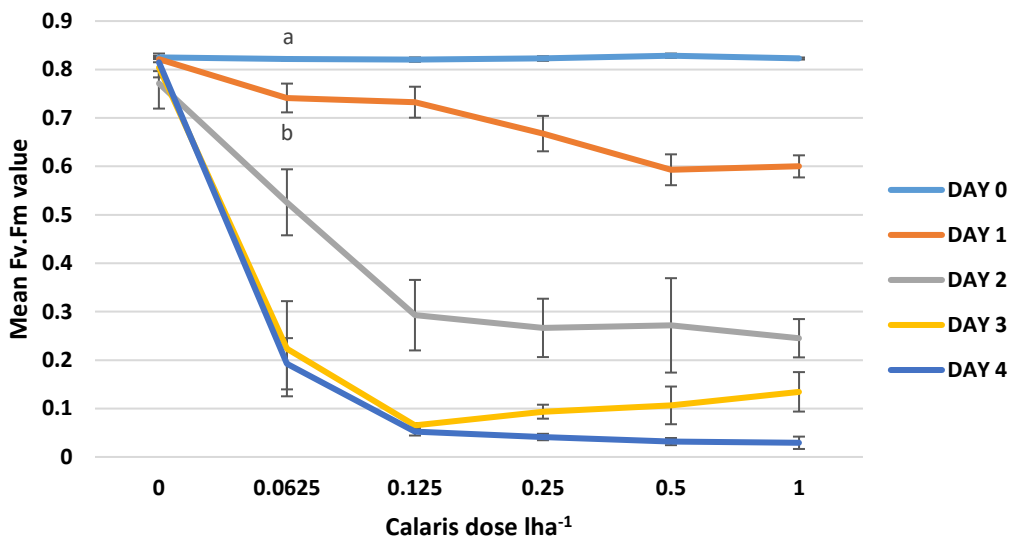
(a)
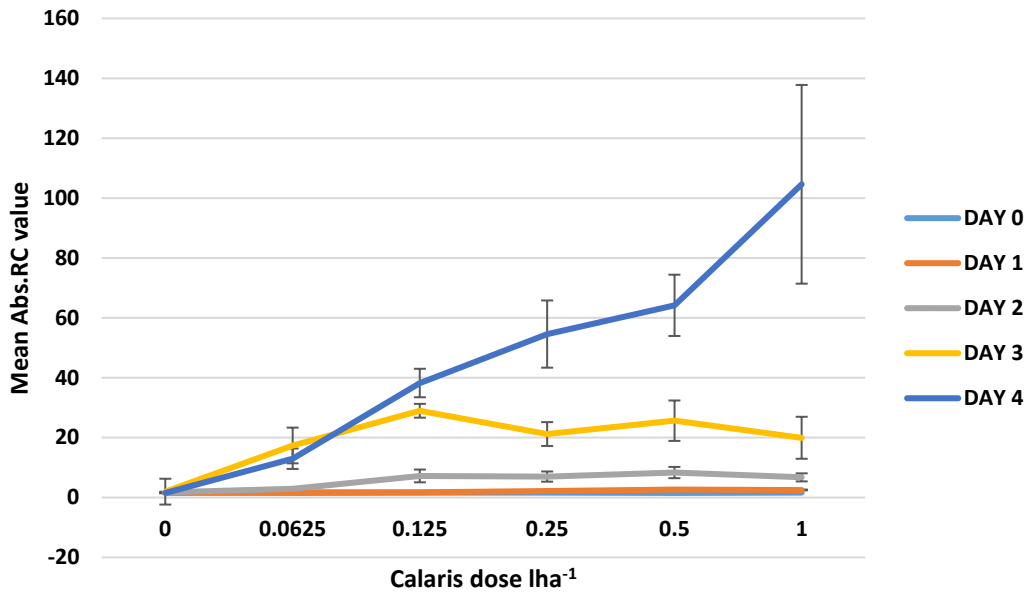
(b)
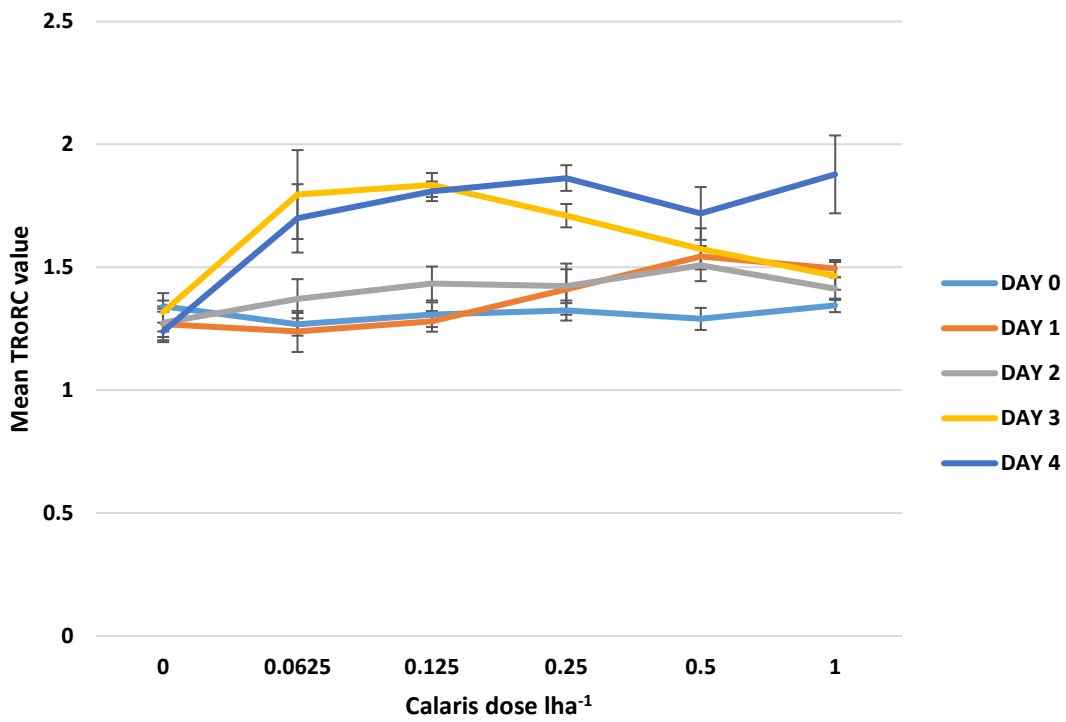
(c)
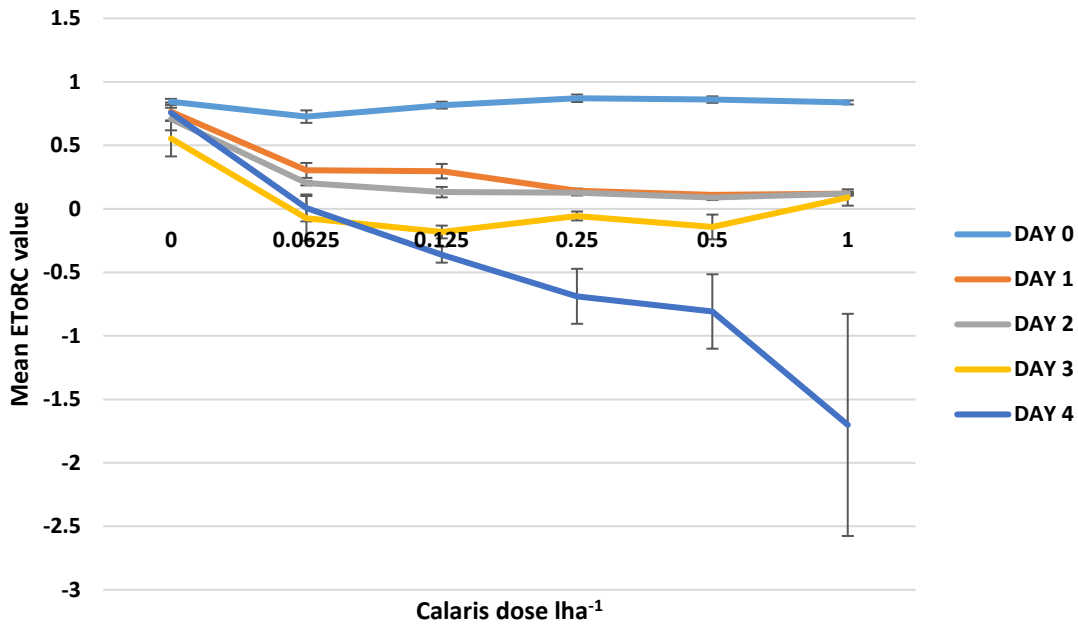
(d)
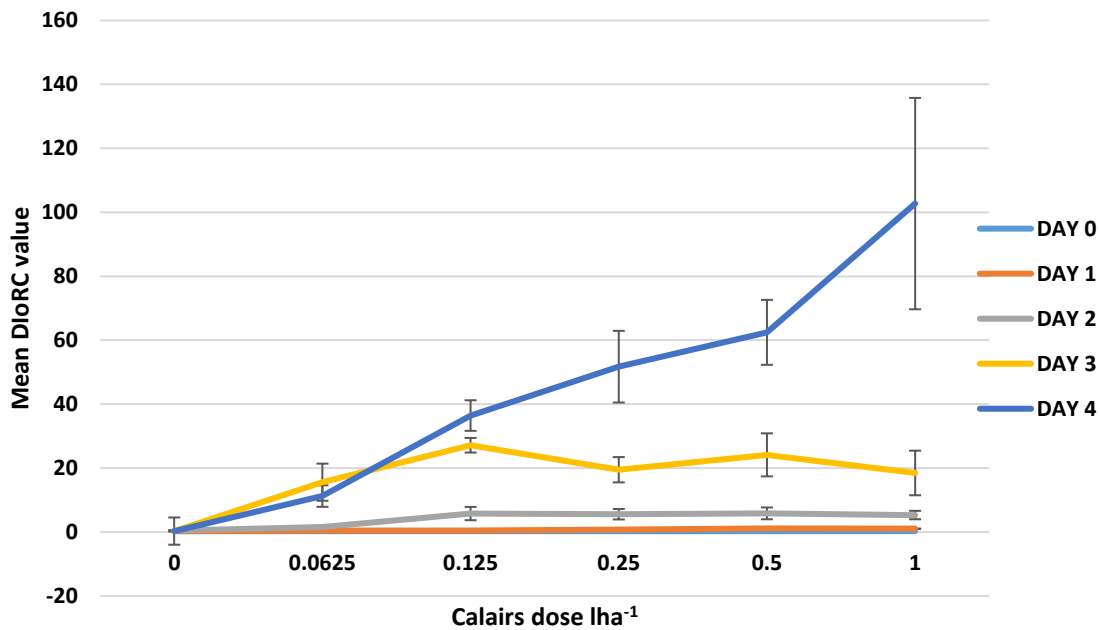
(e)

Figure 10 (a) mean Fv.Fm, (b) mean Abs.RC values, (c) mean DIoRC values, (d) mean EToRC values, and (e) mean DIoRC values of Sinapis arvensis in response to dosage of Calaris® between 0.000lha^{-1} and 1.000lha^{-1} and day post-herbicide application. Day 0 values correspond to values pre-treatment. Error bars represent ± standard error of the mean (SEM), n=8. Data analysed using two-way ANOVA, Tukey's test and T-Tests. Figure 12 (a) data highlighted by letters 'a' and 'b' showing the dose of 0.0625lha^{-1} of Calaris® is significantly different to the control plants on Day 1 for Fv.Fm

values, showing efficacy at the lowest used dosage. Larger error bars for figures 12 (b) to (e) on Day 4 highlight a greater range in data points compared to earlier assessment points.

Figures 10 (a) to (e) present *Sinapis arvensis* OJIP data from Day 0 (pre-treatment) to 4 Days after treatment with Calaris® of varying doses. Fv.Fm shows a decline with increasing Calaris® dose and time post treatment, with Fv.Fm values less than 0.1 reached at doses 0.125lha^{-1} and above on Day 4. Day 1 post-treatment Fv.Fm values at the lowest dose of 0.0625lha^{-1} is significantly different to the control on Day 0 (P=0.037, obtained from a T-Test, highlighted by the 'a' and 'b' on the data points). The pre-treatment Fv.Fm values are consistently above 0.8 showing plants are unstressed before treatment which enables comparisons to be drawn with post-treatment Fv.Fm values.

Abs.RC values show a marked increase on Day 4 post-treatment with values in excess of 100 on Day 4 post-treatment with a dose of 1lha^{-1}. Day 0 to day 2 values remain below 20 for all Calaris® doses with day 3 values significantly greater than day 0 values from 0.0625lha^{-1} to 1.0lha^{-1} (P<0.001). As could be predicted, Abs.RC and DIoRC graphs show high similarity between parameter values for both herbicide dose and time post treatment.

TRoRC values show no clear outcome with no apparent increasing or decreasing pattern for any day post treatment. Day 3 and 4 post-treatment have significantly greater TRoRC vales from 0.0625lha^{-1} to 1.0lha^{-1} compared to the control (P<0.001) with Days 0, 1 and 2 remaining similar across the range of Calaris® doses.

As expected, EToRC values decline rapidly after the application of Calaris®. Day 1 post-treatment is significantly lower than the control at 0.0625lha^{-1}. Days 3 and 4 post-treatment drop to negative values at a dose of 0.0625lha^{-1}.

3.4.2 OJIP analysis for pre and post Calaris®-treated *Chenopodium album*
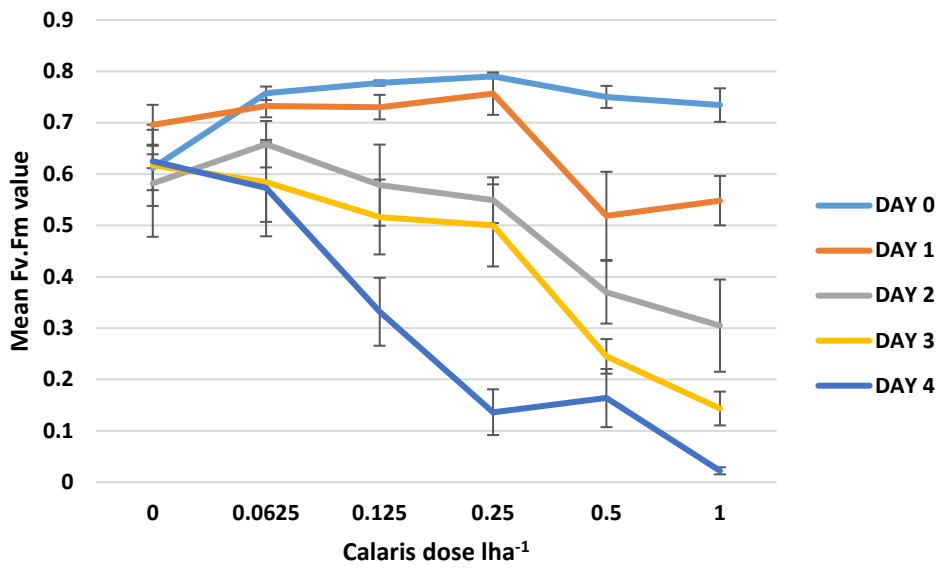
(a)
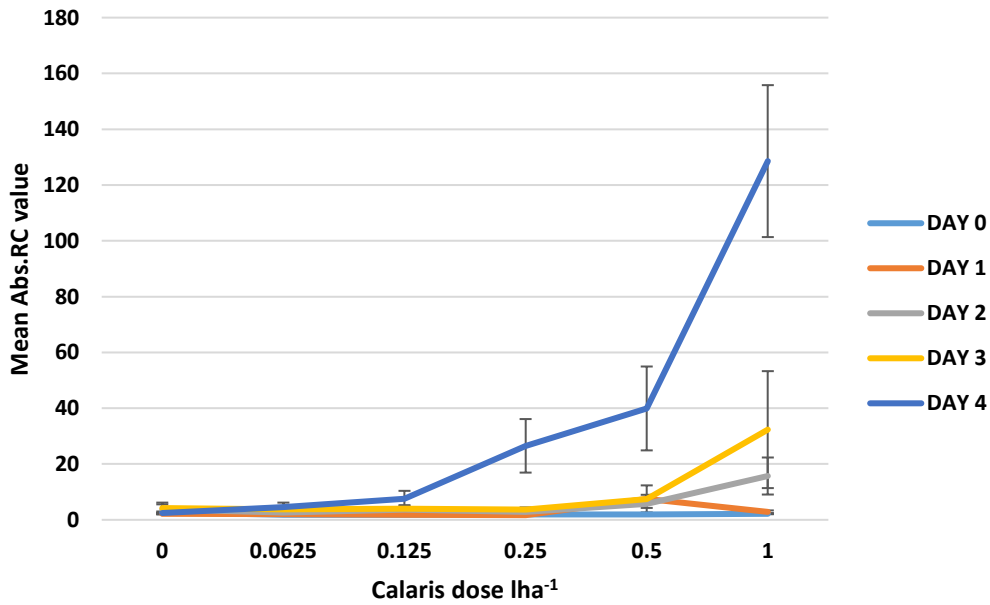
(b)
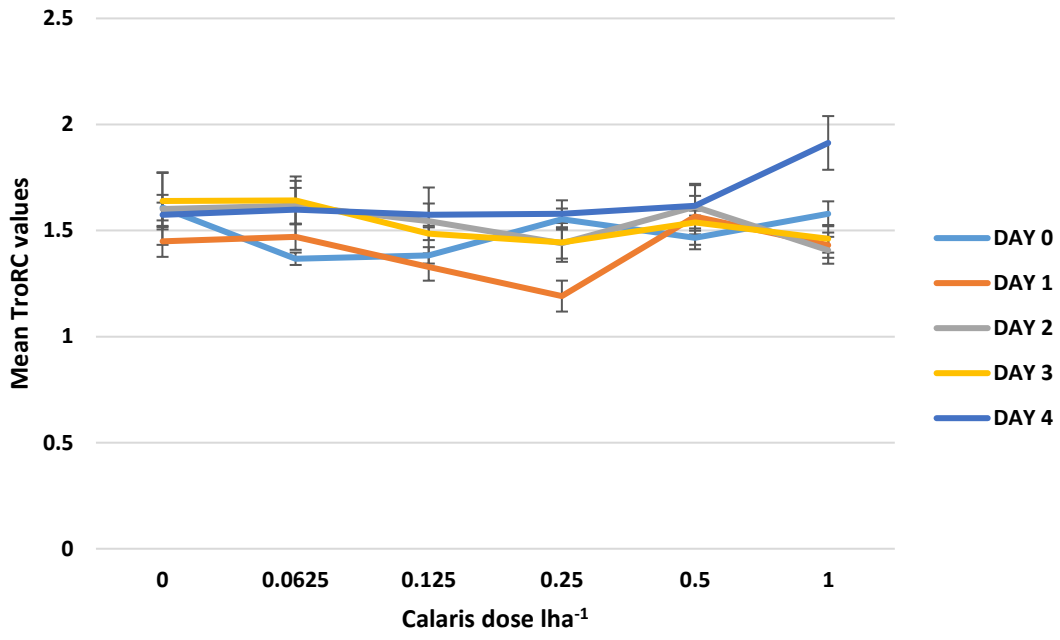
(c)
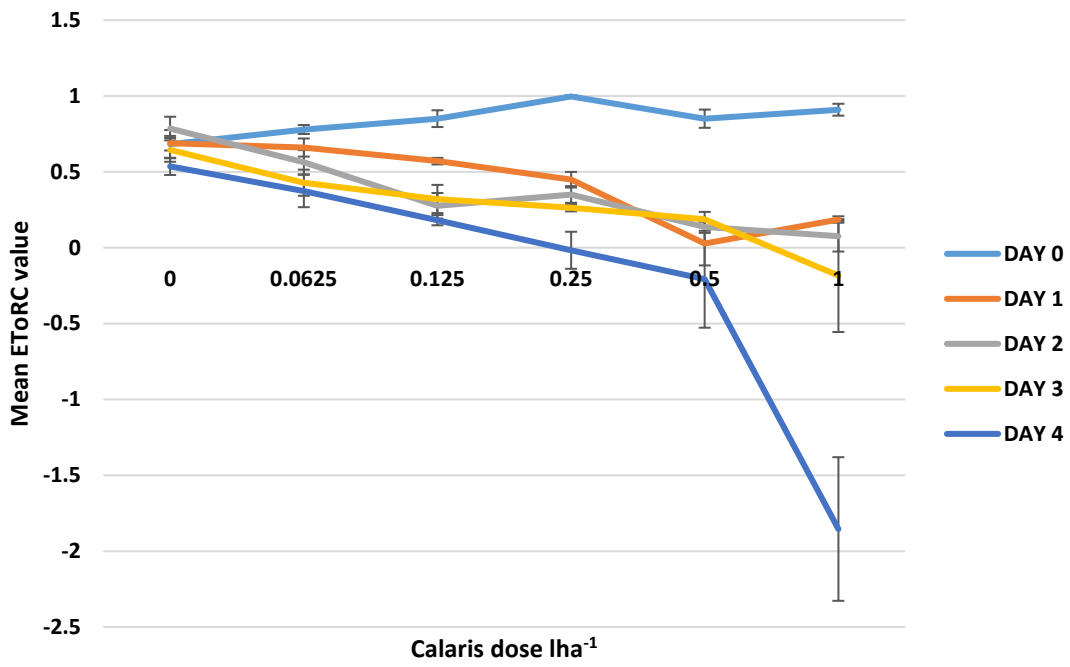
(d)
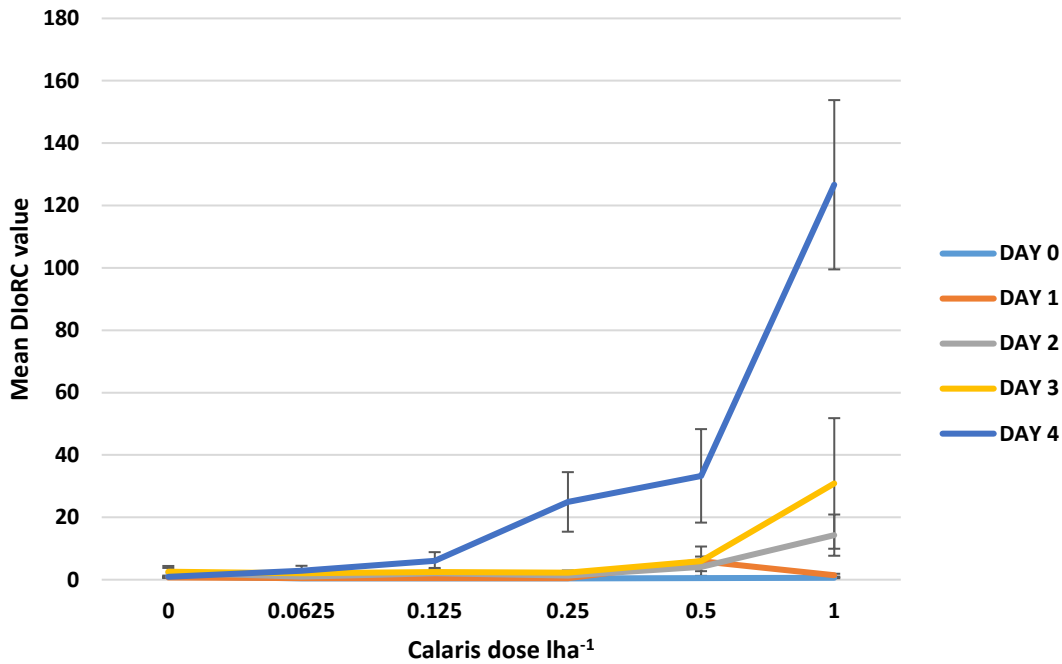
(e)

Figure 11 (a) mean Fv.Fm, (b) mean Abs.RC values, (c) mean DIoRC values, (d) mean EToRC values, and (e) mean DIoRC values in Chenopodium album in response to dosage of Calaris® and day post-herbicide application. Day 0 values correspond to values pre-treatment. Error bars represent ± SEM, n=8. Data analysed using two-way ANOVA, Tukey's test and T-Tests.

Figure 11 OJIP values in *Chenopodium album* Calaris® treated plants are slightly different from Calaris® treated *Sinapis arvensis*. Fv.Fm in *Chenopodium album* declines less rapidly from 0.0625lha^{-1} Calaris® for all days post-treatment compared to *Sinapis arvensis* and Fv.Fm values only drop below 0.1 on Day 4 post-treatment at 1lha^{-1} compared to 0.125lha^{-1} on Day 4 post-treatment in *Sinapis arvensis*.

Abs.RC values remain very similar to the control for Days 0 to 3 across all doses until 0.5lha^{-1} where values diverge and Day 3 is significantly different (P<0.001) day 0 to 2 to post-treatment values at a dose of 1.0lha^{-1}. Day 4 post-treatment values are significantly increased to all other measurement days from 0.25lha^{-1} (P<0.001). Abs.RC and DIoRC values show a high similarity in data patterns.

TRoRC values for Calaris® treated *Chenopodium album* shows no relationship between days and doses, in concordance with *Sinapis arvensis* treated with Calaris®. In addition, the range of values for *Sinapis arvensis* and *Chenopodium album* treated with Calaris® from

0.0lha^{-1} to 1.0lha^{-1} show a similar range from Day 0 to day 4 post treatment. As expected due to the mode of action of Calaris®, EToRC values for *Chenopodium album* decline, but less rapidly than for *Sinapis arvensis*.

3.4.3 OJIP analysis for pre and post Sencorex Flow®- treated *Sinapis arvensis*
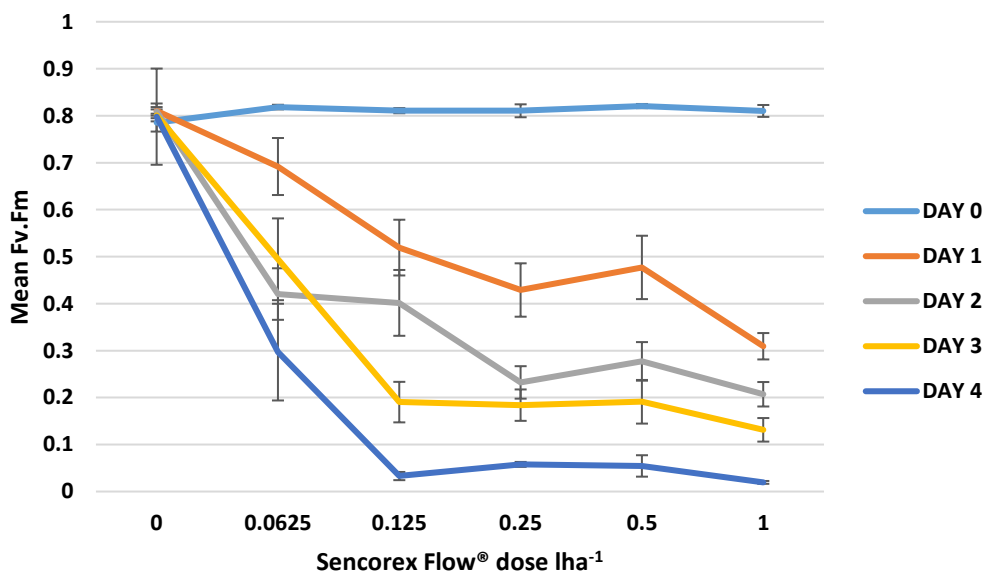
(a)
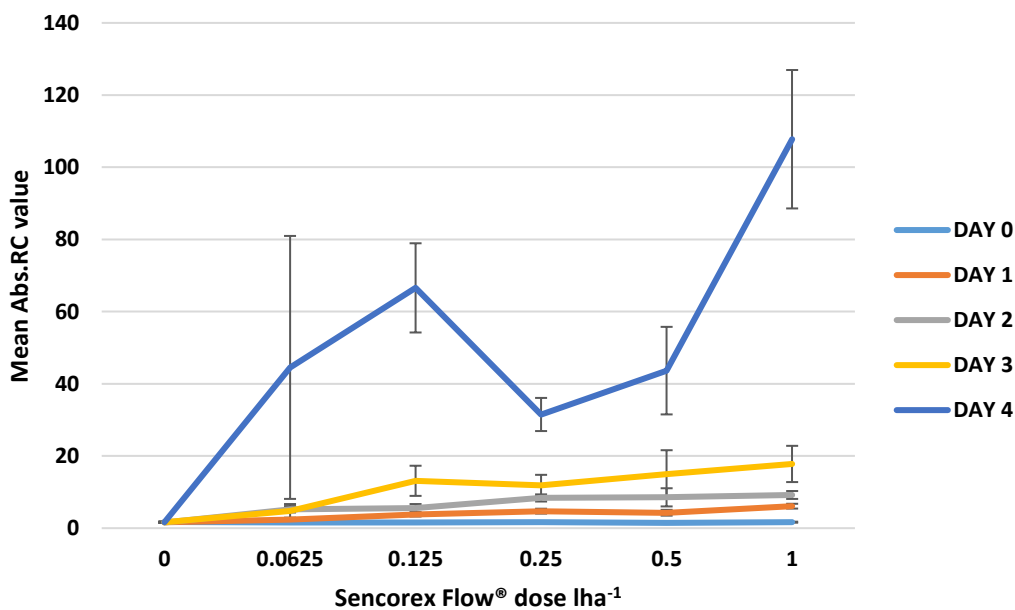
(b)
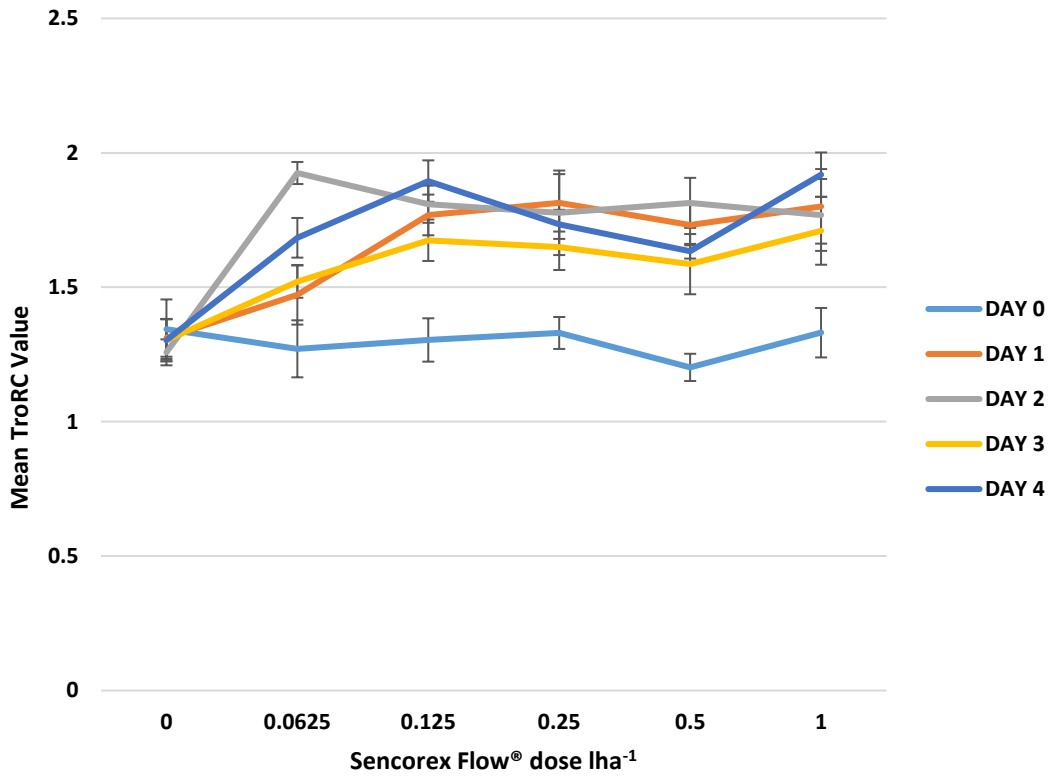
(c)
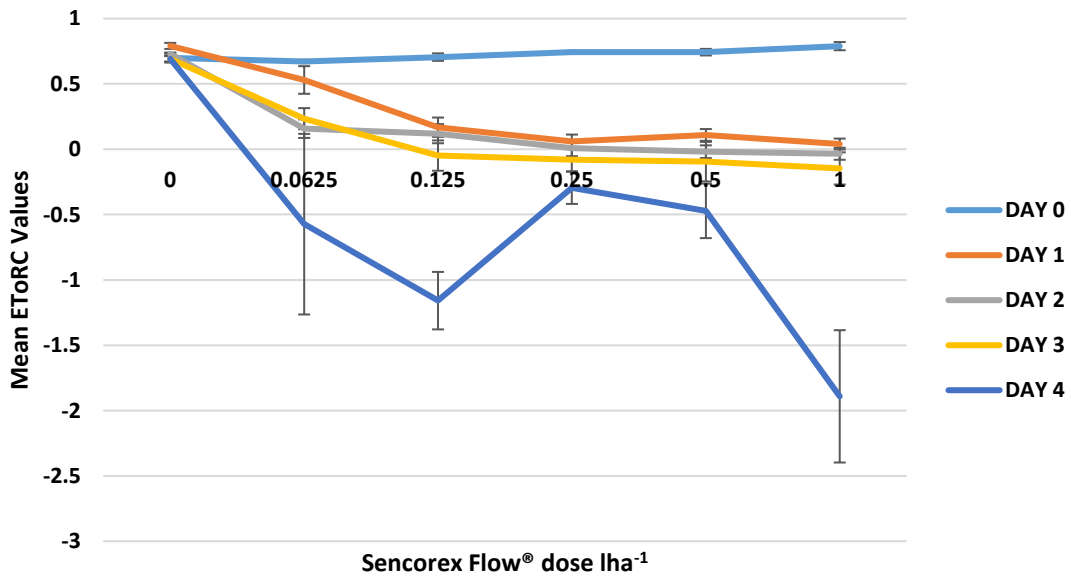
(d)
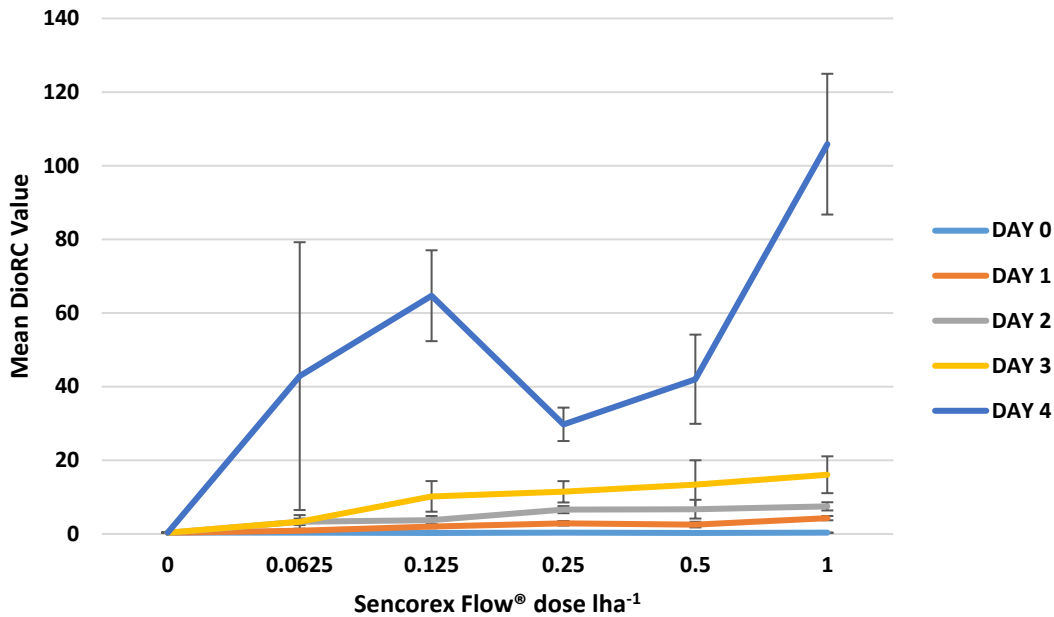
(e)

Figure 12 (a) mean Fv.Fm, (b) mean Abs.RC values, (c) mean DIoRC values, (d) mean EToRC values, and (e) mean DIoRC values in Sinapis arvensis in response to dosage of Sencorex Flow® and day post-herbicide application. Day 0 values correspond to values pre-treatment. Error bars represent ± SEM, n=8. Data analysed using two-way ANOVA, Tukey's test and T-Tests.

As with Calaris® treated *Sinapis arvensis* and *Chenopodium album*, Sencorex Flow® treatment causes a rapid decline in Fv.Fm values in *Sinapis arvensis*, with values on day 4 from $0.0125lha^{-1}$ to $1.0lha^{-1}$ falling below 0.1, highlighting a marked deterioration in overall photosynthetic capability. The Fv.Fm values for day 0 (pre Sencorex Flow® treatment) are consistently above 0.8 meaning plants were in a normal working photosynthetic state before treatment.

As with Calaris® treatment, Abs.RC values are consistently low for days 0 to 3 and only showing a moderate increase with increasing Sencorex Flow® dose. Day 4 shows a dramatic increase in Abs.RC from $0.0625lha^{-1}$ with an unexpected sudden decline between $0.125lha^{-1}$ and $0.5lha^{-1}$. In concordance with results from Calaris® treated *Chenopodium album* and *Sinapis arvensis*, Sencorex Flow® treated *Sinapis arvensis* Abs.RC and DIoRC values show a high similarity across herbicide doses and days post-treatment with the decline in Abs.RC replicated in DIoRC values. TRoRC values are in a similar range to Calaris® treated *Sinapis arvensis* and *Chenopodium album* with no clear finding, the only clear difference being day 0 TRoRC values are significantly (P<0.001) and consistently

lower from 0.0625lha^{-1} onwards compared to days 1 to 4 post treatment. As expected due to the active ingredients of Sencorex Flow® (detailed on page 44) EToRC declines after Sencorex Flow® treatment with day 4 showing a marked decline. Day 4 readings display an unexpected increase in value between 0.125lha^{-1} and 0.5lha^{-1} which inversely mimics Abs.RC and DIoRC.

3.4.4 OJIP analysis for pre and post Sencorex Flow- treated *Chenopodium album*
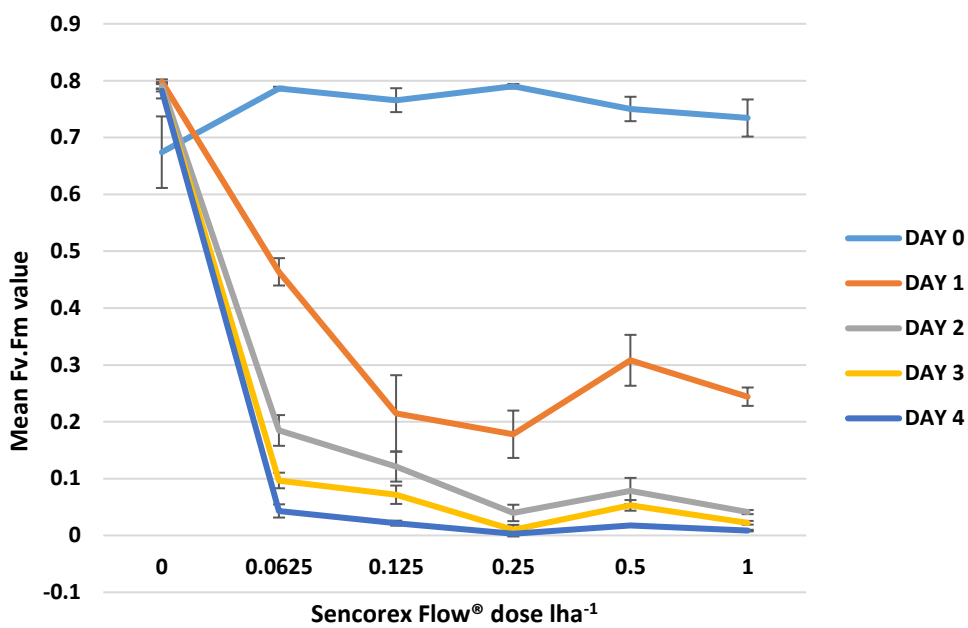
(a)
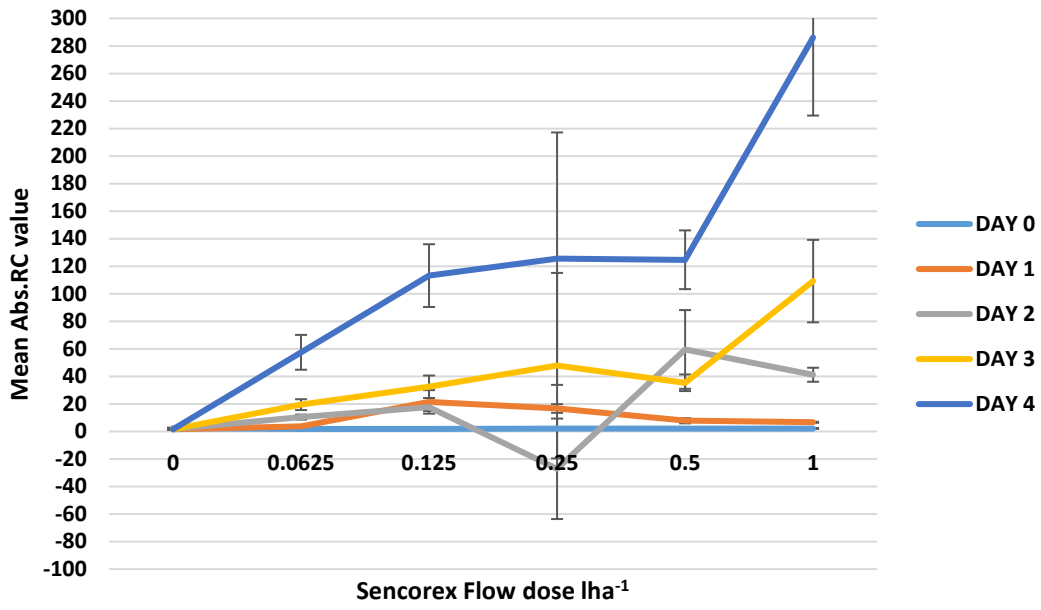
(b)
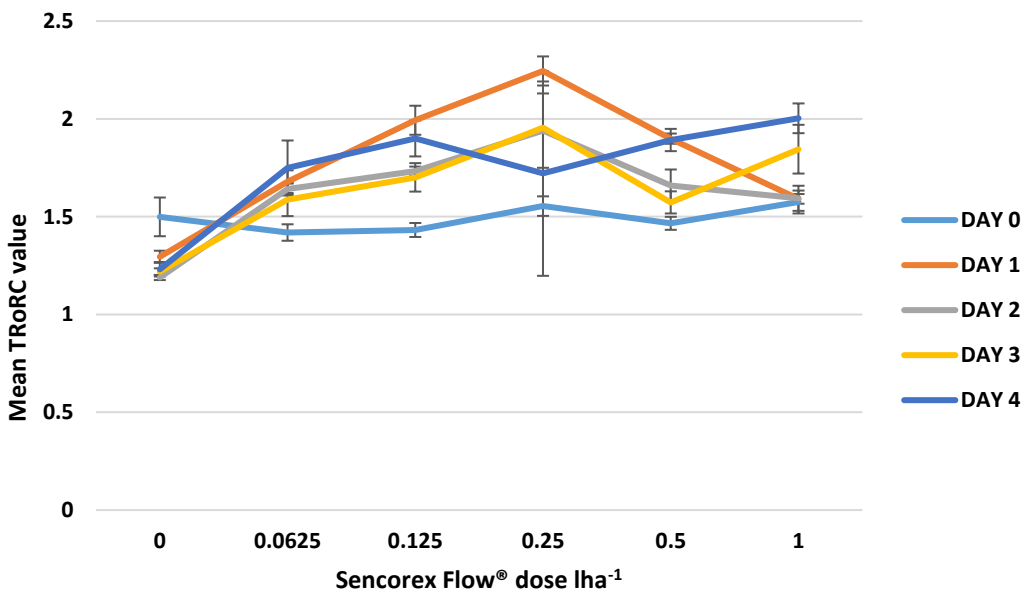
(c)
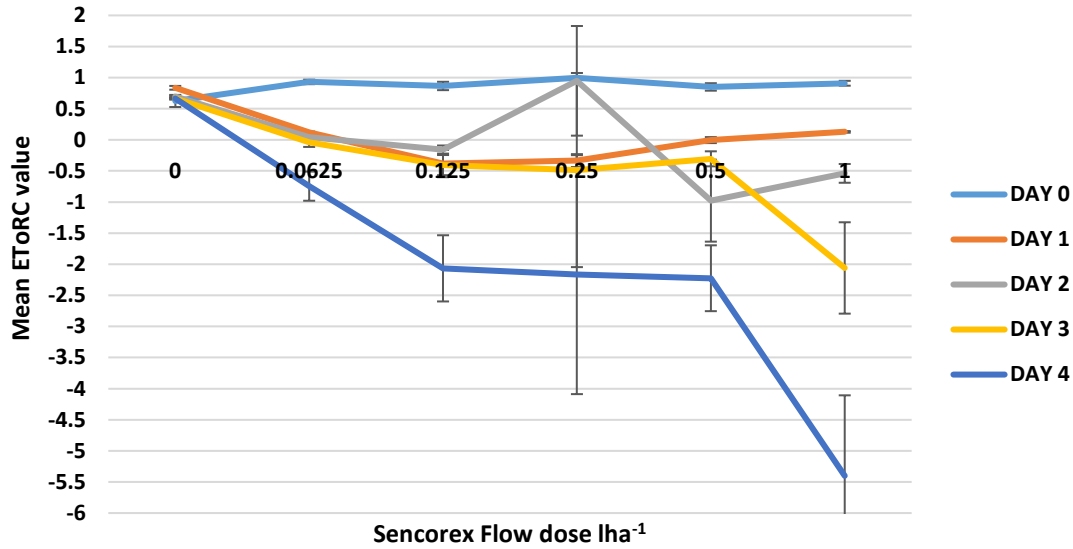
(d)
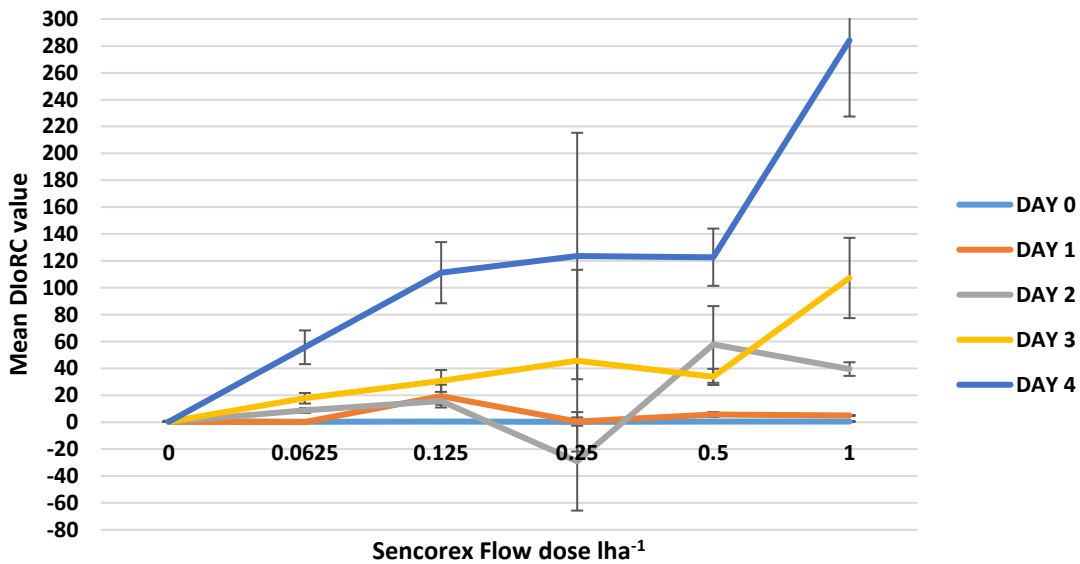
(e)

Figure 13 (a) mean Fv.Fm, (b) mean Abs.RC values, (c) mean DIoRC values, (d) mean EToRC values, and (e) mean DIoRC values in Chenopodium album in response to dosage of Sencorex Flow® and day post-herbicide application. Day 0 values correspond to values pre-treatment. Error bars represent ± SEM, n=8. Data analysed using two-way ANOVA, Tukey's test and T-Tests.

The decline in Fv.Fm values for Sencorex Flow® treated *Chenopodium album* could be predicted due to the mode of action of Sencorex Flow® (as detailed on page 44) and a similar response is evident in Sencorex Flow®-treated *Sinapis arvensis.* As with Abs.RC

and DIoRC values in Sencorex Flow®-treated *Sinapis arvensis* and Calaris® treated *Chenopodium album* and *Sinapis arvensis*, in Sencorex Flow® treated *Chenopodium album* the relationship between Abs.RC and DIoRC are highly similar. TRoRC shows no obvious pattern in response and is similar to Figures 13 to 15. EToRC (Figure 13(d)) shows a decline in value on day 4 across all doses whilst day 1 to 3 show a less steep decline.

## 3.4.5 OJIP analysis for pre and post Nevada®-treated *Sinapis arvensis*
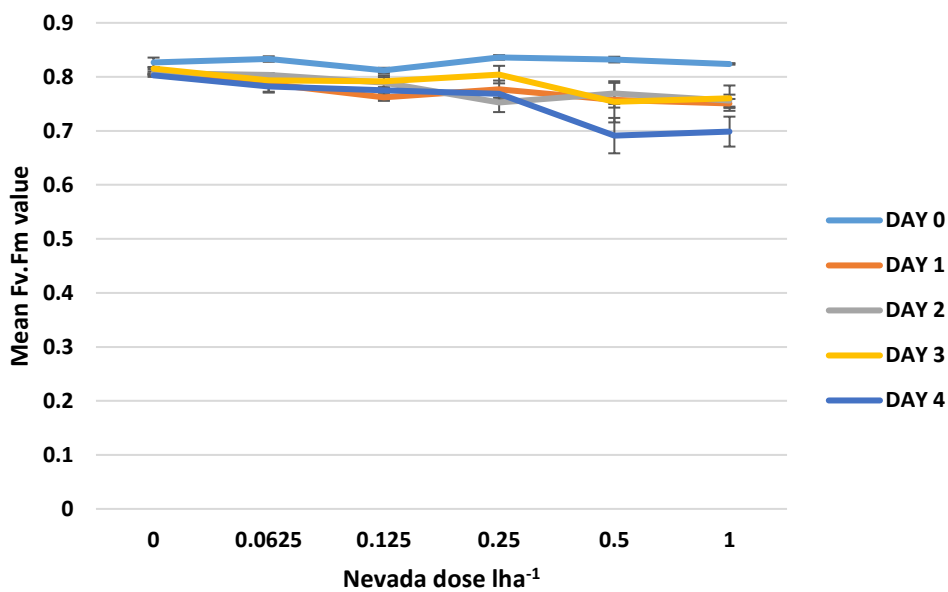
(a)
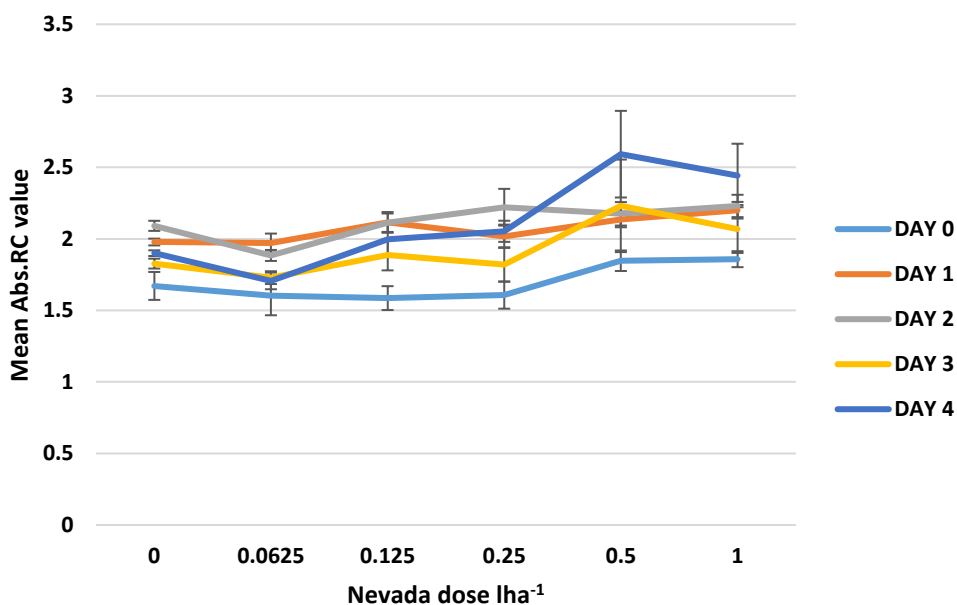
(b)
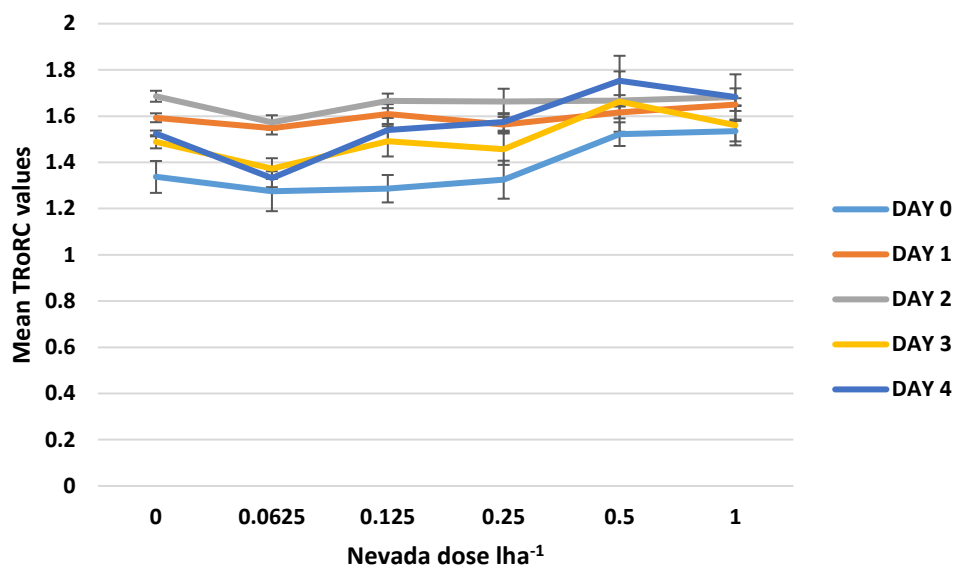
(c)
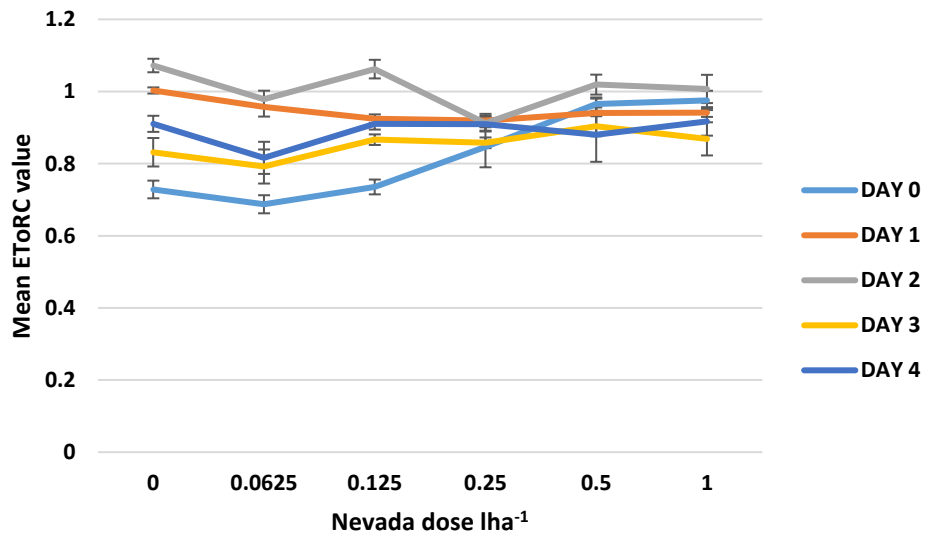
(d)
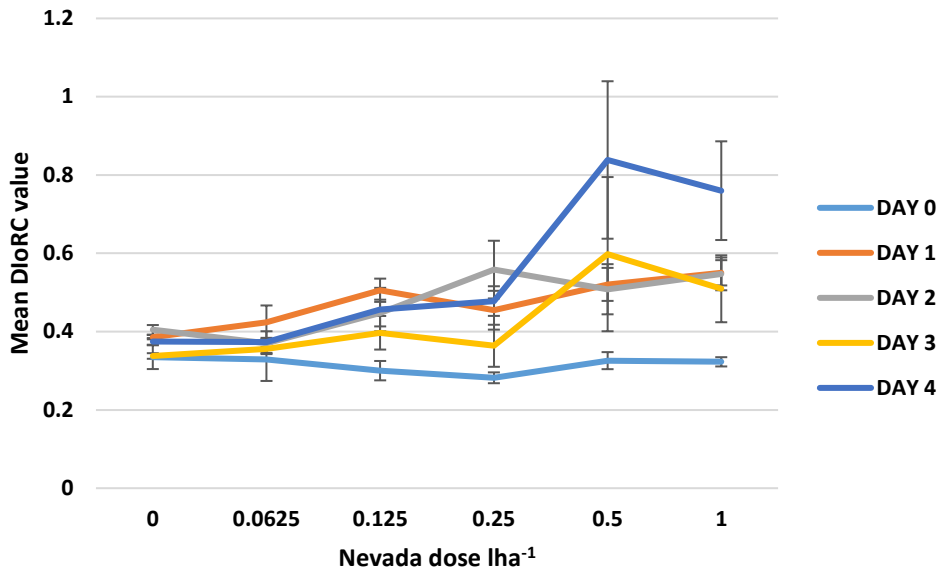
(e)

Figure 14 (a) mean Fv.Fm, (b) mean Abs.RC values, (c) mean DIoRC values, (d) mean EToRC values, and (e) mean DIoRC values in Sinapis arvensis in response to dosage of Nevada® and day post-herbicide application. Day 0 values correspond to values pre-treatment. Error bars represent ± SEM, n=8. Data analysed using two-way ANOVA, Tukey's test and T-Tests, where T-Tests were conducted between data points which were not clearly significantly different from error bars or ANOVA.

The OJIP parameter values shown in Figure 14 for Nevada® treated *Sinapis arvensis* are in contrast to Calaris® and Sencorex Flow®-treated plants. Fv.Fm values show little or no decline over Nevada® doses and over days post-treatment showing minimal effect on the photosynthetic apparatus. Abs.RC data do show increases in values compared to Day 0 data but few data points are significantly increased compared to Day 0 with only 0.5lha^{-1} and 1.0lha^{-1} producing a P Value <0.001 on Day 4 post-treatment. Calaris® and Sencorex Flow®-treated plants, the Abs.RC graphs mimic the response in DIoRC values. In this case (Nevada® treatment) the DIoRC graph is more pronounced than Abs.RC and careful observation of days post-treatment reveals responses are consistent in both parameters.

TRoRC shows a minimal but not significant increase in values across doses and days post-treatment and EToRC shows no significant difference between doses and days, even for 1.0lha^{-1} on day 4 compared to control values.

3.4.6 OJIP analysis for pre and post Nevada®-treated *Chenopodium album*
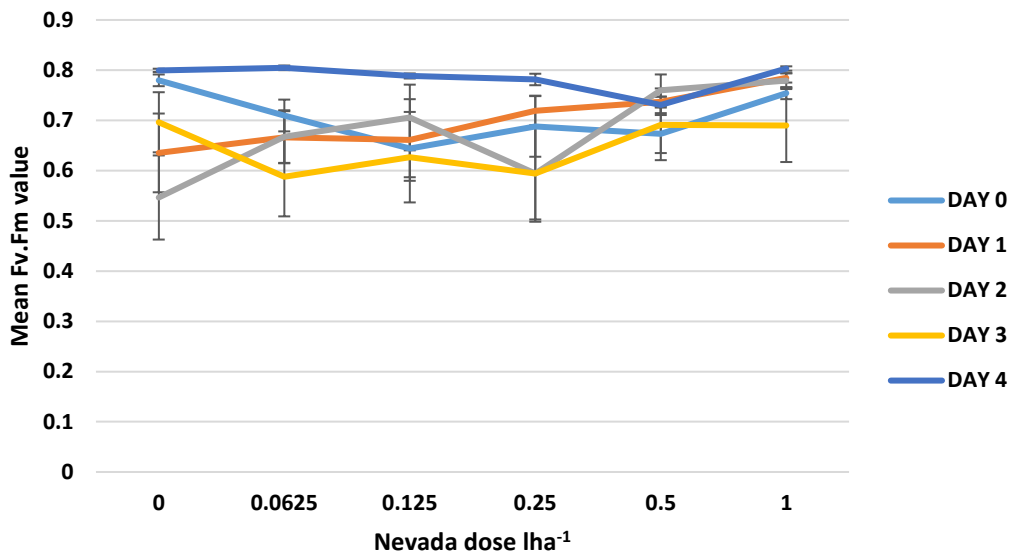
(a)
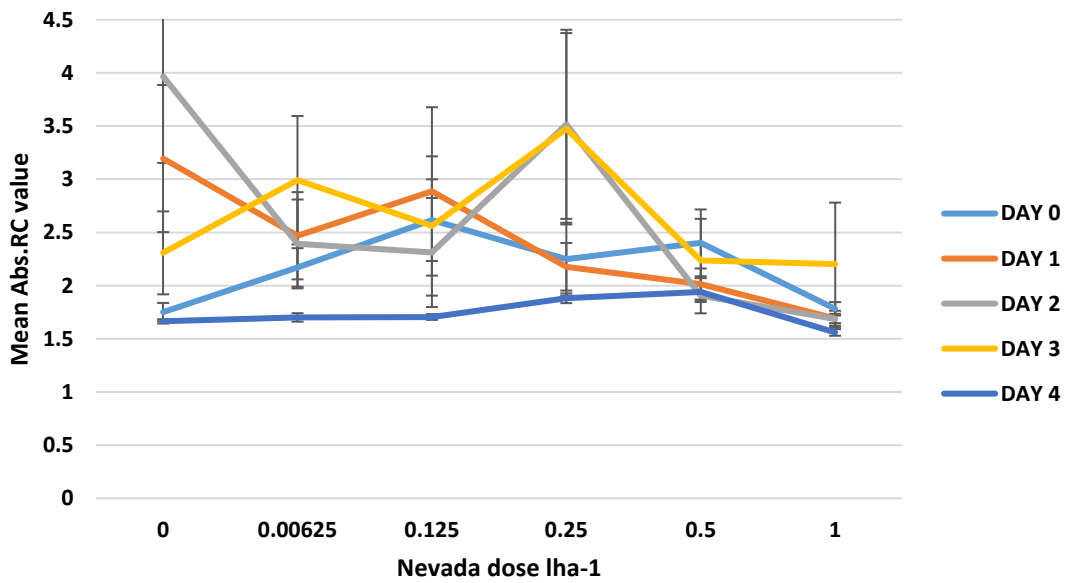
(b)
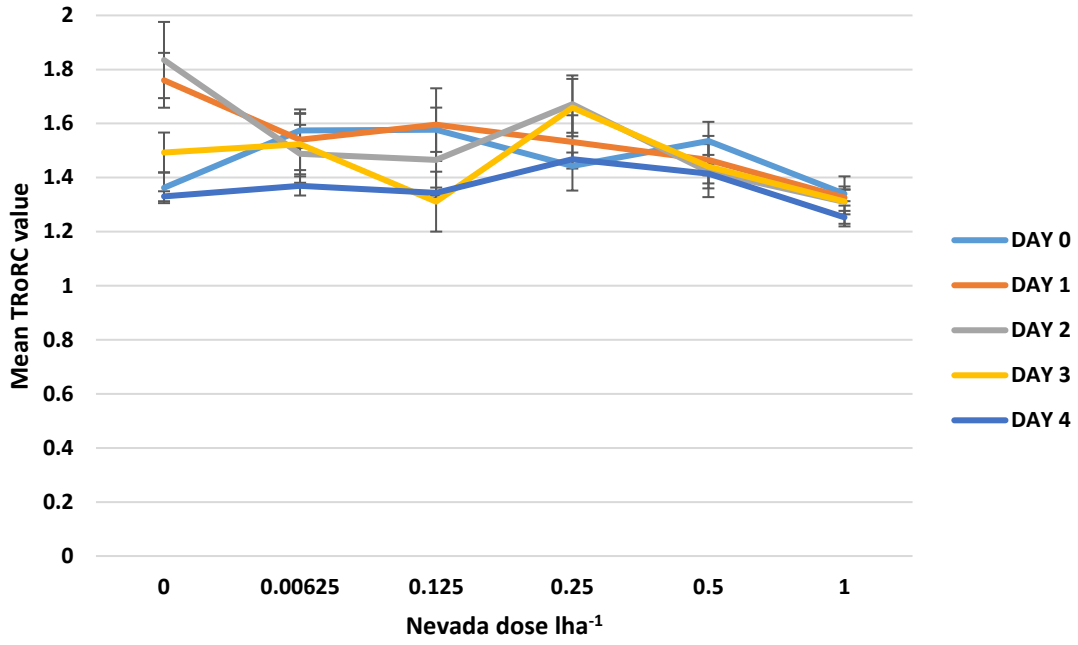
(c)
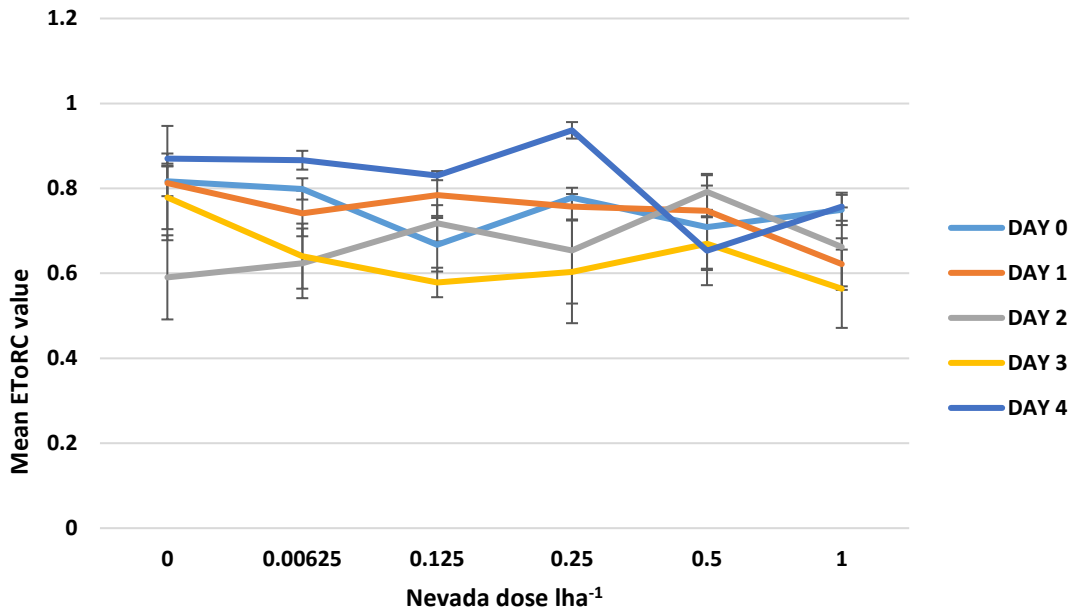
(d)
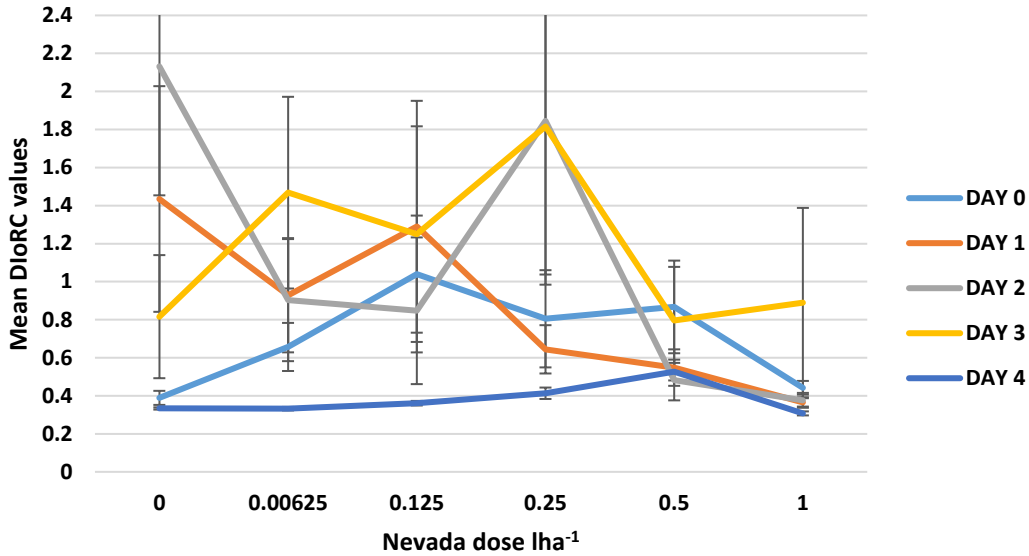
(e)

Figure 15 (a) mean Fv.Fm, (b) mean Abs.RC values, (c) mean DIoRC values, (d) mean EToRC values, and (e) mean DIoRC values in Chenopodium album in response to dosage of Nevada® and day post-herbicide application. Day 0 values correspond to values pre-treatment. Error bars represent ± SEM, n=8. Data analysed using two-way ANOVA, Tukey's test and T-Tests, where T-Tests were conducted between data points which were not clearly significantly different from error bars or ANOVA.

Figure 15 (a) shows the lack of clear outcome in Fv.Fm values for *Chenopodium album* treated with Nevada®. There are values above and below the Day 0 line. The only conclusion which can be drawn from the Fv.Fm data is that Nevada® does not have any influence on the Fv.Fm parameter, and so little if any effect on the photosynthetic apparatus.

The Abs.RC and DIoRC graphs are similar in terms of response, as is the case with Calaris® and Sencorex Flow® treatments, but show a greater range of values compared to Nevada® treated *Sinapis arvensis*. TRoRC shows slight decline in values. Day 1 dose 0lha^{-1} is significantly greater than Day 1 dose 1.0lha^{-1} with a significance value of P=0.007. Similarly, Day 2 shows a significant decline between dose 0lha^{-1} and 1.0lha^{-1} with P=0.012. As expected, Nevada® treatment does not cause a decline in EToRC in *Chenopodium album* due to the mode of action of Nevada®.

3.4.7 Preliminary conclusions from OJIP parameter readings

Determining which herbicide dose to focus on when combining chemical treatment with 680nm LASER treatment is achieved by assessing significant reductions or increases in parameter data compared to the untreated plant values. Day 1 post-treatment will be the chosen day to minimise further variables and to allow for additional changes in parameter values upon 680nm LASER application. The dose of herbicide used cannot be uniform across the three herbicide treatments or plant subjects as each herbicide contains different active ingredients and plant species respond in different ways, as Figures 10 to 15 demonstrate. Tables 2(a) to 2(e) present parameter data where a red box indicates a significant reduction (threshold criteria of $P<0.05$) in parameter values compared to the control and a green box denotes a significant increase in parameter value to the control. Blank boxes denote no significant change from the control. Apart from Nevada® treatments where only TRoRC values for *Chenopodium album* treated with 1.0lha^{-1} are significant, the criteria for dose selection is preferably a significant decline in both Fv.Fm and EToRC compared to the control. EToRC is an important parameter to give weight to as a reduction in EToRC implies a decline in the photosynthetic ETC rate which is a crucial consideration in this project as a whole (detailed on page 38).   In the case of *Chenopodium album* treated with Calaris®, only EToRC values for doses 1.0lha^{-1} and 0.5lha^{-1} show significance, therefore the lowest dose with an effect will be used, 0.5lha^{-1}.

Table 4 Red boxes denote a significant decrease in OJIP parameter value compared to the control, while green boxes denote significant increases in OJIP parameter values compared to the control (0.0lha^{-1}). Blank boxes denote no significant change from the control. SA- *Sinapis arvensis*, CA-*Chenopodium album*, SF- Sencorex Flow®, CAL- Calaris®, NEV - Nevada®, T+1- 24 hours post herbicide treatment.

SA SF T+1	Fv.Fm	Abs.RC	TRoRC	EToRC	DIoRC
1.0lha^{-1}	red	green	green	red	green
0.5lha^{-1}	red	green		red	
0.25lha^{-1}	red	green	green	red	green
0.125lha^{-1}	red		green	red	
0.0625lha^{-1}					
0.0lha^{-1}					

(a)

CA SF T+1	Fv.Fm	Abs.RC	TRoRC	EToRC	DIoRC
1.0lha^{-1}	red		green	red	
0.5lha^{-1}	red		green	red	
0.25lha^{-1}	red		green	red	
0.125lha^{-1}	red	green	green	red	green
0.0625lha^{-1}	red		green	red	
0.0lha^{-1}					

(b)

SA CAL T+1	Fv.Fm	Abs.RC	TRoRC	EToRC	DIoRC
1.0lha^{-1}	red	green		red	green
0.5lha^{-1}	red	green		red	green
0.25lha^{-1}	red			red	
0.125lha^{-1}				red	
0.0625lha^{-1}				red	
0.0lha^{-1}					

(c)

CA CAL T+1	Fv.Fm	Abs.RC	TRoRC	EToRC	DIoRC
1.0lha^{-1}				red	
0.5lha^{-1}				red	
0.25lha^{-1}					
0.125lha^{-1}					
0.0625lha^{-1}					
0.0lha^{-1}					

(d)

SA NEV T+1	Fv.Fm	Abs.RC	TRoRC	EToRC	DIoRC
1.0lha^{-1}					
0.5lha^{-1}					
0.25lha^{-1}					
0.125lha^{-1}					
0.0625lha^{-1}					
0.0lha^{-1}					

(e)

CA NEV T+1	Fv.Fm	Abs.RC	TRoRC	EToRC	DIoRC
1.0lha^{-1}			red		
0.5lha^{-1}					
0.25lha^{-1}					
0.125lha^{-1}					
0.0625lha^{-1}					
0.0lha^{-1}					

(f)

From Table 4 the main observation is the significant increase in Abs.RC values for herbicide treated samples compared to the control samples (P<0.001 for both *Chenopodium album* and *Sinapis arvensis* treated with Calaris® and Sencorex Flow®). This is not the case for Nevada® treated plants and in the case of *Chenopodium album* and *Sinapis arvensis* treated with Nevada®, the control Abs.RC value is significantly greater (P<0.001) than the treated samples.

Other clear responses include the reduction in EToRC value compared to the control for *Chenopodium album* and *Sinapis arvensis* treated with either Calaris® or Sencorex Flow® (P<0.001 for all aforementioned samples) and the increase in dissipation for Calaris® and Sencorex Flow® treated *Chenopodium album* and *Sinapis arvensis*. Calaris® treated *Chenopodium album* shows markedly greater Abs.RC and DIoRC values, 7.5 and 5.9, respectively, than any other treatment and plant type, but the Calaris® dose applied is greater (dose 0.5lha^{-1}). Calaris® treated *Sinapis arvensis* has much lower values than Calaris® treated *Chenopodium album* with less dramatic increases in Abs.RC and DIoRC compared to the untreated plants. This again, is more than likely due to the higher dose of Calaris® used in *Chenopodium album* (dose of 0.5lha^{-1}) compared to the dose of 0.25lha^{-1} in *Sinapis arvensis* (0.25lha^{-1}).

The parameter data for Sencorex Flow® treated *Chenopodium album* and *Sinapis arvensis* are remarkably similar in terms of parameter values even after treatment with a of dose 0.125lha^{-1} in *Sinapis arvensis* and 0.0625lha^{-1} in *Chenopodium album*. The discrepancy in Sencorex Flow® dose appears not to have affected the parameter values. Doses 0.125lha^{-1} and 0.0625lha^{-1} are the two lowest doses used throughout this study. Such a small increase in concentration from dose 0.0625lha^{-1} to 0.125lha^{-1} might not have had a significant effect on the plants. Such similar values for all parameters would not have been expected, especially between two plant species.

Trapping values, denoted by the OJIP parameter TRoRC are also changeable. Sencorex Flow® treated *Sinapis arvensis* and *Chenopodium album* both have P values of <0.001 between treated and control sample TRoRC values, with chemical treatment yielding the greater values. The only other treatment to result in a significant TRoRC value is Nevada® treated *Chenopodium album* where trapping in treated samples is significantly lower than in untreated (P<0.007), a reverse finding to all other treatments.

3.5 Percentage relative conductivity response to herbicide treatment

3.5.1 Percentage relative conductivity post Calaris® treatment
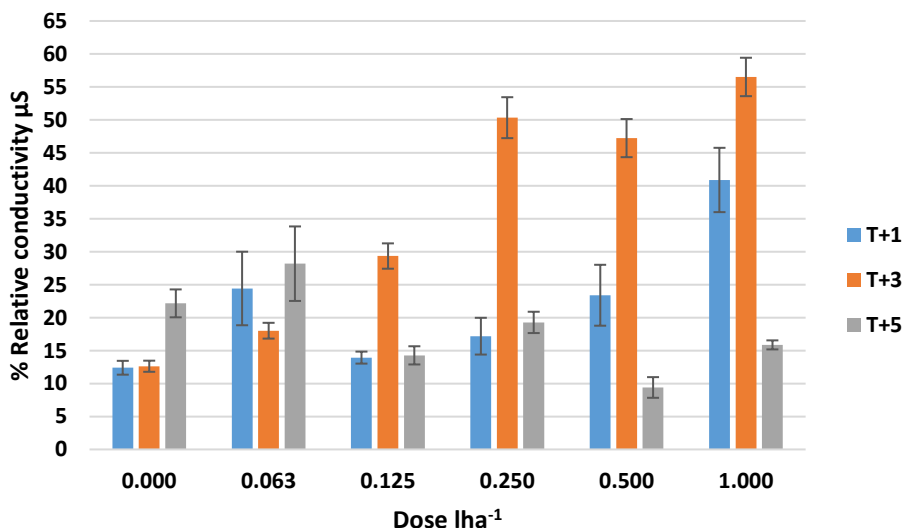
(a)
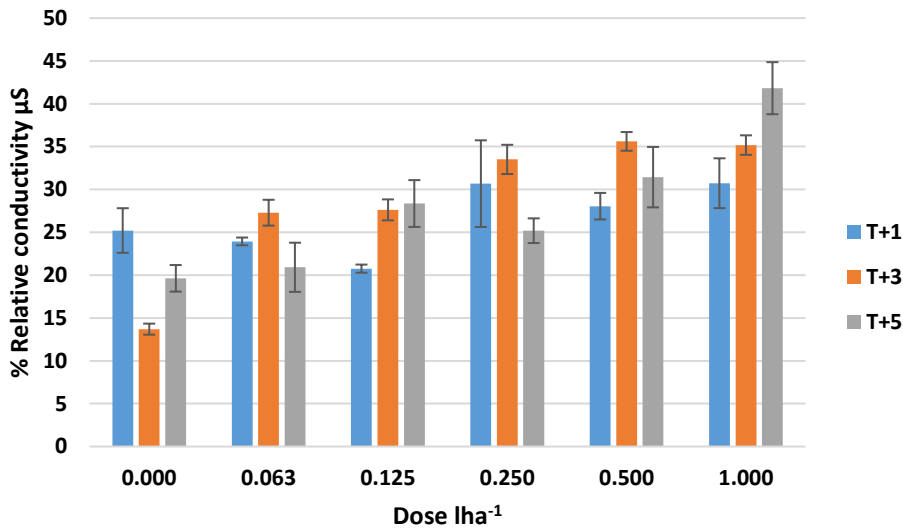
(b)

Figure 16 (a) – Percentage (%) relative conductivity for Sinapis arvensis treated with Calaris® (b) Percentage relative conductivity for Chenopodium album treated with Calaris®. T+1 denotes reading taken 24 hours post Calaris® treatment, T+3 denotes reading taken 72 hours post Calaris® treatment, T+5 denotes reading taken 120 hours post Calaris® treatment. Calaris® dose in litres per hectare. Error bars denotes ±SEM, n=8. Data analysed using two-way ANOVA, Tukey's test and T-Tests.

Percentage relative conductivity is a quantitative representation of the electrolyte leakage from plant cells post treatment. It is widely accepted (Jambunathan, 2010, Leopold et al., 1981, Demidchik et al., 2014) that higher levels of electrolyte leakage correlate with plant stress or damage. Figures 16(a) and 6(b) show an increasing % relative conductivity µS from doses 0.0lha^{-1} to 1.0lha^{-1} with 1.0lha^{-1} Calaris® treatment leading to the greater % relative conductivity values. There is a range of values produced in *Sinapis arvensis* data where Day 3 appears to yield the greatest % relative conductivity readings. *Sinapis arvensis* is likely to contain more water than *Chenopodium album* which might account for the higher readings on Day 3 for doses 0.25lha^{-1} to 1.0lha^{-1} and such Day 3 readings are significantly different to Day 1 readings of the same doses ($P<0.001$). The data could also suggest that *Sinapis arvensis* is repairing leaky membranes between Days 3 and 5. *Chenopodium album* demonstrates greater robustness to Calaris® treatment from the lower % relative conductivity readings, especially on Day 3, which may indicate differences in biochemical responses between the species.

3.5.2 Percentage relative conductivity post Sencorex Flow® treatment
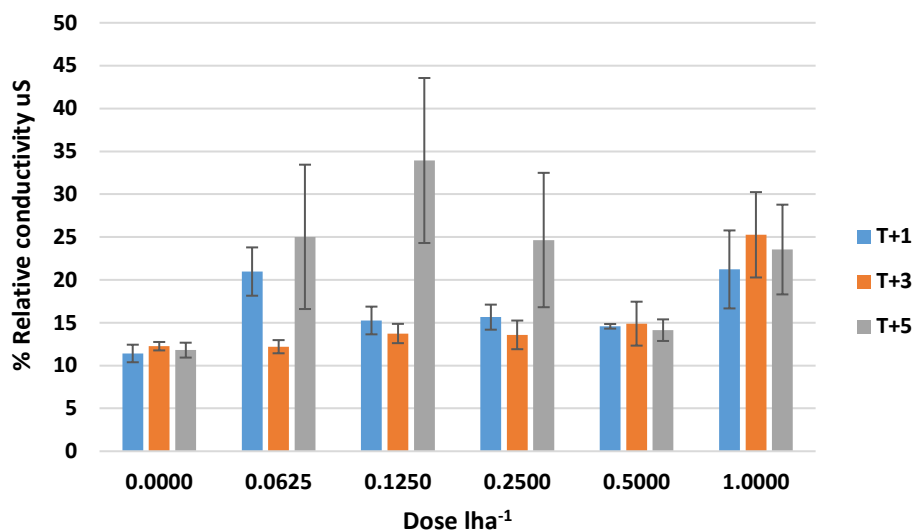
(a)
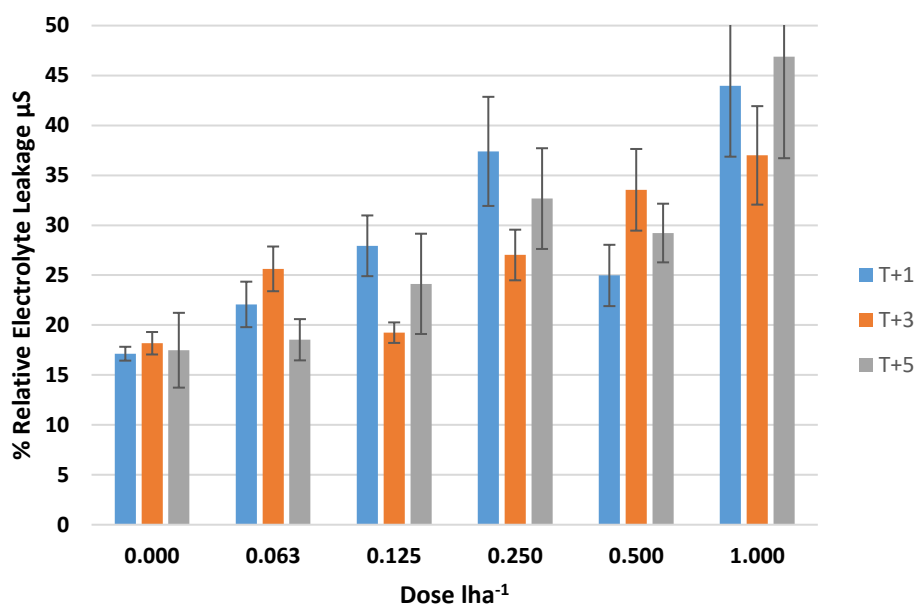
(b)

Figure 17 (a) – Percentage (%) relative conductivity for Sinapis arvensis treated with Sencorex Flow®
(b) Percentage relative conductivity for Chenopodium album treated with Sencorex Flow®®.   T+1
denotes reading taken 24 hours post Sencorex Flow® treatment, T+3 denotes reading taken 72 hours
post Sencorex Flow® treatment, T+5 denotes reading taken 120 hours post Sencorex Flow®
treatment. Sencorex Flow® dose in litres per hectare. Error bars denotes ±SEM, n=8 Data analysed
using two-way ANOVA, Tukey's test and T-Tests.

Figures 17 (a) and (b) shows an increasing *Chenopodium album* % relative conductivity μS values when treated with Sencorex Flow® with 1.0lha^{-1} yielding the greatest % relative conductivity readings out of all other doses. The readings between the two plants species are in a similar range. The greatest % relative conductivity reading for *Sinapis arvensis* is for Day 5 post-treatment treated with Sencorex Flow® at a dose of 0.125lha^{-1} with a P value of 0.001 against the other measurement days for that herbicide dose.

3.5.3 Percentage relative conductivity post Nevada® treatment
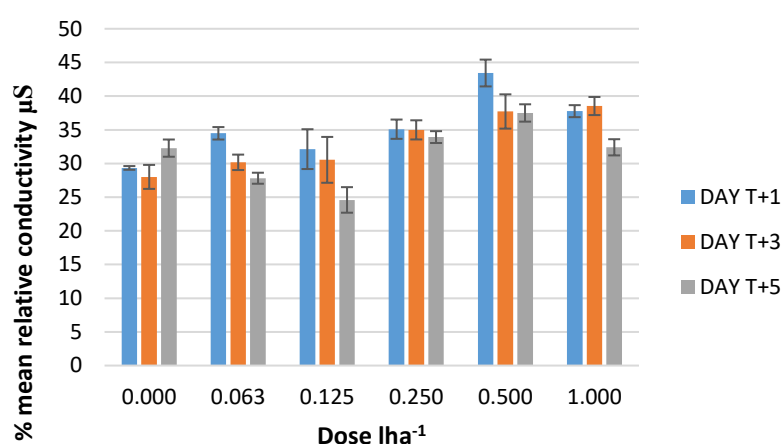
(a)
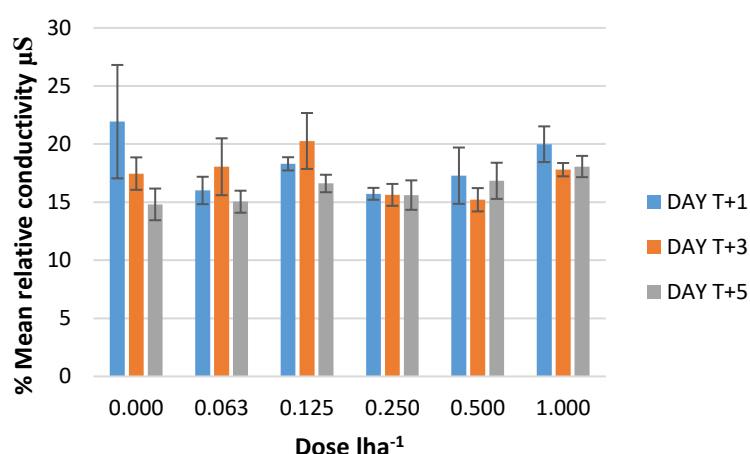
(b)

Figure 18 (a) – Percentage (%) relative conductivity for Sinapis arvensis treated with Nevada® (b)
Percentage relative conductivity for Chenopodium album treated with Nevada®. T+1 denotes

reading taken 24 hours post Nevada® treatment, T+3 denotes reading taken 72 hours post Nevada® treatment, T+5 denotes reading taken 120 hours post Nevada® treatment. Nevada® dose in litres per hectare. Error bars denotes ±SEM, n=8. Data analysed using two-way ANOVA, Tukey's test and T-Tests, where error bars and ANOVA did not clearly show significant differences.

Figures 18 (a) and 10 (b) show no clear pattern with no critical significant differences between data points in either *Sinapis arvensis* or *Chenopodium album* % relative conductivity µS. The readings for *Sinapis arvensis* are generally considerably greater across all herbicide doses than *for Chenopodium album* which could be due to the increased water content of the leaves in *Sinapis arvensis*.

The % relative conductivity values for 0.0lha^{-1} treated plants are higher in the Nevada® treatment cohort compared to the Calaris® and Sencorex Flow® groups. These values should be the same across the study. This suggests there was a difference in growing conditions, e.g., a greater incident light intensity entering the glasshouse, as experimental procedure was consistent.

3.6 SOD units per mg total protein content in herbicide treated plants
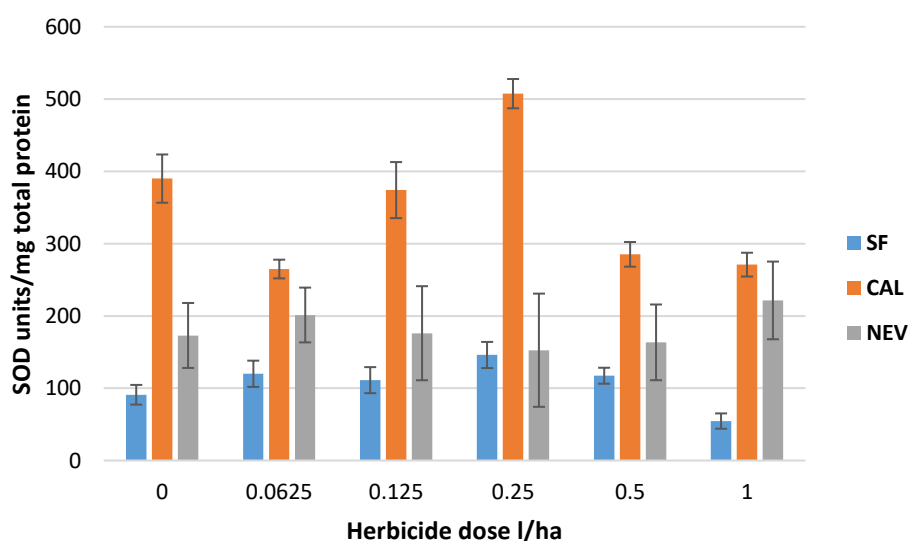
(a)
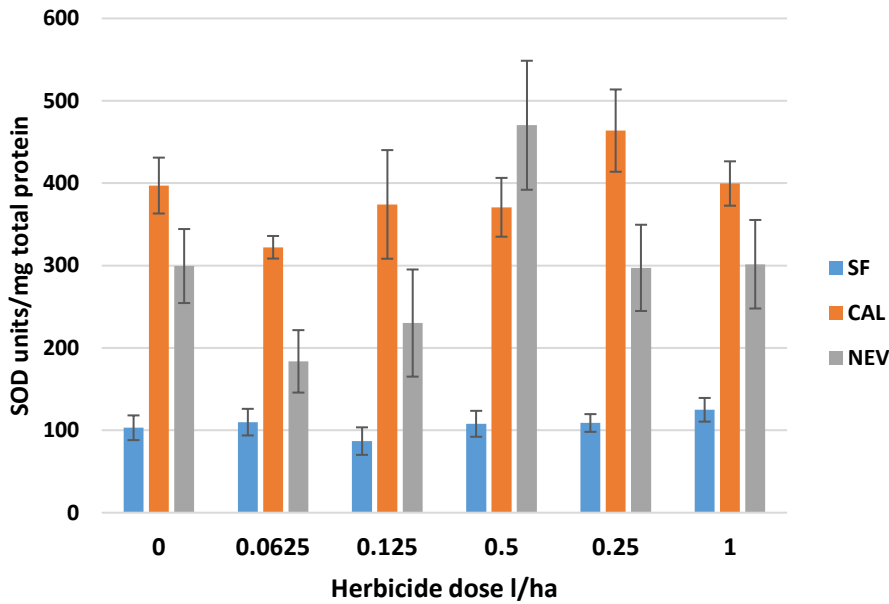
(b)

Figure 19 (a) SOD units/mg total protein in herbicide treated Sinapis arvensis samples, (b) SOD units/mg total protein in herbicide treated Chenopodium album samples. SF – Sencorex Flow® treatment, CAL – Calaris® treatment, NEV – Nevada® treatment. Error bars denote ±SEM, n=10. Data analysed using two-way ANOVA, Tukey's test and T-Tests.

Calaris® treated *Sinapis arvensis* show the greater levels of SOD units/mg total protein compared to Sencorex Flow® and Nevada® treated *Sinapis arvensis* with significantly greater levels for dose $0.0lha^{-1}$, $0.125lha^{-1}$, $0.25lha^{-1}$ and $0.5lha^{-1}$. The fact that the control ($0.0\ lha^{-1}$) dose of Calaris® treated *Sinapis arvensis* is so markedly increased (Figure 19(a)) casts doubt in the validity of this assay as control samples of *Sinapis arvensis* should have similar levels of SOD across all control samples. The SOD levels for Sencorex Flow® and Nevada® treated *Sinapis arvensis* are similar for each herbicide dose with Nevada® application producing the most SOD compared to Sencorex Flow® consistently ($P<0.001$ for Calaris®-treated plants compared to Sencorex Flow®-treated plants for all herbicide doses).

Chenopodium album treated with Sencorex Flow® (Figure 19 (b)) show highly consistent readings of approximately 100 units/mg total protein across the dose range. Calaris® and Nevada® treated *Chenopodium album* show markedly increased SOD readings for each herbicide dose compared to Sencorex Flow®. Greater SOD units/mg total protein for Calaris® and Nevada® treatment compared to Sencorex Flow® treatment shows Calaris® and Nevada® treatment has more biochemical influence on *Chenopodium album* which led

to the production of SOD. But as with *Sinapis arvensis* SOD readings, the control readings are not consistent with the hypothesis that herbicide treatment would increase SOD levels. The control readings are not reliable as there is a vast range of data in these control samples, which in theory should not be the case.

3.7   Discussion

3.7.1 Increase in Abs.RC and DIoRC values with concurrent decline in EToRC

This chapter details the effect three different herbicides have on informative biochemical responses. Absorbance (Abs.RC) and dissipation (DIoRC) values show significant increases compared to dose of $0.0lha^{-1}$ when treated with Sencorex Flow® and Calaris® in *Sinapis arvensis* and *Chenopodium album* and this is more pronounced on Day 4 post-treatment. Concurrently, EToRC values at day 4 dramatically decline. This response is not witnessed in *Sinapis arvensis* and *Chenopodium album* treated with Nevada®. The most likely explanation for this dramatic increase in Abs.RC and DIoRC values is related to the ECT inhibitory effect of the herbicide. As detailed on pages 43-44, Calaris® and Sencorex Flow® contain photosynthetic ETC inhibitors, terbuthylazine in Calaris® and metribuzin in Sencorex Flow®. As the ETC rate is dramatically reduced, markedly so on day 4 post treatment, the plant is failing to keep the rate of photosynthesis in the normal range. As an attempt to rectify the decline in ETC rate, the plant is likely to up-regulate LHCII polypeptides and increases chlorophyll *a* accumulation (Chalifour et al., 2014, Wilson and Huner, 2000). The aforementioned work by Chalifour et al., 2014 and Wilson and Huner, 2000, was conducted in photosynthetic algae, but it has been shown that light deprived rice plants contain greater chlorophyll levels (Zhu. P, 2008, Tian et al., 2017). A recent study conducted by Ceusters et al. (2019) observed an increase in Abs.RC values in plants suffering drought stress. This team concluded that the increase in Abs.RC was due to the inactivation of some PSII RCs (Abs.RC ratio = total number of photons absorbed by Chl molecules in all RC's / total number of active RCs) and increase in antenna size was deemed less likely to cause the increased Abs.RC values due to a lack of significance between the content of photosynthetic pigments between treatments (Ceusters et al., 2019). This is contrary to the findings by Gomes et al. (2012) and van Heerden et al. (2007) who state that increasing antenna size, thus increasing Abs.RC acts as a compensatory

mechanism with an aim of normalising the EToRC levels. This study was also conducted on drought stressed plants.

The studies mentioned focus on drought stress which is likely to affect the electron transport chain through a similar mechanism (Wang et al., 2018) and could aid finding similarities and explanations for the increase in Abs.RC correlated with a decline in EToRC. It is not impossible that the increase in Abs.RC is due to a combination of the two factors highlighted in the Ceusters et al. (2019) study. To solidify this theory, the leaf content of chlorophyll should be determined in future work by extracting plant pigments by immersing leaf material in N,N-dimethylformamide (DMFA) at room temperature for 72 h in darkness. The supernatant can then be used to determine absorbance at 647 nm (A_{647}) and 664 nm (A_{664}) (Ceusters et al., 2019).

DIoRC follows an almost identical graphical response pattern to Abs.RC as absorbed energy cannot be funneled through to the ETC due to the chemical induced blockage at Q_A resulting in the dissipation of energy in a non-photochemical manner.

3.7.2 Photoinhibition of PSII induced by herbicide application

Force et al. (2003) states that an increase in DIoRC and a decline in EToRC values is indicative of photoinhibiton and using these parameters enables a diagnosis of photoinhibition to be made more confidently. DIoRC and EToRC values in Sencorex Flow® and Calaris® treated plants suggest photoinhibitory effects. Photoinhibition could be considered a decline in the functional efficiency of PSII from incident sunlight at a high intensity (Aro et al., 1993, Chan et al., 2012, Long et al., 1994, Powles, 1984, Tikkanen et al., 2014). In this instance, the term 'overload' of PSII could be used to describe the outcome of 680nm light application.

3.7.3 Significant decline in Abs.RC in Nevada®-treated *Chenopodium album*

Figure 15 (b) presents the decrease in Abs.RC upon Nevada® application. As detailed on page 44, Florasulam in Nevada® is a protein synthesis inhibitor (Liu et al., 2015). Florasulam (group B) is an acetohydroxy acid synthase (AHAS) inhibitor. This enzyme is crucial for the biosynthesis of isoleucine, leucine and valine. One possible consequence of

protein synthesis inhibition is the reduction in chlorophyll levels. The amino acid glutamic acid is a precursor to the downstream product of 5-aminolevulinic acid in the porphyrin biosynthesis pathway which leads to the biosynthesis of chlorophyll (Chatterjee and Kundu, 2015, Chen et al., 2018). It is possible that with Nevada®, specifically Florasulam treatment, chlorophyll biosynthesis is inhibited leading to a reduced level of absorbance.

Whilst other pigments capable of absorbing light, including carotenoids are not proteinaceous species, most chloroplasts carotenoids are located in pigment binding proteins in photosynthetic membranes (Demmig-Adams et al., 1996). Thus, inhibition of protein synthesis could impact on the stability of pigments in the thylakoid membranes negating effectiveness. However, the effects of Nevada® treated *Chenopodium album* is not witnessed in *Sinapis arvensis*, and in fact, treatment with Nevada® significantly increases Abs.RC values against the control (P=0.05). This difference further highlights the differences in responses of plants to treatments. Findings such as this add complexity when assessing the potential for treatment in the field when the 680nm LASER is included. In this study, only *Chenopodium album* and *Sinapis arvensis* were used as model species and there is a high level of variation in parameter responses after herbicide treatment. This, coupled with the effects of the 680nm LASER makes finding a general treatment plan for a range of weeds impossible. Therefore, more work is needed with other common UK broadleaf weeds in order to compile a tailored treatment programme.

3.7.4 Trapping increase for Sencorex Flow®-treated *Sinapis arvensis* and *Chenopodium album*

As mentioned in section 3.4, the incident light trapping capability of *Sinapis arvensis* and *Chenopodium album* is significantly increased upon treatment with Sencorex Flow®. It could be argued that more absorbance of light would lead to more trapping in terms of probability. However, when looking at *Chenopodium album* and *Sinapis arvensis* treated with Calaris®, Abs.RC is significantly increased compared to the control (P<0.001 for both *Chenopodium album* and *Sinapis arvensis*) but TRoRC in *Chenopodium album* and *Sinapis arvensis* is increased but not significantly.

Caffarri et al. (2011) found that the health and abundance of LHCs can influence the trapping performance of PSII. One active ingredient of Calaris®, mesotrione inhibits the biosynthesis of carotenoids, α-tocopherol and plastoquinone (Kopsell et al., 2009, Trebst, 2003). It could be assumed that addition of Calaris®, specifically mesotrione leads to a decline in the abundance of LHCs resulting in no significant increase in trapping. However, Abs.RC values, for Calaris® treated *Chenopodium album* increases to 7.5, higher than for

any other sample. It seems hard to believe that trapping is not significantly greater than the control.

One explanation could be the downstream effects of mesotrione from the point of absorbance in the LHC in Calaris® treated plants. Plastoquinone acts as an intermediate electron carrier between carotenoid desaturase and the photosynthetic ETC. Mesotrione treatment is likely to block the transport of electrons between carotenoid desaturase and the photosynthetic ETC due to plastoquinone biosynthesis inhibition induced by mesotrione.

An additional explanation for the lack of trapping in Calaris® treated *Sinapis arvensis* and *Chenopodium album* surrounds the turnover of the D1 protein in PSII. The D1 protein has the highest turnover rate of any other protein located in the thylakoid (Nelson and Yocum, 2006, Wang et al., 2016) and this turnover is responsible for the repair and maintenance of PSII (Adam et al., 2006, Nixon et al., 2005). The other active ingredient of Calaris®, terbuthylazine binds to plastoquinone in the D1 protein. It is likely that the lack of trapping despite significantly higher absorbance compared to the control is due to the dual action of the two active ingredients. Firstly, the binding of terbuthylazine in the D1 binding pocket could induce turnover of the D1 protein. Trebst and Depka (1997) reported that in *Chlamdymonas reinhardtii*, a photosynthetic bacteria, newly synthesised β-carotene is crucial for the repair stage of the D1 turnover. With the inhibition of carotenoid biosyntheiss, it is possible that this stage is not complete, or not as it should be. Faulty or a reduced number of D1 proteins could lead to a significant reduction in both trapping and electron transport rate, highlighted by data presented in Chapter 3.

3.7.5 The increase in absorbance levels for Nevada®-treated *Sinapis arvensis* over 4 days post treatment

The increase in absorbance levels (Abs.RC) for Nevada®-treated *Sinapis arvensis* (Figure 14 (b)) could be an attempt to mitigate *de novo* protein synthesis inhibition as a result of Florasulam treatment by producing more ATP from a greater rate of electron transport. EToRC values are greater at doses 0.0625lha^{-1} and 0.125lha^{-1} for all days compared to the control (Figure 14 (d)). It is possible that at higher herbicide dose, crucial photosynthetic proteins are not replaced due to the action of flurosulam, resulting inefficiency in the electron transport chain, even though the mode of action of Nevada does not directly target PSII.

Dissipation (DIoRC) levels also increase in Nevada®-treated *Sinapis arvensis* (Figure 14 (e)), suggesting that more energy is absorbed than can be funnelled into the electron transport chain and the absence of crucial PSII proteins due to the action of Florasulam.

3.7.6 Percentage relative conductivity protocol suitability

Measuring conductivity of plant samples in turn supplies information of the levels of lipid peroxidation. The 680nm LASER is not used as a treatment in this study and so % relative conductivity levels could be influenced by different factors.

Herbicide induced photoinhibition leads to the production of singlet oxygen predominantly, but also superoxide and OH (Fufezan et al., 2002a). Singlet oxygen is the main ROS which is highly damaging to plant membranes (Jambunathan, 2010, Koh et al., 2016, Triantaphylides et al., 2008). Damage to membranes through the actions of singlet oxygen can occur via two different pathways, i.e., physical membrane disruption or failure of membrane pumps which serve critical roles in homeostasis (Koh et al., 2016). It can be difficult to assess singlet oxygen levels in plant tissue due to the short life time of this species in plant cells, $0.5^{-1}\mu s$ (Li et al., 2012, Telfer, 2014). Therefore, electrolyte leakage quantified by % relative conductivity is a reliable method of quantifying damage by singlet oxygen.

 When comparing OJIP and % relative conductivity responses, there is a noticeable relationship between Abs.RC, DIoRC and EToRC OJIP values and electrolyte leakage levels in herbicide treated plants. It is worth pointing out that % relative conductivity was only measured on Days 1, 3 and 5 post-treatment whereas OJIP was measured every 24 hours post treatment. If this study was to be repeated, measuring % relative conductivity every 24 hours post-treatment would be wise. However, conclusions could still be drawn with a high level of confidence.

Firstly, *Sinapis arvensis* treated with Calaris® sees a sharp increase in % relative conductivity on Day 3 post-treatment for doses $0.25lha^{-1}$ and above (Figure 10(a)). Figure 10 (d) presents a steep decline in EToRC from dose $0.0625lha^{-1}$ of Calaris® and stronger. At the same time, Abs.RC and DIoRC are shown to increase and in a highly similar manner to one another. This is a similar outcome in Calaris® treated *Chenopodium album*. This pattern suggests that with increasing ETC inhibition and due to the mechanism of increased chlorophyll and LHCII polypeptide content, increased absorbance and consequent

dissipation, the production of singlet oxygen is increased. This leads to membrane disintegration and greater % relative conductivity readings.

This close relationship is given yet more strength when analysing the values for Sencorex Flow® treated *Sinapis arvensis*. Figure 10 (d) shows a decline in EToRC value until $0.125lha^{-1}$, followed by a rise in value to $0.25lha^{-1}$ again followed by a steep decline to $1.0lha^{-1}$. The pattern in Abs.RC and DIoRC data mirror this. It is interesting to note that the % relative conductivity graph for Sencorex Flow® treated *Sinapis arvensis* shows a similar response on Day 5 post treatment, with % relative conductivity readings increasing until $0.125lha^{-1}$ and then decreasing between $0.25lha^{-1}$ and $0.5lha^{-1}$. Values increase again for a Sencorex Flow® treatment of $1.0lha^{-1}$. This pattern suggests that % relative conductivity readings are dependent on the ETC and Abs.RC readings. Inhibition of the ETC through chemical action, as reasoned on page 87, leads to increased absorbance. It is entirely plausible that an increased amount of singlet oxygen is produced both from efficient inhibition of the ETC and increased absorbance. As Figure 13 (d) presents there is no such disruption in *Chenopodium album* treated with Sencorex Flow® EToRC pattern as in *Sinapis arvensis* Sencorex Flow®, and this is shown by % relative conductivity consistently increasing over herbicide dose and days post treatment.

Both *Chenopodium album* and *Sinapis arvensis* treated with Nevada® show no distinct findings in either OJIP or % relative conductivity data. This is due to the completely different mode of action of Nevada®. With Nevada® treatment, the electron transport chain does not cease and absorbance and dissipation are also not clearly affected. It is likely that the levels of singlet oxygen produced are very low, supported by the similar % relative conductivity readings for control and treated samples. Having said this, the range of values for Nevada® treated samples and Calaris® and Sencorex Flow® treated plants is similar. This could be due to singlet oxygen production upon wounding of the plants during sample preparation (Prasad et al., 2017, Savatin et al., 2014)

Chlorophyll fluorescence readings are focused around the beginning of the photosynthetic pathway, from absorbance of light to the reduction of Q_A. Fluorescence readings do not give information about other biochemical processes including amino acid synthesis which is the herbicide active site for the active ingredient Flurosulam in Nevada®. One way to quantify amino acid synthesis would be to supply $^{13}CO_2$ to intact plants and analyse enrichment in free amino acids and in amino acid residues in protein during a 24 hour pulse and 4 day chase (Ishihara et al., 2015). Therefore, it is unsurprising that OJIP data shows very little change for days pre and post-treatment or for the dose range as the MOA of Nevada® is not focused on the photosynthetic ETC at all. There are no clear outcomes for Nevada® data in

either *Chenopodium album* or *Sinapis arvensis* over the days of measurements (Day 0 to Day 4) but it could be interesting to see if there is any decline in the photosynthetic efficiency beyond Day 4 as the whole plant integrity begins to decline as plants treated with Nevada[®] can take up to 12 days to die. Any photosynthetic decline is unlikely to be a direct result of the Nevada[®] MOA.

The % relative conductivity data shown in graphs 18(a) and 18 (b) for Nevada[®] show there to be very little difference in the level of % relative conductivity over the course of 5 days post-treatment. This suggests that the cell membranes of the treated plant samples are not losing integrity from lipid peroxidation. This finding is supported by the mode of action of Nevada[®] (as detailed on page 44) which is not widely believed to trigger lipid peroxidation and is more focused on the inhibition of growth. One study found that the pathway of Nevada[®] and other AHAS inhibitors does generate ROS, in particular singlet oxygen but leading to the oxidation of FAD (Lonhienne et al., 2018, Tittmann et al., 2004). Therefore, FAD indirectly mops up singlet oxygen and so it is likely that the rate of damage inflicted by ROS on cellular processes is lower than the rate of repair. This could explain why the mean % relative conductivity levels are not sensitive to change over five days. However, as stated earlier, plants treated with Nevada[®] can take up to 15 days to die from the effects of Nevada[®], so conductivity measurements over a course of 15 days could show more change. An increase in % relative conductivity would have been expected after Nevada® treatment as membranes cannot form or repair as well under the influence of Fluroxpyr, a synthetic auxin (detailed in the Chapter 1 on page 44).

3.7.7 Conclusions to be drawn from the SOD assay

The results from the SOD assay prove unreliable and inconsistent. This could be due to sample preparation or experimental protocol, both of which are critically discussed in the general discussion. Analysis of SOD was used, in part because SOD analysis *in planta* is a common diagnostic for plant stress (Banowetz et al., 2004, Beauchamp and Fridovich, 1971, Bournonville and Diaz-Ricci, 2011) and in this study might have revealed physical biochemical responses herbicide treatment. SOD analysis was also used to assess the effects on PSI to give a complete outlook on the state of the photosynthetic ETC. The lack of consistency in values witnessed in Figures 19 (a) and (b) is likely to be a combination between the insensitivity of the SOD protocol and the lack of SOD produced at PSI and at other photosynthetic sites. Having said this, SOD levels mg^{-1} total protein are elevated in

this study. For example, Giannopolitis and Ries (1976) found in untreated corn, oat and pea shoots, SOD units mg^{-1} total protein ranged from 61 to 22 units mg^{-1} total protein, respectively. In this study, control *Sinapis arvensis* plants contained between approximately 95-505 SOD units per mg total protein and in *Chenopodium album* control plants, between 105-400 SOD units per mg total protein.   However the lack of consistent readings in the control samples casts doubt on the reliability of readings for treated samples. It could be more reliable in future studies to concentrate on physical biochemical markers which can be quantified produced at PSII exclusively. Alternatively, if quantifiable effects on PSI are needed, it could be more accurate and time efficient to use the OJIP parameter REoRC, which is defined as electron flux able to reduce end electron acceptors at the PSI acceptor side, per RC (Ceusters et al., 2019, Fan et al., 2015).

Quantifying singlet oxygen production would be an interesting probe, especially with the use of the 680nm LASER. Singlet oxygen is produced from excess triplet chlorophyll which is hypothesised to be produced upon 680nm LASER treatment. Confocal LASER scanning microscopy with the dye singlet oxygen sensor green (SOSG) could be used to visualize the location of singlet oxygen as in Prasad et al. (2017) who used this method in *Arabidopsis* after wounding. This equipment is not available at Harper Adams University currently, so samples could be sent away to an external laboratory. However, plant sample preparation would be crucial as wounding and low temperatures could cause elevated singlet oxygen production (Fan et al., 2015, Prasad et al., 2017).

3.7.8 Determining the optimal experimental herbicide dosage and time point to use for subsequent trials in this study

The experiments presented in this chapter is to use the lowest dose of herbicide whilst still maintaining efficacy, coupled with the application of 680nm LASER treatment.

The two main OJIP parameters which need to be taken into consideration when dealing with PSII inhibitors are Fv.Fm and EToRC. In this current study, it would be unwise to use a herbicide dose which leads to an unchanged Fv.Fm values compared to the control as this suggests overall plant health has not declined. The EToRC value highlights the effect herbicide treatment has on the electron transport chain. It is ideal to have both Fv.Fm and EToRC significantly lower to dose F to provide robust evidence that this dose and active ingredients prove detrimental to PSII.

The optimal time for 680nm LASER application post herbicide treatment can be decided from the Fv.Fm graphs (see Figures 10-15(a)). Day 1 shows a significant reduction compared to Day 0 for most doses across the Calaris® and Sencorex Flow® and for *Chenopodium album* and *Sinapis arvensis*. Nevada® treated plants show little reduction in Fv.Fm as the MOA of Nevada® is not known to affect PSII. More importantly, at the Day 1 point for most doses, there is room for a reduction in Fv.Fm values upon 680nm LASER treatment, whereas later time points have much lower Fv.Fm values. For consistency across the study, it would be wise to analyze each herbicide, herbicide dose, and plant species at the same time point. It could become too complex to have different time points to suit each plant and herbicide.

From the % relative conductivity data, is it not possible to determine which herbicide dose or time point to use to produce the detrimental effects required. There are distinct value patterns with small error bars, as shown in the results section (headings 3-5), but this does not translate into which dose of herbicide or 680nm LASER treatment day would be best. Similarly, no conclusions can be drawn confidently from the SOD assay data. So far, the OJIP data is by far the more telling and most reliable data.

Table 5 A record of the herbicide doses with which to treat Chenopodium album and Sinapis arvensis in conjunction with the 680nm LASER treatment in accordance with results from Chapter 3.

Plant species	Herbicide	Day of 680nm LASER application post herbicide treatment	Herbicide dose Lha^{-1}
Sinapis arvensis	Calaris®	1	0.25
Sinapis arvensis	Sencorex Flow®	1	0.125
Sinapis arvensis	Nevada®	1	1.0
Chenopodium album	Calaris®	1	1.0
Chenopodium album	Sencorex Flow®	1	0.0625
Chenopodium album	Nevada®	1	1.0

3.8   Conclusion

Calaris® and Sencorex Flow® both contain PSII inhibitors the effects of treatment is evident from the OJIP data as detailed in section 3.4. Alternatively, Nevada® did not display any PSII inhibitory effects from the OJIP data. This is expected due to the mode of action of Fluroxypyr and Florasulam, which focus on triggering an auxin type response and the inhibition of amino acid biosynthesis, respectively.

In terms of the suitability of the procedures in this study (detailed in the general discussion), the OJIP data could be considered more valuable than the % relative conductivity and SOD data due to its high accuracy and clear patterns which can be logically explained. % relative conductivity data is useful in terms of supporting lipid peroxidation occurrence but some sets of data proving surprisingly turbulent with large error bars cast doubt on the accuracy of this method.

SOD analysis reveals very little regarding SOD production, primarily from PSI. It is highly possible that the method used is not sensitive enough to detect such subtle changes. For future work, it might be more prudent to employ alternative assays to detect other ROS produced from PSII, including downstream products of singlet oxygen production.

This current study is invaluable when assessing the likelihood of 680nm LASER treatment in addition to herbicide treatment having an enhanced detrimental effect on the state of PSII. For Calaris® and Sencorex Flow® (PSII inhibitors) the added 680nm LASER energy application could prove further detrimental to the state of PSII due to the dual line of attack focusing on PSII. Nevada® treatment with 680nm LASER treatment may prove efficacious due to the nature of the treatment; the mode of action of Nevada® is not PSII inhibition and two lines of attack with unrelated modes of action could be effective.

It is worth noting that this work is testing a concept of tailoring chemical and LASER treatment to specific weed species so that less herbicide is used whilst still killing the plant to prevent resistance cases. At the moment, the on-farm technology to do this is not yet developed and so the practicalities for a farmer to tailor chemical treatments to weeds are prohibitive. The technology would be required to recognise weed species and possibly growth stages in order to administer the correct dose of herbicide and to be an autonomous robot capable of continuous work. Adding LASER treatment onto this increases the complexity, but researching the biochemical responses now adds to the understanding of this method and has the potential to speed up a technology being brought to market.

Chapter 4

The biochemical responses of *Sinapis arvensis* and *Chenopodium album* post 680nm LASER treatment

4.1   Objective

The research in this chapter served a dual purpose; to assess responses of plants to the 680nm LASER of different doses and to decide which dose could be more effective once herbicides were included in the treatment regime.

4.2   Abstract

The use of 680nm LASER light had different effects on *Sinapis arvensis* compared to *Chenopodium album* at higher LASER doses or above 1800mA for 5s, 7s and 10s dwell times compared to the control. From OJIP parameter data, it would appear that the PSII in *Sinapis arvensis* plants utilised the 680nm readily and LASER treatment was not detrimental. *Chenopodium album* responded minimally to the addition of 680nm light. Percentage relative conductivity readings for *Sinapis arvensis* increased significantly to the control with increasing 680nm LASER dose but and *Chenopodium album* shows markedly increased readings with the application of 680nm at 2000mA for 10s a dwell time. SOD units per mg total protein analysis showed levels to decline in *Sinapis arvensis* with doses above 1800mA whereas *Chenopodium album* SOD levels showed inconsistency. The potential for impacting PSII by administering LASER light in a positive or detrimental way exists but more work needs to be carried out using a number of different wavelengths to target different processes of photosynthesis.

4.3   Introduction

The purpose of the experimental work outlined in this chapter was to assess the effectiveness of different doses of 680nm LASER when aiming to disrupt the photosynthetic electron transport chain (ETC) with special focus on photosystem II (PSII).

As described in detail on pages 24 to 26, the chlorophyll *a* special pair P680 in the PSII reaction centre (RC) absorbs light directly at 680nm (Anderson and Chow, 2002, Matsubara et al., 2011, Pospisil, 2016) as well as after photosynthetically active radiation (PAR)

96

radiation has been absorbed through the antenna (commonly known as light harvesting complexes (LHCs)) systems. These antenna systems are able to convert the energy to a useable form for the special pair P680 to absorb to avoid the production of ROS and free radicals (Krieger-Liszkay, 2005, Krieger-Liszkay et al., 2008b) due to excessive energy reaching the RC. It is hypothesised that if light of 680nm from the LASER can be administered to a plant already in steady state unstressed photosynthesis, the light would either bypass the antenna complex and reach P680 directly, or be transferred down the antenna system without filtration. Either way, it is hypothesised that excess energy will accumulate at P680 leading to overload and subsequent shutdown of this protein complex. Whether an accumulation at P680 is managed and the biochemical consequences of this will be the focus of this chapter. To analyse the effects of the laser, OJIP parameters were analysed along with percentage relative conductivity data and superoxide dismutase (SOD) levels in treated plant samples.

The data from the 680nm LASER treatment study and the data from the herbicide treatment only study will provide comparisons and will allow assumptions to be made regarding the efficacy and effectiveness of the combined or individual treatments.

4.4   Results

4.4.1 OJIP parameter analysis

The OJIP parameters Fv.Fm, Abs.RC, TRoRC, EToRC, and DIoRC were focused on in this chapter. Fv.Fm relates to the overall state of PSII, where a low ratio i.e., <0.75 highlights a decline in photosynthetic capability. Abs.RC relates to the absorption of light in the LHC and RCs and TRoRC details the success of absorbed light potentially being funnelled into the ETC. EToRC denotes the rate of electron transport where DIoRC quantifies the dissipation of energy from the system which has not been utilised photo-chemically. OJIP data are markedly different between the *Sinapis arvensis* and *Chenopodium album*. For a complete description of the meaning of the parameters analysed, see page 35-38.

Figures 21 to 31 contains a summary of all OJIP parameter data enabling comparisons to be drawn between the photosynthetic behaviour *Chenopodium album* and *Sinapis arvensis.*

4.4.2 Fv.Fm response to 680nm LASER treatment

Figure 20 Mean Fv.Fm values in Chenopodium album after 680nm LASER treatment. Error bars represent ± standard error of the mean (SEM) n=10. Data analysed using two-way ANOVA, Tukey's Test and T-Test.

Figure 21 Mean Fv.Fm values in Sinapis arvensis after 680nm LASER treatment. Error bars represent ± standard error of the mean (SEM) n=10. The notation 'a', 'b' and 'c' denote Tukey's 95% confidence intervals indicating significance between values. Data analysed using two-way ANOVA, Tukey's test and T-Tests.

From Figure 20, it is evident that *Chenopodium album*, as suggested by the other parameters, is the more robust species compared to *Sinapis arvensis* (Figure 21) in terms of resisting biochemical effects initiated by the 680nm LASER at 0s, 5s and 7s dwell times. The 10s dwell time is consistently lower between 1400mA and 2000mA and there is a convergence of values at 2000mA to a point, which is a consistency across the other 4 parameters assessed. Predictably, Fv.Fm values for *Sinapis arvensis* dramatically decrease and diverge from 1800mA, a similarity across the *Sinapis arvensis* parameter data. Interestingly, mean Fv.Fm values for *Sinapis arvensis* 0s, 5s and 7s dwell times increase and decrease between 1300mA and 1800mA, but the 10s dwell time Fv.Fm values decrease from 1300mA onwards. As with all other OJIP parameters analysed with 680nm LASER treated *Sinapis arvensis,* there is a marked divergence of values for each dwell time at 2000mA with highly significant values for each dwell time ($P < 0.001$).

4.4.3 Abs.RC values in response to 680nm LASER treatment
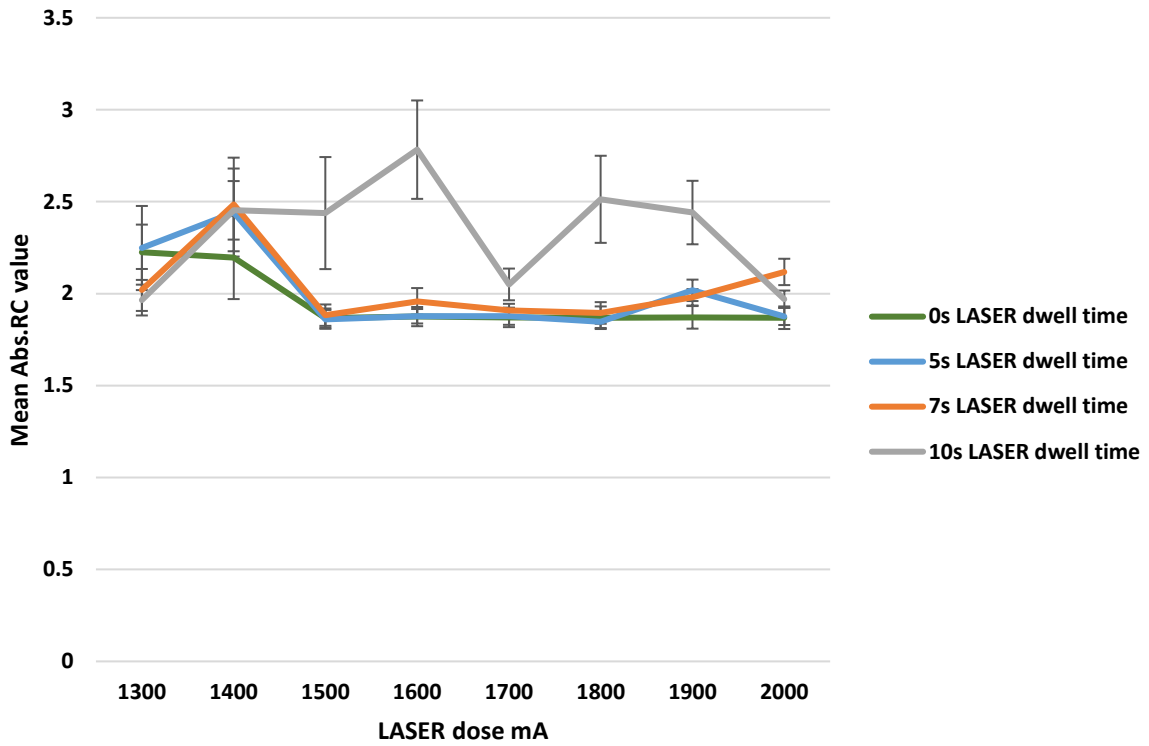
Figure 22 Mean Abs.RC values in Chenopodium album after 680nm LASER treatment. Error bars represent ± standard error of the mean (SEM) n=10, Data analysed using two-way ANOVA, Tukey's test and T-Tests.
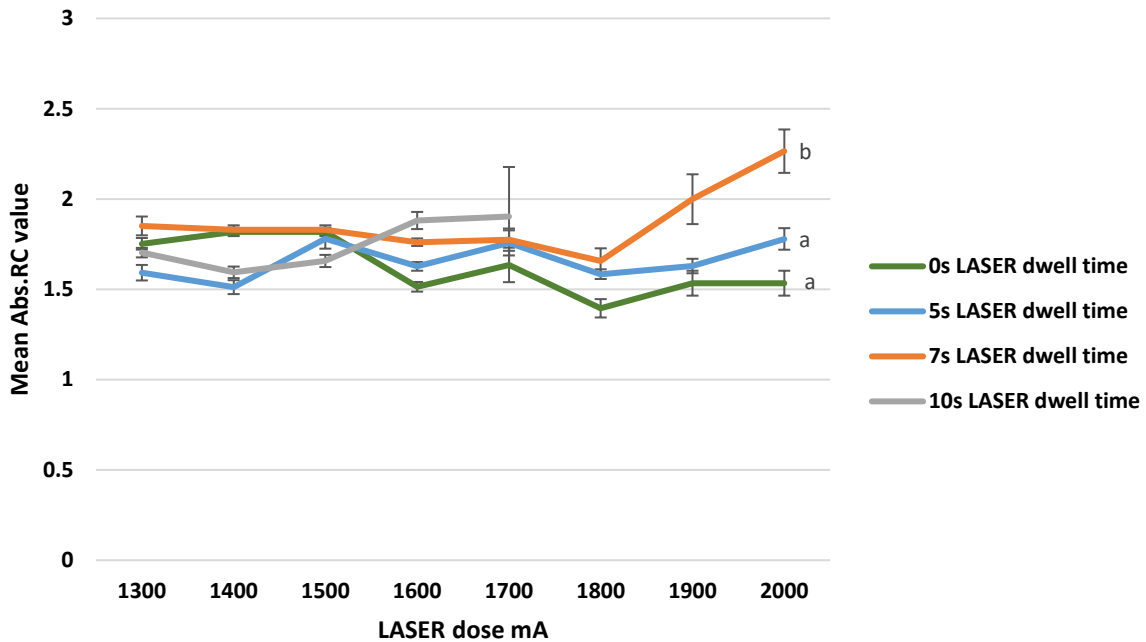
Figure 23 Mean Abs.RC values in Sinapis arvensis after 680nm LASER treatment. Error bars represent ± standard error of the mean (SEM) n=10, Data analysed using two way ANOVA, Tukey's test and T-Tests.

Figure 22, *Chenopodium album* graph displays Abs.RC readings for a range of 680nm LASER doses and dwell times.   Figure 22 suggests *Chenopodium album* possesses a level of resistance to change in the Abs.RC parameter for LASER dwell times of 0s, 5s and 7s highlighted by similar mean Abs.RC values for these dwell times. It is only with a dwell time of 10s where values are significantly different at 1600mA and 1800mA values (P<0.001). Figure 23 shows at 2000mA, the 4 dwell times converge at a similar Abs.RC value for *Chenopodium album* suggesting the 680nm LASER at these doses is neither increasing nor decreasing absorbance values quantified by Abs.RC data.

Figure 23 shows that *Sinapis arvensis* had a narrower range of mean Abs.RC values for a dwell time of 10s up to 1700mA suggesting a reduced susceptibility to change in the Abs.RC parameter compared to *Chenopodium album*. Compared to *Chenopodium album*, the lines on Figure 23 for dwell times 0s, 5s and 7s show divergence at the greater mA levels of 680nm LASER (instead of convergence as in *Chenopodium album* (Figure 22) suggesting that the 680nm LASER does have an effect on absorbance levels in *Sinapis arvensis* at higher doses. An increase in Abs.RC values at greater 680nm LASER doses suggests the P680 RC is absorbing more 680nm light compared to lower 680nm LASER doses.   The 7s

dwell time shows the highest mean Abs.RC value which is expected with a P value of 0.001 against 5s and 0s dwell times at a dose of 2000mA. The 10s dwell time was not administered beyond 1700mA due to the visible damage inflicted on the plant leaf.

4.4.4 TRoRC values in response to 680nm LASER treatment
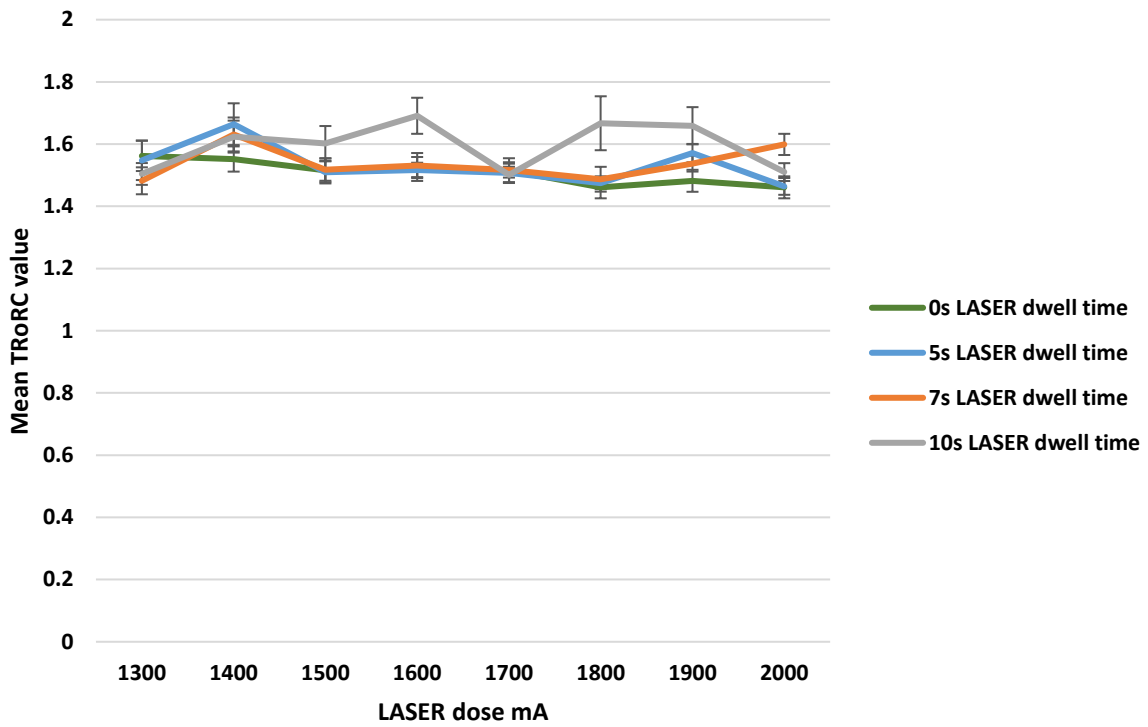
Figure 24 Mean TRoRC values in Chenopodium album after 680nm LASER treatment. Error bars represent ± standard error of the mean (SEM) n=10, Data analysed using two-way ANOVA, Tukey's test and T-Tests.
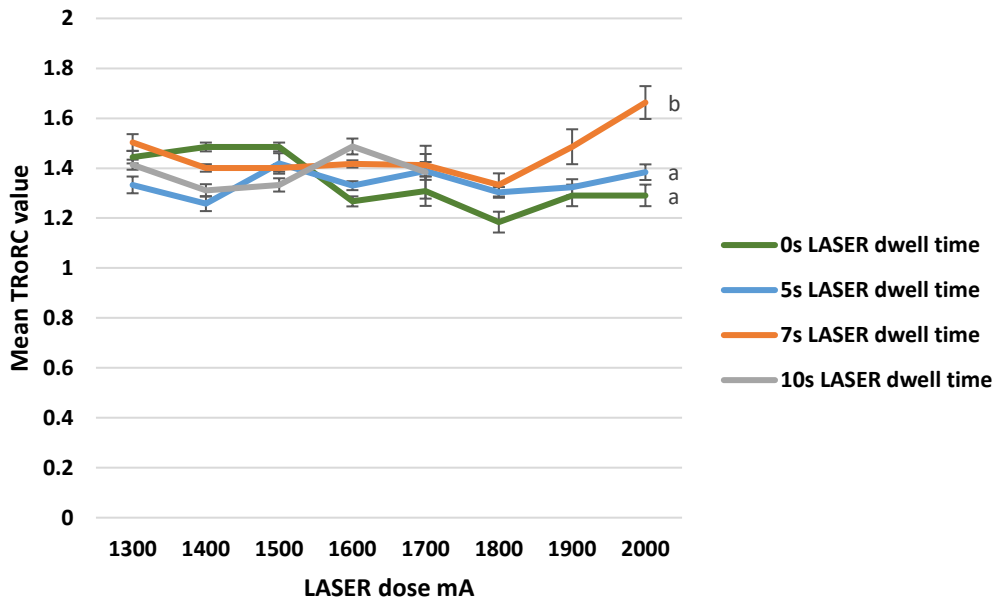
Figure 25 Mean TRoRC values in Sinapis arvensis after 680nm LASER treatment. Error bars represent ± standard error of the mean (SEM) n=10. The notation 'a' and 'b' denote Tukey's 95% confidence intervals indicating significance between values. Data analysed using two way ANOVA, Tukey's test and T-Tests.

Figure 24 shows that TRoRC values for all dwell times in 680nm LASER treated *Chenopodium album* lie between 1.4 and 1.8 and show very high similarity in TRoRC values between 1500mA and 1800mA. Figure 24 shows how the dwell time of 10s lacks a distinct outcome and is unpredictable which has been the case in the other OJIP parameters as previously observed.

Sinapis arvensis TRoRC data shown in Figure 25 begins from between 1.3 and 1.6 for all dwell times but values begin to diverge at 1800mA with a marked increase in TRoRC values with a dwell time of 7s (P<0.001) compared to the control from 1800mA and above. This is consistent with Abs.RC and DIoRC responses.

4.4.5 EToRC values in response to 680nm LASER treatment
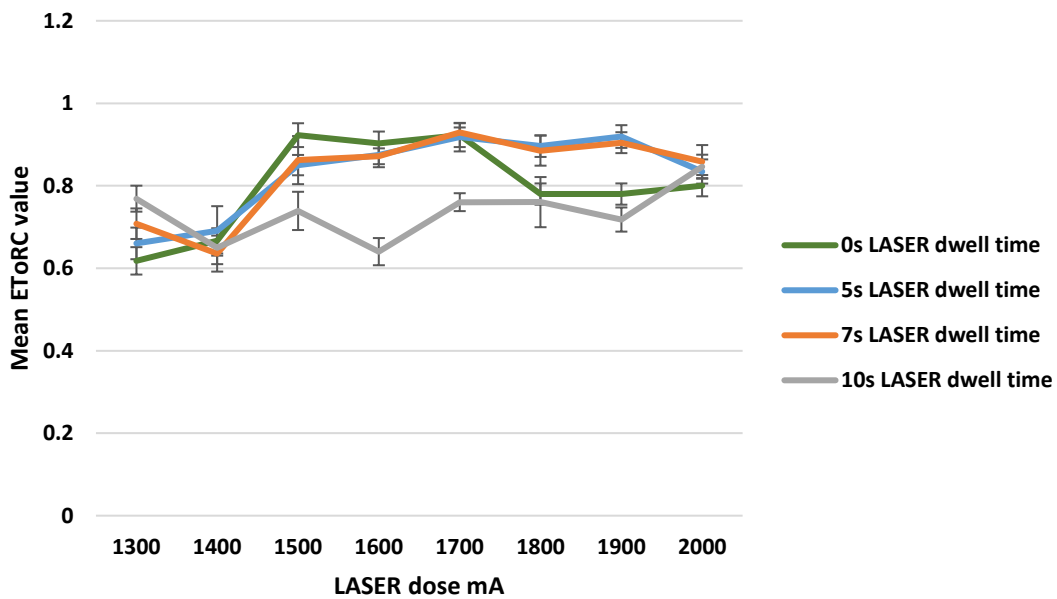
Figure 26 Mean EToRC values in Chenopodium album after 680nm LASER treatment. Error bars represent ± standard error of the mean (SEM) n=10, Data analysed using two-way ANOVA, Tukey's test and T-Tests.
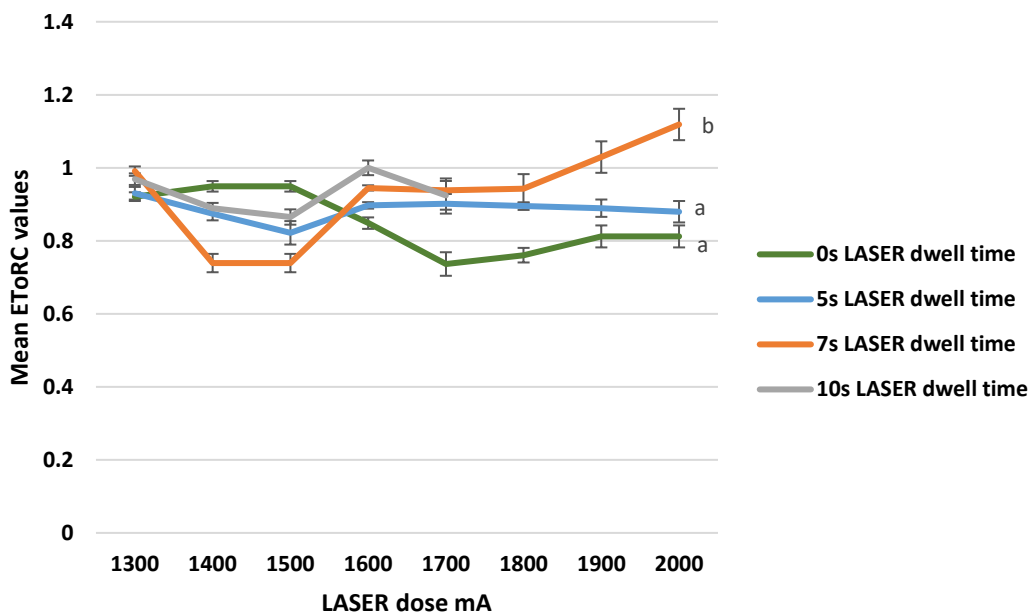
Figure 27 Mean EToRC values in Sinapis arvensis after 680nm LASER treatment. Error bars represent ± standard error of the mean (SEM) n=10. The notation 'a' and 'b' denote Tukey's 95%

confidence intervals indicating significance between values. Data analysed using two-way ANOVA, Tukey's test and T-Tests.

Figure 26 shows how *Chenopodium album* EToRC values begin at 1300mA consistently. The 10s dwell time from 1400mA to 1900mA is consistently lower than the control and 5s and 7s dwell times, with a P value of <0.001 for the 10s dwell time at 1500mA, 1600mA and 1700mA compared to the control plants (0s dwell time). All dwell times converge at a uniformed point at 2000mA suggesting the 680nm LASER at this high dose is no longer having an effect on the electron transport probability. The data for *Chenopodium album* remains consistent across the parameters discussed as data for dwell times of 0s, 5s and 7s diverge in a predictable way (7s greatest, 0s lowest, P<0.001) at 2000mA.

Figure 27 shows how with the previously explained parameter results, there is a divergence in data at 2000mA, specifically with a dwell time of 7s (P<0.001).
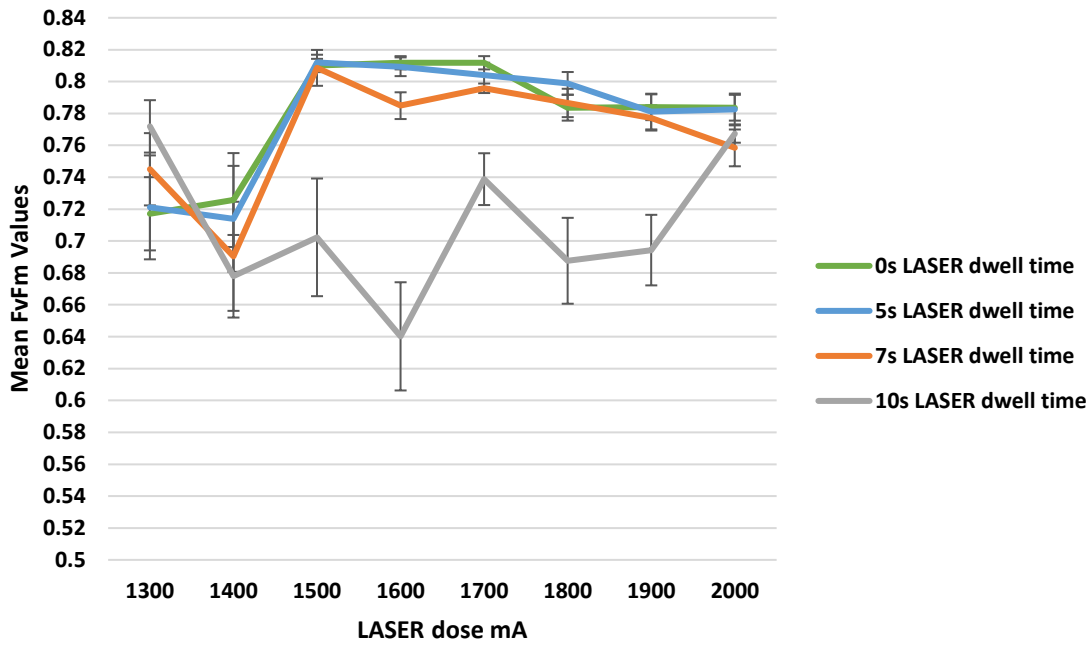
4.4.6 DIoRC values in response to 680nm LASER treatment
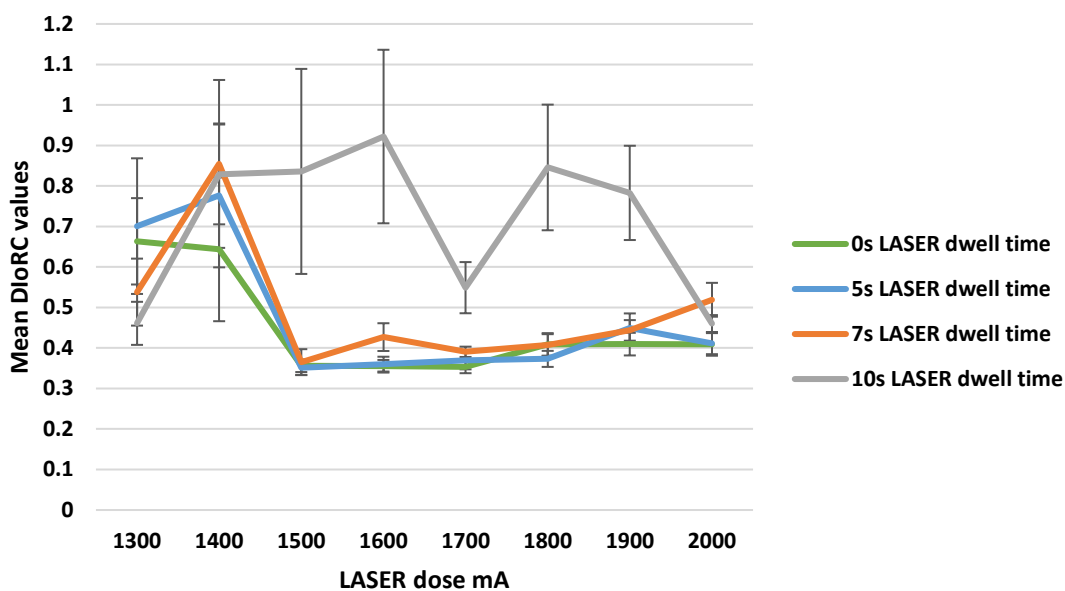
Figure 28 Mean DIoRC values in Chenopodium album after 680nm LASER treatment. Error bars represent ± standard error of the mean (SEM) n=10, Data analysed using two-way ANOVA, Tukey's test and T-Tests.
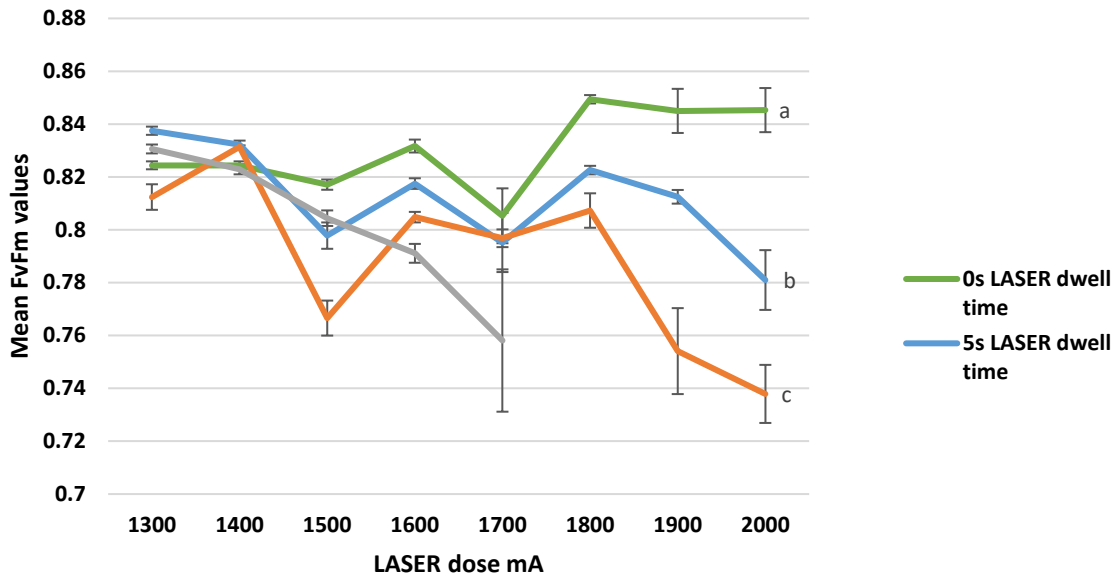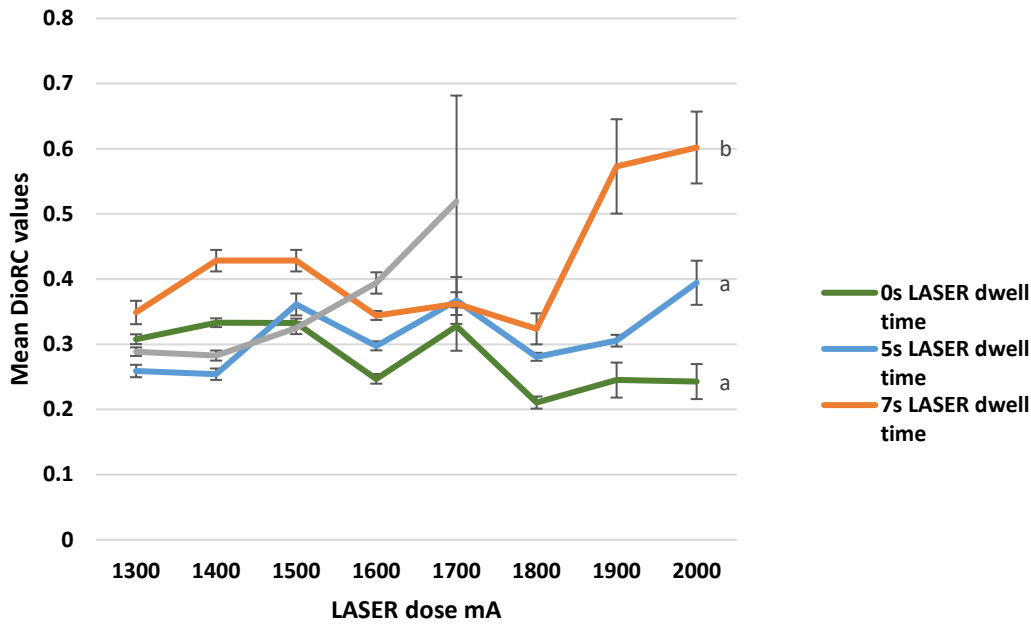
Figure 29 Mean DIoRC values in Sinapis arvensis after 680nm LASER treatment. Error bars represent ± standard error of the mean (SEM) n=10. The notation 'a' and 'b' denote Tukey's 95% confidence intervals indicating significance between values. Data analysed using two-way ANOVA, Tukey's test and T-Tests.

Figures 28 and 29 suggests that *Chenopodium album* is more robust to the 680nm LASER energy compared to *Sinapis arvensis*. This is suggested by the high similarity between value plots for *Chenopodium album* at dwell times of 0s, 5s and 7s whereas 10s dwell time is less unpredictable but consistently greater. The DIoRC parameter data points for *Chenopodium album* converge to a point for all 680nm LASER dwell times at high mA doses (2000mA).

For the *Sinapis arvensis* DIoRC, the data is more diverse in comparison to DIoRC for *Chenopodium album*. The data lines on Figure 31 show divergence beyond 1800mA with 7s showing the greatest dissipation levels. The 10s dwell time appears to increase in an exponential way, however this dwell time was not used at doses above 1700mA due to the damage inflicted on the leaf. At 2000mA with a 7s dwell time, there is a high level of significance compared to 5s and 0s dwell times at 2000mA (P<0.001).

Table 6 *(a) OJIP parameter responses in* C.album *after 680nm LASER doses. Red boxes = significantly decreased values compared to control (0mA) values, green boxes = significantly greater values compared to control (0mA) values. (b) OJIP parameter responses in* S.arvensis *after 680nm LASER doses. Red* ▰ *boxes = significantly decreased values compared to control (0mA) values, green* ▰ *boxes = significantly greater values compared to control (0mA) values. Dashed* ▨ *boxes denote plants where no 680nm LASER was applied due to leaf damage caused by 680nm LASER treatment. Blank boxes represent neither a significant increase or decrease in parameter value compared to the control.* Data analysed using two way ANOVA, Tukey's test and T-Tests.

a)

CA LASER Dose mA		FvFm	AbsRC	TroRC	EtoRC	DIoRC
1300	0					
	5					
	7					
	10					
1400	0					
	5					
	7					
	10					
1500	0					
	5					
	7					
	10	red			red	
1600	0					
	5					
	7					
	10	red	green	green	red	green
1700	0					
	5					
	7					
	10	red			red	green
1800	0					
	5					
	7					
	10	red	green			green
1900	0					
	5				green	
	7					
	10	red	green	green		green
2000	0					
	5					
	7		green	green		
	10	red				

b)

SA LASER Dose mA		FvFm	AbsRC	TroRC	EtoRC	DIoRC
1300	0					
	5	green	red			red
	7					
	10					
1400	0					
	5	green	red	red	red	red
	7					
	10					
1500	0					
	5	red			red	
	7					green
	10			red		
1600	0					
	5	red				
	7		green	green	green	
	10					
1700	0					
	5				green	
	7					
	10					
1800	0					
	5	red			green	green
	7		green	green		
	10	dashed	dashed	dashed	dashed	dashed
1900	0					
	5	red				
	7		green	green	green	green
	10	dashed	dashed	dashed	dashed	dashed
2000	0					
	5	red				
	7		green	green	green	green
	10	dashed	dashed	dashed	dashed	dashed

Table 6 (b) highlights that *C.album* is more susceptible to changes in OJIP parameters post 680nm LASER treatment compared to *S.arvensis*. This assessment is made from the greater level of significant changes against the controls shown in Table 6 (b) compared to Table 6 (b). In addition, in *Sinapis arvensis* Table 6 (b), lower LASER doses including

1300mA for 5s dwell time and 1400mA for 5s dwell time, have more influence on OJIP parameters. At these aforementioned doses, Fv.Fm in *Sinapis arvensis* is significantly increased, which is contrary to all other cases where if Fv.Fm is affected, it is negatively influenced (red boxes).

Chenopodium album Table 6 (a) treated with the dose of 1600mA at 10s dwell time results in a set of changes to the OJIP parameter values which is promising in terms of the 680nm LASER having an effect on PSII. Both Fv.Fm and EToRC are significantly lower upon 680nm LASER treatment to the control which highlights disruption in the electron transport chain. At the same time, Abs.RC, TRoRC and DIoRC values are all significantly increased compared to the control, suggesting the 680nm LASER energy is readily absorbed by PSII but energy is also readily lost through dissipation (DIoRC). This correlation implies that the electron transport chain is less efficient than pre-680nm LASER treatment.

4.4.8 Representation of inter-related OJIP parameters via correlation matrix in *Chenopodium album* and *Sinapis arvensis*
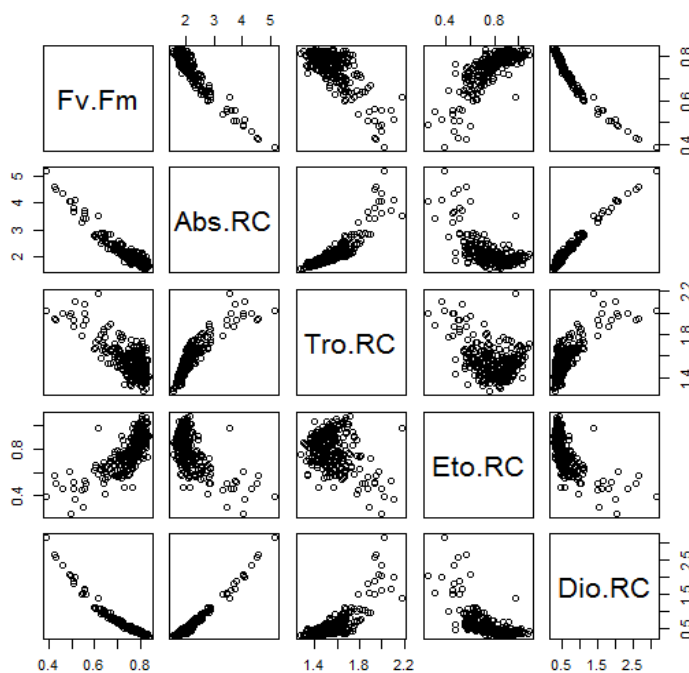
Figure 30 Paired correlation matrix representation for Chenopodium album after 680nm LASER treatment. For a detailed description of parameter definitions, refer to page 36-38. The left had side of the matrix represents mirror images of the data on the right hand side of the parameters. Significant differences in parameter data were calculated using the Kruskal-Wallis Test using the statistical program 'R'.

Figure 30 presents the paired correlations between all measured OJIP parameters after *Chenopodium album* 680nm LASER treatment of varying doses. As with the paired correlation matrix of *Sinapis arvensis,* there are similarities in that each pair of parameters has a significant correlation (P<0.001). Differences between *Sinapis arvensis* and *Chenopodium album* correlation matrixes include a positive correlation between Fv.Fm and EToRC in *Chenopodium album* samples, where in *Sinapis arvensis,* the same OJIP pair is negatively correlated. Figure 21 shows a marked decline in Fv.Fm values in *Sinapis arvensis* from 1800mA and the dwell times of 5s and 7s are significantly lower than the control (0s dwell time) (P<0.001). In addition, correlations presented in Figure 30 are not as defined as in Figure 31, an example being the correlation between TRoRC and EToRC in *Chenopodium album* compared to the more defined correlation in *Sinapis arvensis.* This difference could be due to the way the two species use the 680nm light. The lack of defined correlations in *Chenopodium album* correlations between parameters could suggest more variation in the response on the plant at certain points in PSII, highlighted by the OJIP parameters.
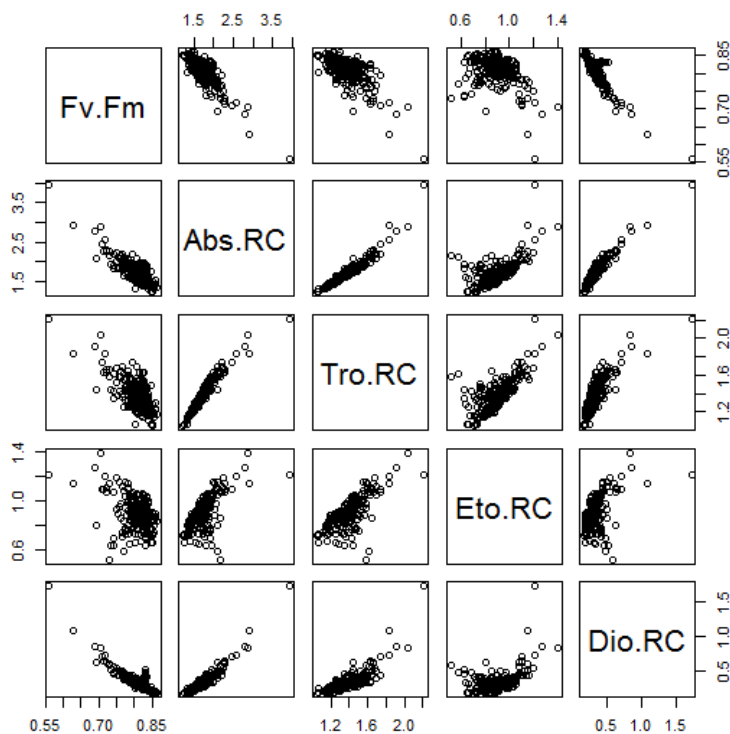
Figure 31 Correlation matrix representation for Sinapis arvensis after 680nm LASER treatment. For a detailed description of parameter definitions, refer to page 36-38. The left had side of the matrix represents mirror images of the data on the right hand side of the parameters. Significant differences in parameter data were calculated using the Kruskal-Wallis Test using the statistical program 'R'.

Figure 31 presents correlations between all five OJIP parameters in *Sinapis arvensis* measured after 680nm LASER treatment. Fv.Fm declines with each measured OJIP parameter (P<0.001), whereas the correlations between Abs.RC, TRoRC, EToRC and DIoRC are all positive (P<0.001). Each correlation whether positive or negative has a P value <0.001. It is important to remember that this schematic does not take into account the variation in 680nm LASER mA settings and dwell times. Nevertheless, there are very strong patterns from which certain assumptions can be made. Abs.RC and TRoRC has a defined significant positive trend (P<0.001) suggesting a greater level of absorption results in more trapping.

4.4.9 Percentage relative conductivity readings post 680nm LASER treatment
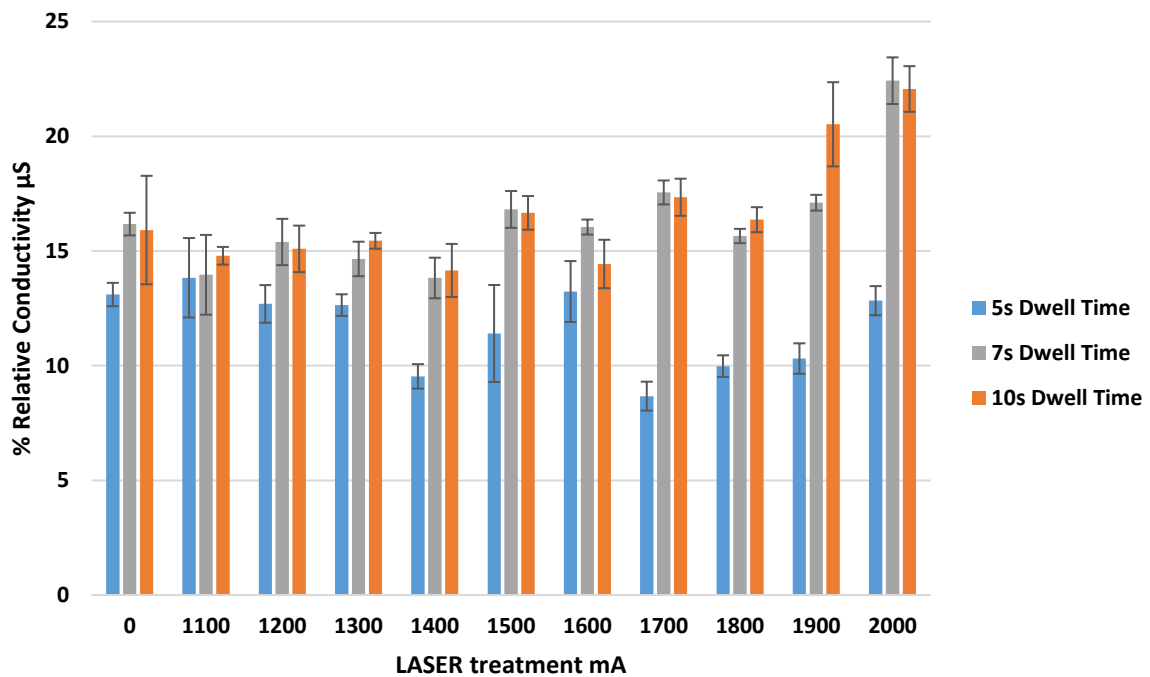
Figure 32 Percentage (%) relative conductivity for Chenopodium album treated with 680nm LASER doses. Error bars represent ±SEM. n=7, Data analysed using two-way ANOVA, Tukey's test and T-Tests.
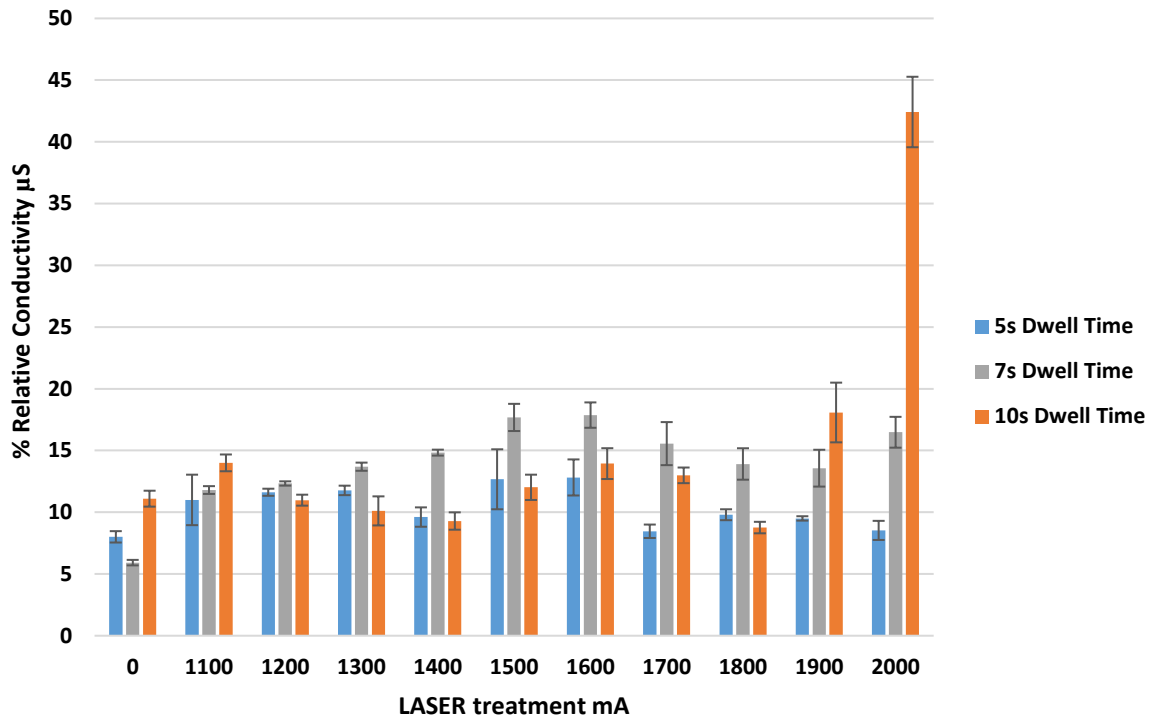
Figure 33 Percentage (%) relative conductivity for Sinapis arvensis treated with 680nm LASER doses. Error bars represent ±SEM. n=7, Data analysed using two way ANOVA, Tukey's test and T-Tests.

Figure 32 shows % relative conductivity in *Chenopodium album*. From 1700mA, dwell times of 7s and 10s are significantly different (P<0.001) to the 5s dwell time. The maximum dose of 10s and 2000mA in *Chenopodium album* does not show as great a conductivity reading as *Sinapis arvensis* (*Sinapis arvensis* = 43µs, *Chenopodium album* = 22µS). There appears to be very little difference between most treatment doses for *Chenopodium album* and *Sinapis arvensis* and the control values (control = 0mA LASER).

Figures 33 shows concordance in % relative conductivity data between *Sinapis arvensis and Chenopodium album*. Values for both plant species remained similar between 0mA (no treatment) and 1800mA for all dwell times and are not dissimilar to the control. A 10s dwell time at 2000mA shows a dramatically greater conductivity reading with a high level of significance to 7s with a P value <0.001. At this higher dose this values is unsurprising. The maximum dose of 2000mA for a 10s dwell time was applied in this conductivity protocol despite the visible damage to the leaf so such high values are likely to be caused by cellular ablation.

4.4.10   SOD units per mg total protein content post 680nm LASER treatment
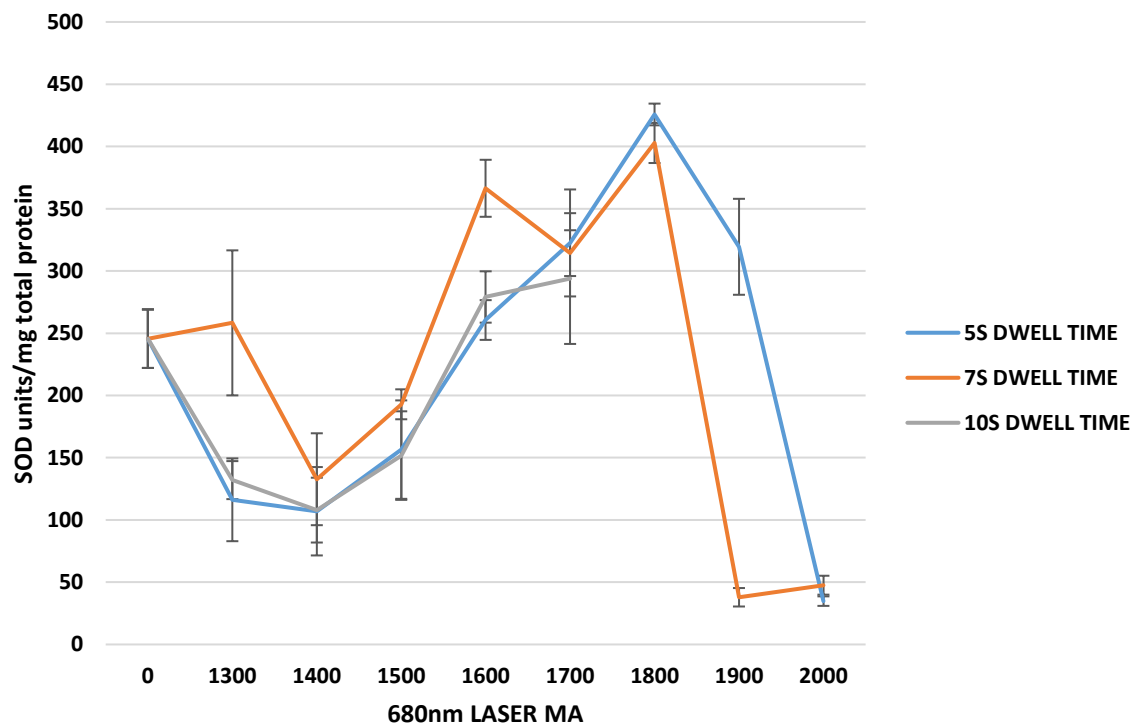
Figure 34 SOD levels per unit/mg total protein in Sinapis arvensis post 680nm LASER treatment. Error bars denote ±SEM, 680nm LASER treated doses n=6, control n=12, Data analysed using two-way ANOVA, Tukey's test and T-Tests.
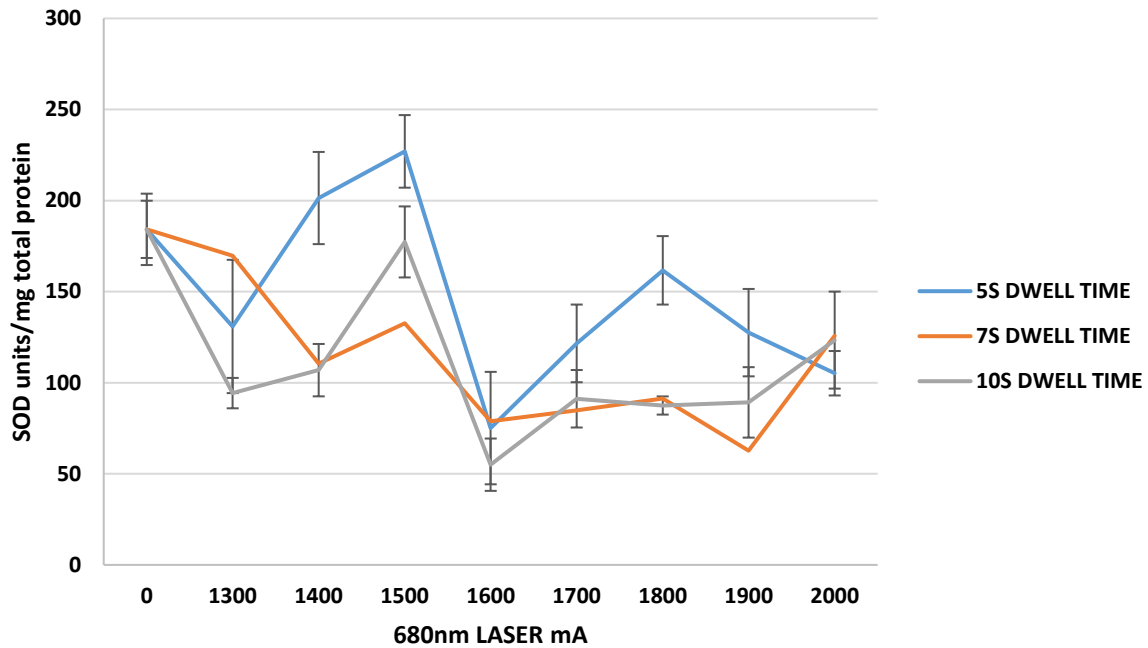
Figure 35 SOD levels per unit/mg total protein in Chenopodium album post 680nm LASER treatment. Error bars denote ±SEM, 680nm LASER treated doses n=6, control n=12, Data analysed using two-way ANOVA, Tukey's test and T-Tests.

The SOD units/mg of total protein for *Sinapis arvensis* (Figure 34) shows a steep decline between 1500mA and 1600mA for the 5 dwell time, possibly highlighting denaturation of the SOD proteins post 680nm LASER treatment at high doses. The 5s dwell time treatment group contains the highest and lowest average value within the mA treatment groups, i.e., 426 units/mg total protein for 1800mA and 34.8 units/mg total protein for 2000mA.

SOD units/mg total protein for *Chenopodium album* (Figure 35) displays peaks and troughs across all 680nm LASER mA doses. The 5s dwell time yields consistently greater SOD unit/mg total protein levels from 0s to 2000mA. The range of values in *Chenopodium album* is much lower than in *Sinapis arvensis*, from 55 units of SOD/mg total protein at a dose of 1600mA at 10s to 227 units SOD/mg total protein at 1500mA and a 5s dwell time. As with OJIP data, the values converge at 2000mA for all dwell times.

4.4.11 Comparison of OJIP values for herbicide only treated plants compared to 680nm LASER treated *Sinapis arvensis* and *Chenopodium album*

OJIP parameter data for plants treated with herbicide exclusively is in contrast to 680nm LASER treated samples for both *Sinapis arvensis* and *Chenopodium album*. Whilst herbicide treated plants demonstrate very clear and explainable responses according to the herbicide used across a time scale post herbicide application, OJIP parameters in 680nm LASER treated plants is not as straight forward except for higher doses of 680nm LASER in *Sinapis arvensis* (see pages 99-109). Fv.Fm values in both control samples in the herbicide only treatment group (Chapter 3) and control samples in the 680nm LASER only treatment group (Chapter 4) show little deviation from a Fv.Fm value of ~0.8 showing plants are unstressed. In *Chenopodium album*, it is only with the addition of the 680nm LASER at 10s where values drop below 0.8 highlighting a change in photosynthetic capacity and in *Sinapis arvensis*, there is more disruption of Fv.Fm values but few lie outside the range of 0.75-0.83. Only from doses beyond 1800mA in *Sinapis arvensis* do Fv.Fm values decrease with increasing dwell time. These Fv.Fm values in 680nm LASER treated plants are markedly greater than for herbicide treated plants. In Sencorex Flow® treated *Chenopodium album*, which according to Table 4 in Chapter 3 is the most effective chemical treatment, Fv.Fm values show a decline as soon as Day 1 post treatment for the lowest dose of 0.0625lha^{-1} and continuing to rapidly decline to Fv.Fm=0.19 for a dose of 0.25lha^{-1} Sencorex Flow®. There is a similar response for Sencorex Flow® and Calaris® treated *Chenopodium album* and *Sinapis arvensis*, suggesting these herbicide treatments are highly effective at targeting PSII.

Abs.RC values in 680nm LASER treated *Chenopodium album* shows no deviation from the control values bar the 10s dwell time which is consistently greater, usually reaching values of 2.5. 680nm LASER treated *Sinapis arvensis* also shows very little deviation in Abs.RC value for all dwell times between 1300-1800mA and are within Abs.RC=1.5-2.0. Abs.RC values for control samples in the herbicide only treatment group range from 1.5-2.0 (except Nevada® treated *Chenopodium album* which rises above 3.0). This is to be expected in control samples. However, upon application of the chemical treatments at the doses which will be used when combining chemical and 680nm LASER treatments (detailed in Chapter 5), Day 1 post Sencorex Flow® treatment leads to Abs.RC rising above 3.5 for *Chenopodium album* (Sencorex Flow® dose 0.0625lha^{-1}) and *Sinapis arvensis* (Sencorex Flow® dose of 0.125lha^{-1}) with Calaris® treated *Chenopodium album* (Calaris® dose 0.5lha^{-1}) achieving Abs.RC values greater than 7.0. An explanation for an increase in absorbance

for herbicide treated plants is detailed on page 87. It is hypothesised that the 680nm LASER will be absorbed efficiently by the P680 RC thus leading to elevated Abs.RC levels. However, Abs.RC values in 680nm LASER only treated samples show very little change upon 680nm LASER treatment and in the next chapter where herbicide treatment is used in conjunction with 680nm LASER treatment, it is likely that the effects of the 680nm LASER with be lost within the efficient herbicide treatment. Change in Abs.RC values upon herbicide and 680nm LASER treatment is more likely to be achieved with Nevada® treatment as even with a dose of 1.0lha^{-1} of Nevada®, Abs.RC values were largely unchanged (between 1.5-2.5 in both *Chenopodium album* and *Sinapis arvensis*), meaning there is scope to increase Abs.RC values in Nevada® treated plants to highlight increased absorbance of the 680nm LASER.

Trapping (TRoRC) values for 680nm LASER treated *Chenopodium album* and *Sinapis arvensis* remain in a similar range across all doses and dwell times, ie., 1.1-1.7. Trapping values in herbicide treated plants are within a similar range to 680nm LASER treated plants suggesting the effect on trapping from photosystem II inhibitor (Calaris® and Sencorex Flow®) usage is limited. The expectation therefore, is for trapping values to increase upon 680nm LASER combined with herbicide treatment as herbicide treatment alone has had no effect on TRoRC values and plant may readily use the energy being supplied by the 680nm LASER to attempt to mitigate against the block in electron flow (mechanism detailed on pages 42-44).

Dissipation (DIoRC) in 680nm LASER treated *Chenopodium album* is increased after dwell times of 10s for most 680nm LASER doses. The other dwell times (5s and 7s) display very similar outcomes to the control, visible in Figure 28. The greatest DIoRC value is 0.9 at a dose of 1600mA with a 10s dwell time. The highest DIoRC value reached in *Sinapis arvensis* treated with the 680nm LASER is 0.6 at 2000mA and 7s. With herbicide only treatment, Day 1 data shows Sencorex Flow® treated plants to have DIoRC=2.0 (Sencorex Flow® doses 0.125lha^{-1} and 0.0625lha^{-1} in *Sinapis arvensis* and Calaris®, respectively) and Calaris® treated *Chenopodium album* (Calaris® dose of 0.5lha^{-1}) to reach just below 6.0. For herbicide and 680nm LASER treatment combined the expectation is for there to be greater dissipation due to the increase in absorbance of the 680nm light as the plants' attempt to mitigate against the decline in photosynthetic viability and from the block in electron flow induced by the herbicides. Again, the likelihood is there to be no observed increase in dissipation upon addition of the 680nm LASER due to the effectiveness of the chemical treatments. As with Abs.RC, an increase in DIoRC could be observed in Nevada® treated plants as even with a dose of 1.0lha^{-1}, the DIoRC values are insensitive to change.

The EToRC values for LASER treated *Chenopodium album* are between 0.6-1.0 and between 0.7-1.2 for *Sinapis arvensis*. When comparing with Day 1 EToRC average values for herbicide only treated samples, EToRC average values for Sencorex Flow® treated *Chenopodium album* is 0.12 and *Sinapis arvensis* 0.17 (Sencorex Flow® doses 0.0625lha^{-1} and 0.125lha^{-1}, respectively) and Calaris® treated *Sinapis arvensis*, 0.14. Day 1 post Calaris® treatment of *Chenopodium album* (Calaris® dose of 0.5lha^{-1}) yielded an EToRC average value as low as 0.027. From these average EToRC values after herbicide treatment, a further decrease in EToRC value upon addition of 680nm LASER treatment is perceived as unlikely due to the strength of the chemical treatment. Even with increase in EToRC value in *Sinapis arvensis* at high 680nm LASER doses (Figure 27) which leads to the assumption of an increased rate of ETC promoted by 680nm LASER treatment, it is unlikely that the 680nm LASER will be able to overpower the electron block caused by Calaris® and Sencorex Flow®.

4.4.12 Comparison of percentage relative conductivity values for herbicide only treated plants compared to 680nm LASER treated *Sinapis arvensis* and *Chenopodium album*

The % relative conductivity levels for Calaris® treated *Sinapis arvensis* and *Chenopodium album* are generally greater than the values of 680nm LASER treated plants. The majority of 680nm LASER treated *Chenopodium album* plant samples have a % relative conductivity value of ~15μS with only doses of 1900mA and a 10s dwell time, and 2000mA 7s and 10s dwell time breaking above 20μS. Similarly 680nm LASER treated *Sinapis arvensis* (Figure 33) values are largely between 10-15μS with only 2000mA 10S dwell time reaching 42.6μS. Calaris® treated *Chenopodium album* yields % relative conductivity values all above 20μS. Calaris® treated *Sinapis arvensis* is more sporadic but Day 3 values for doses 0.25lha^{-1} and above all exceed 45μS.

Sinapis arvensis treated with Sencorex Flow® has % relative conductivity values generally in a similar range to 680nm LASER treated *Sinapis arvensis* with the exception of 3 high values on Day 5 for 0.0625, 0.125 and 0.25lha^{-1}. This is one case where an increase in % relative conductivity might be observed after dual treatment (herbicide+680nm LASER in conjunction). Sencorex Flow® treated *Chenopodium album* has greater % relative conductivity values in general compared to LASER treated *Chenopodium album*, with the

majority of values above 20µS and a Sencorex Flow® dose of 1.0lha^{-1} on Day 1 exceeding 40µS. The expectation here is that the addition of 680nm LASER energy alongside Sencorex Flow® will not influence % relative conductivity levels as % relative conductivity responses to 680nm LASER energy are mild, especially at lower doses.

Nevada® treated *Chenopodium album* (Figure 18 (b)) has a lower range of % relative conductivity values compared to responses with Sencorex Flow® and Calaris® and is in a similar range to 680nm LASER treated *Chenopodium album*. Nevada® treated *Sinapis arvensis* does have a higher range of values with % relative conductivity levels often exceeding 30µS.

As Nevada® has a mode of action not related to PSII, addition of 680nm LASER energy is proposed to create a dual effect so there is scope for the % relative conductivity value range to increase. As with OJIP data, Sencorex Flow® and Calaris® % relative conductivity results highlight the fact that with herbicide and 680nm LASER treatment working in conjunction, % relative conductivity levels may be pre-determined more by the dose of herbicide used instead of subtle biochemical effects consequent of 680nm LASER treatment.

4.4.13   Comparison of SOD levels per mg total protein for herbicide only treated plants compared to 680nm LASER treated *Sinapis arvensis* and *Chenopodium album*

SOD data in herbicide only treated samples show clear differences between the three herbicides in *Chenopodium album* and *Sinapis arvensis*. The same cannot be said for 680nm LASER treated *Chenopodium album* and *Sinapis arvensis* for which there is no logical explanation. In addition, 680nm LASER treated *Chenopodium album* and *Sinapis arvensis* SOD values have a large range across 680nm LASER doses making reliable comparison difficult. In order to provide any sort of comparison, specific herbicide and 680nm LASER doses would need to be individually analysed.

4.5   Discussion

4.5.1 Salt bladder protection

From the OJIP data, it would appear that the two species, *Sinapis arvensis* and *Chenopodium album* behave differently in response to the 680nm LASER. As highlighted in the results section, for *Chenopodium album* there are numerous occasions where significance in OJIP parameter data is more commonly observed at the dwell time of 10s.

One reason for this discrepancy between these species could be the physiology of the plants. One visible difference between *Chenopodium album* and *Sinapis arvensis* is the presence of a covering of micelles known as salt bladders (Bohm et al., 2018) found on the leaves and stems of *Chenopodium album* (Figure 36). Whilst Bohm et al. (2018) studied the salt bladders present on *Chenopodium quinoa*, this is highly related to *Chenopodium album* and so the same mechanisms of salt sequestration would apply. It is possible that salt bladders act as an energy absorbing barrier to the incident 680nm LASER thus preventing alteration to PSII. In most cases for *Chenopodium album* it is only the application of 680nm LASER at a dwell time of 10s which has an effect on the parameter values. This might suggest that 10s is a great enough dwell time to overcome the potentially indirect protective role of the salt bladders. Having said this, salt bladders are in lower quantities on the upper surface of the leaf compared to the underside, so this theory might not be reliable. Younger leaves possess more salt bladders in all parts of the leaf and especially on unopened cotyledons (Figure 36).
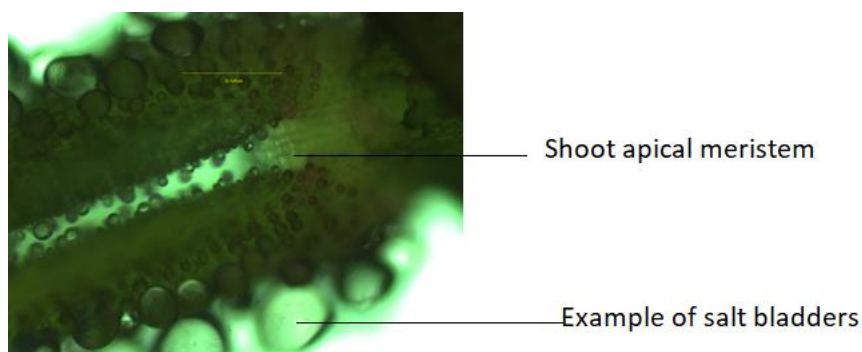
Figure 36 image taken of salt bladders located on unopened cotyledons of Chenopodium album. The shoot apical meristem (SAM) can also be seen

It might be interesting to run a study testing the same OJIP parameters as in this study for *Chenopodium album* grown in high light intensities with salt bladders present and where salt bladders have been removed. The results of this may also help to explain why *Chenopodium album* does appear more resistant to the 680nm LASER than *Sinapis arvensis* in terms of OJIP parameter responses.

4.5.2 Explanation for Sinapis arvensis appearing to benefit from 680nm LASER treatment

From the Figures 10 to 15 particularly focusing on *Sinapis arvensis*, there is a stark contrast in data for dwell times at 2000mA. The graphs show that for *Chenopodium album* treated with varying dwell times, there is a convergence of values at 2000mA, whereas for *Sinapis arvensis*, there is a divergence from 1800mA with increasing values for 5s and 7s. This occurs across all parameters excluding TRoRC for *Chenopodium album* which shows a weak convergence and Fv.Fm highlighting a decline in *Chenopodium album* photosynthetic efficiency. This could suggest that the photosynthetic pathways of *Sinapis arvensis* are more efficient than in *Chenopodium album* with 680nm LASER energy being used in the photosynthetic processes. For *Sinapis arvensis*, a significant (P<0.001) Abs.RC increase for the 7s dwell time indicates a high level of absorbance of 680nm in the RCs. DIoRC also increases dramatically for *Sinapis arvensis* 2000mA 7s dwell time meaning non-photochemical dissipation is markedly increased. This suggest the 680nm LASER energy is absorbed well but is not in safe quantities for downstream proteins including P680, so is released. Releasing excess energy avoids production of triplet chlorophyll and subsequent ROS production. TRoRC is significantly (P<0.001) greater for *Sinapis arvensis* treated with 7s at 2000mA indicating a high trapping (TRoRC) probability and an increase in EToRC could be due to a greater electron transport from increased electron availability. This suggests that remaining energy which has not been dissipated has been trapped and funnelled into the ETC. This relationship is shown in Figure 31 where the correlation between TRoRC and EToRC has a strong positive correlation where P<0.001. To add further strength to this argument, the correlation between EToRC and DIoRC shown in Figure 31 has a steep positive correlation (P<0.001). This implies that for a high electron transport flow, there is minimal dissipation of energy. This could explain why at greater doses of 680nm LASER, *Sinapis arvensis* plants appear to benefit photosynthetically.

It is important to remember here that the LASER at 680nm is highly specific to the P680 RC. Therefore, it is probable that in a situation where the whole spectrum of PAR is available to

plants, i.e., from sunlight, energy is absorbed in excess and so a higher level dissipated, but due to the specificity of the 680nm light, a lower intensity is needed to power the ETC.

For *Sinapis arvensis*, Fv.Fm values decline rapidly for all dwell times. OJIP parameter values barring Fv.Fm for *Sinapis arvensis* suggest this plant is in an improved photosynthetic condition when a dwell time of 7s at 2000mA is used as highlighted by P<0.001 between a 7s dwell time and the control and 5s dwell time values for Abs.RC, DIoRC, EToRC and TRoRC. The paired correlation for *Sinapis arvensis* (Figure 31) shows Fv.Fm to have negative correlations with all OJIP parameters whereas all other OJIP correlations show significantly positive relationships. Whilst all parameters excluding Fv.Fm could suggest the photosynthetic system of *Sinapis arvensis* is benefiting from 680nm LASER treatment, Fv.Fm correlations with the remaining parameters state the opposite. This contradictory finding suggests that the *Sinapis arvensis* plant is under stress if only Fv.Fm is taken into account, but may also support the idea that Fv.Fm is not the most reliable parameter to assess photosynthetic stress and is less sensitive to stress changes compared to the other parameters (Force et al., 2003). An experiment comparing OJIP parameter correlations between *Sinapis arvensis* plants treated with 680nm LASER doses as in this study and *Sinapis arvensis* plants treated with extremely intense photosynthetic photon flux density, (for example, that of natural sunlight has a PAR value of 900-1500µMol/m2/s or 3.8 x 1026 Joules a second when the sun is directly overhead (Varella et al., 2011)) could prove if *Sinapis arvensis* plants treated with 680nm do benefit from this treatment or if Fv.Fm is an inferior OJIP parameter and should not be relied upon.

In *Sinapis arvensis*, the Fv.Fm readings for the control, 5s and 7s dwell times are all significantly different to each other with P<0.001 (Figure 21) at 2000mA. Seppanen et al. (2000) stated that a plant with low Fv.Fm values indicate that reaction centres have been damaged which also leads to a reduction in electron transport. In this study, *Sinapis arvensis* at high doses (2000mA) have low Fv.Fm values but the EToRC for *Sinapis arvensis* at 2000mA and 7s dwell time is significantly greater (P<0.001) than the control (0s) and the 5s dwell time. In support of this, the pairs plot correlation (Figure 31) for Fv.Fm vs EToRC is negative (P<0.001), visibly demonstrating that an increasing EToRC leads to lower Fv.Fm values. One explanation is that the other RCs in the PSII LHC are damaged by the 680nm light at this dose but the chlorophyll *a* in P680 is not damaged by this intensity hence the increase in EToRC values at greater 680nm LASER doses. Figure 37 is a schematic of the organisation of LHCs and the P680 RC in the PSII complex. This could explain why Abs.RC is significantly greater at 2000mA 7s and why EToRC continues to increase at 7s dwell time 2000mA; the last and most crucial RC (as shown in Figure 37) in this process is working very well. EToRC quantifies the re-oxidation of reduced Q_A via electron transport in an

active RC. A high EToRC value means that P680 is unstressed and is able to pass on the electrons from the RC and release them to move onto Q_A. This is supported by Allakhverdiev and Murata (2004) and Ohnishi et al. (2005) who state that the electron transport rate through PSII does not relate to photodamage of PSII. This could explain why all parameters excluding Fv.Fm suggest the plant is benefitting from the 680nm LASER treatment.
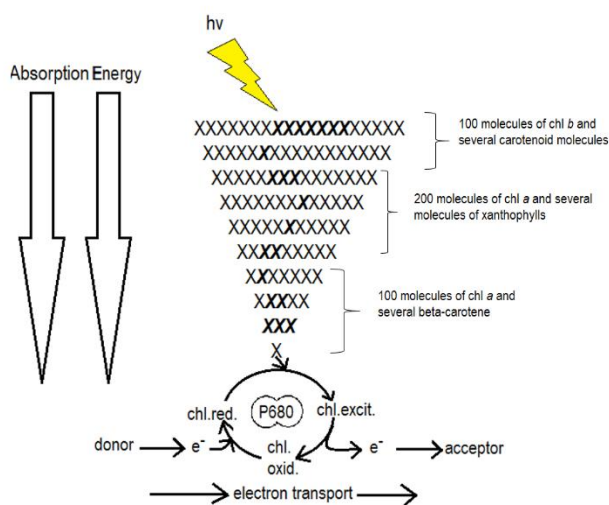
Figure 37 Schematic representation of the route taken by incident light photons, hv, from the antenna complexes to the P680RC. The special chlorophyll pair 'a' is reduced and then excited and subsequently reoxidised. The ejected electron enters into the electron transport chain via Q_A and Q_B.

4.5.3 Photoinhibition versus overload

As a general rule, photoinhibition occurs when photon flux densities exceed the photosynthetic capacity (Roach and Krieger-Liszkay, 2014) and the term is used to describe light induced inhibition of the normal workings of PSII (Murata et al., 2007a). When the photosynthetic capacity exceeds the biochemical systems' ability to minimise and mitigate damage to cellular components, a decline in photosynthetic efficiency occurs. This is due to the production of ROS and free radicals which can be detrimental to cellular and photosynthetic proteins and membranes. When damage exceeds the ability of the repair mechanisms to cope with the onslaught, the photosynthetic rate rapidly declines, hence,

photoinhibition (Aro et al., 1993, Hideg et al., 1998, Murata et al., 2007b, Takahashi et al., 2009, Takahashi and Murata, 2008, Tikkanen et al., 2014).

Traditionally, the OJIP parameter Fv.Fm has been used to detect photoinhibition (Burritt and Mackenzie, 2003, Kato et al., 2002, Long et al., 1994, Maxwell et al., 1994). There is now a plethora of published work which supports the idea that Fv.Fm is not the most reliable parameter (Demmig-Adams and Adams, 2006, Murchie and Niyogi, 2011, Takahashi et al., 2009, Takahashi and Murata, 2008). Force et al. (2003) states that photoinhibition is more reliably detected not by a decline in Fv.Fm values, but by a concurrent increase in DIoRC and decline in EToRC. The results in this study show no difference in the Fv.Fm ratio values for *Chenopodium album*, but for *Sinapis arvensis* treated with 2000mA, each dwell time (0s, 5s and 7s) are significantly different from one another and show marked decline (Figure 21). The DIoRC values for *Sinapis arvensis* do significantly increase with a 7s dwell time at 2000mA, but there is no such decline in EToRC, but a significant increase. This suggests that as Force et al. (2003) eludes to, photoinhibition is not occurring, but P680 is being affected through a more direct approach from the 680nm LASER but not in a detrimental way.

4.5.4 Leaf chlorosis

The leaves of *Chenopodium album* often demonstrated visible chlorosis during growth in the glasshouse environment. It has previously been argued in the literature that changes in the chlorophyll content of leaves has a marked influence on fluorescence readings thus casting doubt on the validity of data (Hsu and Leu, 2003, Susila et al., 2004). It could be expected that chlorophyll fluorescence emissions depend on the abundance of chlorophyll present in leaves. Hsu and Leu (2003) demonstrated that when two leaves were sitting on top of each other, the chlorophyll *a* fluorescence was more than from one leaf. However, physical layout of leaves in terms of adaxial or abaxial orientation dramatically influences fluorescence emissions (Dinc et al., 2012) so the results of Hsu and Leu (2003) should not be relied upon. It is now accepted that chloroplasts can adapt to light environments over time through adaptations in antenna size or changes in PSI:PSII ratio. *Chenopodium album* was grown in the glasshouse for approximately 20 days from germination so the fluorescence data from *Chenopodium album* can be relied upon even with chlorosis of the leaves. In addition, Fm and Fo values (used to calculate Fv.Fm) are not related to the chlorophyll content in leaves (Dinc et al., 2012). However, for future studies, it might be wise to measure fluorescence parameters every day to ensure that fluorescence emissions do not have a wide range of values.

4.5.5 Percentage relative conductivity readings

The dramatic increase in conductivity levels for *Sinapis arvensis* at 2000mA and a 10s dwell time is not unexpected. This increase is most likely due to physical damage to the leaf material by heat from the 680nm LASER through cellular ablation. OJIP was not measured at doses 1800mA to 2000mA for a dwell time of 10s because of visible physical damage which affected the optics.

4.5.6 SOD units per mg total protein analysis

The SOD assay data does not show any definitive finding for either *Sinapis arvensis* or *Chenopodium album*. Plants under stressful conditions are likely to suffer oxidative stress and it is generally accepted that as oxidative stress in a plant increases, the levels of antioxidant enzymes produced to counteract detrimental effects of ROS also increase (Alscher et al., 2002, Asada, 2006). It is hypothesised that the high intensity 680nm LASER would overload special pair of chlorophyll a in the P680 RC which could be conceived as a stressful environment for the plant generating ROS including superoxide.

Aside for assessing if high 680nm light intensity inducing the production of ROS, focusing on superoxide, another aim of conducing the SOD units assay was to give a complete and detailed picture on the effects of the 680nm LASER downstream from PSII. Specifically, clarification is needed regarding the fate of energy leaving PSII. It was hypothesised that the 680nm LASER could overload the P680 RC in PSII thus resulting in the shutdown of this domain. But as OJIP data shows, particularly for *Sinapis arvensis*, 680nm LASER treatment alone appears to influence the photosynthetic ETC is a positive way.

The method used to quantify oxidative stress levels in 680nm LASER treated plant samples is the SOD assay. SOD neutralises the superoxide anion radical into O_2 or H_2O_2 (Alscher et al., 2002). Superoxide anion radicals can be generated in photosynthesis, but more so from the PSI complex rather than PSII (Asada, 1999, Asada, 2006, Rizhsky et al., 2003, Scheller and Haldrup, 2005). The water-water cycle is an effective generator of superoxide on the reducing side of PSI, the aim of which is to dissipate excess light by increasing the rate of electron transport (Asada, 1999, Asada, 2006, Rizhsky et al., 2003). It is possible that with an increased absorption of 680nm, excess energy would be funnelled through to PSI resulting in superoxide production via the water-water cycle in order to clear the backlog of excess absorbed light. SOD unit analysis could therefore provide an insight as to the fate of

incident 680nm light if it is passed on from the PSII P680 RC to Pheo and so on. The expectation might therefore be a positive correlation between increased EToRC values (as in 680nm LASER treated *Sinapis arvensis*) and greater SOD production.

Superoxide production from PSII is acknowledged (Ananyev et al., 1994, Pospisil et al., 2006). As stated on page 30 back electron transport from Q_A^- to Pheo results in the formation of the highly deleterious singlet oxygen. To prevent back electron transport, electrons from Q_A^- leak onto O_2 forming superoxide (Pospisil, 2016). Producing superoxide does not threaten the integrity of the cell as superoxide is nullified by enzymatic dismutation to H_2O_2 by FeSOD in the vicinity of PSII (Pospisil, 2016). This back-electron transport is more likely to occur when herbicides are used, including Calaris® and Sencorex Flow® which cease the flow of electrons from Q_A to Q_B. Therefore, SOD analysis could provide useful information when herbicide treatment is combined with 680nm LASER treatment to determine if reverse electron flow increase upon combined treatment.

The results of SOD analysis when treating *Chenopodium album* and *Sinapis arvensis* with 680nm LASER treatment only do not show any clear responses and any conclusions drawn from this data should be taken carefully. A possible reason for the lack of a data concordance in the SOD assay results could mean that the 680nm light is targeting the P680 RC efficiently and only causing stress to a small section of PSII. Chlorophylls are coupled with carotenoids in order to quench excess energy (Pospisil, 2016). However, some researchers have stated that the carotenoids in the P680 RC are located too far away from the chlorophyll a special pair (the 680nm LASER target) to have any quenching activity (Loll et al., 2005, Umena et al., 2011). Taking these findings into account, large production of superoxide at PSII is unlikely so the focus of superoxide and subsequently SOD production concentrates on PSI. As stated, the water-water cycle in PSI aims to clear the backlog of absorbed excess energy (Asada, 1999, Asada, 2006, Rizhsky et al., 2003). In *Sinapis arvensis*, increasing EToRC at higher LASER doses implies energy has successfully been passed on through PSII and is now powering the ETC. The aim of administering high doses of 680nm light is not to benefit the plant but to decrease photosynthetic capacity. It would appear, judging from the lack of a pattern in SOD unit levels that PSI is capable of processing absorbed energy whether it be in excess or not from PSII. An explanation for the decline in SOD activity, specifically in *Sinapis arvensis* (Figure 34) may be due to enzyme denaturation at greater 680nm LASER doses.

One possible explanation for the peaks and troughs and seemingly unpredictable relationship between 680nm LASER treatment and SOD production could be due to the sample preparation procedure. Wounding plant tissue is positively correlates with oxidative

damage of lipids and proteins (Savatin et al., 2014) and wounding of *Pisum sativum* seedlings has been shown to result in oxidative burst (Roach et al., 2015). Further, wounding in *Arabidopsis* has led to the direct detection of superoxide anion radical and H_2O_2 through NBT and DAB staining, respectively (Morker and Roberts, 2011). Therefore, the presence of SOD in the plant samples could be due to sample processing flaws or cellular ablation of the plant tissue from the 680nm LASER which is possible at higher doses, or through freezing of samples post 680nm LASER treatment. However, sample preparation for all plant samples was consistent. It is likely that the decline in SOD units/mg total protein in Sinapis arvensis with increasing 680nm LASER dose is due to the denaturation of SOD enzymes through heat and cellular ablation effects (Figure 34).

With the current set up of equipment, this flaw in the experimental protocol would be difficult to mitigate against. The 680nm LASER was shone through an aperture with a diameter of 7mm to mimic OJIP analysis with the leaf clips. Excision of the treated leaf area from the whole intact leaf is unavoidable. Ideally, a larger area of leaf treated with the 680nm LASER is needed in order to minimise the error and wounding of the plant. Samples were stored on ice immediately after treatment to prevent further biochemical reactions but excision of the treated area took place prior to storing on ice. The production of superoxide is therefore likely to be greater through wounding instead of the subtle biochemistry hypothesised as a result of 680nm incident light.

For further investigation of this, it could be interesting to see the comparison between superoxide production in PSII compared to PSI using PSII and PSI isolates separated along a sucrose gradient and measuring changes in NBT absorbance (Dunahay and Staehelin, 1985). In addition, assessment of superoxide production in plant samples under high light intensity of 700nm could determine if inducing photoinhibition of PSI with LASER energy is more effective than in PSII.

As the main ROS produced in PSII is singlet oxygen, it could be prudent in a future experiment to assess for singlet oxygen responses rather than for superoxide after LASER treatment. This can be achieved with a confocal LASER scanning microscope as in Prasad et al. (2017), currently not available at HAU.

4.6 Determination of the correct dosage of 680nm LASER for the dual treatment of LASER plus herbicide

4.6.1 Sinapis arvensis 680nm LASER dose determination

When looking at Table 6(b) containing OJIP parameter data for *Sinapis arvensis*, there appear to be two possible 680nm LASER settings suitable.

Ideally, for an effective treatment with a view to overload PSII, the Abs.RC values should ideally be greater than the control as a light source of 680nm should be readily be absorbed by PSII. Similarly TRoRC would ideally increase for the same logic as Abs.RC. The EToRC parameter should be significantly reduced to the control highlighting damage to the P680 RC. DIoRC should be significantly increased in value compared to untreated samples as the plant is not able to power the ETC using this intensity of light (suggested by the drop in the EToRC value) and so energy is dissipated. The Fv.Fm value shows a significant rise compared to the control. Whilst work in this field (Force et al., 2003) has suggested Fv.Fm is not the most reliable OJIP parameter, it should not be completely ignored.

In light of this reasoning, the more efficient dose to use could be 1500mA with a 5s dwell time. The OJIP readings for this show Fv.Fm and EToRC to have a significant reduction compared to control readings whilst Abs.RC, TRoRC and DIoRC show little deviation from the control values. Whilst there is less distinct information compared to the dose of 1400mA and 5s dwell time, Fv.Fm shows an overall decline in the state of PSII (compared to an increase for 1400mA, 5s dwell time) and EToRC shows a significant reduction suggesting damage in the P680 RC and inhibition of electron transport. Whilst there is little information regarding Abs.RC, TRoRC and DIoRC, these have not significantly declined.

In conclusion, it would be unwise to choose a 680nm LASER dose to use, when combining with the herbicide treatment, which shows an increase in the health of PSII (as shown by Fv.Fm for the dose of 1400mA, 5s dwell time). Further to this, the main focus of the 680nm LASER treatment is to inhibit the ETC. There are only two 680nm LASER doses which significantly reduce EToRC; the aforementioned doses (1500mA with a 5s dwell time and 1400mA, also a 5s dwell time). There is not a higher dose which has the same effect as this but actually promote a significant increase in EToRC (see Table 6(b)).

The % relative conductivity data from the *Sinapis arvensis* 680nm LASER treated samples shows very little in regards to these aforementioned doses and throws further doubt as to whether conductivity readings are the best approach for such fine biochemical reactions.

SOD assay data also gives very minimal insight into SOD responses to increasing 680nm LASER doses.

4.6.2 Chenopodium album 680nm LASER dose determination

Determining the appropriate 680nm LASER dose for *Chenopodium album* is more straight forward than for *Sinapis arvensis*. The dose of 1600mA and 10s dwell time has ideal OJIP outcomes (see Table 6(a). The parameters Abs.RC and TRoRC show significant increases in value compared to the control, suggesting the light is absorbed well and trapped well. EToRC shows a significant reduction to the control highlighting inhibition of the ETC. DIoRC shows as significant increase to the control, which is preferable; energy has been absorbed well, but cannot be passed on to the ETC so is dissipated. Overall, PSII is showing a decline in health suggested by the significant reduction in the Fv.Fm value.

4.7   Conclusion and further work

The findings in this chapter demonstrate 680nm LASER energy having very little, if any, detrimental effect on the plants studied in terms of OJIP parameters in particular. Ohnishi et al. (2005) suggested that the working state of photosystem II could be affected by supplying the plant with two different wavelengths of light in a two-step process. Firstly, 500nm light (blue region) which is highly effective for OEC inactivation but not effective for PSII RC inactivation was illuminated onto thylakoid membranes. Following this, the same membranes were illuminated with 680nm light (red region) thus inactivating the PSII RC but having little influence on the OEC. Ohnishi et al. (2005) concluded that P680 only becomes sensitive to 680nm light when the OEC has been inactivated by the 500nm light.

If further work was possible, it would be interesting to treat plants with 500nm as well as 680nm and OJIP parameters measured to see if a dual wavelength approach has a greater effect on PSII. In addition, it would be intriguing to see the outcomes regarding OJIP parameters when light targeting PSI, 700nm is applied either in combination with 680nm or 680nm plus 500nm. How PSII inhibiting herbicides further interact with these light treatment combinations could be a highly rewarding addition to this area of research.

Using only 680nm LASER energy as the treatment, it is clear from OJIP data analysis in particular, that the 680nm LASER alone does have an effect on the plants studied, especially *Sinapis arvensis*. The different responses have been displayed on pages 99-109. It would appear instead of photoinhibition of PSII, overload of the P680 RC is occurring in

some instances. The next step is to use a dual treatment of PS ETC inhibiting herbicides along with the 680nm LASER energy to cause further detrimental effects on the plants' photosynthetic machinery. The role of the herbicides will be to stop the flow of electrons from P680 RC onwards. It is therefore hypothesised that this electron transport inhibition could cause further stress to upstream machinery leading to free radical and ROS production, leading to a shutdown of PS in the affected plant areas of treatment.

The % relative conductivity data suggests that *Sinapis arvensis* is more susceptible to lipid peroxidation than *Chenopodium album*. This could be due differences in the water content of the leaves of *Sinapis arvensis* and *Chenopodium album*. The higher conductivity readings for both *Sinapis arvensis* and *Chenopodium album* at 2000mA and a 7s dwell time is not surprising and the likelihood of this being down to cellular ablation due to heat from the 680nm LASER is high. This is the more likely scenario than the 680nm LASER triggering ROS and free radical production and increasing the conductivity reading so significantly.

Chapter 5

Combining 680nm LASER energy with electron transport chain inhibiting herbicides to further compromise the working state of PSII

5.1 Objective

The objective in this chapter was to determine the optimal dose of herbicide in conjunction with 680nm LASER treatment in *S.arvensis* and *C.album* to overload PSII.

5.2 Abstract

This chapter focused on the combination of 680nm LASER doses with pre-determined herbicide doses as detailed in Chapter 3. This chapter is the amalgamation of findings from Chapters 3 and 4 in order to devise a treatment plan with the combination of 680nm LASER and herbicide treatment. The overall aim of the project was to use low energy LASER doses and a minimal herbicide dose whilst still maintaining effective weed control. This chapter assesses if a dual treatment of LASER and herbicide, albeit both at low doses, can combine to form a powerful treatment.

5.3 Introduction

This chapter focuses on the dual treatment of PSII inhibitors and the use of 680nm LASER energy at 680nm. Treatment with Nevada® which does not directly target PSII is to provide comparison of outcomes when plants are treated with chemicals of different modes of action in conjunction with 680nm LASER energy.

It is hypothesised that after treatment of Calaris® or Sencorex Flow®, any excitation energy generated by P680, will not be dissipated by normal electron transport after the Q_A^- step due to the herbicide induced blockage at Q_A^-. With a dose of 680nm LASER energy administered thus overloading P680, this effect could be accentuated, markedly increasing the fluorescence yield and potentially leading to the production of ROS.

Work has shown PSII to be the most sensitive part of the photosynthetic apparatus to stressors including light and heat (Baker, 2008, Baker and Rosenqvist, 2004). The 680nm LASER is likely to include light and heat stress on treated plants. This abiotic stress could

lead to biochemical damage from the production of reactive oxygen species (ROS) along with free radical formation indirectly quantified by SOD production. Lipid peroxidation according to the mechanisms outlined in Chapter 1 are also a likely outcome of 680nm LASER and herbicide treatment and this is quantified by relative conductivity readings of treated plant samples. It is unlikely that the resultant biochemical effects after LASER treatment are due to heat effects from the LASER as the diode was low energy and was temperature controlled and there was no visible change in the leaf surface after treatment after visualisation under a microscope at the doses used. For future work, it would be wise to measure the temperature of the leaf surface whilst the LASER is being administered to rule out heat stress effects.

5.4   OJIP reading results

For clarity in the preceding discussion, it is worth noting that all OJIP measurements were taken after addition of 680nm LASER energy (see materials and methods chapter). 680nm LASER light was applied 24 hours after herbicide treatment for all plants, doses and herbicide types. The reasoning behind this decision is detailed on page 26. Similarly, the logic behind herbicide dose treatments is explained on page 94.

5.4.1 OJIP readings for *Chenopodium album* treated with 680nm LASER and Sencorex Flow® at a rate of 0.0625lha^{-1}

A factorial ANOVA was carried out to determine the presence of any interactions between factors, i.e., 680nm LASER usage, dwell time and mA dose. Across all five OJIP parameters (Fv.Fm, Abs.RC, TRoRC, EToRC and DIoRC), there is no demonstration of an interaction between mA and Dwell time. As factors, block and 680nm LASER show significance ($p < 0.001$) across all parameters suggesting a discrepancy in conditions between treatment day.

Figure 38 displays how all five measured OJIP parameters are influenced by LASER dwell time. The parameters of Fv.Fm and DIoRC show a wide range in data points across 680nm LASER dose but with little coherence. Figure 38(a) shows how Fv.Fm values remain in the normal range (0.79±0.3) for untreated plants and show a decline for 680nm LASER+Sencorex Flow® treatment and Sencorex Flow® treatment alone. This is unsurprising and likely to be a result of the herbicide rather than the LASER treatment, mostly suggested by the similarity of results for Sencorex Flow® treated plants and Sencorex Flow®+ 680nm LASER treated plants, albeit at the low dose of 0.0625lha^{-1}. The

dramatic decline in Fv.Fm value for 5s dwell time at 1800mA is unlikely to be a result of the 680nm LASER and more likely to be a collection of erroneous data points as this result is not supported by other findings in previous trials focusing on the 680nm LASER treatment exclusively.

Abs.RC values (light absorption) (Figure 38(b)) are generally greater upon 680nm LASER treatment but as with Fv.Fm values, lack distinct outcomes. A dwell time of 10s at 1900mA and 2000mA yields significantly greater Abs.RC values than all other dwell times ($P<0.001$). This result suggests that for a more prolonged length of time, PSII is absorbing the 680nm energy well compared with other dwell times. As Figure 38 (e) shows, dissipation (DIoRC) at the aforementioned doses is significantly greater than plants treated with Sencorex Flow® only (no LASER) suggesting energy at these doses is absorbed well but cannot be funnelled into the ETC due to the block in electron transport induced by Sencorex Flow®. Elevated dissipation (DIoRC) levels could be exacerbated by a low electron transport rate which necessitates the need to remove energy through non-photochemical quenching methods.

Trapping (TRoRC) (Figure 38 (c)) and electron transport (EToRC) (Figure 38 (d)) rate values both show very little deviation from a consistent range of values after 680nm LASER treatment. This suggests that the 680nm LASER is not influential to these parameters or that actions of Sencorex Flow® are overpowering any effects of the 680nm LASER at these OJIP 'check-points'. EToRC values contain no significant differences to the control when 680nm LASER is applied at any mA, possibly highlighting the block in the PSII ETC induced by Sencorex Flow® treatment where application of 680nm energy has no influence. The decline in EToRC values is possible even at this low dose (dose 0.0625lha) as highlighted in Chapter 3. More concentrated doses of Sencorex Flow® could result in larger deviations from the range shown in Figures 38 (a) to (e).

One interesting observation is the spike in values present in all OJIP parameters in *Chenopodium album*. This sharp increase in values is not consistent with a single dwell time but appears to be produced at either 1800mA or 1900mA. It is worth noting that when OJIP parameters were analysed when *Chenopodium album* plants were treated with only the 680nm LASER, in the 1800mA and 1900mA dose levels, there were signs that the 680nm LASER was influencing the state of PSII. Typically, this was highlighted by significantly decreased Fv.Fm values compared to the control, significantly increased Abs.RC and DIoRC values compared to the control and for a dose of 1900mA, significantly increased TRoRC values compared to the control. EToRC for both 1800mA and 1900mA remained significantly unchanged compared to the control. It is also worth noting that with 680nm LASER treatment exclusively, *Chenopodium album* plants displayed a convergence of data

points at 2000mA with more turbulent data at lower 680nm LASER doses with little or no response evident other than convergence at 2000mA. With the addition of Sencorex Flow® alongside 680nm LASER energy, a convergence in data points is only the case in EToRC data (Figure 38(d)) and with the exception of spikes in data, values follow a more consistent path compared with when the 680nm LASER is used exclusively. This could suggest that as expected, the action of Sencorex Flow® acts as a leveller and hides the action of the 680nm LASER.
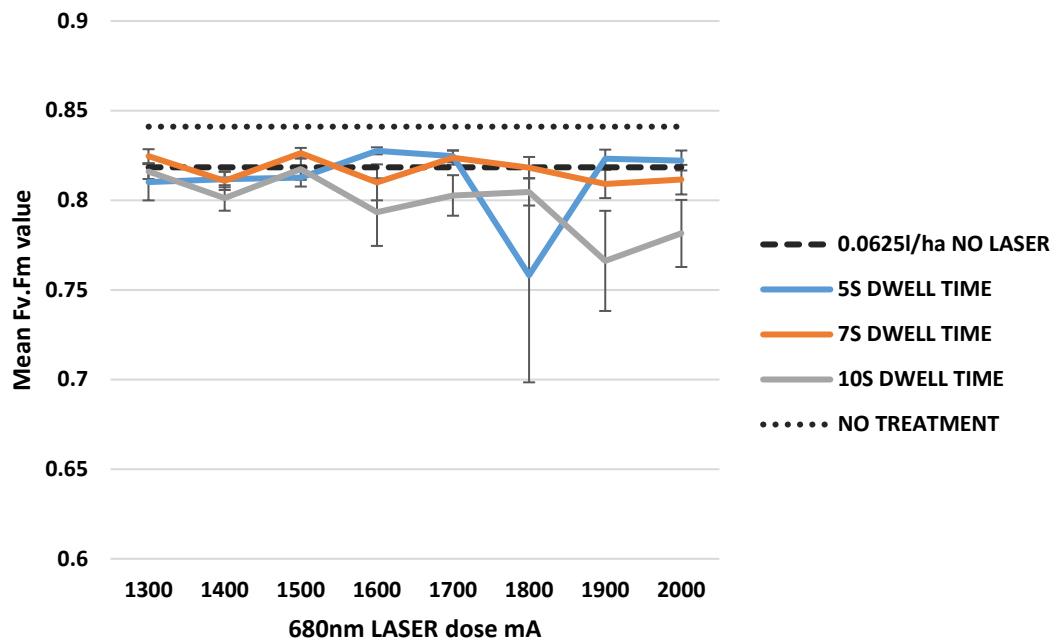
(a)
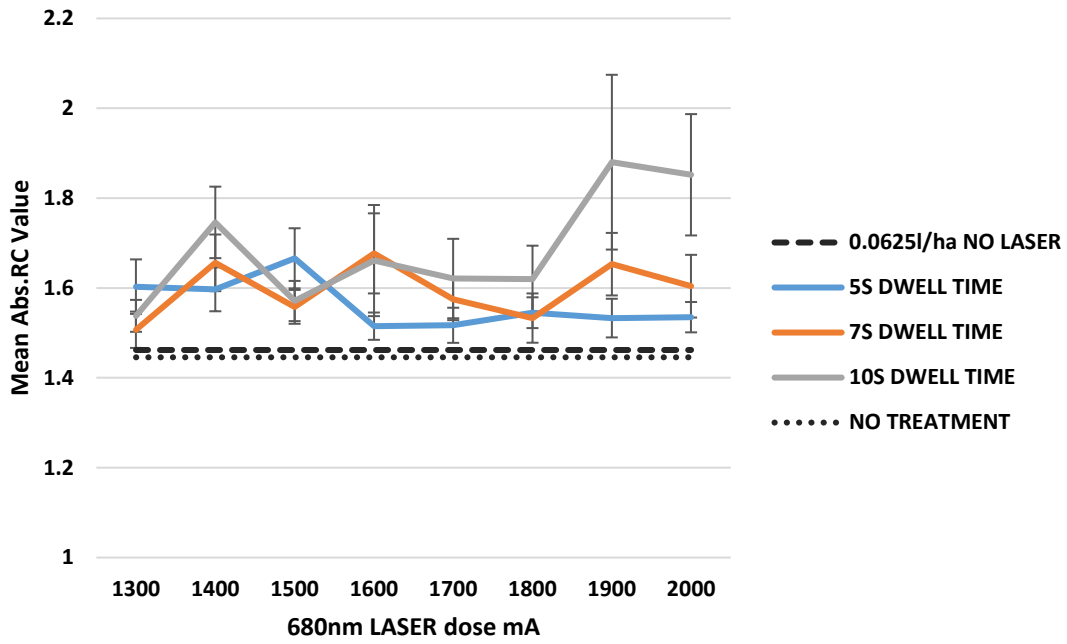
(b)
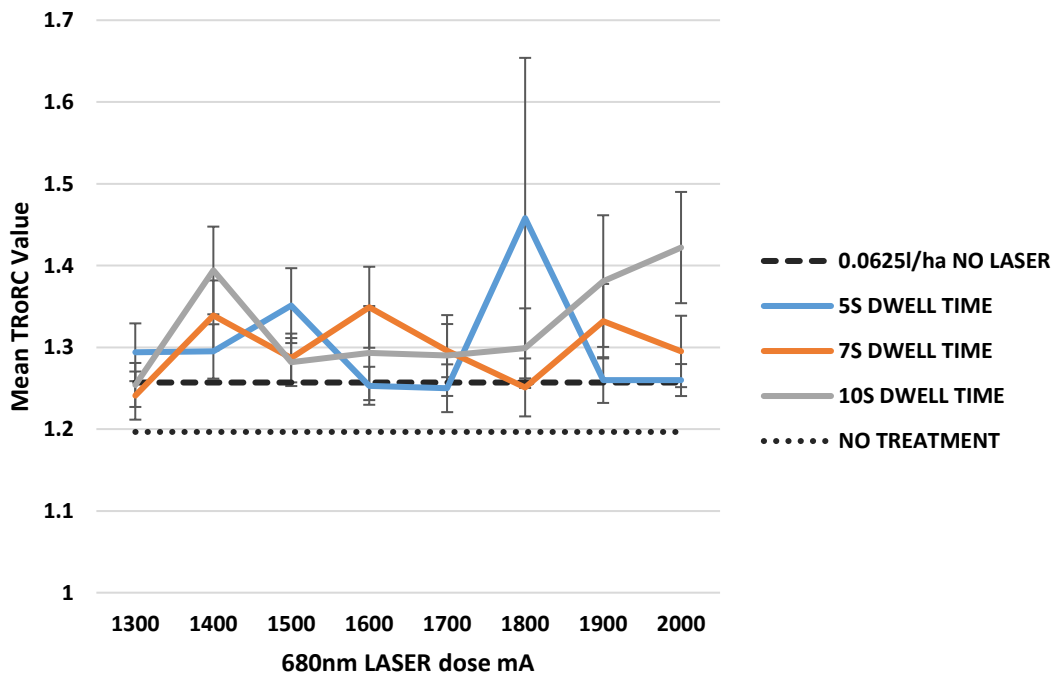
(c)

(d)

(e)

Figure 38 The (a) mean Fv.Fm values, (b) mean Abs.RC values, (c) mean TRoRC values, (d) mean EToRC values and (e) mean DIoRC values in Chenopodium album plants in response to 680nm LASER doses (mA) and Sencorex Flow® at a dose of 0.0625lha⁻¹. NO TREATMENT is classified by plants not treated with herbicide or 680nm LASER energy.   0.0625l/ha NO LASER denotes

0.0625lha⁻¹ of Sencorex Flow® exclusively. Error bars denote ± standard error of the mean (SEM), n=12. Significant outcomes calculated using factorial ANOVA and T-Test.

As previously mentioned (page 35-41), all of the OJIP parameters analysed form interlinking relationships. Figure 38 highlights the relationships between each OJIP parameter in *Chenopodium album* after Sencorex Flow® treatment at dose 0.0625lha treated at 680nm LASER doses. 680nm LASER treatments are not specified in Figure 41, it is merely to demonstrate the intertwined nature of the five OJIP parameters. The strongest positive correlations are between Abs.RC and TRoRC, Abs.RC and DIoRC and finally TRoRC and DIoRC (P<0.001). Strong negative correlations can be observed between Fv.Fm and Abs.RC, Fv.Fm and TRoRC and between Fv.Fm and DIoRC (P<0.001). No correlation exists when EToRC is a factor, highlighting the disruptive effect of Sencorex Flow® on the photosynthetic ETC. A detailed explanation of the interlinking relationships of OJIP parameters is discussed on pages 35-41.
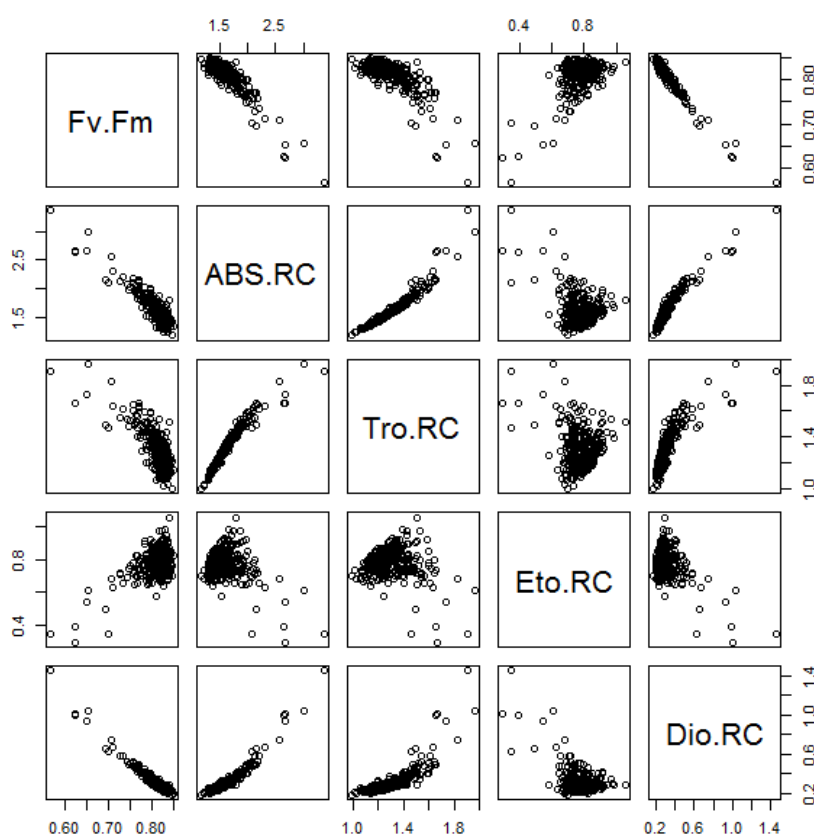
Figure 39 Pairs correlation matrix for Chenopodium album treated with Sencorex Flow® at a dose of 0.0625lha⁻¹. Significant differences in parameter data were calculated using the Kruskal-Wallis Test using the statistical program 'R'.

5.4.2 OJIP readings for *Chenopodium album* treated with 680nm LASER and Calaris® at a rate of 0.5lha^{-1}

An ANOVA was run to determine the presence of any interactions between factors, i.e., 680nm LASER usage, dwell time and mA dose. Across all five parameters, there is no demonstration of an interaction between mA and Dwell time. Block and LASER factors show significance ($p<0.001$) across all parameters.

When looking more specifically into certain points of the PSII energy transfer process, the outcomes do not necessarily reflect the promising decline of Fv.Fm, which could suggest reduced efficiency of PSII. For example, EToRC levels across all 680nm LASER doses in *Chenopodium album* in conjunction with Calaris® treatment (dose 0.5lha^{-1}) (Figure 40(d)) show no significant different values for 680nm LASER dwell times and EToRC values from the range of doses follow a similar pattern for all 680nm LASER doses. However, 680nm LASER treated samples show consistently significantly reduced EToRC values than untreated plants samples ($P<0.001$). Plants treated with Calaris® at a dose of 0.5lha exclusively have EToRC values in a similar range as 680nm LASER treated samples highlighting the probability that any lowering of EToRC values is independent of 680nm LASER treatment and that herbicidal effects are wholly responsible for any reduction in values.

Figure 40 (b) shows that absorbance (Abs.RC) is consistently significantly increased compared to the untreated plants. It is therefore unsurprising that dissipation values are also increased for herbicide treated plants compared to the untreated samples, i.e., greater absorption leading to greater dissipation. Dissipation (DIoRC) levels (Figure 40(e)) are likely to be enhanced by the block in ETC induced by herbicidal action.

Trapping responses to 680nm LASER application are elevated but few 680nm LASER doses produce significantly greater trapping levels compared to plants treated with Calaris® but lacking 680nm LASER treatment. A T-Test reveals no significant difference between untreated plants and Calaris® only treated plants ($P=0.570$). Most plants treated with both 680nm LASER+Calaris® show significantly greater trapping values compared to completely untreated plants. 680nm LASER+Calaris® treatment in conjunction does not result in significantly greater TRoRC values compared to Calaris® treatment alone. Figure 40 (c) (trapping/TRoRC) shows trapping levels to be raised after 680nm LASER+Calaris®

treatment, suggesting the 680nm LASER is having an influence on trapping capability. As absorbance is increased, this leaves a greater opportunity for energy to be trapped.

In general in this cohort of parameter responses, there is little alteration in values upon 680nm LASER application, except for the Fv.Fm parameter which shows a promising reduction in values upon 680nm LASER treatment. This reduction in Fv.Fm, albeit non-significant compared to herbicide only treated samples (see Chapter 3) for most doses, is not supported by the other OJIP parameters in terms of PSII decline in response to 680nm LASER treatment. This could suggest that other factors are responsible for the decline in Fv.Fm. As Figure 41 displays, there is a large discrepancy in data values between blocks 1 and 2 (Figure 41, right), which is likely to have swayed the data and resulted in lower average values. A discrepancy such as this could be a result of general plant condition on the treatment or measurement day as all measurements for individual blocks were taken on the same days.

As in Sencorex Flow® treated *Chenopodium album*, there are spikes in the data at consistent doses highlighted in all parameters. With Calaris® treated *Chenopodium album*, spikes are consistently at 1900mA. Whilst not all spikes have significantly different values to the control, it is still an important observation worth highlighting.
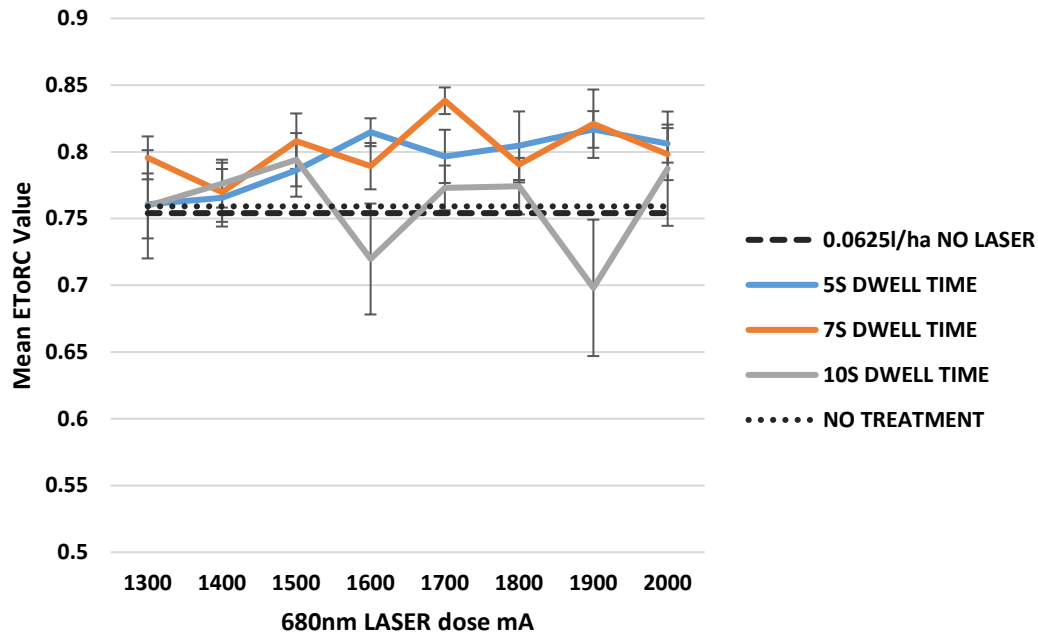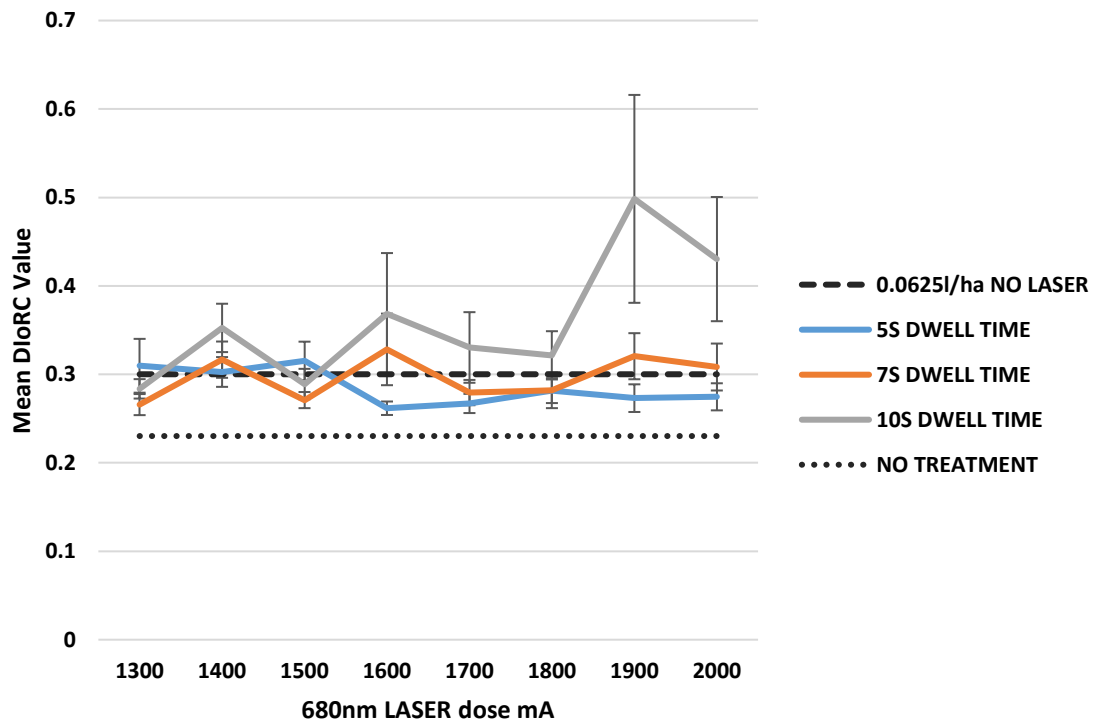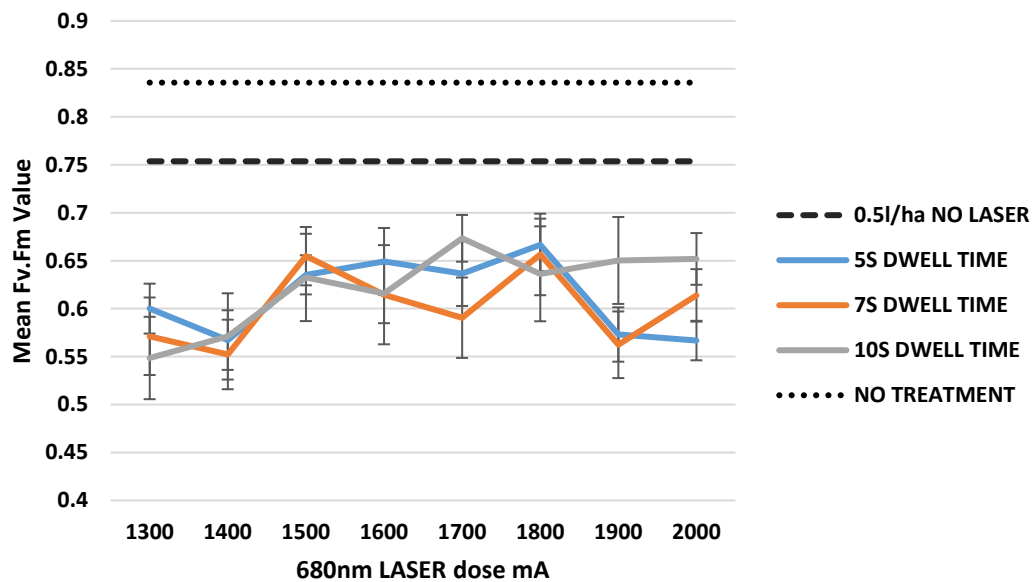

(a)
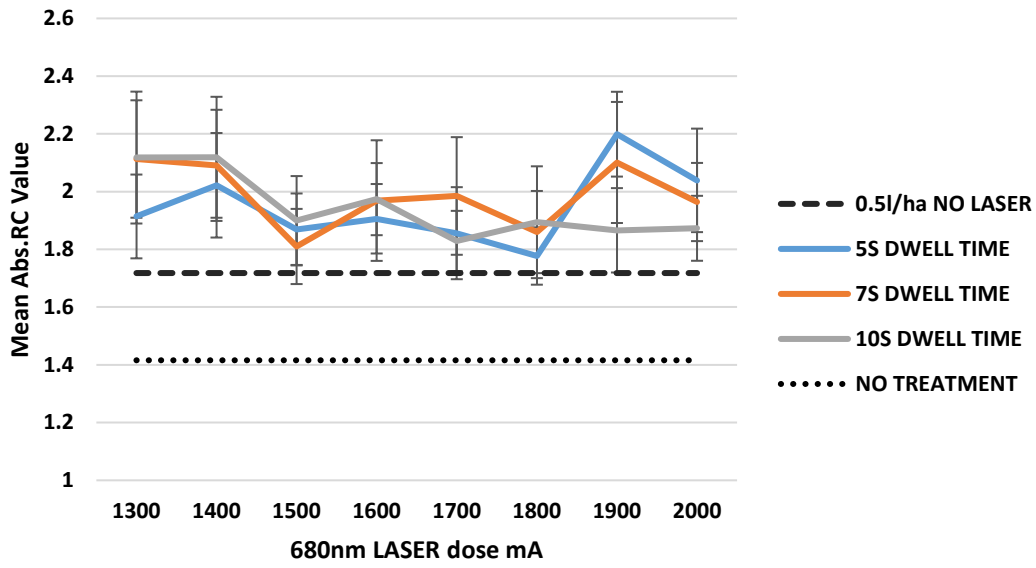
(b)
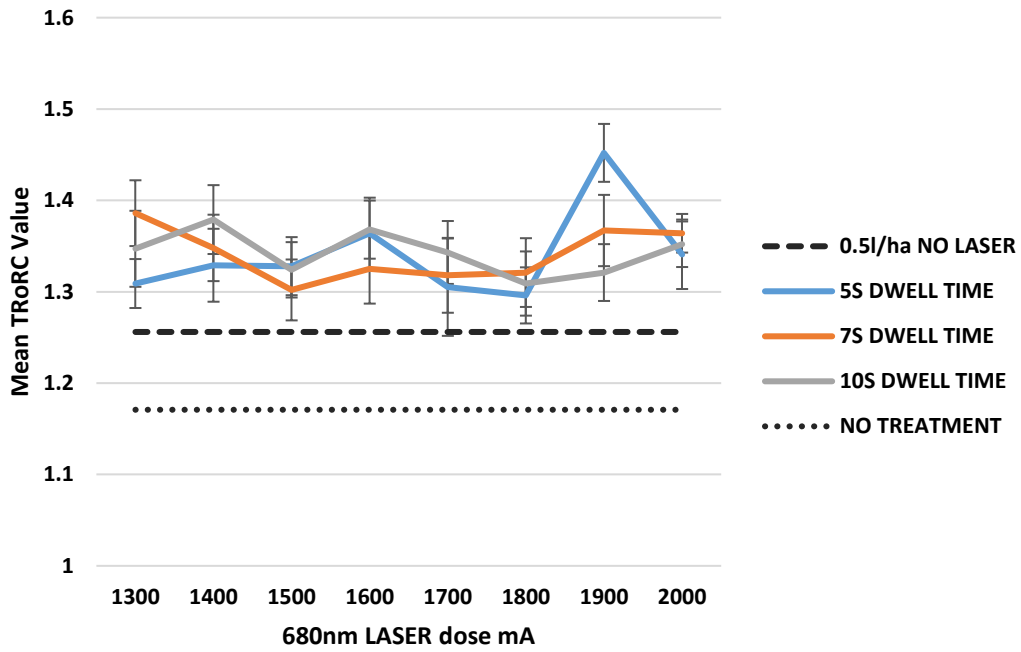
(c)

(d)

(e)

Figure 40 The (a) mean Fv.Fm values, (b) mean Abs.RC values, (c) mean TRoRC values, (d) mean EToRC values and (e) mean DIoRC values in Chenopodium album plants in response to 680nm LASER doses (mA) and Calaris® at a dose of 0.5lha^{-1}. NO TREATMENT is classified by plants not treated with herbicide or 680nm LASER energy. 0.5l/ha NO LASER denotes 0.5lha^{-1} of Calaris® exclusively. Error bars denote ± standard error of the mean (SEM), n=12. Significant outcomes calculated using factorial ANOVA and T-Test.

Figure 41 presents interlinking relationships of the five assessed OJIP parameters. All five parameters show significant correlations on a pairs correlation test with all P values <0.001. There is a large discrepancy within this data set. Figure 41 (right) more clearly shows the discrepancy lies between blocks. Nevertheless, P value data is not affected by this. This difference between blocks could account for the lack of significant interactions between treatment factors when running the unbalanced ANOVA. Further, the difference between data in blocks 1 and 2 is responsible for the data distribution as shown in Figure 41 (right).

In conclusion, it would be highly valuable to re-run this trial to remove the discrepancy between blocks and yield more accurate data.
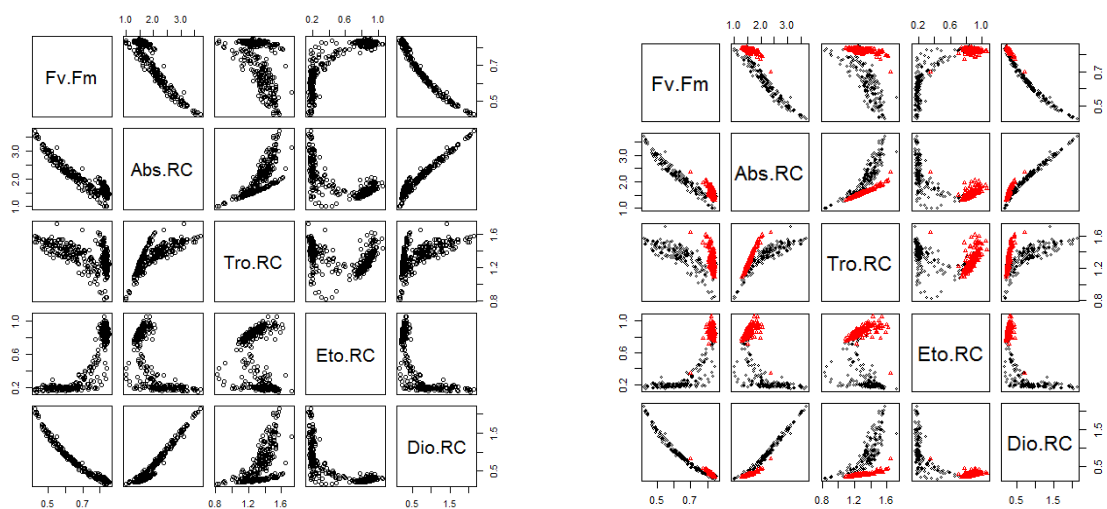
Figure 41 (left) pairs correlation matrix for Chenopodium album plants in response to 680nm LASER energy + Calaris® treatment at a dose of 0.5lha⁻¹ Tro.RC = TRoRC, Eto.RC = EToRC, Dio.RC = DIoRC,. (right) pairs correlation matrix for Chenopodium album plants in response to 680nm LASER energy + Calaris® treatment at a dose of 0.5lha⁻¹ Tro.RC = TRoRC, Eto.RC = EToRC, Dio.RC = DIoRC Black data points represent block 1, red data points represent block 2, blocks treated as factors. Significant differences in parameter data were calculated using the Kruskal-Wallis Test using the statistical program 'R'.

5.4.3 OJIP readings for *Chenopodium album* treated with 680nm LASER and Nevada® at a rate of 1.0lha^{-1}

As documented, the mode of action of Nevada® does not affect PSII, supported by the highly similar EToRC values between untreated and Nevada® treated plants (Figure 42 (d)). Fv.Fm values (Figure 42 (a)) are significantly reduced (P<0.001) when dwell times of 5s and 10s at 1900mA are used compared to Nevada® only (w/o 680nm LASER) treated plants. Plants treated with dose 1.0lha^{-1} of Nevada® alone, also show reduced Fv.Fm levels compared to untreated plants (P=0.008), suggesting it is not the application of 680nm LASER which is responsible for the reduction of Fv.Fm values. This finding remains intriguing due to the fact the mode of action of Nevada® is not related to PSII in any way. The decline in Fv.Fm is possibly due to the overall plant decline upon Nevada® treatment and a decreased supply of photosynthetic proteins resulting from the mode of action of Florasulam (5g/l). Florasulam acts as a protein synthesis inhibitor (Liu et al., 2015). Turnover of proteins including the D1 protein which is crucial to the functioning of PSII will therefore cease under the action of Nevada®. It is this effect which could result in a decline PSII viability leading to Fv.Fm reduction. A further interesting finding is the dramatic increase in trapping capability upon Nevada® application compared to untreated plants. It could be assumed that an increase in trapping could lead to a subsequent increase in EToRC, but this is not the case. Furthermore, dissipation levels are also not subsequently increased after Nevada® treatment. This begs the question of where the increase in trapped energy has been transferred to if it has not been dissipated. One possibility is the loss of energy through repeated attempts of initiating the ETC flow.

There is a consistent spike in values at 1900mA, a finding which is not dissimilar to values in Calaris® and Sencorex Flow® treated *Chenopodium album* plants. Findings from *Chenopodium album* plants treated with the 680nm LASER alone, show differences in OJIP data with after treatment with 1900mA. This was characterised by a significant decline in Fv.Fm at a dose of 1900mA for a period of 10s compared to the control (without 680nm LASER treatment) and a significant increase in Abs.RC, DIoRC and TRoRC parameters compared to the control. EToRC values after 680nm LASER only treatment remained largely unchanged which is consistent across 680nm LASER treatment alongside Calaris® and Sencorex Flow® application. It could be prudent to explore the effects of this dosage further as this spike is present in Sencorex Flow® and Calaris® treated samples but is more pronounced after Nevada® treatment. As Nevada® does not contain an active ingredient responsible for the disruption of the ETC, this data could be seen as more valuable than with Calaris® and Sencorex Flow® treatment as it exposes the action of the 680nm LASER,

whereas Calaris® and Sencorex Flow® treatment is hypothesised to negate the effects of the LASER. It is therefore plausible that the action of the 680nm LASER is highly effective at 1900mA with a strong dual action effect present.
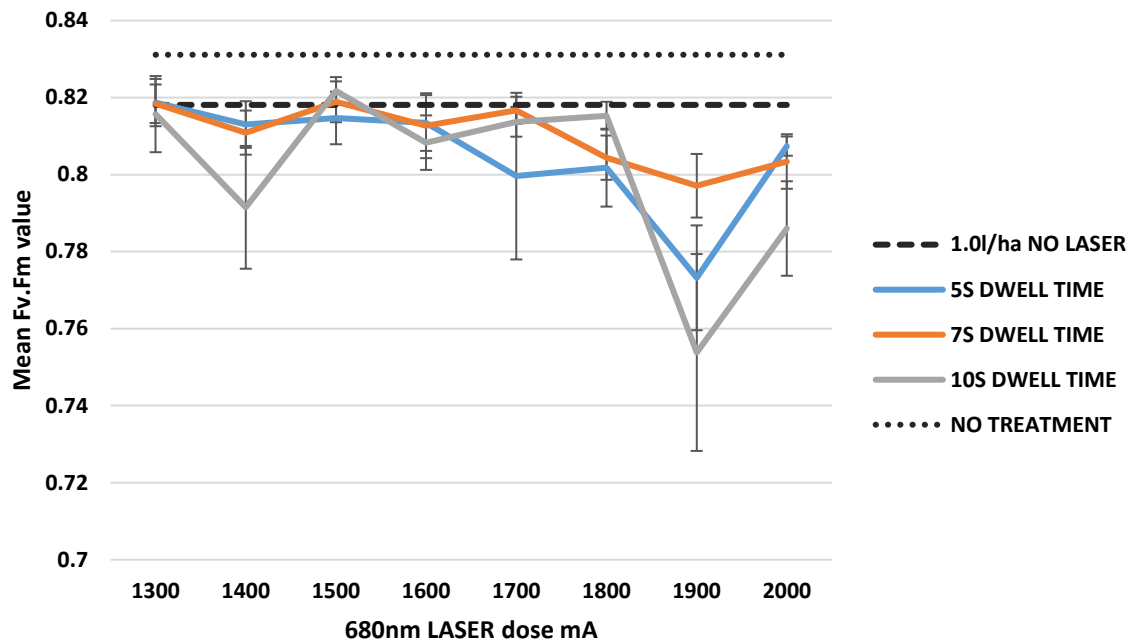
(a)
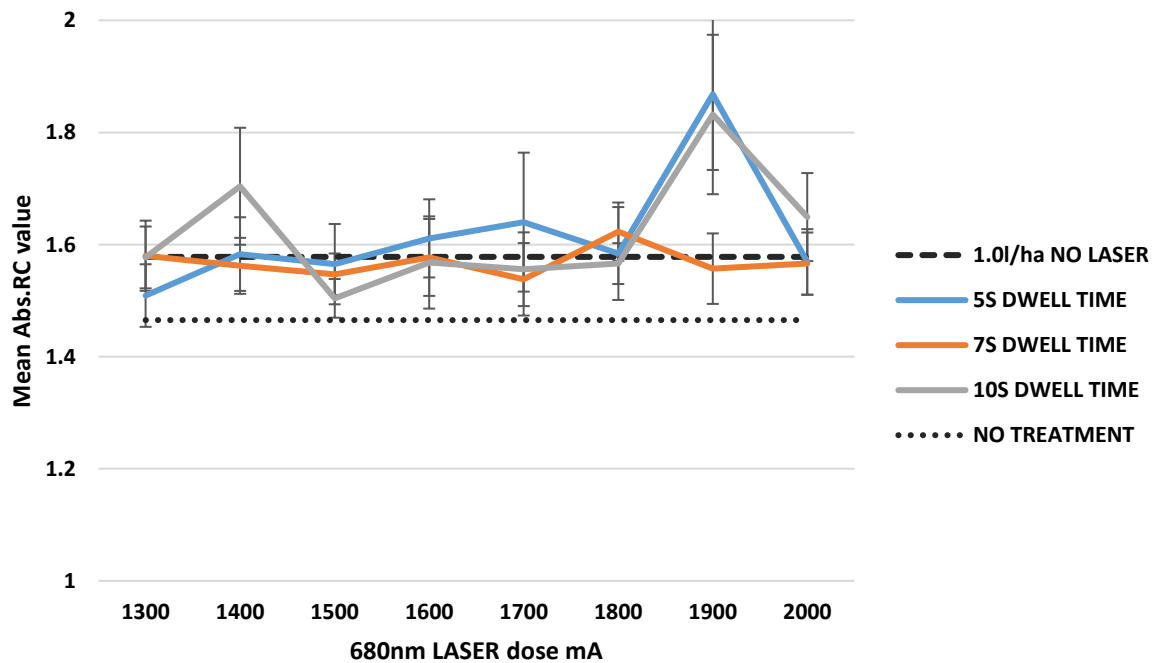
(b)
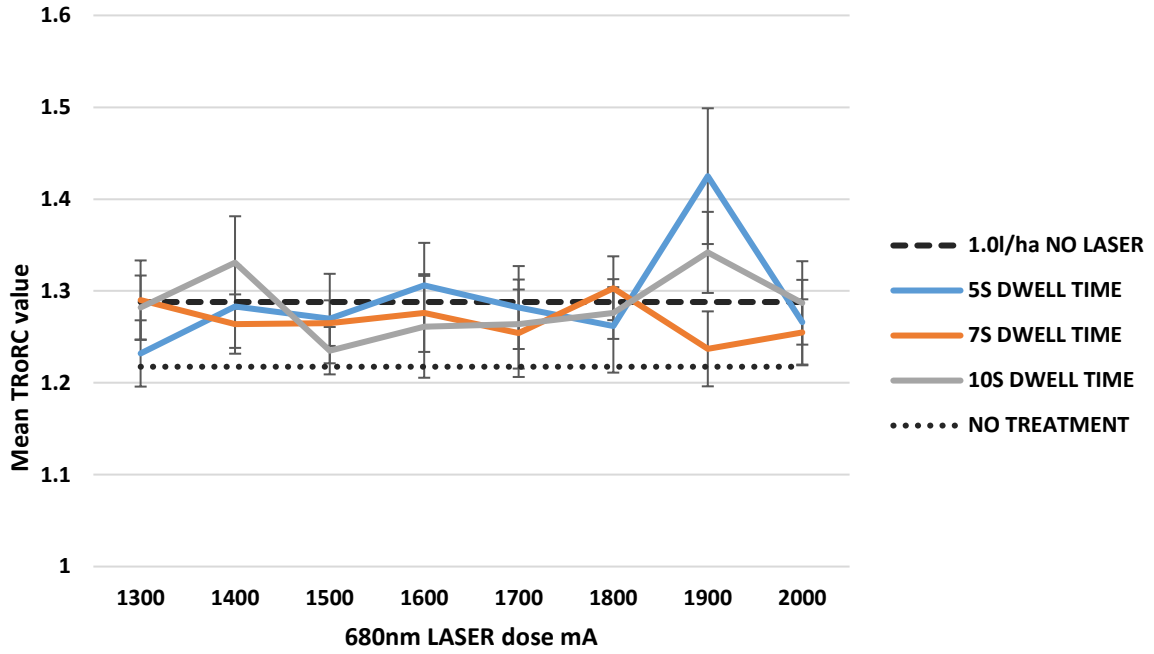
(c)

(d)

(e)

Figure 42 The (a) mean Fv.Fm values, (b) mean Abs.RC values, (c) mean TRoRC values, (d) mean EToRC values and (e) mean DIoRC values in Chenopodium album plants in response to 680nm LASER doses (mA) and Nevada® at a dose of 1.0lha^{-1}. NO TREATMENT is classified by plants not treated with herbicide or 680nm L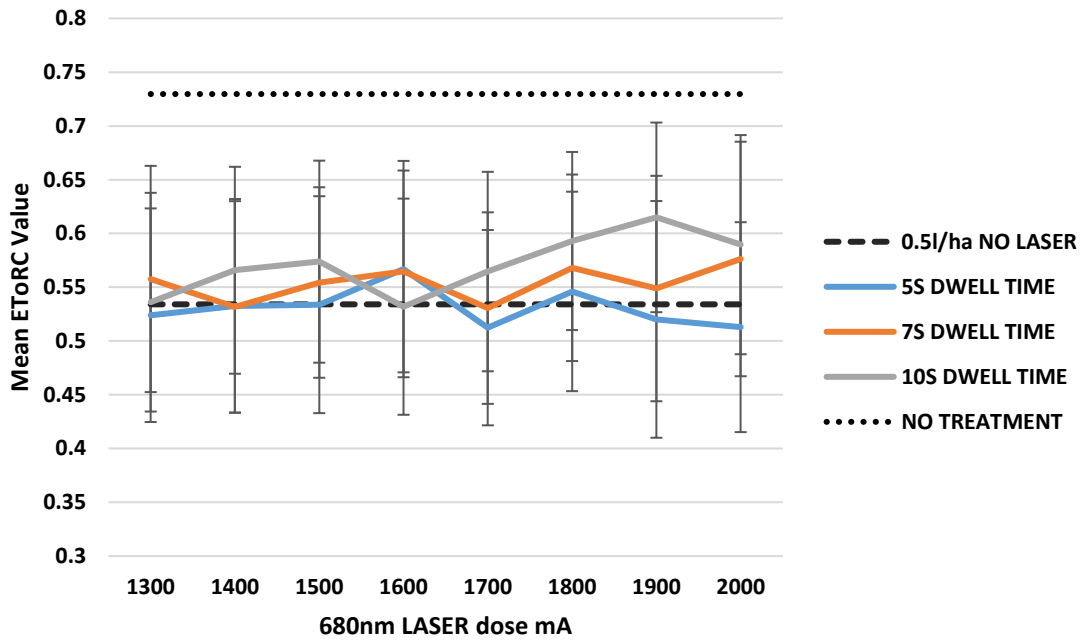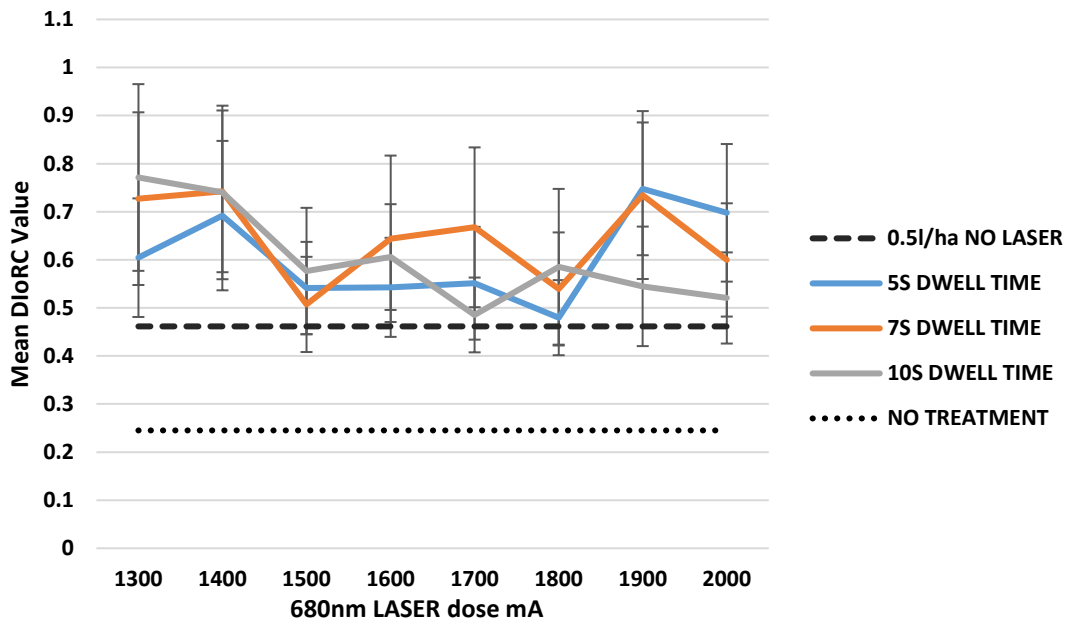ASER energy. 1.0l/ha NO LASER denotes 1.0lha^{-1} of Nevada® exclusively. Error bars denote ± standard error of the mean (SEM), n=12. Significant outcomes calculated using factorial ANOVA and T-Test.

Figure 43 shows the interlinked relationships of all five OJIP parameters upon Nevada® and 680nm LASER treatment. As with previous paired correlation matrices, defined 680nm LASER doses are not detailed, but this matrix is a useful tool when comparing the OJIP results of other treatments. Nevada® treated *Chenopodium album* (dose of 1.0lha^{-1}) generates significant correlations for all paired OJIP (P<0.001) parameters excluding the pair of Abs.RC and EToRC which shows very little interlinking relationship.

Figure 43 Pairs correlation matrix for Chenopodium album plants in response to 680nm LASER treatment + Nevada® treatment at 1.0lha^{-1} Tro.RC = TRoRC, Eto.RC = EToRC, Dio.RC = DIoRC. Significant differences in parameter data were calculated using the Kruskal-Wallis Test using the statistical program 'R'.

5.4.4 OJIP readings for *Sinapis arvensis* treated with 680nm LASER and Sencorex Flow® at a rate of 0.125lha^{-1}

As with previously analysed 680nm LASER treated plant samples in conjunction with herbicide treatment, there is a distinct lack of any pattern in OJIP parameter response to varying dwell times and mA 680nm LASER doses. Upon Sencorex Flow® treatment (Figure 44), *Sinapis arvensis* plants show a decline in Fv.Fm values with significantly lower values for 5s, 7s and 10s dwell times across all mA settings (P<0.001) compared to untreated samples. The 0s dwell time response shows a significant decrease in Fv.Fm value compared to control plants, likely to be a response of the Sencorex Flow® active ingredients. Absorbance (Abs.RC) and dissipation (DIoRC) readings for 5s, 7s and 10s dwell times are significantly greater for all mA settings compared to untreated plants with some significant values between 680nm LASER treated and exclusively Sencorex Flow® treated plants (i.e., 1400mA and 1900mA at 7s dwell time). This is likely to be in response to

the 680nm LASER application as 0s dwell time values are significantly lower for most mA settings compared to other dwell times. As EToRC values are dramatically reduced with Sencorex Flow® application, the dissipation and absorbance values are unsurprisingly increased. Trapping (TRoRC) shows extremely little variation in values for varying 680nm LASER treatments providing the argument that TRoRC is a relatively weak diagnostic for assessing responses to 680nm LASER and herbicide treatment in PSII.

As with *Chenopodium album* treated plants, there are spikes in parameter values at either 1800mA or 1900mA. When *Sinapis arvensis* plants were treated with 680nm LASER energy exclusively, a much lower dose of 1500mA for a period of 5s resulted in a significant decline in Fv.Fm and EToRC compared to the control. Upon this finding, this was nominated as the most efficient dose of 680nm LASER to apply to the plants in order to achieve the goal of reduced electron transport and signified the overload of PSII. It is interesting to note that EToRC in 680nm LASER+Sencorex Flow® treated plants is dramatically increased at 1800mA, the opposite of the effect the dose of 1500mA for a period of 5s has on EToRC.
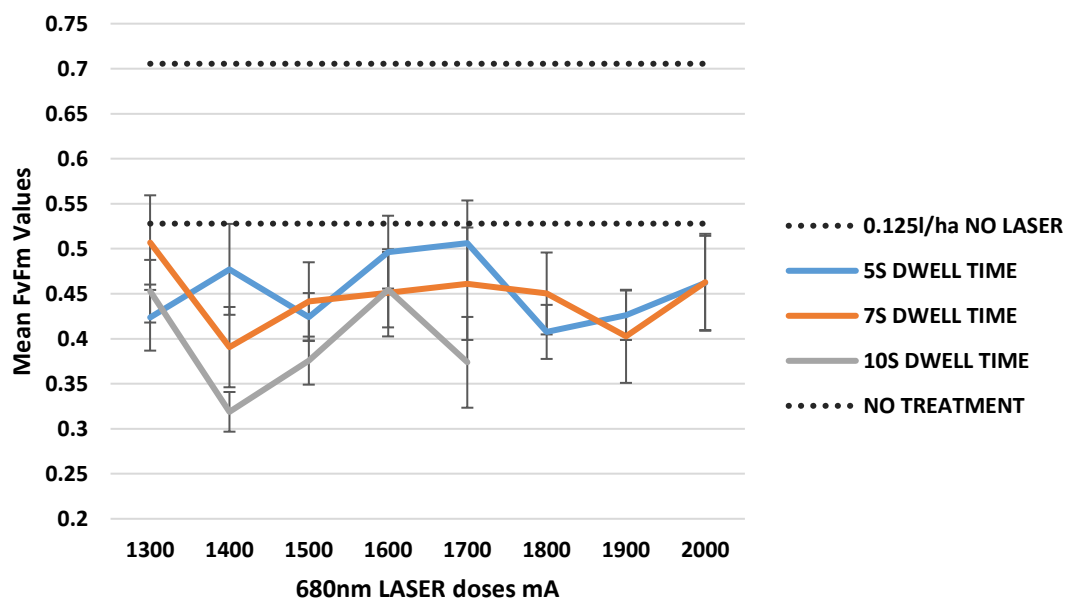
(a)
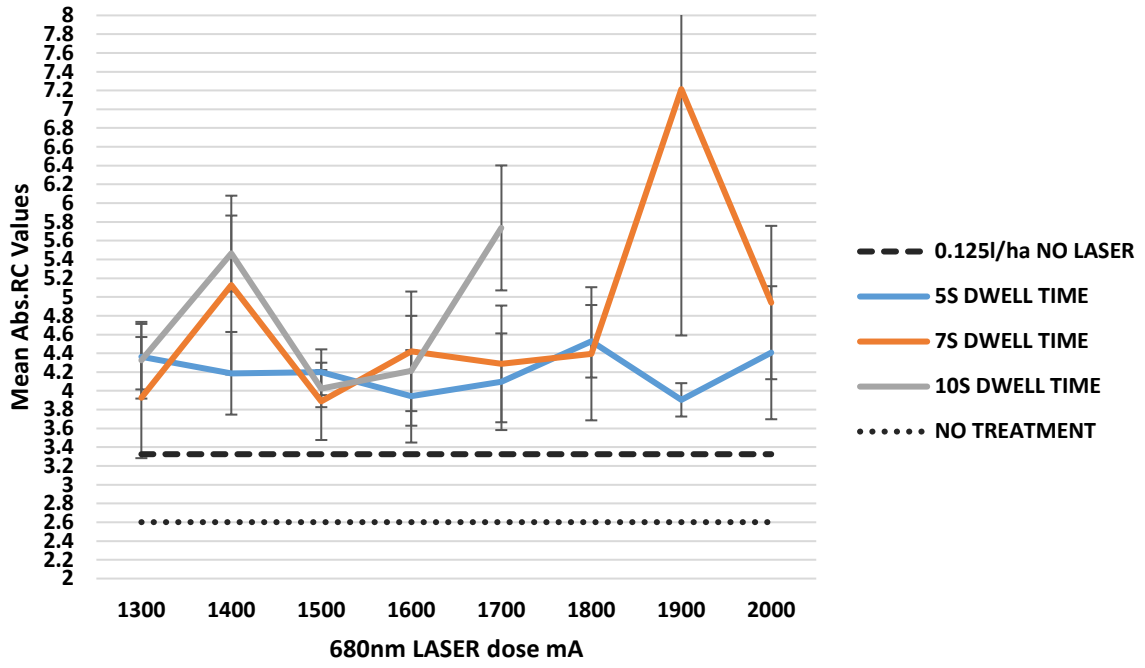
(b)
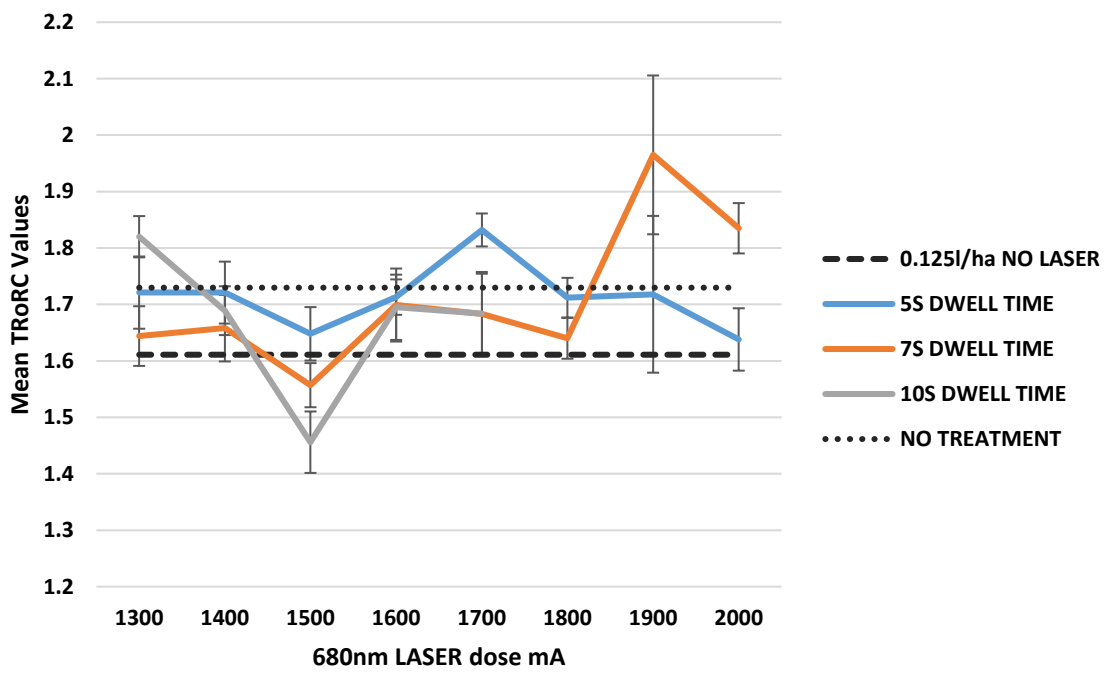
(c)

(d)

(e)

Figure 44 The (a) mean Fv.Fm values, (b) mean Abs.RC values, (c) mean TRoRC values, (d) mean EToRC values and (e) mean DIoRC values in Sinapis arvensis plants in response to 680nm LASER doses (mA) and Sencorex Flow® at a dose of 0.125lha⁻¹. NO TREATMENT is classified by plants not treated with herbicide or 680nm LASER energy.   0.125l/ha NO LASER denotes 0.125lha⁻¹ of Sencorex Flow® exclusively. Error bars denote ± standard error of the mean (SEM), n=12. Significant outcomes calculated using factorial ANOVA and T-Test.

The pairs correlation matrix shown in Figure 45 highlights a significant correlation between Abs.RC and DIoRC (P<0.001 (Kruskal test)). This is predictable as the OJIP parameters of Abs.RC and DIoRC are highly related and often mirror correlations between graphs. Fv.Fm values display highly similar negative relationship between Abs.RC and DIoRC; another unsurprising finding as Abs.RC and DIoRC generally share concordance in results. The pair's correlation plots for *Chenopodium album* shows more defined outcomes between parameters. This suggests the treatment effects of the 680nm LASER+Sencorex Flow® application produce OJIP values with a narrower range in *Chenopodium album* compared to *Sinapis arvensis*.

Figure 45 Pairs correlation matrix for Sinapis arvensis plants in response to 680nm LASER treatment + Sencorex Flow® treatment at 0.125lha^{-1} Tro.RC = TRoRC, Eto.RC = EToRC, Dio.RC = DIoRC. Significant differences in parameter data were calculated using the Kruskal-Wallis Test using the statistical program 'R'.

5.4.5 OJIP readings for *Sinapis arvensis* treated with 680nm LASER and Calaris® at a rate of 0.25lha^{-1}

Calaris®+680nm LASER treated *Sinapis arvensis* yields largely unremarkable OJIP parameter data. The spikes present at 1800mA and 1900mA are markedly less pronounced in this set of data (Figure 46) than in sets previously analysed. There are similar absorbance (Abs.RC) and dissipation (DIoRC) values and show that a 5s dwell time at 2000mA is absorbed very effectively, but equally produced the greatest dissipation levels. As an attempt to rectify the decline in ETC rate (shown in Figure 46 (d)) induced by Calaris®, the plant is likely to up-regulate LHCII polypeptides and increase chlorophyll *a* accumulation (Chalifour et al., 2014, Wilson and Huner, 2000). It is possible that a dose of 2000mA for a period of 5s is readily absorbed by the increased abundance of LHCII polypeptides and this could provide an explanation for the dramatic increase in Abs.RC levels at this point. However, Figure 10 in Chapter 3 shows how absorbance and subsequent dissipation levels only show marked increased on day 4 post-treatment. There is no significant difference between Abs.RC values on Day 0 and Day 1 post-treatment at a dose of 0.25lha^{-1} (P=0.073). This similarity between pretreatment and 24 hours post treatment values provides a baseline. Therefore, the increase in Abs.RC in Calaris® and 680nm LASER treated *Sinapis arvensis* is likely to be as a result of efficient absorption of 680nm on application.

EToRC values are all significantly reduced compared to untreated plants (P<0.001) with the addition of 5s and 7s dwell times from 1600mA leading to a further decline in EToRC values. Trapping (TRoRC) values show signs of increasing with increasing 680nm LASER dose.
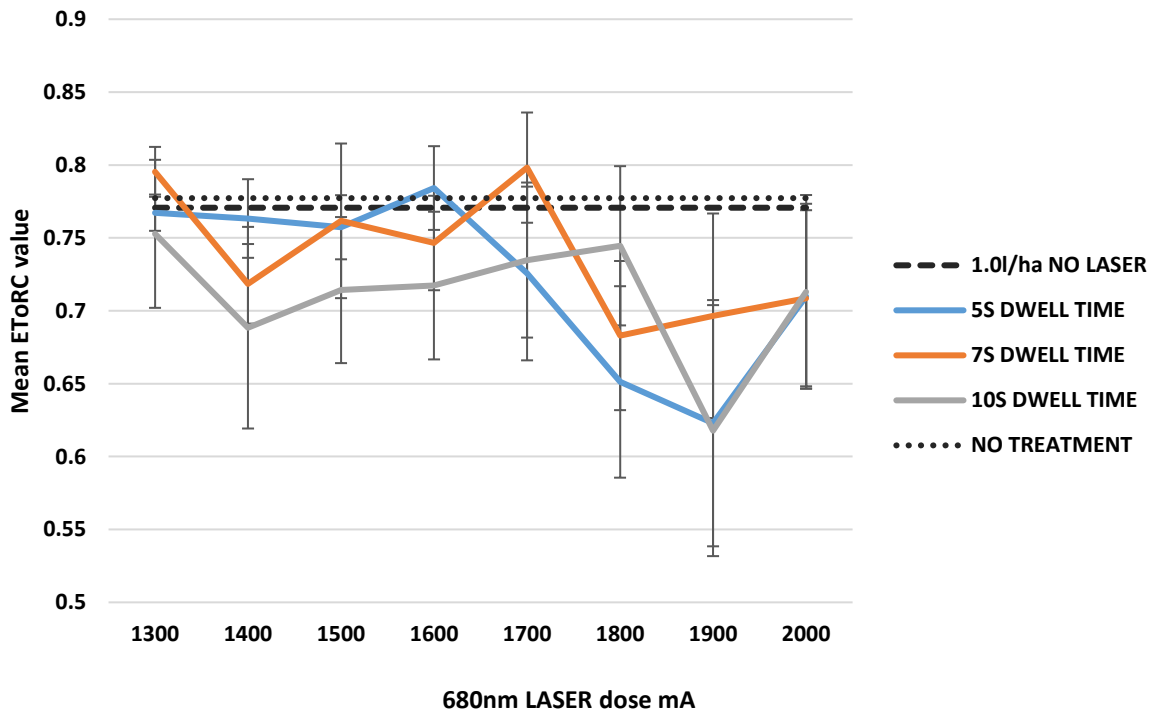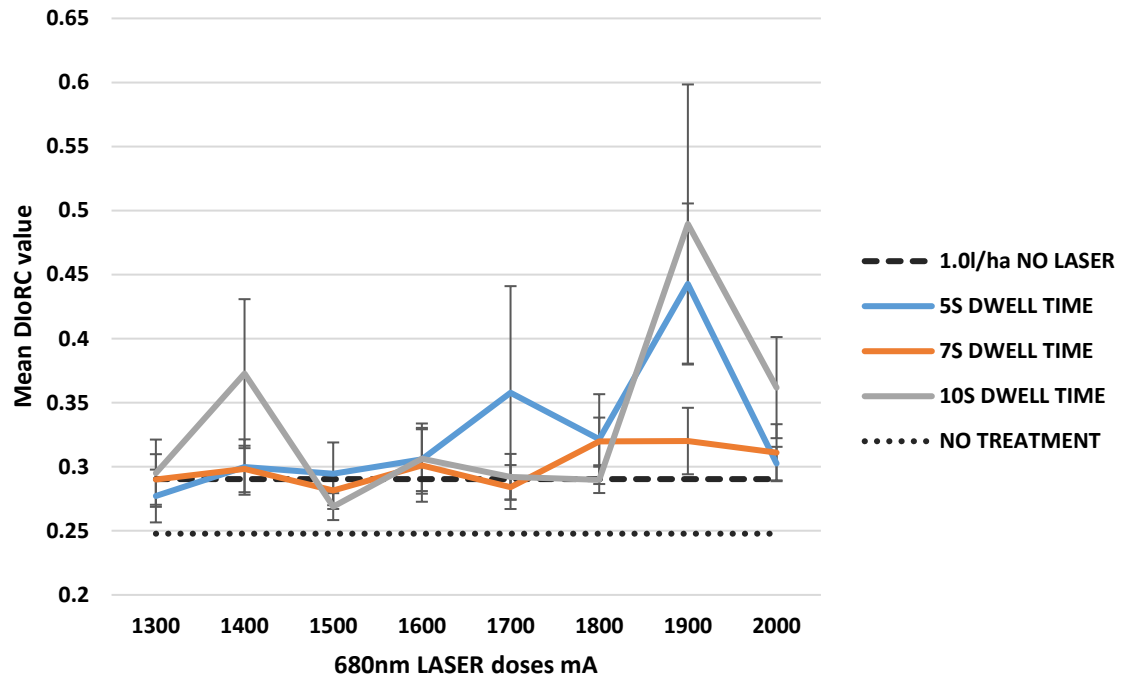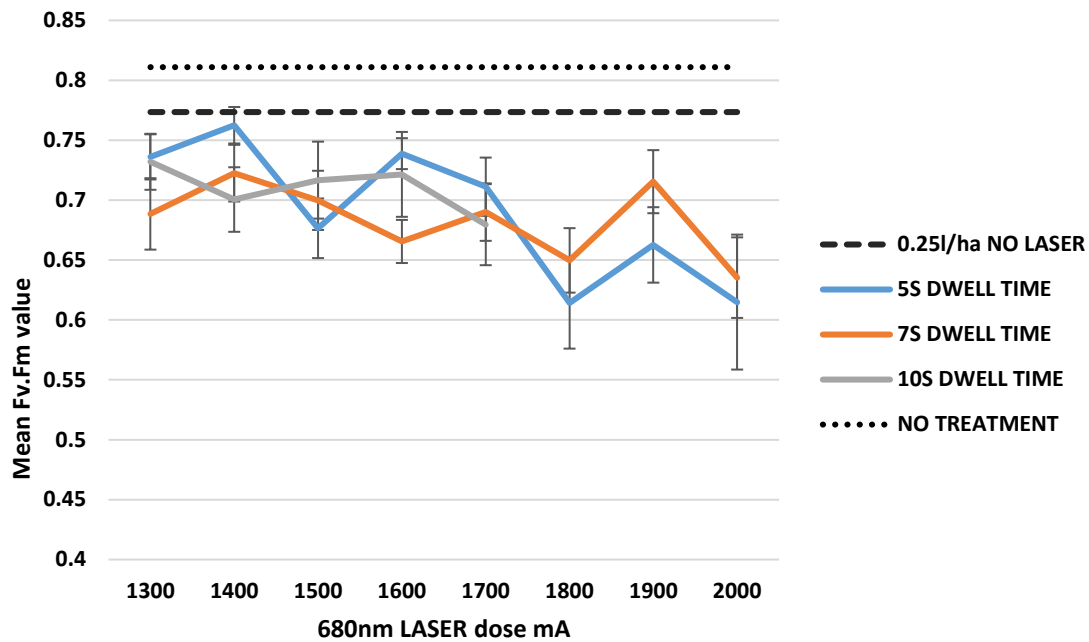
(a)
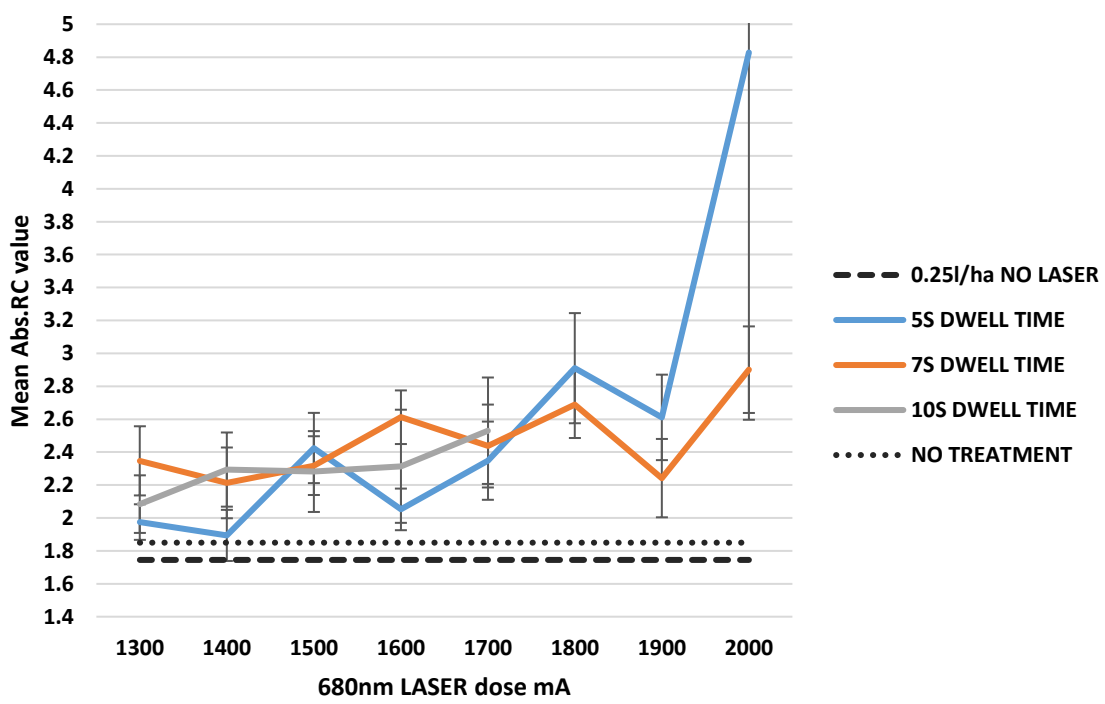
(b)
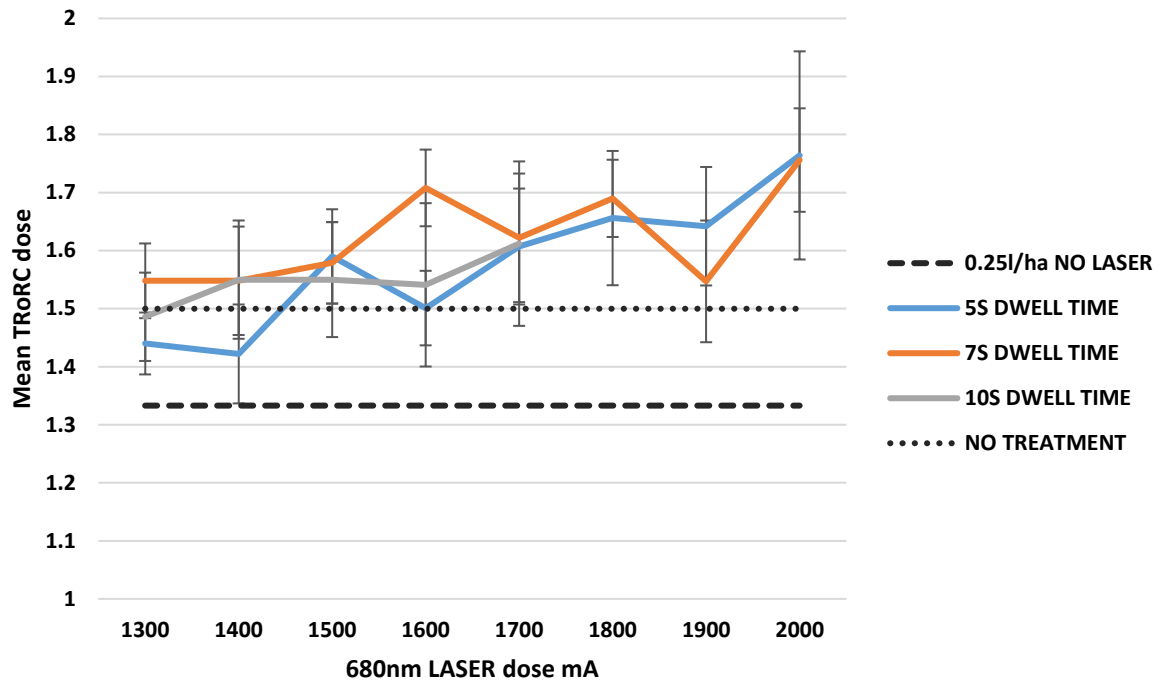
(c)
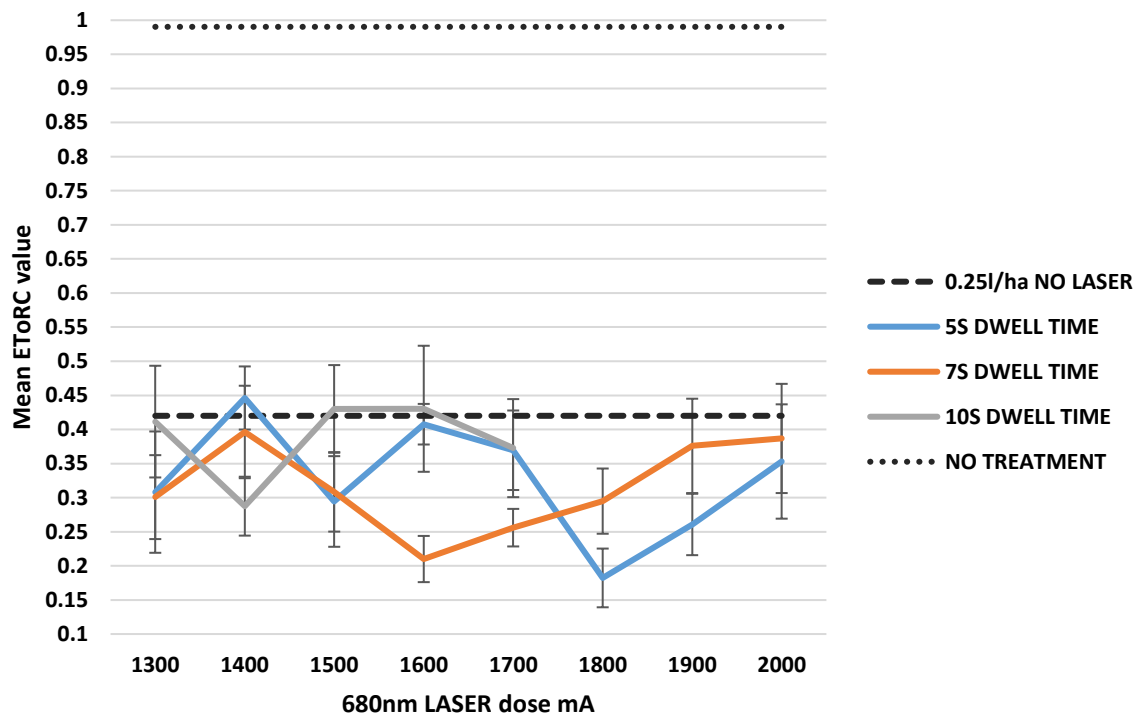
(d)
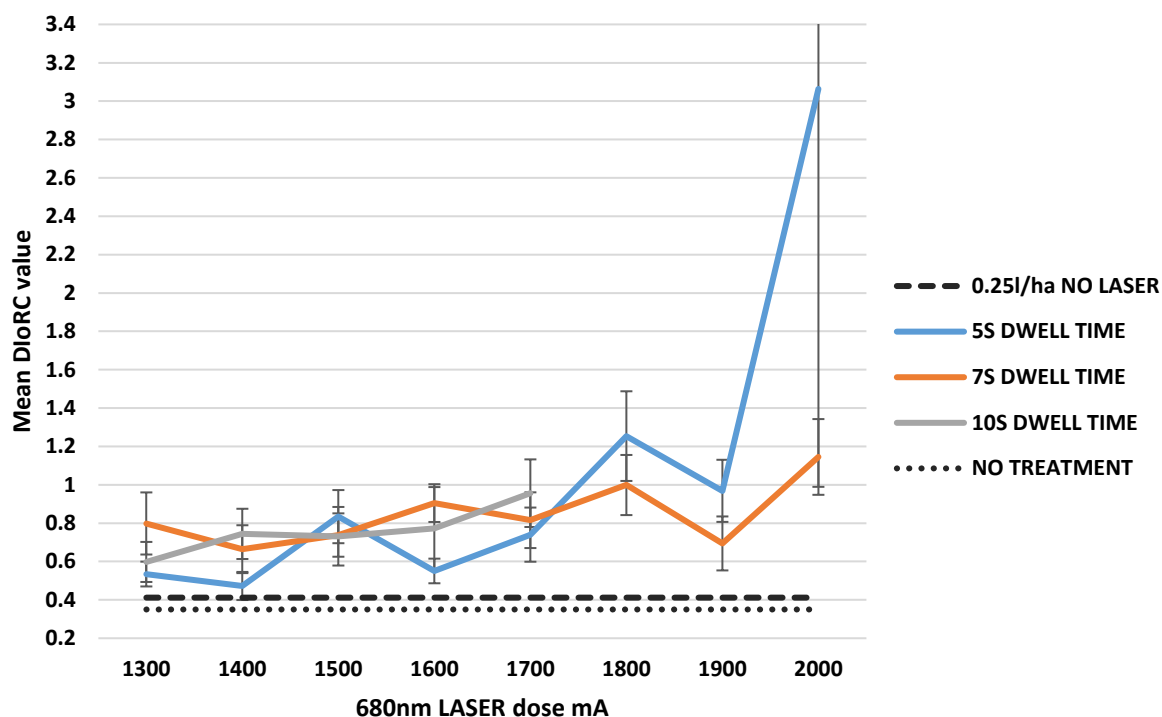
(e)

Figure 46 The (a) mean Fv.Fm values, (b) mean Abs.RC values, (c) mean TRoRC values, (d) mean EToRC values and (e) mean DIoRC values in Sinapis arvensis plants in response to 680nm LASER doses (mA) and Calaris® at a dose of 0.25lha^{-1}. NO TREATMENT is classified by plants not treated with herbicide or 680nm LASER energy. 0.25l/ha NO LASER denotes 0.25lha^{-1} of Calaris® exclusively. Error bars denote ± standard error of the mean (SEM), n=12. Significant outcomes calculated using factorial ANOVA and T-Test.

The pairs correlation plot shown in Figure 47 displays OJIP data with narrow ranges for all OJIP parameters apart from the relationship between TRoRC and EToRC where no clear finding is observed. This could be a result of the disruption inflicted upon the ETC by the active ingredients of Calaris®. Fv.Fm and TRoRC demonstrate a strong negative correlation (P<0.001) suggesting as the overall function of PSII declines, trapping capability also declines.
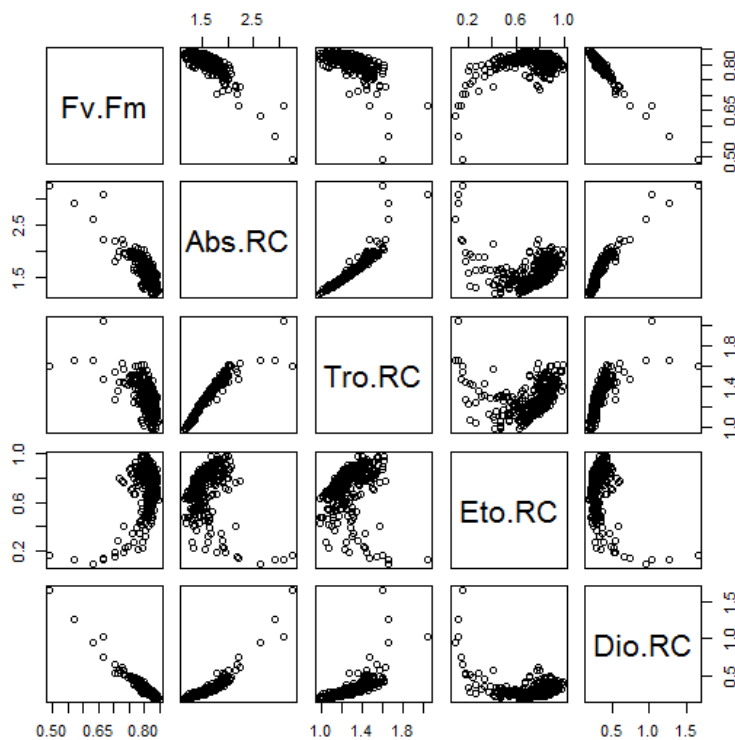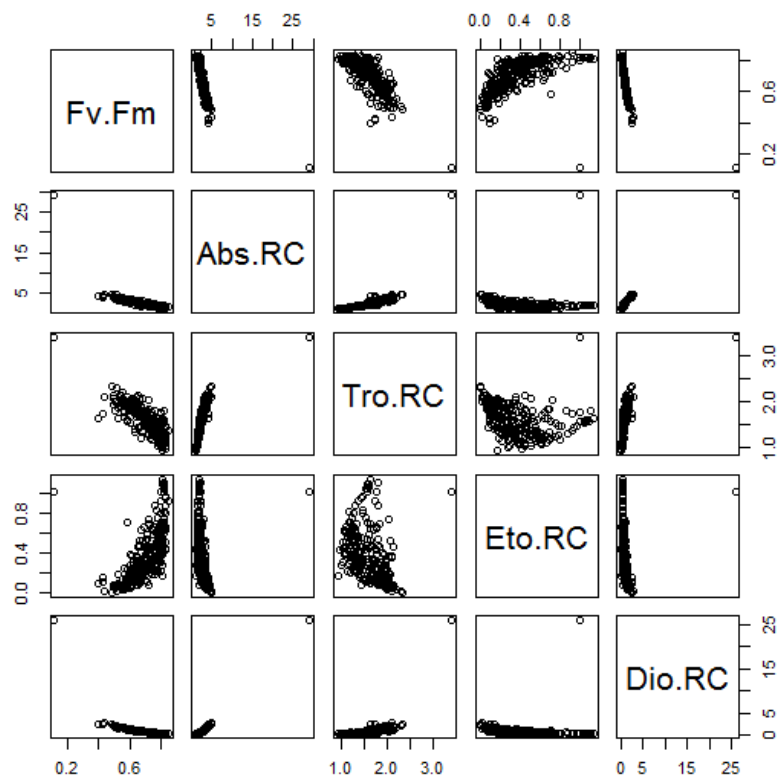
Figure 47 Pairs correlation matrix for Sinapis arvensis plants in response to 680nm LASER treatment + Calaris® treatment at 0.25lha⁻¹ Tro.RC = TRoRC, Eto.RC = EToRC, Dio.RC = DIoRC. Significant differences in parameter data were calculated using the Kruskal-Wallis Test using the statistical program 'R'.

## 5.4.6 OJIP readings for *Sinapis arvensis* treated with 680nm LASER and Nevada® at a rate of 1.0lha⁻¹

Figure 48 ((a), (b) and (e)) show how Fv.Fm, Abs.RC and DIoRC values are unchanged upon addition of Nevada® compared to the untreated samples. This is unsurprising as Nevada® is not known to inflict any photosynthetic inhibitory action on PSII at all (detailed on page 44). It is therefore unexpected to find average EToRC values (Figure 48 (d)) significantly increase (values taken at intervals during the treatment period (see Chapter 2) upon addition of Nevada® at a dose of 1.0lh⁻¹ (◆◆◆◆ line in Figure 48 (e)) compared to untreated plants. This is likely to be a damage mitigation response from the plant to produce more ATP in order to increase protein production and repair membranes (see page 44 action of Nevada®). Trapping (TRoRC) shows a significant increase (P=0.024) upon Nevada® treatment compared to untreated samples, suggesting a similar motivation for up regulating

154

electron transport (EToRC), i.e., a greater amount of energy trapped thus more energy funnelled into the ETC. Interestingly, Nevada® treated *Chenopodium album* plants do not display a rise in EToRC value upon herbicide treatment compared to the untreated plants but trapping values after Nevada® application in *Chenopodium album* are markedly increased. There is evidently a disconnect between energy transfer after trapping leading into the ETC in *Chenopodium album*. This could be due to differences in the effect of Nevada® in *Chenopodium album* and *Sinapis arvensis* and is likely to be as a result of chemical action on crucial proteins between trapping and the ETC.

Continuing a consistent response through the OJIP results in this chapter, a spike in data is found for each parameter after 680nm LASER+Nevada® treatment at 1800mA, albeit with a less defined spike for Abs.RC. As previously mentioned, *Sinapis arvensis* plants treated with Calaris® and Sencorex Flow® display a similar spike in data at a similar dosage but is more pronounced in *Chenopodium album* plants, especially so for Nevada® treated *Chenopodium album* plants (spike at 1900mA).
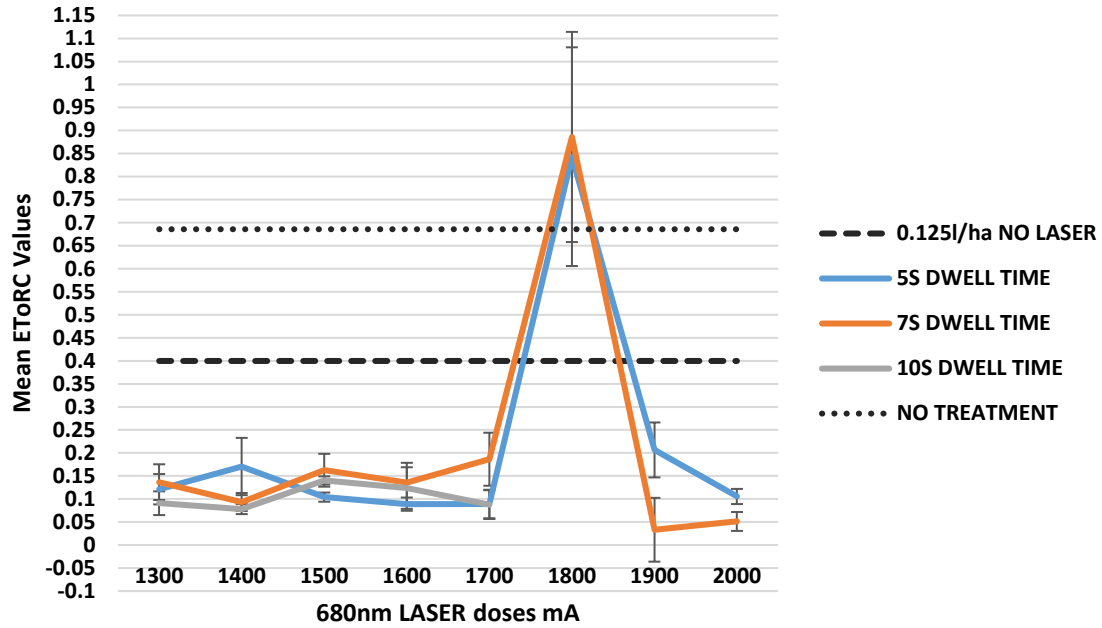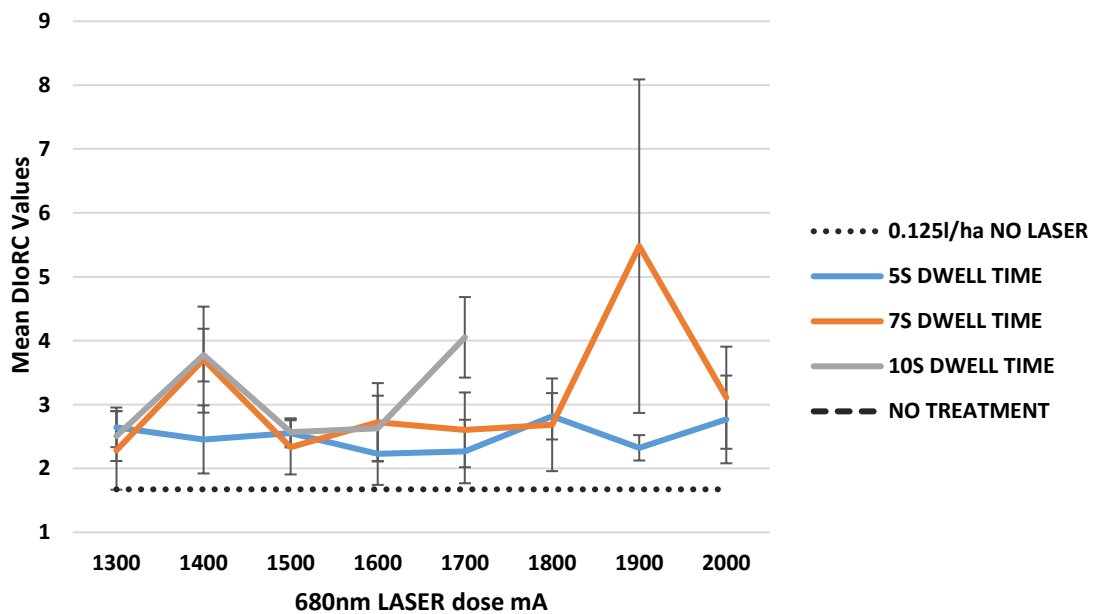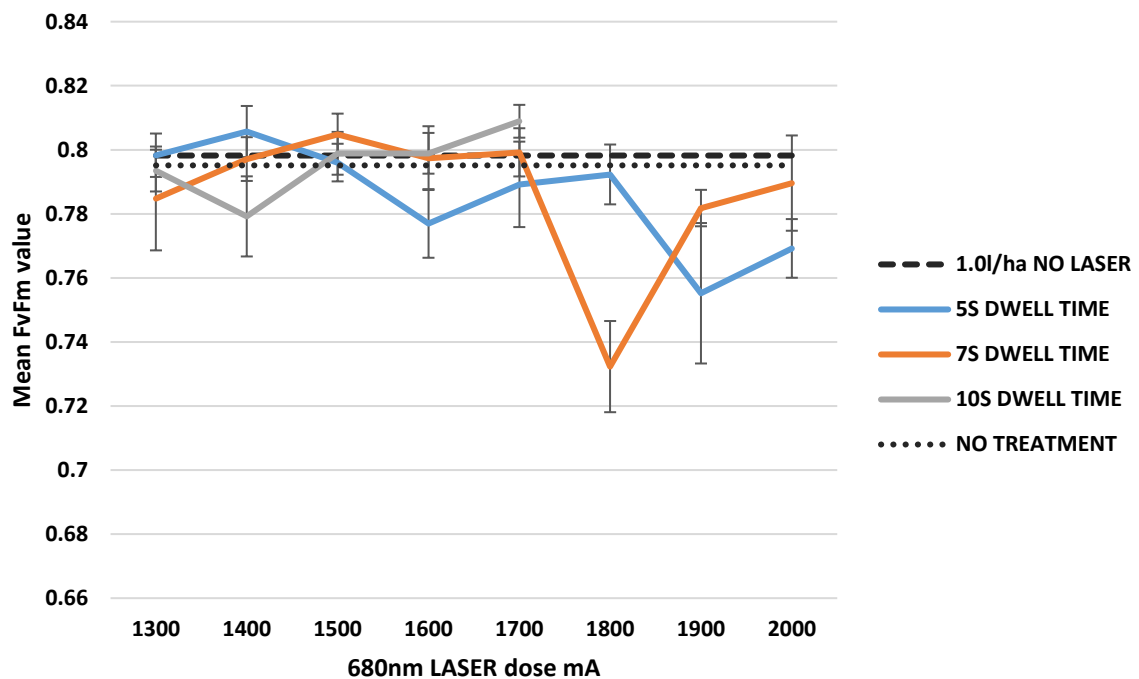

(a)
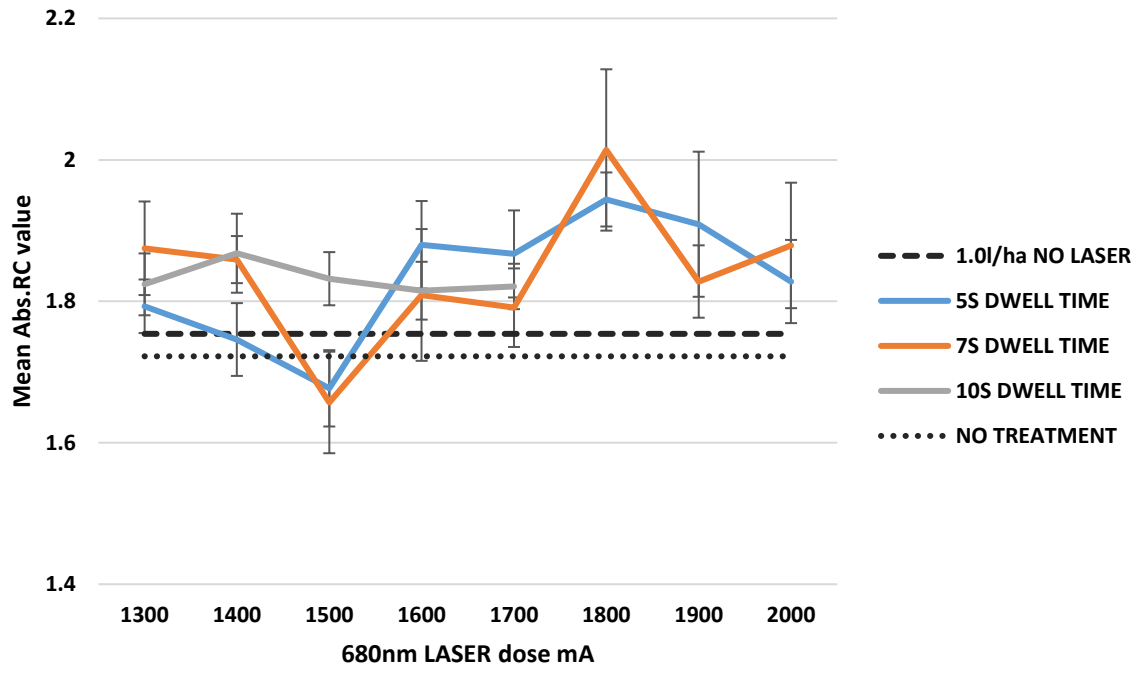
(b)
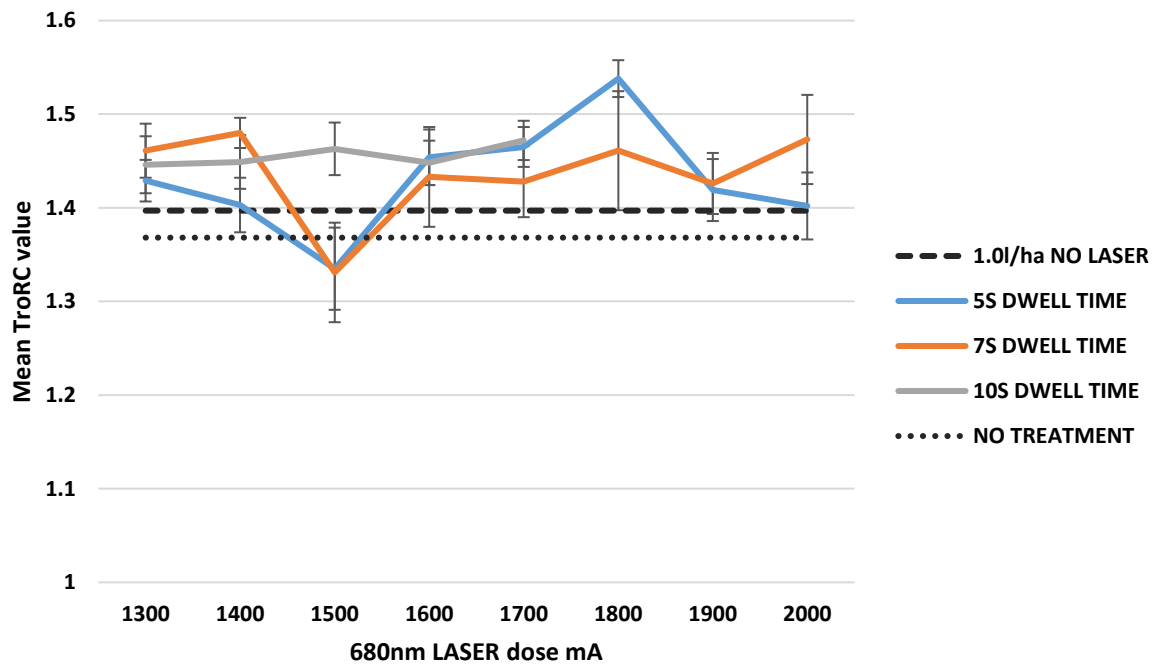
(c)
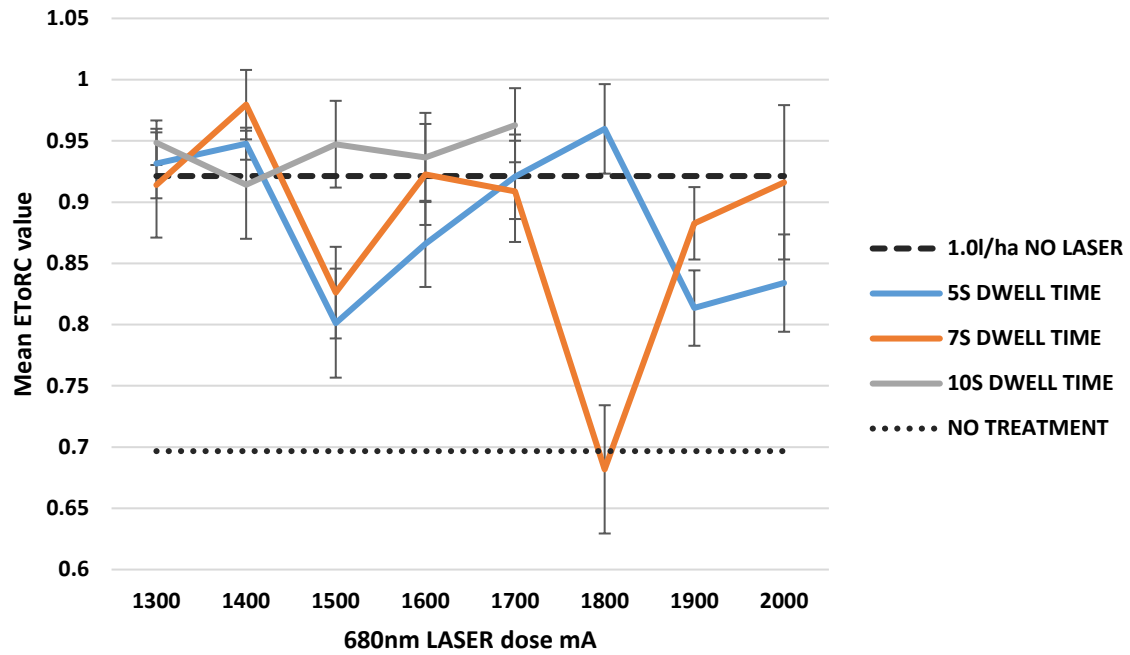
(d)
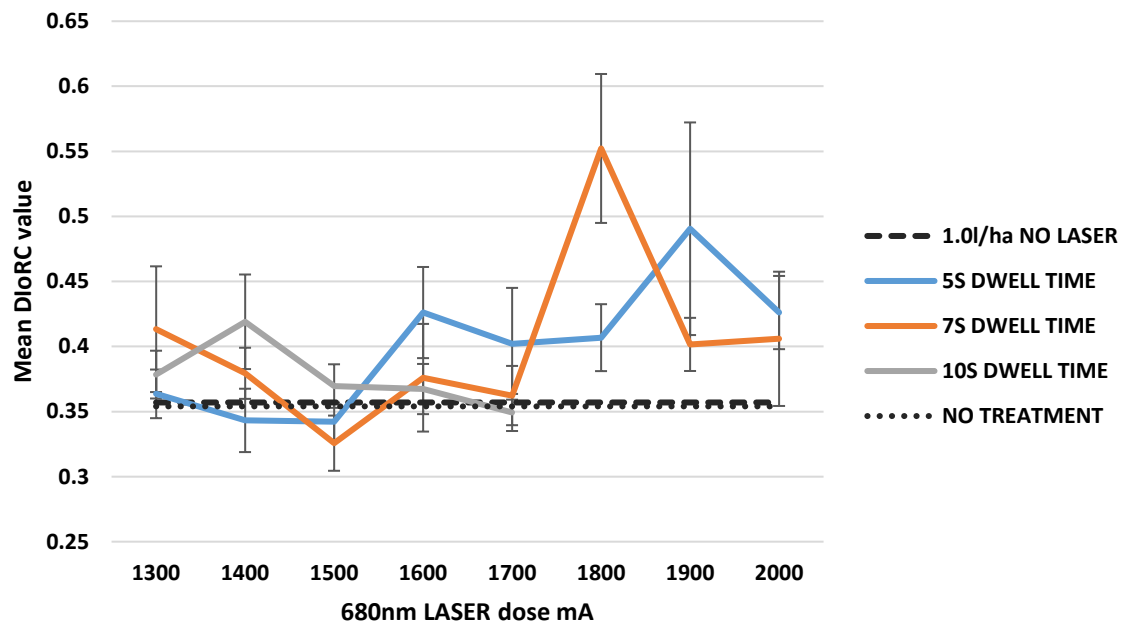
(e)

Figure 48 *The (a) mean Fv.Fm values, (b) mean Abs.RC values, (c) mean TRoRC values, (d) mean EToRC values and (e) mean DIoRC values in Sinapis arvensis plants in response to 680nm LASER doses (mA) and Nevada® at a dose of 1.0lha^{-1}. NO TREATMENT is classified by plants not treated with herbicide or 680nm LASER energy.   1.0l/ha NO LASER denotes 1.0lha^{-1} of Nevada® exclusively. Error bars denote ± standard error of the mean (SEM), n=12. Significant outcomes calculated using factorial ANOVA and T-Test.*

Figure 49 shows a negative correlation between Fv.Fm and DIoRC (P<0.001) highlighting the overall decline of the PSII system post treatment. This is interesting as the active ingredients of Nevada® are not directly related to a reduction in photosynthetic capability. Abs.RC and TRoRC display a strong positive correlation (P<0.001); this is predictable as a greater level of light absorption increases the likelihood of light trapping. Fv.Fm and DIoRC display a strong negative correlation (P<0.001) showing an overall decline in the PSII capability leads to greater dissipation as it is no longer possible to use all of the absorbed light.
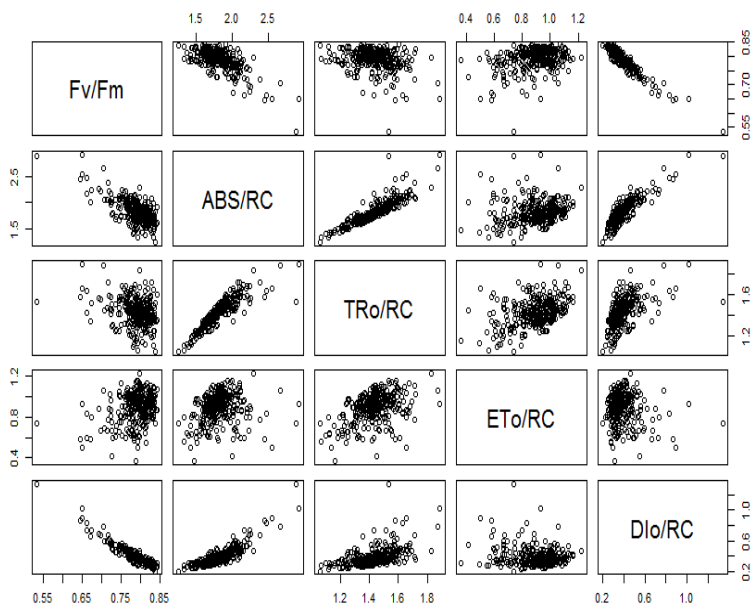
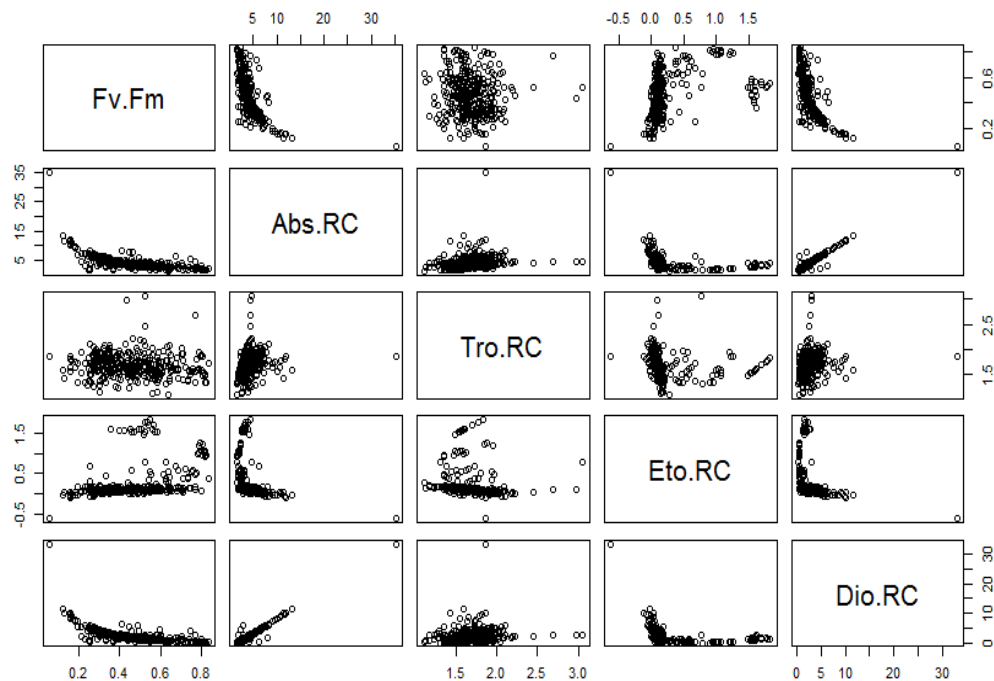*Figure 49 Pairs correlation matrix for Sinapis arvensis plants in response to 680nm LASER treatment + Nevada® treatment at 1.0lha⁻¹ Fv/Fm = Fv.Fm, ABS/RC = Abs.RC, Tro/RC = TRoRC, Eto/RC = EToRC, Dio/RC = DIoRC. Significant differences in parameter data were calculated using the Kruskal-Wallis Test using the statistical program 'R'.*

5.5 Percentage relative conductivity readings for *Chenopodium album* and *Sinapis arvensis* treated with 680nm LASER in conjunction with herbicide treatment

Conductivity data for both *Chenopodium album* and *Sinapis arvensis* plants treated with Calaris® show a generally positive relationship between 680nm LASER dose and percentage conductivity readings indicating the addition of 680nm LASER energy does have an influence on the electrolyte leakage status of plant cells. In both plants, untreated samples (i.e., control plants not treated with herbicide or 680nm LASER energy) demonstrate lower percentage conductivity readings compared to herbicide treated plants, but the difference is not significantly lower in each case (*Sinapis arvensis* P=0.062, *Chenopodium album* P=0.072).

Sencorex Flow® treated plants lack a distinct response in electrolyte leakage profile according to LASER dosage. In *Sinapis arvensis*, untreated and Sencorex Flow® treated (dose 0.125lha^{-1}) show highly similar average readings. Whilst on the surface this appears unlikely, this data is supported by findings in Chapter 3, which show % relative conductivity readings for Sencorex Flow® treated *Sinapis arvensis* on T+1 at a dosage of 0.125lha^{-1} to be non-significantly increased to the control (dose F, 0.00lha^{-1}). The combination of findings suggests the mode of action of Sencorex Flow® has a minimal effect of the integrity of cell membranes in *Sinapis arvensis*. Sencorex Flow® treated *Chenopodium album* shows an increase in percentage relative conductivity compared to untreated plants, but a T-Test reveals a lack of significant difference (P=0.118). For both *Chenopodium album* and *Sinapis arvensis* treated with Sencorex Flow®, there is, as with Calaris® treated plants, a distinct lack of a coherent outcome in % relative conductivity data according to LASER dosage.

Perhaps the only interesting finding arising as a result of Sencorex Flow® treatment in *Sinapis arvensis* is the spike in percentage relative conductivity at 1500mA dose and 10s dwell time. When *Sinapis arvensis* plants were treated with 680nm LASER energy exclusively, the 1500mA dosage level contained the most OJIP parameter responses which indicated photoinhibition, or more specifically, PSII overload than any other dosage level. At a dose of 1500mA for a period of 5s, both Fv.Fm and EToRC were significantly reduced compared to untreated plants. Both OJIP parameters being significantly reduced was exclusive to this dose across all other tested 680nm LASER doses. It is possible that, when plants were treated with a dose of 1500mA at a period of 5 and 7 seconds as in Figure 38, a similar effect was triggered. However, this finding is not echoed in OJIP data in response to

Sencorex Flow®+LASER treatment in *Sinapis arvensis* where a spike in OJIP parameters is only present at 1800mA and 1900mA.

Nevada® treated *Sinapis arvensis* and *Chenopodium album* demonstrate no clear outcome in percentage relative conductivity readings.
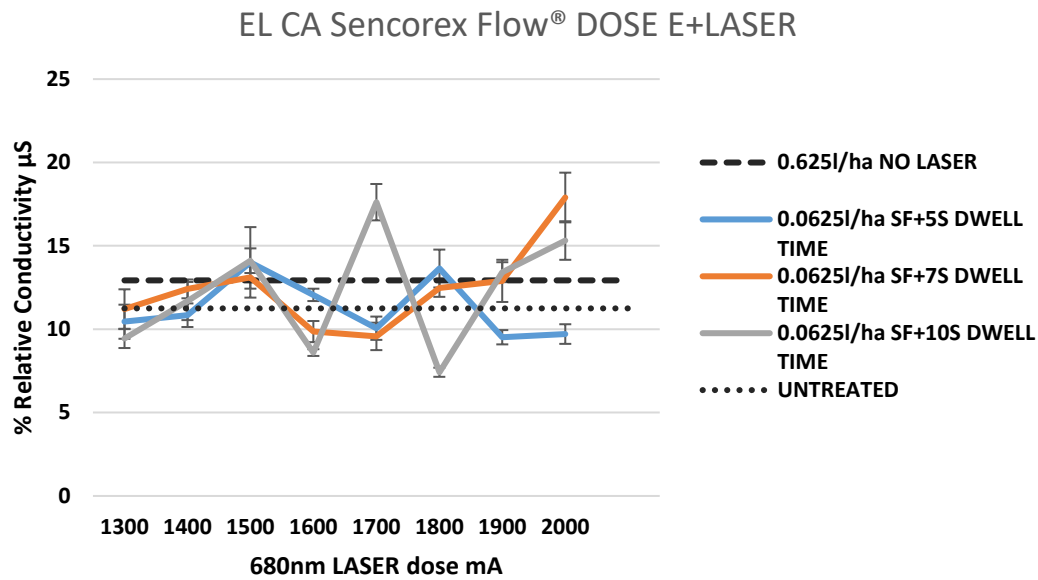
(a)
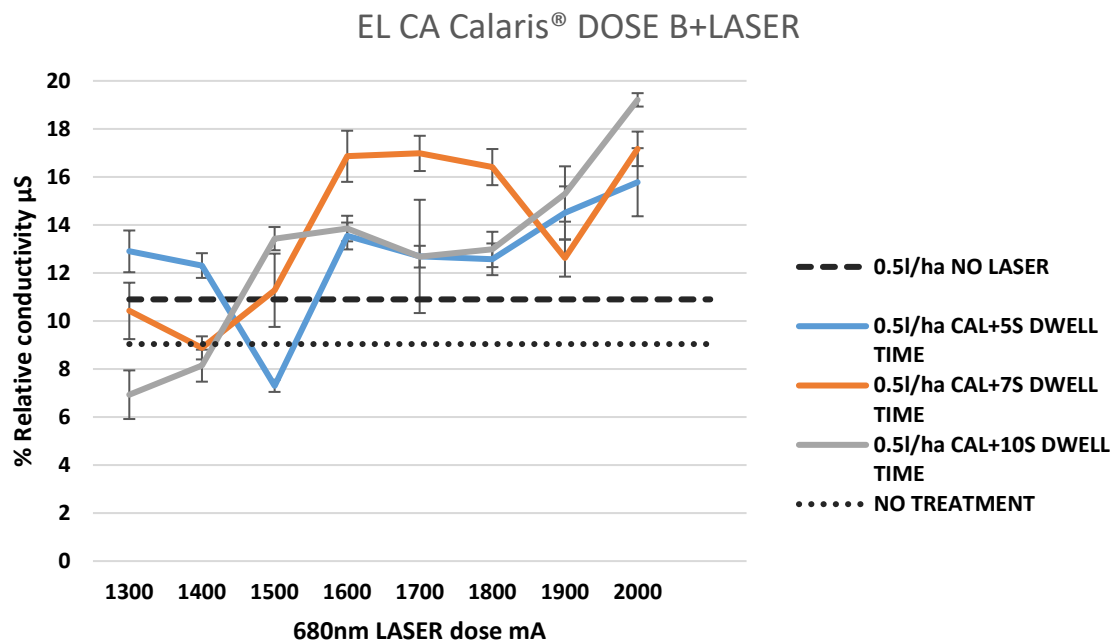
(b)

EL CA Nevada® DOSE A+LASER
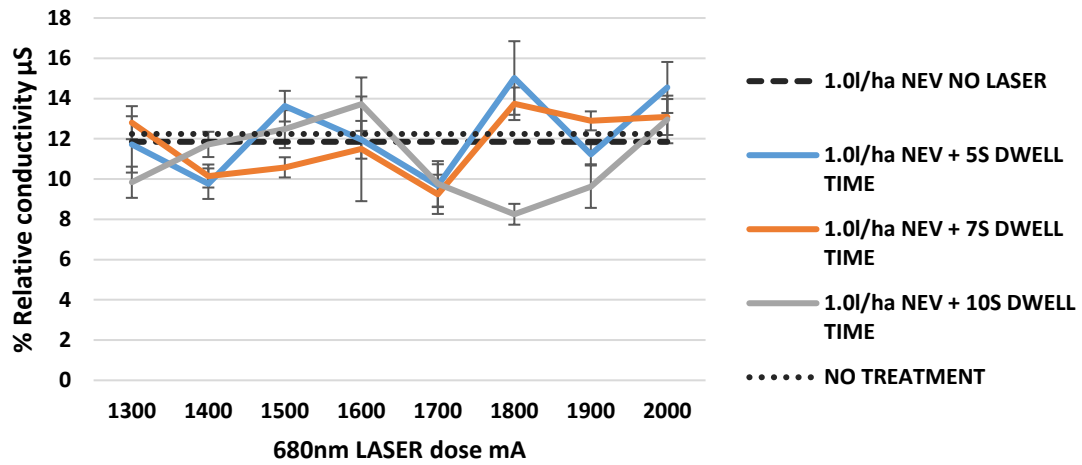
(c)

EL SA Sencorex Flow® DOSE D + LASER

(d)

EL SA Calaris® DOSE C + LASER

(e)

SA EL Nevada® DOSE A + LASER
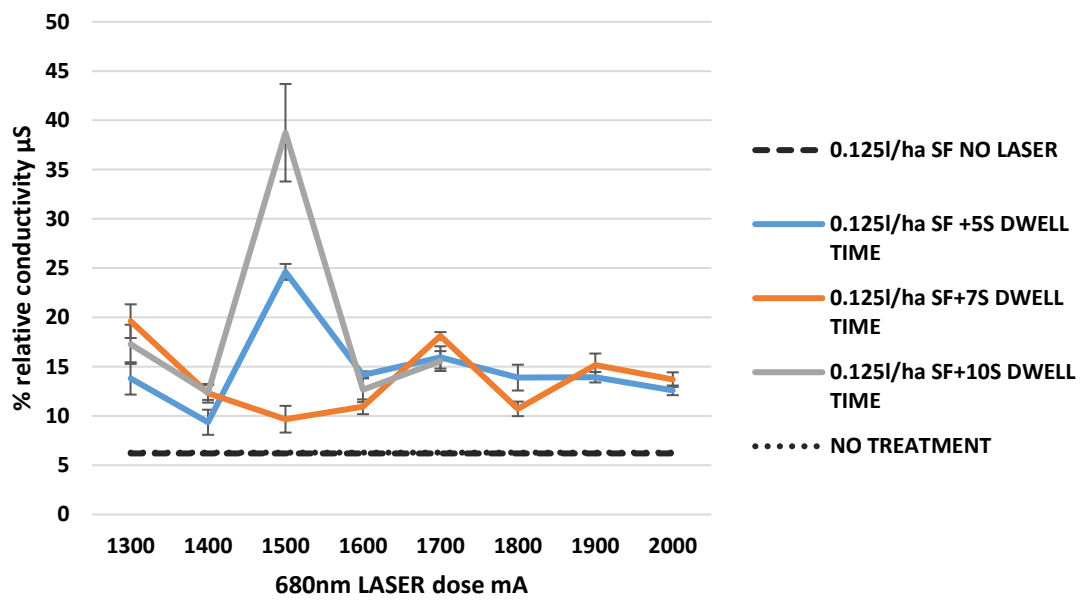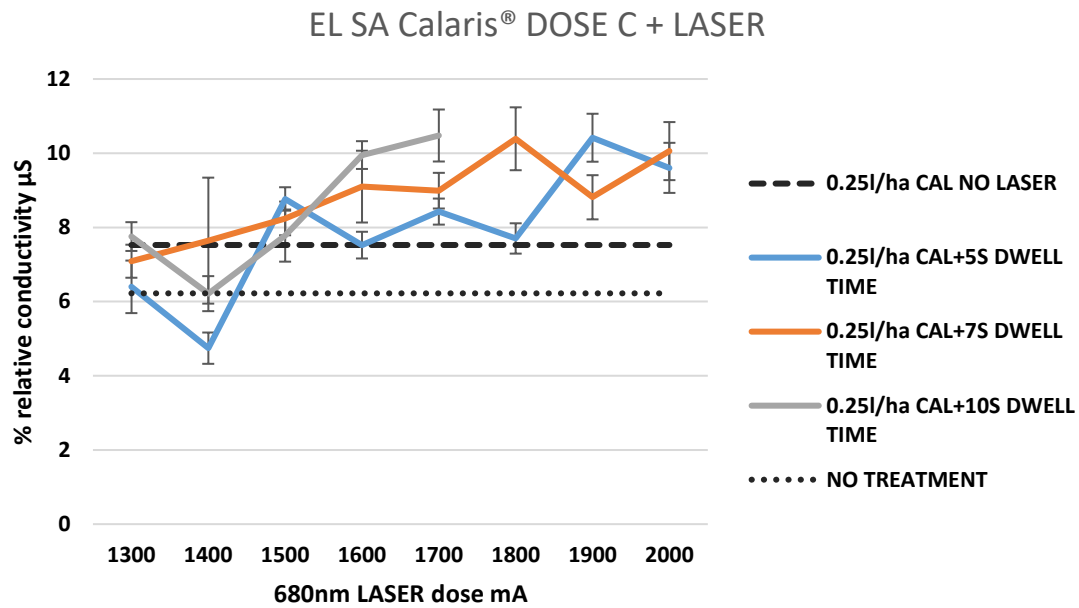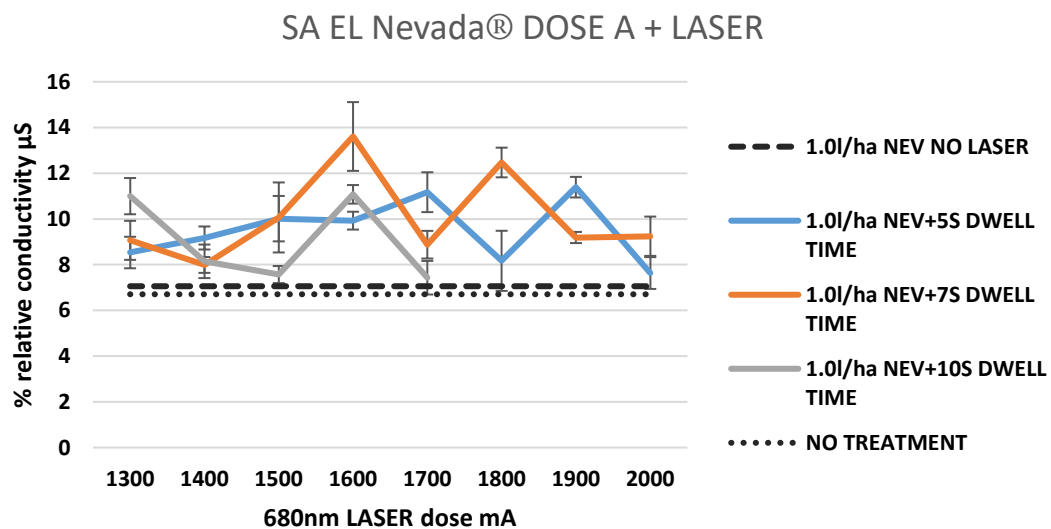
(f)

Figure 50 The percentage (%) relative conductivity of (a) Chenopodium album treated with Sencorex Flow® at a rate of 0.0625lha[-1], (b) Chenopodium album treated with Calaris® at a rate of 0.5lha[-1] , (c) Chenopodium album treated with Nevada® at a rate of 1.0lha[-1] (d) Sinapis arvensis treated with Sencorex Flow® at a rate of 0.125lha[-1], (e) Sinapis arvensis treated with Calaris® at a rate of 0.25lha[-1], (f) Sinapis arvensis treated with Nevada® at a rate of 1.0lha[-1] in response to 680nm LASER dose (mA) Legend: Sencorex Flow®-denotes Sencorex Flow® treatment, Calaris®- denotes Calaris® treatment, NEV- denotes Nevada® treatment. NO TREATMENT corresponds to Chenopodium album or Sinapis arvensis plants receiving no herbicide or 680nm LASER treatment. Error bars denote ± standard error of the mean (SEM), n=6. Significant outcomes calculated using factorial ANOVA and T-Test.

5.6 The determination of SOD units/mg total protein in 680nm LASER and herbicide treated *Chenopodium album* and *Sinapis arvensis*

Figure 51 displays how *Chenopodium album* and *Sinapis arvensis* respond in terms of SOD levels after herbicide and herbicide and 680nm LASER treatment used in conjunction. In all treatment types excluding Nevada® treated plants, the herbicide treated plant samples contain significantly greater levels of SOD mg^{-1} total protein than completely untreated samples. Such an increase in SOD levels is likely to be in response to the stressful environment the active ingredient of Sencorex Flow® and Calaris® inflict on the plant, specifically targeting photosynthetic processes (see pages 42-44 for a detailed description of the modes of action of the herbicidal active ingredients used in this trial). Other than this response, for Calaris® and Sencorex Flow® treated plants, there are few other reliable conclusions that can be drawn from this data. For example, for Sencorex Flow® and Calaris® treated plants, the addition of 680nm LASER treatments at the doses specified in Chapter 5, does not prove to be highly influential to the production or upregulation of SOD. Few doses lead to significantly increased levels of SOD compared to plants treated with herbicide exclusively. This said, after Calaris® treatment and in Sencorex Flow® treated *Chenopodium album*, there is a dramatic increase in SOD units mg^{-1} total protein for the 7s dwell time at higher mA levels of 1800-2000mA. This response is not echoed for the higher dwell time of 10s. In addition, the average values for SOD levels are markedly increased in *Sinapis arvensis* treated with Sencorex Flow® and Calaris® compared to *Chenopodium album* plants.

There are spikes in SOD units levels, especially evident in Figures 50 (d) for the 5s dwell time. These spikes in values occur at 1800mA and 1900mA and are consistent with the sudden rise in OJIP values discussed. This could highlight the link between the inhibition of PSII and the production of SOD.

Nevada® treated *Chenopodium album* and *Sinapis arvensis* yield highly inconsistent levels of SOD. Nevada® treated *Chenopodium album* and *Sinapis arvensis* plants do not yield a significant difference between untreated plants and herbicide treated plants. Furthermore, upon 680nm LASER treatment, levels of SOD in *Chenopodium album* decline with increasing LASER dosage. In *Sinapis arvensis* treated with Nevada®, this is less evident with no significant response.
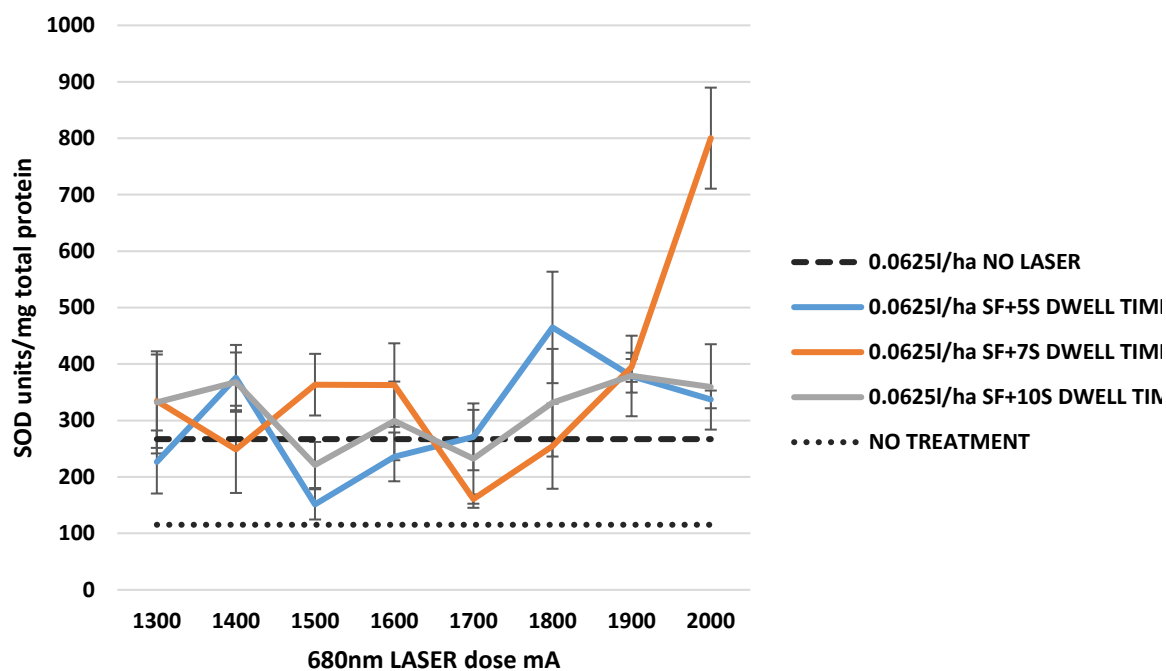
(a)
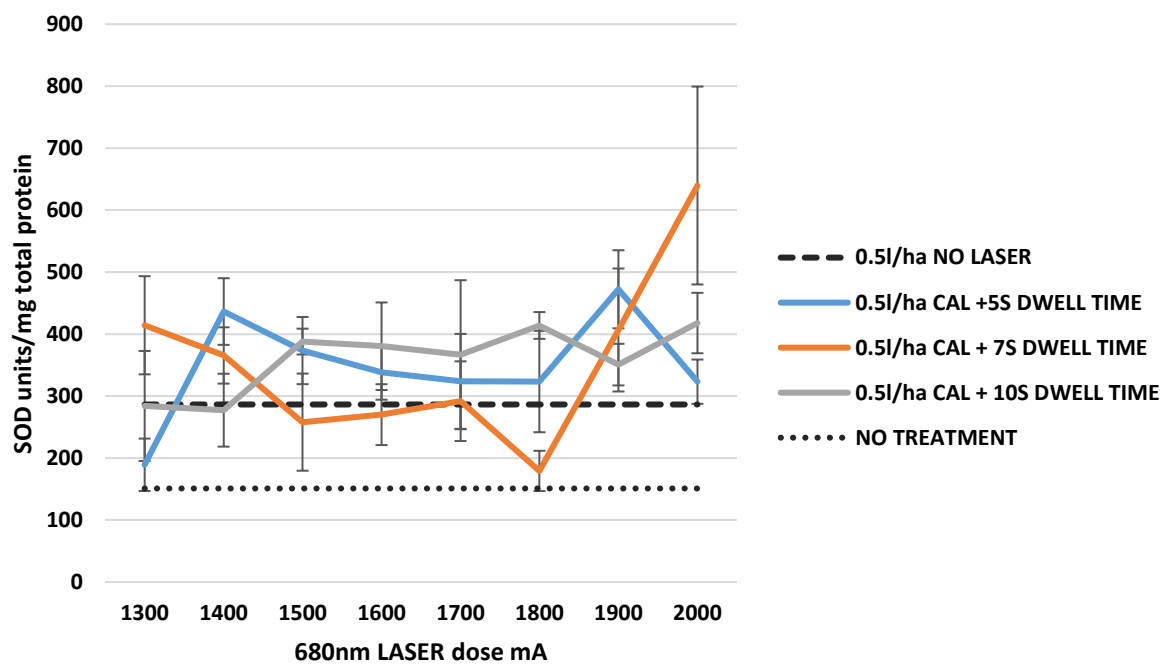
(b)
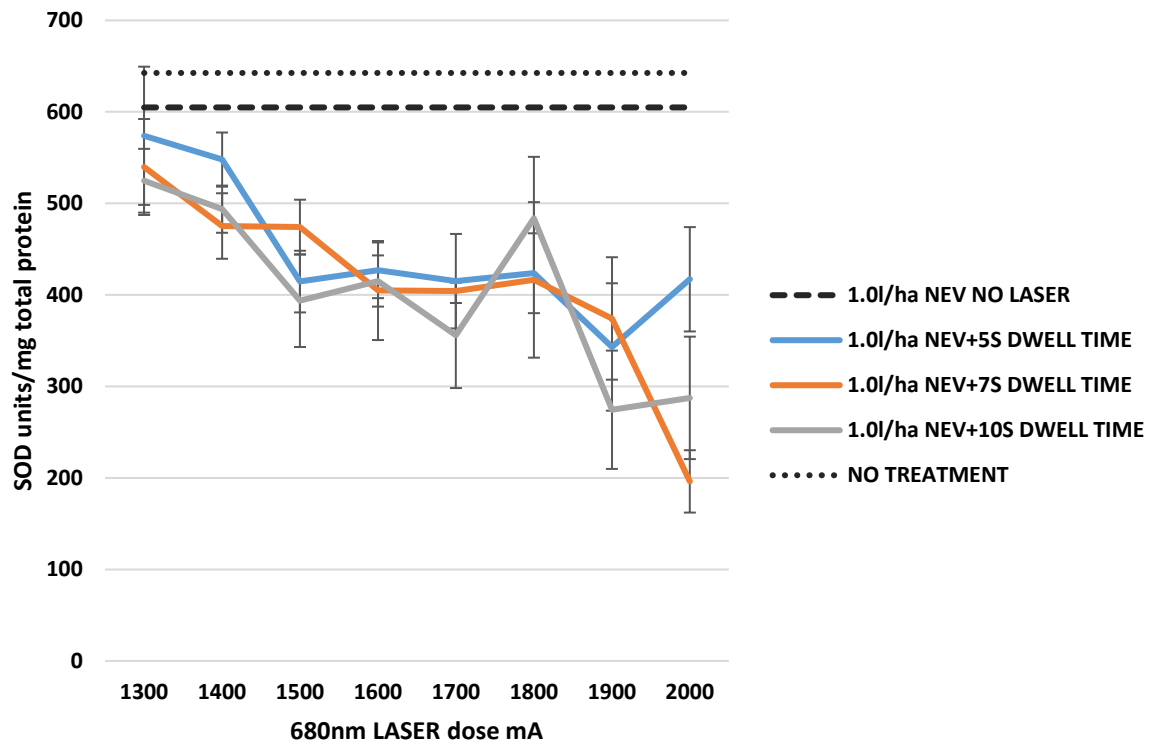
(c)
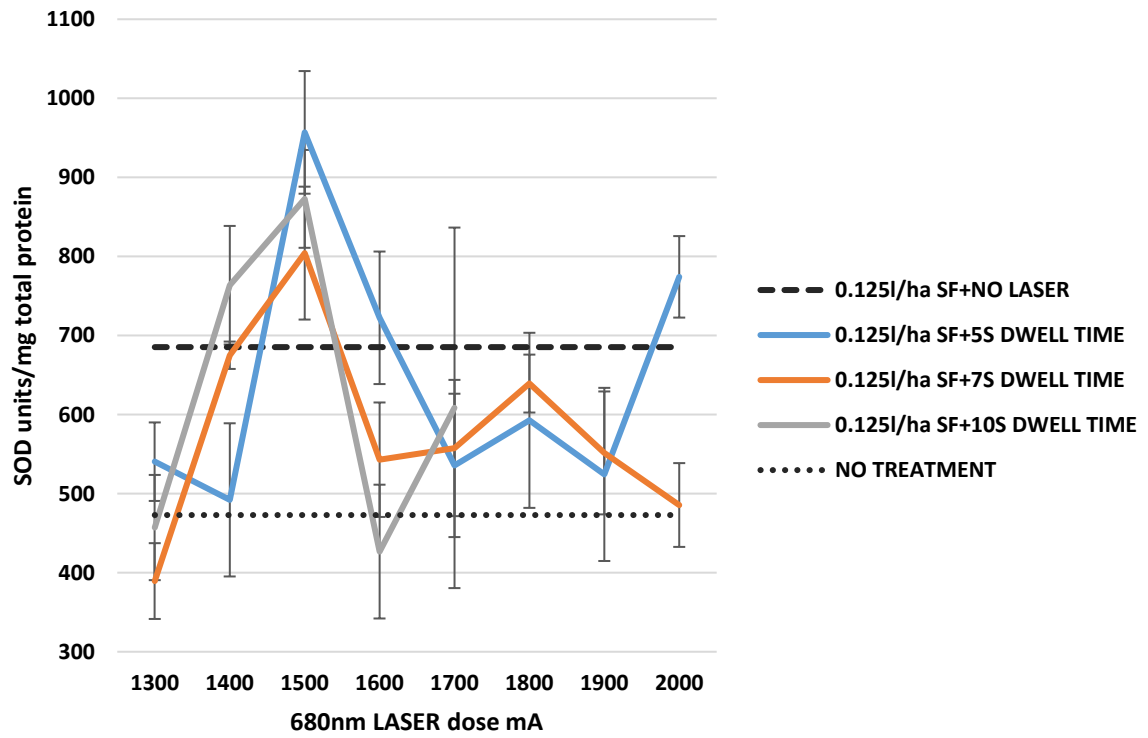
(d)
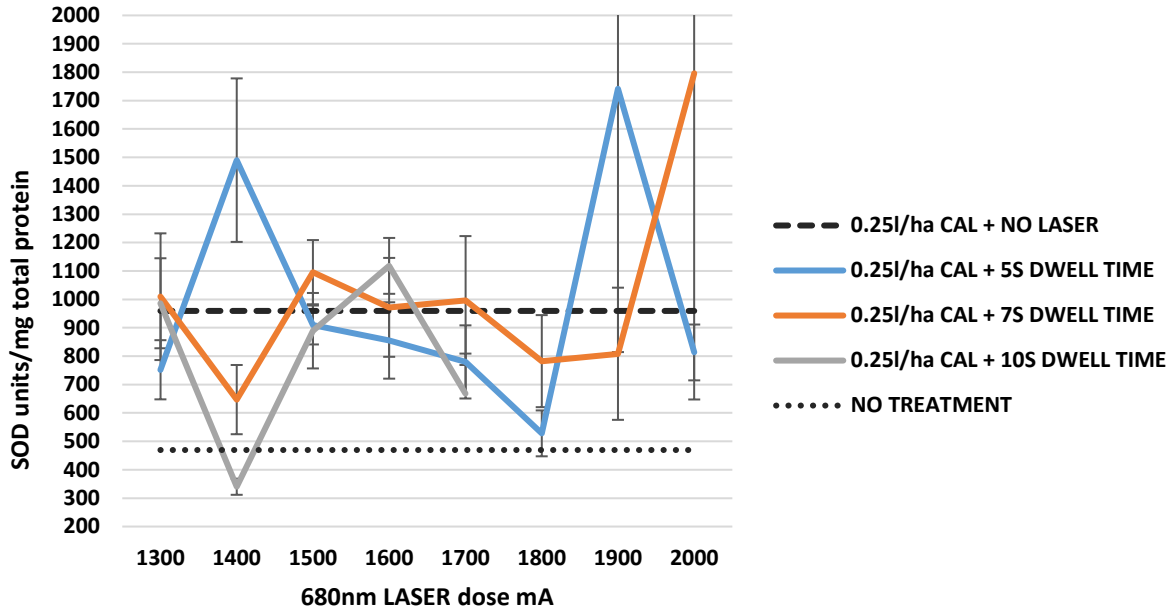
(e)
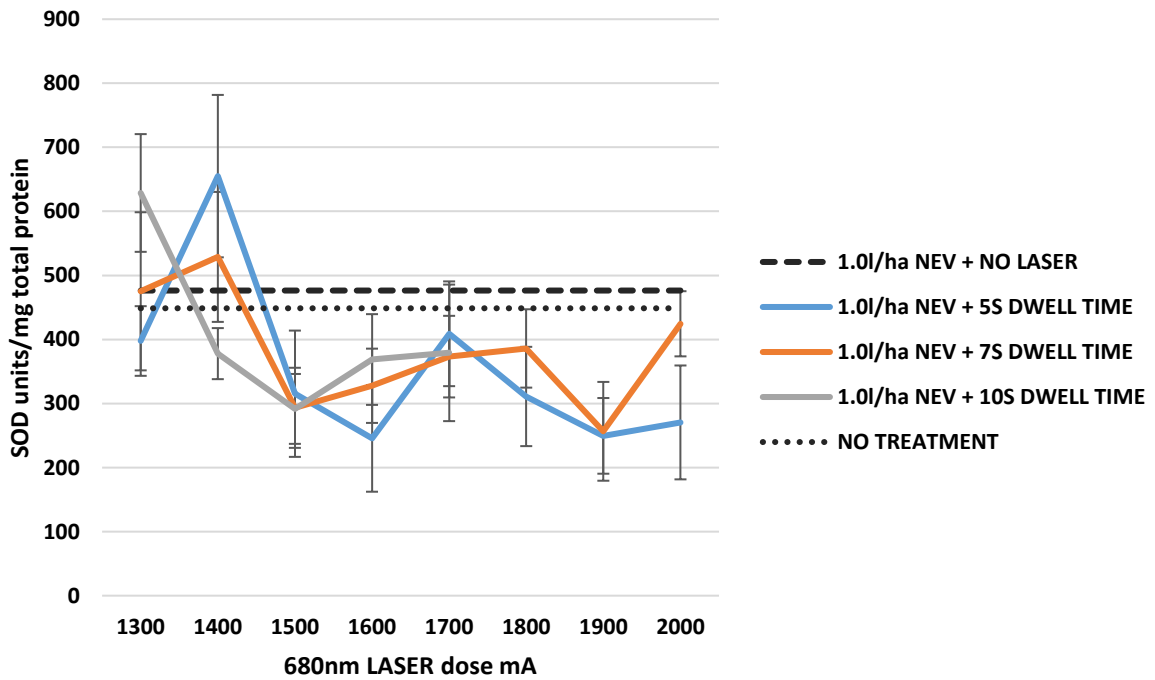
(f)

Figure 51 The units of SOD/mg total protein of (a) Chenopodium album treated with Sencorex Flow®
at a rate of 0.0625lha^{-1}, (b) Chenopodium album treated with Calaris® at a rate of 0.5lha^{-1} , (c)
Chenopodium album treated with Nevada® at a rate of 1.0lha^{-1} (d) Sinapis arvensis treated with
Sencorex Flow® at a rate of 0.125lha^{-1} , (e) Sinapis arvensis treated with Calaris® at a rate of 0.25lha^{-1}
^{1}, (f) Sinapis arvensis treated with Nevada® at a rate of 1.0lha^{-1} in response to 680nm LASER dose
(mA) Legend: Sencorex Flow®-denotes Sencorex Flow® treatment, Calaris®- denotes Calaris®

treatment, NEV- denotes Nevada® treatment. NO TREATMENT corresponds to Chenopodium album or Sinapis arvensis plants receiving no herbicide or 680nm LASER treatment. Error bars denote ± standard error of the mean (SEM), n=6. Significant outcomes calculated using factorial ANOVA and T-Test.

5.7   Discussion

5.7.1 Spikes in OJIP data

The spikes visible in OJIP data usually present at 1800mA and 1900mA after herbicide and 680nm LASER treatment is difficult to explain. It is unlikely that such specific doses of 680nm LASER energy of no consistent dwell time influence every OJIP parameter individually. At 680nm LASER doses of 1800mA and 1900mA, there is a generally a significant increase in Abs.RC values. This increase in absorption (quantified by the OJIP parameter Abs.RC) results in energy accumulation in the system, leading to a higher chance of trapping (quantified by the OJIP parameter TRoRC), electron flow (quantified by the OJIP parameter EToRC) and dissipation (quantified by the OJIP parameter DIoRC). Alterations in aforementioned OJIP parameters therefore originates from the amount of energy absorbed from the supply of 680nm LASER energy, which could be considered unsurprising due to the readiness of PSII to absorb light at 680nm.

The question of, why do the specific 680nm LASER currents of 1800mA and 1900mA alter OJIP parameters from the norm, remains. It is interesting that such a specific 680nm LASER current, albeit not consistent in terms of dwell time has this effect. All that can be theorised is that this level of current is absorbed efficiently by either the LHC or is funnelled and absorbed directly by the chlorophyll *a* special pair. The second scenario is more likely due to the concomitant increase in TRoRC and EToRC when Abs.RC is raised. It is plausible that a current level of 1800mA and 1900mA is strong enough to force the 680nm LASER energy through to the chlorophyll a special pair. Plant leaves, specifically Sinapis arvensis at greater 680nm LASER mA doses and at dwell times exceeding 7s suffered visible leaf surface damage. This is likely to have been caused by cellular ablation. In studies conducted by Abushita et al. (1997) and D'Evoli et al. (2013) it was found that β-carotene and lutein were only partially degraded by 20 minutes of 100°C heat treatment, at levels of 29% and 3%, respectively. This suggests carotenoids are relatively stable under heat pressure. Exposure to such a high temperature and increased duration compared to treatment by the 680nm LASER which had a maximum chosen dwell time of 10s is therefore

unlikely to have denatured the carotenoids in the LHC which contribute to the absorption of light, in turn suggesting that carotenoids could also be responsible for absorbing increased levels of energy.

Photoinhibition is defined as the light dependent decrease in photosynthetic rate which may occur whenever the photon flux is in excess of that required for photosynthesis (Aro et al., 1993, Chan et al., 2012, Hakala et al., 2005, Murata et al., 2007a, Takahashi and Murata, 2008, Tikkanen et al., 2014, Vass and Cser, 2009)It is not unreasonable to suggest that the reduction in OJIP values after the pinnacle of the spike in OJIP parameters signifies a decline in photosynthetic capability. A more far-fetched hypothesis could be that the high current of 2000mA forces the LASER energy through the plant leaving no opportunity for absorption.

5.7.2 The shift in optimal dose for 680nm LASER only treatment to higher 680nm LASER doses after herbicide application

When 680nm LASER energy was applied to *Chenopodium album* and *Sinapis arvensis* exclusively, the optimal doses of 680nm LASER which led to the symptoms of photoinhibition in terms of OJIP parameter readings were 1700mA for a period of 10s for *Chenopodium album* and in the 1400mA and 1500mA regions for *Sinapis arvensis*. For *Sinapis arvensis* especially, the apparent LASER doses most effective at inducing photoinhibition/overload are in the 1800mA to 1900mA region. The difference in OJIP parameter results for *Chenopodium album* in terms of treatment type is less stark, where photoinhibition/overload is induced with LASER+herbicide according to OJIP parameters at 1800mA or 1900mA. The change in effective dose for *Sinapis arvensis* is particularly marked.

Possible explanations for this change are scarce in published literature. One theory could be that a higher dose of energy is needed to impact PSII. It is worth noting that spikes in OJIP parameters are less pronounced after Calaris® treatment. Calaris® contains the active ingredient mesotrione, the action of which is detailed on pages 42-44. Mesotrione is responsible for the inhibition or carotenoid biosynthesis, which could suggest why there is no accentuated spike in Abs.RC data for LASER+Calaris® treated plants therefore a lack of a knock-on effect shown in the remaining OJIP parameters. As detailed on pages 35-40, TRoRC, EToRC, DIoRC parameters are strongly influenced by the Abs.RC values. Sencorex Flow® does not contain mesotrione and the spikes in OJIP data upon LASER+Sencorex Flow® treatment are defined suggesting a greater rate of absorbance (Abs.RC) where absorbance by carotenoid pigments is a contributing factor.

Another explanation for a greater dose of 680nm LASER required to influence OJIP parameters after Calaris® and Sencorex Flow® treatment surrounds the block in electron transport. It is possible that more energy is needed to overcome the block in electron transport caused by the photosynthetic inhibiting active ingredients of Calaris® and Sencorex Flow®, terbuthylazine and metribuzin respectively. Ungerer et al. (2018) details the pull effect that is inflicted upon electrons through the PSII and PSI complexes, where P700+ pulls electrons from cytochrome F after electrons arrive from PSII. It is possible that electrons are pulled through PSII after they pass beyond PSII and onto PSI (P700). It would be interesting to see the changes in REoRC values after herbicide+LASER treatment to assess if electrons reach PSI. If the REoRC value is greater upon LASER treatment, the plausibility of the electron pull theory could increase. It would also be interesting to focus on a range of herbicide and 680nm LASER doses applied to the plants to determine if there is consistent evidence of this 'pull' theory. It would be important to record REoRC in addition to the five OJIP parameters measured in this study. It could be hypothesised that increasing herbicide dose could lead to a greater 'pull' from the increased level of absorbance, onwards through the PSII complex in order to overcome the electron block enforced by the herbicide.

5.7.3 The increase in EToRC values in response to Nevada® treated *Sinapis arvensis*

The increase in EToRC values at shown in Figure 48 (d) after Nevada® application is opposite to the effect Sencorex Flow® and Calaris® treatment have on *Chenopodium album* and *Sinapis arvensis*. As Sencorex Flow® and Calaris® are photosystem II inhibitors, it was predicted that EToRC levels would decline in response to herbicide treatment compared to the control. The mode of action of the active ingredients of Nevada®, florasulam and fluorpoxyr are independent of PSII entirely. This is not to say that the active ingredients of Nevada® do not affect photosynthetic mechanisms indirectly. Florasulam in Nevada® is a protein synthesis inhibitor (Liu et al., 2015). After Nevada® treatment, global plant health can begin to visibly decline one day post treatment, but plants treated with Nevada® can generally cling to viability for around 10 days. As a result of this global decline, it is plausible to suggest that electron transport is increased in order to generate ATP as an attempt to increase protein production and rectify the block in *de novo* protein synthesis as well as transporting proteins across membranes

An increase in EToRC is apparent when treated with Nevada® exclusively in Chapter 3 between Days 0 (pre-treatment) and Day 1, but is more apparent at lower doses (0.0625lha^{-1}

and 0.125lha^{-1}), P<0.001 between Day 0 (pre-treatment) and Day 1 (post-treatment) for dose 0.0625lha, and similarly P<0.001 between Day 0 (pre-treatment) and Day 1 (post-treatment) for dose 0.125lha. However, beyond 0.25lha^{-1} EToRC values between Days 0 and day 1 converge and normalise. This suggests Day 1 EToRC values were misleadingly low. This test should be repeated to determine if this difference in value is accurate.

5.7.4 The increase in TRo.RC values in response to 680nm LASER+Nevada® treatment in *Chenopodium album*

The increase in TRoRC values in Nevada® treated *Chenopodium album* is probably due to the increased absorbance and trapping capability and efficiency to mitigate against plant health decline by increasing the ETC in order to produce ATP. However, other OJIP parameter data for Nevada® treated *Chenopodium album* are inconsistent. For example, Abs.RC values are largely unaltered and EToRC unchanged from the control. Dissipation (DIoRC) is slightly but not significantly increased upon Nevada® application. This data set is inconsistent and highlights an unusual disconnect between OJIP parameters upon Nevada® treatment. Trapping values are also inconsistent where TRo.RC values are significantly lower than in untreated plants (P=0.007) (page 147) after treatment with 1.0lha^{-1} Nevada®. This could be highlighting an attempt made by the plant to trap an increased amount of light to mitigate against the continuing decline in overall plant health. However, as shown in (Chapter 5), Fv.Fm levels in Nevada® treated *Chenopodium album* do not significantly decline suggesting no overall decline in photosynthetic state in the days post treatment. Therefore this logic for increased trapping after Nevada® treatment may not follow. However, Force et al. (2003) states that Fv.Fm is an OJIP parameter insensitive to change and cannot be completely relied upon and other OJIP parameters including TRo.RC reveal finer details.   The addition of 680nm LASER energy to 1.0lha^{-1} Nevada® treated *Chenopodium album* plants, leads to a spike at 1900mA in all OJIP parameters measured and yields a more interrelated set of OJIP parameters. The spike in values at 1900mA upon 680nm LASER+Nevada® treatment could suggest trapping proteins are more stable or less frequently turned over and so do not require newly synthesised proteins, a process which is inhibited by Nevada®. Absorption levels also increase at 1900mA upon 680nm LASER+Nevada® treatment supporting the idea that the plant is attempting to rectify the loss of overall plant health and making use of the 680nm LASER light supplied.

5.7.5 The decline in SOD units per mg total protein in Nevada® treated *Chenopodium album*

As Figure 51 (c) displays, there is a correlated decline in SOD units mg total protein with increasing 680nm LASER dose after 1.0lha Nevada® treatment in *Chenopodium album* and less so in *Sinapis arvensis*. One active ingredients of Nevada®, florasulam is a protein synthesis inhibitor. It is possible that upon 680nm LASER application, especially at higher 680nm LASER doses, proteins denatured by free radicals generated in response to 680nm LASER application are not replenished due to florasulam. SOD is an enzymatic protein and so is produced in the same way as other cellular proteins. This effect could be accentuated by the high dose of Nevada®, at 1.0lha^{-1}. However, the same dose of Nevada®, 1.0lha^{-1} was applied to *Sinapis arvensis* pre-680nm LASER treatment and the correlated decline between SOD units per mg total protein and 680nm LASER dose is much less pronounced. It is possible that different plant species have different biochemical responses after Nevada® treatment. It would be interesting to treat *Chenopodium album* with lower doses of Nevada® and then apply 680nm LASER energy to assess if the active ingredients of Nevada® do result in the block in the replenishment of denatured SOD even at lower doses of active ingredients.

Chenopodium album and *Sinapis arvensis* plants treated with Calaris® and Sencorex Flow® do not exhibit such a decline in SOD units per mg total protein post 680nm LASER treatment and this could be due to the different active ingredients in Calaris® and Sencorex Flow®. Mesotrione and metribuzin in Calaris® and Sencorex Flow® respectively do not have a role in protein synthesis inhibition as Florasulam does in Nevada®. It is possible that any SOD denatured after 680nm LASER treatment through free radical formation is replenished more readily.

5.7.6 The general increase in percentage relative conductivity for Calaris® treated plants and unpredictability in values for Sencorex Flow® and Nevada® treated plants

The % relative conductivity readings for *Sinapis arvensis* and *Chenopodium album* treated with Calaris® show increasing values with greater 680nm LASER doses irrespective of dwell times. This is not apparent in *Chenopodium album* and *Sinapis arvensis* treated with Sencorex Flow® or Nevada® where the data points are erratic in nature. One possible reason behind the increasing % relative conductivity is due to the active ingredients of Calaris®. Mesotrione, as stated on Page 43 reduced the plants' ability to scavenge ROS

leading to lipid peroxidation and subsequent membrane damage (Hess, 2000). It is possible that as 680nm LASER is applied with increasing dose, ROS are produced in response to the high light intensity and due to the action of mesotrione, are left to inflict damage on cellular membranes.

It is interesting to see the lack of a clear response for Nevada® treated *Sinapis arvensis* and *Chenopodium album* as fluroxpyr (group O) and 5g/L florasulam (group B) disrupt cell wall structure. However, the cell wall is independent of the cell membrane and is composed of glucan-based cellulose microfibrils bound in a hydrated matrix made of pectins, hemicelluloses, structural proteins and proteoglycans (Burton et al., 2010, Cosgrove, 2005) whereas the cell membrane is composed of phospholipids. It is possible that the action of fluroxpyr and Florasulam cause a loss of turgor pressure and restrictions in growth but do not cause direct damage to cell membranes. It could be due to this difference in mechanism why the cell membrane remains largely intact resulting in low electrolyte leakage thus low % relative conductivity readings. In addition, 680nm LASER treatment in conjunction with Nevada® treatment did not result in an increasing % relative conductivity value as it is likely that the biochemical responses in after 680nm LASER treatment which could include ROS production were minimised by the cellular scavenging systems which were unhindered by Nevada® action.

Sencorex Flow®+680nm LASER treatment also produced erratic % relative conductivity readings with increasing 680nm LASER dose. The active ingredient of Sencorex Flow® is 600g/L metribuzin which is a photosystem II inhibitor. It is possible that any ROS produced in response to the 680nm light is scavenged as carotenoid and a-tocopherol biosynthesis is unaffected by Metribuzin which directly inhibits electron flow by binding to plastoquinone (Arntzen et al., 1981, Blyden and Gray, 1986, Ort et al., 1983). As a result, ROS production is scavenged and cell membranes remain intact.

% relative conductivity readings for Sencorex Flow® and Nevada® treated plants are likely to be erratic due to the decline in plant viability and only somewhat due to the combined action of the herbicide and 680nm LASER treatments.

5.7.7 No observable response in Nevada® data regarding percentage relative conductivity

Nevada® is a protein synth inhibitor which could lead to failure of the membrane repair processes. Data from Chapter 3 detailing biochemical plant responses prior to herbicide treatment show little change in %RC between days 1, 3 and 5 post treatment. %RC should

be measured up to day 10 post Nevada® treatment as plants treated with Nevada® take up to 10 days to senesce. It is possible that longer time is needed between the day of treatment and post treatment measurement of %RC in order to show a difference between %RC values. However, the absence of change in %RC values is consistent in the results across chapters. The erratic range in data points for Nevada®+LASER treated samples could be as a result of the action of the LASER but without a defined outcome, forming definite explanations could be misleading. Having said this, plants treated with Nevada®, exclusively look to have highly inconsistent %RC readings, but the reality is that the %RC range is between 7µS and 14µs with small error bars for both *Sinapis arvensis* and *Chenopodium album.* In comparison to Sencorex Flow® treated *Sinapis arvensis* at a dose of 0.125lha^{-1} where %RC data points range from 5-40µS, the range in %RC data points in Nevada® treated plants is minimal.

5.8   Conclusion

To conclude, there is evidence of enhanced disruption upon a dual treatment of 680nm LASER and PSII inhibiting herbicide application on the function of PSII. Such changes are small but could be increased by the inclusion of various other wavelengths of light, including 700nm to target PSI. In general, the marked changes in the state of PSII are largely due to the effect of the herbicide treatment and not the 680nm LASER treatment.

Chapter 6

General discussion

6.1   680nm LASER

The overall set up of the 680nm LASER was effective in contributing to this field of weed growth management. Focusing on OJIP parameter data, addition of the 680nm LASER on both herbicide treated and herbicide un-treated plants yielded both positive and negative changes in the PSII complex. The 680nm LASER influenced *Chenopodium album* and *Sinapis arvensis* differently, suggesting that in a field setting, tailoring of treatments to specie weed species is needed to achieve optimal weed control outcomes. Percentage relative conductivity and SOD assay data did contribute to the findings in this study, but it is chlorophyll fluorescence, specifically OJIP parameter readings which provides a quick and non-invasive method to assess biochemical changes in PSII in response to herbicide and or 680 LASER treatment.

6.1.1 Spot size

The beam size emitted from the 680nm LD was 300µm diameter, the area of which is 544 times smaller than the area of the leaf clip aperture (see Chapter 2, page 46). Whilst the spot size of the 680nm LASER is small compared to the leaf clip aperture and thousands of times smaller than a whole leaf area, the addition of the 680nm LASER is having an effect on PSII from the OJIP data detailed in Chapter 4 and 5. This can be seen in Chapter 4 which details the biochemical changes when the 680nm LASER is the sole treatment. A larger spot size could yield more accurate data if it was to cover a larger area of the leaf clip aperture. From some data gathered from the herbicide + 680nm LASER treatment, it could be concluded that the effects of the 680nm LASER were 'lost' in the efficient biochemical effects of the herbicide. Having a larger beam size whilst maintaining power and wavelength could provide a better insight and more reliable data. In an ideal situation where these findings could be applied to a field setting, a whole plant should be illuminated with 680nm light. This would be very costly to produce a set up with LDs as used in this study, so LEDs could be trialled.

6.1.2 Choice of wavelength

The decision to use a LASER emitting 680nm was based upon the ability of photosystem II (PSII) to absorb light efficiently at this wavelength. The aim was to overload PSII with energy leading to a decline in photosynthetic capacity. The results of this study, particularly when the LASER was used as a treatment in conjunction with herbicides (Chapter 5), found that the effects of the LASER were overpowered by the biochemical effects of the herbicide, even at low chemical doses.

There are a number of possible developments which could be added to the LASER treatment protocol in order to increase efficacy. Firstly, 680nm LASER treated *Sinapis arvensis* was shown to be affected by treatment, whereas *Chenopodium album* plants showed very little change through OJIP parameter data. Photosystem I (PSI) absorbs light efficiently at 700nm. It would be interesting to see the effect on the ETC if both 680nm and 700nm light was administered to the plants. Further, measuring the IP phase of OJIP which details the reduction of plastocyanin and P700$^+$ after initial oxidation (Schansker et al., 2003, Schreiber et al., 1989) could highlight effects on PSI after 680nm LASER treatment.

The oxygen evolving complex is an important complex which could also be targeted by LASERs emitting different wavelengths. Ohnishi et al. (2005) suggested that the working state of photosystem II could be affected by supplying the plant with two different wavelengths of light in a two-step process. Firstly, 500nm light (blue region) which is highly effective for OEC inactivation but not effective for PSII RC inactivation was illuminated onto thylakoid membranes. Following this, the same membranes were illuminated with 680nm light (red region) thus inactivating the PSII RC but having little influence on the OEC. Ohnishi et al. (2005) concluded that P680 only becomes sensitive to 680nm light when the OEC has been inactivated by the 500nm light.

However, having to supply a range of light rather negates the aim of the theory of using one specific wavelength of light to target specific processes. Further, adding more wavelengths could contribute to cost and complexity of a LASER emission system. Future work using a number of LASER diodes covering a wider area on the leaf and able to emit either one determined wavelength or a number of wavelengths would be needed in order to assess effects on the wider photosynthetic systems. However, again, adding these conditions to an already complex and technically difficult set up is likely to add further complications and cost reducing feasibility for in field applications.

The distance treated plants are placed from the 680nm LASER is another factor which can be adjusted. In theory, when using a multimode model as in this study (page 46) the 680nm

LASER beam is not collimated as a parallel beam. Nevertheless, as long as the leaf area to undergo analysis i.e., OJIP analysis is covered by the LASER beam area, the flux density across that area should be unchanged. However, it would be worth making sure this is the case and that distance from the source is not a factor in OJIP, % relative conductivity or SOD production variations.

A major caveat in this study was the limitation of dwell times available. Dwell times of only 1s increments were possible. When administering already short dwell times, it would be useful to be able to treat plants for half second intervals to aid in the equal spread of doses. For example, a 7.5s dwell time would have been useful to make the doses between 5s and 10s dwell times equal. A 5s dwell time was shown to be the lowest dwell time capable of initiating biochemical change to PSII and a 10s dwell time was chosen as this dwell time effectively doubled the dose of energy. 7s dwell was chosen to be a go between dose but ideally this should have been 7.5s. Dwell times above 7s for LASER treated *Sinapis arvensis* visible damaged *Sinapis arvensis* so could not be used at mA values above 1800mA.

6.2   OJIP readings

In the field of chlorophyll fluorescence, OJIP parameter readings are considered highly robust and accurate (Baker, 2008, Baker and Rosenqvist, 2004, Barbagallo et al., 2003, Maxwell and Johnson, 2000, Murchie and Lawson, 2013). Time course analysis in regular intervals, i.e., every 15 minutes post LASER treatment could give a clear picture as to the recovery of PSII or the wider ETC instead of solely at 45 minutes after treatment to allow for dark adaptation. However recording OJIP every 15 minutes post treatment is difficult in terms of labour and time would be needed for dark adaptation.

6.3   Conductivity reading method

The percentage relative conductivity data gathered supports some of the OJIP data and provides explainable outcomes according to the herbicide and type of herbicide used. In general, the error bars for the % relative conductivity data are small, indicating a small range in data values. Notwithstanding, there is some doubt in the field regarding the accuracy of this method (Kato et al., 2002, Leopold et al., 1981) in terms of quantifying the correct biochemical processes occurring in the leaf.

For example, it is possible that the salt bladders present on the *Chenopodium album* leaves influence the conductivity readings, but this is not suggested by these current results as the difference between *Sinapis arvensis* and *Chenopodium album* % relative conductivity values are not marked enough. *Chenopodium album* has significantly thicker leaves than *Sinapis arvensis* ($P<0.001$, via a T-Test) so the water content could vary between species so may alter % relative conductivity readings. This is a factor which should be certified in future work. Therefore, it could be possible that the salt bladders do contribute the conductivity readings, but as yet this is a very tenuous assumption. It would be interesting to determine the composition of the salt bladders. It could be possible that as the name suggests, the bladders have a high salt content which would increase conductivity readings.

As stated in the protocol on page 49, leaves were floated in a sealed tube on 25ml deionised water and subsequent conductivity readings measured to quantify electrolyte leakage through % relative conductivity readings. Leaf discs floated on water are different from intact leaves in photosynthetic efficiency terms according to Kato et al. (2002); this study was not assessing the % relative conductivity from treated plants but highlights some useful findings and differences to this present study. The results from Kato et al., (2002) show that floating leaf discs on water affects the susceptibility of the plant to photoinhibition which may have influenced the findings in this experiment. A non-destructive method to visually assess membrane damage could be via Fluorescein diacetate staining followed by visualization through a confocal microscope (Jones et al., 2016).

Leaf discs stored on water experience a CO_2 exchange reduction (Ishibashi and Terashima, 1995) and a lower partial pressure (pp) of CO_2 in intercellular spaces. Lower pp of CO_2 decelerates the ribulose-1,5-bisphosphate carboxylase/oxygenase reaction which in turn retards the rate of the ETC (Sage et al., 1990). The result of this is the inhibition of ATP production resulting in a lower rate of repair to cellular proteins and membranes which could translate into greater electrolyte leakage form cells.

The 680nm LASER treated samples were stored in the dark preventing the production of ATP. This ATP production inhibition results in the failure to supply the energy required for cellular repair processes leaving ROS level unchanged. This mechanism could confound the membrane damage, leading to greater % relative conductivity. The leaves in the Kato et al. (2002) study were exposed to light whilst floating in the water, which highlights a major difference in experimental protocol between these studies. As stated Kato et al. (2002) were not analysing % relative conductivity from treated samples, but storing leaf samples in the light could produce misleading % relative conductivity readings in the Kato et al. (2002) study as ROS could be scavenged and membranes repaired with the continuation of

photosynthesis and ATP production. It would be interesting to compare the conductivity of leaf discs stored in water in light, and those stored in the dark to determine if this variable makes a significant difference to conductivity readings.

A further finding from Kato et al. (2002) relevant to this current study is the amphistomatic nature of *Chenopodium album* leaves. *Chenopodium album* leaves possess 39% of total stomatal pores on the adaxial side in high light grown plants (Kato et al., 2002) but the high light intensity was supplied after leaf excision and not during plant growth as in this current study. When the leaf discs are floated on water in Kato et al. (2002) the leaves were placed on the water with the adaxial side up to prevent desiccation. CO_2 diffusion at the abaxial surface might have been limited, which lowered CO_2 pp at intercellular spaces (see above why this is important). In this current study, there was no consideration regarding the orientation of the leaf pieces on the water. It could be worth running a trial where leaf orientation was consistent to determine if this has an effect on %RC findings.

It is likely that these seemingly minor differences between study protocols are not enough to affect conductivity readings with the method chosen for this present study. Kato et al. (2002) analysed plant susceptibility to photoinhibition in detached and intact plant samples using highly accurate equipment. It is possible that even if the amendments mentioned above where adhered to, the conductivity probe used in this present study is not accurate enough to pick up any subtle and minor differences in readings. It could be wise to run a malondialdehyde (MDA) assay to quantify lipid peroxidation (Garcia et al., 2005, Jambunathan, 2010) alongside the conductivity probe method to support these findings

6.4   SOD assay

The oxidative stress status in plants can be quantified by measuring ROS levels, modifications to certain proteins and redox metabolites. In this study, ROS levels were quantified using SOD as an indication of superoxide levels in the plant after either herbicide, 680nm LASER or herbicide and 680nm LASER combined treatment. Quantifying SOD does not give a definitive version of oxidative stress levels in the cell but can contribute useful information.

It is recognized in the field of oxidative stresses that SOD and other antioxidant enzymes are upregulated in response to an increase in stress in the plant (Alscher et al., 2002). Having said this, more recently there has been evidence put forward to suggest that the increase in ROS levels in a sample does not merely indicate an increase in oxidative stress as ROS are

unlikely to accumulate in a consistent pattern across the cell and only accumulate in areas where oxidation is required (Foyer and Noctor, 2005, Foyer and Noctor, 2016). Thus, ROS accumulation may not be a result of cellular stress. In addition, the levels of upregulated SOD may not be due to external treatment such as the 680nm LASER as SOD and H_2O_2 scavenging enzymes are highly expressed even in optimal conditions for the plant (Noctor et al., 2016). In light of this, careful thought should be taken when conducting the SOD assay in vitro. The main problem in this current study is the fact that the 680nm LASER theoretically should target P680 in the PSII complex and data from the OJIP measurements (detailed in Chapters 4 and 5) would suggest that this is the case. PSI in turn could generate superoxide due to the water-water cycle (Asada, 1999, Rizhsky et al., 2003). The protocol for this SOD assay requires the plant sample to be ultra-centrifuged at 15000g for 15 minutes in order to separate cellular homogenate into fractions after lysing of cells. Centrifuging samples separates cell components by size and density, where low speeds are able to force large components including nuclei to the bottom of the centrifuge tube. The remaining fraction after resuspension contains SOD released from lysed cells. In this study, the plant cells were lysed through mechanical pressure thus releasing cellular contents. Therefore, any reading of SOD regards the levels in the cell and is not specific to certain areas of the cell, i.e. relevant to this study, isolation of the chloroplasts (Shao et al., 2011) might give a more accurate reading.

6.4.1 The use of NBT

One technical caveat in the protocol used to quantify SOD in the plant samples is the use of NBT. A measurable colour change as a result of monoformazan production is usually taken as proof that superoxide is the cause. A factor often ignored in this field of science is NBT is not specific to superoxide and can highlight ascorbate (Conklin et al., 1996) or dehydrogenases (Fridovich, 1997) and changing oxygen levels can also influence the colour change reaction. However, this limitation is more likely to be a problem with *in situ* analyses but regarding this study, it could be wise to run other assays which do not use NBT as the supernatant used for the assay may contain the complicating moieties. In addition, there is evidence to suggest NBT can produce ROS (Fridovich, 1997) thus an artificial production may reduce NBT and confound the colour change through production of monoformazan which is also antagonized by SOD.

6.4.2 *In vitro* and *in vivo* misconceptions

Antioxidative enzyme assays, of which the SOD assay used in this study is included, have further limitations. Quantifying the extracted enzyme activity can be used to provide only indirect evidence of an increase in ROS in the plant before sampling, but a common misconception is that relative increases in antioxidant enzymes such as SOD correlate to relative ROS levels. In addition, it is unwise to draw precise conclusions from data received from assays conducted *in vitro* and transfer them to *in vivo* systems. One reason for this, relevant to this study is that often in *in vitro* assays, the activity of the identified enzyme is an amalgamation of the activity of a number of enzyme isoforms coded by a gene family. Hence, different subcellular compartments could have different varying levels of the isoform depending on the organelle. The theoretical MOA of the 680nm LASER would be to increase oxidative stress in PSII and PSI contained in the thylakoid membranes. In light of this, it would be prudent to only analyze the SOD isoform present in chloroplasts for a higher level of accuracy.

6.4.3 SOD vs singlet oxygen assay conclusion

The choice of assay to reveal the intricacies of ROS production after plant treatment was decided by the theoretical outcome of the 680nm LASER treatment in terms of the biochemical processes taking place. With this in mind, the choice of the SOD assay might not have been the best diagnostic tool to quantify superoxide levels. Singlet oxygen ($^1O_2$) is formed in PSII from the transfer of energy from triplet chlorophyll to triplet oxygen (Fufezan et al., 2002b, Hideg et al., 2007). It is likely that the excited state of triplet chlorophyll is formed after 680nm LASER application. The 680nm LASER is hypothesized to target the chlorophyll special pair (Chl *a*) in the P680 reaction center (RC) and as Chl *a* should theoretically absorb this wavelength of light very efficiently, the lower energy excited state of triplet chlorophyll can arise. Triplet chlorophyll has a long life time (2-3µs) and can react with $3O_2$ to produce $^1O_2$ (Krieger-Liszkay, 2005, Krieger-Liszkay et al., 2008b). In addition, the more likely location, according to Krieger-Liszkay (2005) for large amounts of $^1O_2$ to be produced is in the P680 RC where the Chl *a* special pair are located, rather than from triplet chlorophyll production in the antenna. With this evidence in mind, the most appropriate diagnostic to determine the effects of the 680nm LASER could be through $^1O_2$ quantification. Relevant to this study, this $^1O_2$ oxygen production (Krieger-Liszkay, 2005). Further, Fufezan et al. (2002b) also showed that in the presence of PSII targeting herbicides, the production

of $^1O_2$ is markedly increased so this same approach could be used to assess the suitability of the herbicides used. In general, the SOD assay is suitable to assess superoxide produced in response to stress. However $^1O_2$ production is more specific to the P680 RC and so quantification of $^1O_2$ could yield a more valuable data set.

6.5   Bradford assay

The Bradford assay was run in order to be able to express specific SOD activity of plant samples as SOD units per mg of total protein. The assay produced highly reliable and repeatable data. The standard curve produced by a bovine serum albumin serial dilution produced a curve with a high R^2 value. Sample and reagent preparation was minimal with few individual processes whilst still producing accurate data sets.

6.6   The suitability of the chosen protocols

The SOD assay, whilst containing protocol caveats, aims to quantify levels of SOD in the plant tissue sample. This SOD level does not directly translate into the level of lipid peroxidation but provides information of the level of a stress response after treatment. Lipid peroxidation is a likely outcome of both herbicide treatment (see page 31) and LASER treatment. At certain doses of the 680nm LASER specifically 1800mA to 2000mA with a 10s dwell time on *Sinapis arvensis*, there was visible deformation of the leaf surface. This suggested heat ablation of the cells of the upper epidermis. Lipid peroxidation assays are able to distinguish between chemical i.e. the lipid peroxidation cascade (see page 31) and heat ablation as the bursting of cells due to high temperature is a different mechanism to lipid peroxidation; physical rather than chemical. Conductivity readings, in this study translating into electrolyte leakage does not distinguish between lipid peroxidation and cellular ablation. It is would be advisable, in order to fill this gap, to run malondialdehyde assays (see section 7 (Further work)) alongside the current methods to make findings more robust and conclusive. It would be interesting to run a small trial to compare % relative conductivity and malondialdehyde data where cells have been ablated through heat and those treated with a known lipid peroxidation trigger such as aluminium (Yamamoto et al., 2001) to compare protocol suitability.

6.7 Further work

Another OJIP parameter which could be measured in future work is REoRC. REoRC is defined as the electron flux able to reduce end electron acceptors at the PSI acceptor side per RC (Ceusters et al., 2019, Fan et al., 2015). Put simply, Reo.RC values give an indication of the proportion of electrons arriving at PSI. Reo.RC values of approximately 0.4-0.5 would be found in a typical unstressed plant. Lower values indicate faults in the ability of PSII to absorb photons and funnel this energy into the photosynthetic ETC. This OJIP parameter could strengthen the findings of the project as a whole as Reo.RC could reveal if light from the 680nm LASER is reaching PSI. Whilst EToRC supplies evidence for the promotion or inhibition of the photosynthetic ETC, it does not reveal information as to the fate of this energy.

Malondialdehyde is a widely used marker of oxidative lipid injury whose concentration varies in response to biotic and abiotic stress. Usually, it is membrane lipid peroxidation induced by environmental stress in plants which is detected by measuring MDA (Kong et al., 2016). MDA is quantified as a strong light-absorbing and fluorescing adduct following reaction with thiobarbituric acid (TBA) (Ayala et al., 2014). As with many scientific protocols, they are not completely accurate and have caveats. For example, the MDA assay can be affected by the compounds plants naturally contain and the concentrations of these compounds can be altered by the plants' environmental conditions. There are newer MDA assay techniques to minimize this interference including reverse phased HPLC developed by Ayala et al. (2014). This technique is beyond the scope of the research able to be conducted at Harper Adams University but samples could be sent away. It could be interesting to use the MDA assay alongside the EL and SOD assay in support but not as a replacement to these other methods.

6.8 Key findings

The findings from this project suggest the use of LASER energy in the control of weed growth does have potential, but the focus in future work should be on the use of multiple different wavelengths of light in order to target various processes of photosynthesis. This could allow the movement away from the use of herbicides as weed control methods. This study did find that administering 680nm LASER light promoted the rate of electron transport in *Sinapis arvensis* and so this could be a secondary finding of this study which was not originally the focus.

The use of herbicides is still the one of the most effective methods of weed control and if this method is to be used less, research into using novel methods of weed control such as with the use of LASER energy is needed. Complete control of weeds with methods such as administering LASER energy are a long way from being commercially viable. In addition, the use of different herbicide dose rates on *Sinapis arvensis* and *Chenopodium album* is not a method a busy farmer would have time to do. The combination of 680nm LASER and varying herbicide doses to form a tailored weed control method to different species solely relies upon the availability of the correct equipment and technology to carry this out, without the need for human intervention. To have an autonomous robot capable of administering the correct dosages of 680nm LASER and herbicide is plausible and this research was conducted with this view in mind.

The more commercially viable finding from this study is the promotion of the ETC after 680nm in *Sinapis arvensis*. This approach could be used in artificial growing conditions in order to use less energy in production. It is clear from the results that whether the aim is promotion of photosynthesis or inhibition, a tailored approach to the use with different plants is needed.

7 References

ABUSHITA, A. A., HEBSHI, E. A., DAOOD, H. G. & BIACS, P. A. 1997. Determination of antioxidant vitamins in tomatoes. *Food Chemistry,* 60**,** 207-212.

ADAM, Z., RUDELLA, A. & VAN WIJK, K. J. 2006. Recent advances in the study of Clp, FtsH and other proteases located in chloroplasts. *Curr Opin Plant Biol,* 9**,** 234-40.

ALLAKHVERDIEV, S. I. & MURATA, N. 2004. Environmental stress inhibits the synthesis de novo of proteins involved in the photodamage-repair cycle of Photosystem II in Synechocystis sp. PCC 6803. *Biochim Biophys Acta,* 1657**,** 23-32.

ALSCHER, R. G., ERTURK, N. & HEATH, L. S. 2002. Role of superoxide dismutases (SODs) in controlling oxidative stress in plants. *J Exp Bot,* 53**,** 1331-41.

ANANYEV, G., RENGER, G., WACKER, U. & KLIMOV, V. 1994. The photoproduction of superoxide radicals and the superoxide dismutase activity of Photosystem II. The possible involvement of cytochrome b559. *Photosynth Res,* 41**,** 327-38.

ANDERSON, G. C., FILLERY, I. R. P., DOLLING, P. J. & ASSENG, S. 1998. Nitrogen and water flows under pasture-wheat and lupin-wheat rotations in deep sands in Western Australia - 1. Nitrogen fixation in legumes, net N mineralisation, and utilisation of soil-derived nitrogen. *Australian Journal of Agricultural Research,* 49**,** 329-343.

ANDERSON, J. M. & CHOW, W. S. 2002. Structural and functional dynamics of plant photosystem II. *Philosophical Transactions of the Royal Society of London, Series B: Biological Sciences,* 357**,** 1421-30; discussion 1469-70.

APEL, K. & HIRT, H. 2004a. Reactive oxygen species: metabolism, oxidative stress, and signal transduction. *Annu Rev Plant Biol,* 55**,** 373-99.

APEL, K. & HIRT, H. 2004b. Reactive oxygen species: Metabolism, oxidative stress, and signal transduction. *Annual Review of Plant Biology,* 55**,** 373-399.

ARMEL, G. R., HALL, G. J., WILSON, H. P. & CULLEN, N. 2005. Mesotrione plus atrazine mixtures for control of Canada thistle (Cirsium arvense). *Weed Science,* 53**,** 202-211.

ARNTZEN, C. J., PFISTER, K. & STEINBACK, K. E. 1981. The mechanisms of chloroplast triazine resistance: Alteration in the site of herbicide action. *In:* LEBARON, H. M. & GRESSEL, J. (eds.) *Herbicide Resistance in Plants.* New York: John Wiley & Sons, Inc.

ARO, E. M., SUORSA, M., ROKKA, A., ALLAHVERDIYEVA, Y., PAAKKARINEN, V., SALEEM, A., BATTCHIKOVA, N. & RINTAMAKI, E. 2005. Dynamics of photosystem II: a proteomic approach to thylakoid protein complexes. *J Exp Bot,* 56**,** 347-56.

ARO, E. M., VIRGIN, I. & ANDERSSON, B. 1993. Photoinhibition of Photosystem-2 - Inactivation, Protein Damage and Turnover. *Biochimica Et Biophysica Acta,* 1143**,** 113-134.

ASADA, K. 1999. THE WATER-WATER CYCLE IN CHLOROPLASTS: Scavenging of Active Oxygens and Dissipation of Excess Photons. *Annu Rev Plant Physiol Plant Mol Biol,* 50**,** 601-639.

ASADA, K. 2006. Production and scavenging of reactive oxygen species in chloroplasts and their functions. *Plant Physiology,* 141**,** 391-396.

ASCARD, J. 1989. Thrmal Weed Control with Flaming in Onions. *30th Swedish Crop Protection Conference: Weeds and Weed Control.* Uppsala, Sweden.

ASTATKIE, T., RIFAI, M. N., HAVARD, P., ADSETT, J., LACKO-BARTOSOVA, M. & OTEPKA, P. 2007. Effectiveness of hot water, infrared and open flame thermal units for controlling weeds. *Biological Agriculture & Horticulture,* 25**,** 1-12.

AVERY, A. A. 2006. *Nature's Toxic Tools: The Organic Myth of Pesticide-Free Farming.,* Churchwille, Center for Global Food Issues.

AYALA, A., MUNOZ, M. F. & ARGUELLES, S. 2014. Lipid Peroxidation: Production, Metabolism, and Signaling Mechanisms of Malondialdehyde and 4-Hydroxy-2-Nonenal. *Oxidative Medicine and Cellular Longevity*.

BABAR, M. A., REYNOLDS, M. P., VAN GINKEL, M., KLATT, A. R., RAUN, W. R. & STONE, M. L. 2006. Spectral reflectance indices as a potential indirect selection criteria for wheat yield under irrigation. *Crop Science,* 46**,** 578-588.

BAJJI, M., KINET, J. M. & LUTTS, S. 2002. Osmotic and ionic effects of NaCl on germination, early seedling growth, and ion content of Atriplex halimus (Chenopodiaceae). *Canadian Journal of Botany-Revue Canadienne De Botanique,* 80**,** 297-304.

BAKER, C. J. & ORLANDI, E. W. 1995. Active oxygen in plant pathogenesis. *Annu Rev Phytopathol,* 33**,** 299-321.

BAKER, N. R. 2008. Chlorophyll fluorescence: A probe of photosynthesis in vivo. *Annual Review of Plant Biology,* 59**,** 89-113.

BAKER, N. R. & ROSENQVIST, E. 2004. Applications of chlorophyll fluorescence can improve crop production strategies: an examination of future possibilities. *J Exp Bot,* 55**,** 1607-21.

BALYKIN, V. I. & SIDOROV, A. I. 1987. Collimation and Decollimation of Atomic-Beams by Laser-Radiation. *Applied Physics B-Photophysics and Laser Chemistry,* 42**,** 51-54.

BANOWETZ, G. M., DIERKSEN, K. P., AZEVEDO, M. D. & STOUT, R. 2004. Microplate quantification of plant leaf superoxide dismutases. *Analytical Biochemistry,* 332**,** 314-320.

BARBA-ESPIN, G., DIAZ-VIVANCOS, P., CLEMENTE-MORENO, M. J., ALBACETE, A., FAIZE, L., FAIZE, M., PEREZ-ALFOCEA, F. & HERNANDEZ, J. A. 2010. Interaction between hydrogen peroxide and plant hormones during germination and the early growth of pea seedlings. *Plant Cell Environ,* 33**,** 981-94.

BARBAGALLO, R. P., OXBOROUGH, K., PALLETT, K. E. & BAKER, N. R. 2003. Rapid, noninvasive screening for perturbations of metabolism and plant growth using chlorophyll fluorescence imaging. *Plant Physiology,* 132**,** 485-493.

BARTON, M. K. 2010. Twenty years on: the inner workings of the shoot apical meristem, a developmental dynamo. *Dev Biol,* 341**,** 95-113.

BAYRAMIAN, A., FAY, P.E., DYER, W.E. Weed control using carbon dioxide lasers. In: Proceedings Western Society of Weed Science, 1993 Logan, UT, USA. 55-56.

BEAUCHAMP, C. & FRIDOVICH, I. 1971. Superoxide dismutase: improved assays and an assay applicable to acrylamide gels. *Anal Biochem,* 44**,** 276-87.

BECKIE, H. J., ASHWORTH, M. B. & FLOWER, K. C. 2019. Herbicide Resistance Management: Recent Developments and Trends. *Plants (Basel),* 8.

BERCA, M. 2004. Perspectives Regarding Weeds Control. *In:* DEVELOPMENT, U. F. C. F. A. A. R. (ed.). Chelmsford.

BHATTACHARJEE, S. 2005. Reactive oxygen species and oxidative burst: Roles in stress, senescence and signal transduction in plants. *Current Science,* 89**,** 1113-1121.

BLYDEN, E. R. & GRAY, J. C. 1986. The Molecular-Basis of Triazine Herbicide Resistance in Senecio-Vulgaris L. *Biochemical Society Transactions,* 14**,** 62-62.

BOHM, J., MESSERER, M., MULLER, H. M., SCHOLZ-STARKE, J., GRADOGNA, A., SCHERZER, S., MAIERHOFER, T., BAZIHIZINA, N., ZHANG, H., STIGLOHER, C., ACHE, P., AL-RASHEID, K. A. S., MAYER, K. F. X., SHABALA, S., CARPANETO, A., HABERER, G., ZHU, J. K. & HEDRICH, R. 2018. Understanding the Molecular Basis of Salt Sequestration in Epidermal Bladder Cells of Chenopodium quinoa. *Curr Biol,* 28**,** 3075-3085 e7.

BOND, W. & GRUNDY, A. C. 2001. Non-chemical weed management in organic farming systems. *Weed Research,* 41**,** 383-405.

BOOTH, B. D., MURPHY, S.D. AND SWANTON, C.J., 2003. *Weed Ecology in Natural and Agricultural Systems.,* Wallingford, UK, CABI publishing.

BOURNONVILLE, C. F. & DIAZ-RICCI, J. C. 2011. Quantitative determination of superoxide in plant leaves using a modified NBT staining method. *Phytochem Anal,* 22**,** 268-71.

BRADFORD, M. M. 1976. A rapid and sensitive method for the quantitation of microgram quantities of protein utilizing the principle of protein-dye binding. *Anal Biochem,* 72**,** 248-54.

BRASLAVSKY, S. E. & HOLZWARTH, A. R. 2012. Role of Carotenoids in Photosystem II (PSII) Reaction Centers. *International Journal of Thermophysics,* 33**,** 2021-2025.

BUCHANAN, B. B. 1984. The ferredoxin/thioredoxin system: a key element in the regulatory function of light in photosynthesis. *Bioscience,* 34**,** 378-83.

BUNTING, A. H., DENNETT, M.D., ELSTON, J., AND SPEED, C.B. 1982. Climate and crop distribution. *In:* BLAXTER, K. L., FOWDEN, L. (ed.) *Food, Nutrition and Climate.* London: Applied Science Publisher.

BURRITT, D. J. & MACKENZIE, S. 2003. Antioxidant metabolism during acclimation of Begonia x erythrophylla to high light levels. *Ann Bot,* 91**,** 783-94.

BURTON, R. A., GIDLEY, M. J. & FINCHER, G. B. 2010. Heterogeneity in the chemistry, structure and function of plant cell walls. *Nature Chemical Biology,* 6**,** 724-732.

CAFFARRI, S., BROESS, K., CROCE, R. & VAN AMERONGEN, H. 2011. Excitation energy transfer and trapping in higher plant Photosystem II complexes with different antenna sizes. *Biophys J,* 100**,** 2094-103.

CAFFARRI, S., TIBILETTI, T., JENNINGS, R. C. & SANTABARBARA, S. 2014. A Comparison Between Plant Photosystem I and Photosystem II Architecture and Functioning. *Current Protein & Peptide Science,* 15**,** 296-331.

CAMPE, R., HOLLENBACH, E., KAMMERER, L., HENDRIKS, J., HOFFKEN, H. W., KRAUS, H., LERCHL, J., MIETZNER, T., TRESCH, S., WITSCHEL, M. & HUTZLER, J. 2018. A new herbicidal site of action: Cinmethylin binds to acyl-ACP thioesterase and inhibits plant fatty acid biosynthesis. *Pestic Biochem Physiol,* 148**,** 116-125.

CARRILLO, N., LUCERO, H. A. & VALLEJOS, R. H. 1981. Light modulation of chloroplast membrane-bound ferredoxin-NADP+ oxidoreductase. *J Biol Chem,* 256**,** 1058-9.

CELESTI-GRAPOW, L., AND BLASI, C., 2004. The Role of Alien and Native Weeds in the Deterioration of Archaeological Remains in Italy. *Weed Technology,* 18**,** 1508-1513.

CEUSTERS, N., VALCKE, R., FRANS, M., CLAES, J. E., VAN DEN ENDE, W. & CEUSTERS, J. 2019. Performance Index and PSII Connectivity Under Drought and Contrasting Light Regimes in the CAM Orchid Phalaenopsis. *Front Plant Sci,* 10**,** 1012.

CHALIFOUR, A., ARTS, M. T., KAINZ, M. J. & JUNEAU, P. 2014. Combined effect of temperature and bleaching herbicides on photosynthesis, pigment and fatty acid composition of Chlamydomonas reinhardtii. *European Journal of Phycology,* 49**,** 508-515.

CHAN, T., SHIMIZU, Y., POSPISIL, P., NIJO, N., FUJIWARA, A., TANINAKA, Y., ISHIKAWA, T., HORI, H., NANBA, D., IMAI, A., MORITA, N., YOSHIOKA-NISHIMURA, M., IZUMI, Y., YAMAMOTO, Y., KOBAYASHI, H., MIZUSAWA, N., WADA, H. & YAMAMOTO, Y. 2012. Quality control of photosystem II: lipid peroxidation accelerates photoinhibition under excessive illumination. *PLoS One,* 7**,** e52100.

CHATTERJEE, A. & KUNDU, S. 2015. Revisiting the chlorophyll biosynthesis pathway using genome scale metabolic model of Oryza sativa japonica. *Sci Rep,* 5**,** 14975.

CHEN, G. E., CANNIFFE, D. P., BARNETT, S. F. H., HOLLINGSHEAD, S., BRINDLEY, A. A., VASILEV, C., BRYANT, D. A. & HUNTER, C. N. 2018. Complete enzyme set for chlorophyll biosynthesis in Escherichia coli. *Sci Adv,* 4**,** eaaq1407.

CHOUDHURY, S., PANDA, P., SAHOO, L. & PANDA, S. K. 2013. Reactive oxygen species signaling in plants under abiotic stress. *Plant Signal Behav,* 8**,** e23681.

CONKLIN, P. L., WILLIAMS, E. H. & LAST, R. L. 1996. Environmental stress sensitivity of an ascorbic acid-deficient Arabidopsis mutant. *Proceedings of the National Academy of Sciences of the United States of America,* 93**,** 9970-9974.

CONSTANTINE, N., GIANNOPOLITIS & REIS, S. K. 1977. Superoxide Dismutases. *Plant Physiology,* 59**,** 309-314.

COSGROVE, D. J. 2005. Growth of the plant cell wall. *Nature Reviews Molecular Cell Biology,* 6**,** 850-861.

COSGROVE, D. J. 2016. Plant cell wall extensibility: connecting plant cell growth with cell wall structure, mechanics, and the action of wall-modifying enzymes. *Journal of Experimental Botany,* 67**,** 463-476.

D'EVOLI, L., LOMBARDI-BOCCIA, G. & LUCARINI, M. 2013. Influence of Heat Treatments on Carotenoid Content of Cherry Tomatoes. *Foods,* 2**,** 352-363.

DACOSTA, M., WANG, Z. L. & HUANG, B. R. 2004. Physiological adaptation of Kentucky bluegrass to localized soil drying. *Crop Science,* 44**,** 1307-1314.

DALL'OSTO, L., HOLT, N. E., KALIGOTLA, S., FUCIMAN, M., CAZZANIGA, S., CARBONERA, D., FRANK, H. A., ALRIC, J. & BASSI, R. 2012. Zeaxanthin protects plant photosynthesis by modulating chlorophyll triplet yield in specific light-harvesting antenna subunits. *J Biol Chem,* 287**,** 41820-34.

DAT, J. F., LOPEZ-DELGADO, H., FOYER, C. H. & SCOTT, I. M. 1998. Parallel changes in H2O2 and catalase during thermotolerance induced by salicylic acid or heat acclimation in mustard seedlings. *Plant Physiology,* 116**,** 1351-1357.

DEFRA. 2014. *Agriculture in the United Kingdom* [Online]. Department For Environment, Food And Rural Affairs. [Accessed [Accessed on 19/06/2014] 2014].

DEMIDCHIK, V., STRALTSOVA, D., MEDVEDEV, S. S., POZHVANOV, G. A., SOKOLIK, A. & YURIN, V. 2014. Stress-induced electrolyte leakage: the role of K+-permeable channels and involvement in programmed cell death and metabolic adjustment. *J Exp Bot,* 65**,** 1259-70.

DEMMIG-ADAMS, B. & ADAMS, W. W., 3RD 2006. Photoprotection in an ecological context: the remarkable complexity of thermal energy dissipation. *New Phytol,* 172**,** 11-21.

DEMMIG-ADAMS, B., GILMORE, A. M. & ADAMS, W. W., 3RD 1996. Carotenoids 3: in vivo function of carotenoids in higher plants. *FASEB J,* 10**,** 403-12.

DIAZ, R., MANRIQUE, V., HIBBARD, K., FOX, A., RODA, A., GANDOLFO, D., MCKAY, F., MEDAL, J., HIGHT, S. & OVERHOLT, W. A. 2014. Successful Biological Control of Tropical Soda Apple (Solanales: Solanaceae) in Florida: A Review of Key Program Components. *Florida Entomologist,* 97**,** 179-190.

DINC, E., CEPPI, M. G., TOTH, S. Z., BOTTKA, S. & SCHANSKER, G. 2012. The chl a fluorescence intensity is remarkably insensitive to changes in the chlorophyll content of the leaf as long as the chl a/b ratio remains unaffected. *Biochim Biophys Acta,* 1817**,** 770-9.

DUNAHAY, T. G. & STAEHELIN, L. A. 1985. Isolation of photosystem I complexes from octyl glucoside/sodium dodecyl sulfate solubilized spinach thylakoids : characterization and reconstitution into liposomes. *Plant Physiol,* 78**,** 606-13.

EICHELMANN, H., OJA, V., RASULOV, B., PADU, E., BICHELE, I., PETTAI, H., MAND, P., KULL, O. & LAISK, A. 2005. Adjustment of leaf photosynthesis to shade in a natural canopy: reallocation of nitrogen. *Plant Cell and Environment,* 28**,** 389-401.

ELAVARTHI, S. & MARTIN, B. 2010. Spectrophotometric assays for antioxidant enzymes in plants. *Methods Mol Biol,* 639**,** 273-81.

ELLIOTT, M. S., MASSEY, B., CUI, X., HIEBERT, E., CHARUDATTAN, R., WAIPARA, N. & HAYES, L. 2009. Supplemental host range of Araujia mosaic virus, a potential biological control agent of moth plant in New Zealand. *Australasian Plant Pathology,* 38**,** 603-607.

FAN, J., HU, Z., XIE, Y., CHAN, Z., CHEN, K., AMOMBO, E., CHEN, L. & FU, J. 2015. Alleviation of cold damage to photosystem II and metabolisms by melatonin in Bermudagrass. *Front Plant Sci,* 6**,** 925.

FERNANDEZ-QUINTANILLA, C., PENA, J. M., ANDUJAR, D., DORADO, J., RIBEIRO, A. & LOPEZ-GRANADOS, F. 2018. Is the current state of the art of weed monitoring suitable for site-specific weed management in arable crops? *Weed Research,* 58**,** 259-272.

FERRELL, J., CHARUDATTAN, R., ELLIOTT, M. & HIEBERT, E. 2008. Effects of selected herbicides on the efficacy of tobacco mild green mosaic virus to control tropical soda apple (Solanum warm). *Weed Science,* 56**,** 128-132.

FORCE, L., CRITCHLEY, C. & VAN RENSEN, J. J. 2003. New fluorescence parameters for monitoring photosynthesis in plants. *Photosynth Res,* 78**,** 17-33.

FOREMAN, J., DEMIDCHIK, V., BOTHWELL, J. H. F., MYLONA, P., MIEDEMA, H., TORRES, M. A., LINSTEAD, P., COSTA, S., BROWNLEE, C., JONES, J. D. G., DAVIES, J. M. & DOLAN, L. 2003. Reactive oxygen species produced by NADPH oxidase regulate plant cell growth. *Nature,* 422**,** 442-446.

FOYER, C. H. & NOCTOR, G. 2005. Oxidant and antioxidant signalling in plants: a re-evaluation of the concept of oxidative stress in a physiological context. *Plant Cell and Environment,* 28**,** 1056-1071.

FOYER, C. H. & NOCTOR, G. 2016. Stress-triggered redox signalling: what's in pROSpect? *Plant Cell and Environment,* 39**,** 951-964.

FRIDOVICH, I. 1986. Superoxide dismutases. *Adv Enzymol Relat Areas Mol Biol,* 58**,** 61-97.

FRIDOVICH, I. 1997. Superoxide anion radical (O-2 radical anion), superoxide dismutases, and related matters. *Journal of Biological Chemistry,* 272**,** 18515-18517.

FUFEZAN, C., RUTHERFORD, A. W. & KRIEGER-LISZKAY, A. 2002a. Singlet oxygen production in herbicide-treated photosystem II. *FEBS Lett,* 532**,** 407-10.

FUFEZAN, C., RUTHERFORD, A. W. & KRIEGER-LISZKAY, A. 2002b. Singlet oxygen production in herbicide-treated photosystem II. *Febs Letters,* 532**,** 407-410.

GAO, C., ZHANG, L., WEN, F. & XING, D. 2008. Sorting out the role of reactive oxygen species during plant programmed cell death induced by ultraviolet-C overexposure. *Plant Signal Behav,* 3**,** 197-8.

GARCIA, Y. J., RODRIGUEZ-MALAVER, A. J. & PENALOZA, N. 2005. Lipid peroxidation measurement by thiobarbituric acid assay in rat cerebellar slices. *Journal of Neuroscience Methods,* 144**,** 127-135.

GECHEV, T., GADJEV, I., VAN BREUSEGEM, F., INZE, D., DUKIANDJIEV, S., TONEVA, V. & MINKOV, I. 2002. Hydrogen peroxide protects tobacco from oxidative stress by inducing a set of antioxidant enzymes. *Cell Mol Life Sci,* 59**,** 708-14.

GIANNOPOLITIS, C. N. & RIES, S. K. 1976. Superoxide Dismutases: Occurence in Higher Plants. *Journal of Plant Physiology,* 59**,** 309-314.

GIANNOPOLITIS, C. N. & RIES, S. K. 1977. Superoxide dismutases: I. Occurrence in higher plants. *Plant Physiol,* 59**,** 309-14.

GIROTTI, A. W. 1998. Lipid hydroperoxide generation, turnover, and effector action in biological systems. *J Lipid Res,* 39**,** 1529-42.

GOMES, M. T. G., DA LUZ, A. C., DOS SANTOS, M. R., BATITUCCI, M. D. P., SILVA, D. M. & FALQUETO, A. R. 2012. Drought tolerance of passion fruit plants assessed by the OJIP chlorophyll a fluorescence transient. *Scientia Horticulturae,* 142**,** 49-56.

GOULD 1959. The LASER, Light Amplification by Stimulated Emission of Radiation. *The Ann Arbor Conference on Optical Pumping, the University of Michigan.*

GRAHAM, M. D., REES, S. L., STEINER, M. & FLEMING, A. S. 2006. The effects of adrenalectomy and corticosterone replacement on maternal memory in postpartum rats. *Horm Behav,* 49**,** 353-61.

GUYOT, C. 1962. Semences et Plantules des Principales des Mauvaises Herbes. *Association de Coordination Technique Agricole*.

HAFEZ, Y. M., BACSO, R., KIRALY, Z., KUNSTLER, A. & KIRALY, L. 2012. Up-regulation of antioxidants in tobacco by low concentrations of H(2)O(2) suppresses necrotic disease symptoms. *Phytopathology,* 102**,** 848-56.

HAKALA, M., TUOMINEN, I., KERANEN, M., TYYSTJARVI, T. & TYYSTJARVI, E. 2005. Evidence for the role of the oxygen-evolving manganese complex in photoinhibition of Photosystem II. *Biochim Biophys Acta,* 1706**,** 68-80.

HALL, A. J., REBELLA, C.M., GHERSA, C.M., AND CULOT, J., 1982. Field-crop systems of the Pampas. *In:* PEARSON, C. J. (ed.) *Field Crop Ecosystems Series: Ecosystems of the World.* Amsterdam: Elsevier Science Publishers B.V.

HALLIWELL, B. 2006. Reactive species and antioxidants. Redox biology is a fundamental theme of aerobic life. *Plant Physiol,* 141**,** 312-22.

HANSSON, D. & ASCARD, J. 2002. Influence of developmental stage and time of assessment on hot water weed control (vol 42, pg 307, 2002). *Weed Research,* 42**,** 414-414.

HARDING, D. P. & RAIZADA, M. N. 2015. Controlling weeds with fungi, bacteria and viruses: a review. *Front Plant Sci,* 6**,** 659.

HAVAUX, M., EYMERY, F., PORFIROVA, S., REY, P. & DORMANN, P. 2005. Vitamin E protects against photoinhibition and photooxidative stress in Arabidopsis thaliana. *Plant Cell,* 17**,** 3451-69.

HAY, J. R. 1974. Gains to Grower from Weed Science. *Weed Science,* 22**,** 439-442.

HEAP, I. 2008. *The International Survey of Resistant Weeds* [Online]. www.weedscience.com. [Accessed 25/01/2016 2016].

Heap, I.M. International Survey of Herbicide Resistant Weeds. 2019. Available online: http://www.weedscience.org (accessed on 23rd June 2019).

HEAP, I. 2014. Global perspective of herbicide-resistant weeds. *Pest Management Science,* 70**,** 1306-1315.

HEAP, I. 2020. The International Herbicide-Resistant Weed Database.

HEISEL, T., SCHOU, J., ANDREASEN, C. & CHRISTENSEN, S. 2002. Using laser to measure stem thickness and cut weed stems. *Weed Research,* 42**,** 242-248.

HEISEL, T., SCHOU, J., CHRISTENSEN, S. & ANDREASEN, C. 2001. Cutting weeds with a CO2 laser. *Weed Research,* 41**,** 19-29.

HESS, F. D. 2000. Light-dependent herbicides: an overview. *Weed Science,* 48**,** 160-170.

HGCA. 2005a. *Avoiding lodging in winter wheat, practical guidelines.* [Online]. Home Grown Cereals Authority. [Accessed [Accessed 03/08/2015] 2015].

HGCA. 2005b. *The Barley Growth Guide* [Online]. Home Growth Cereals Authority. [Accessed [Accessed 03/08/2015] 2015].

HIDEG, E., KALAI, T. & HIDEG, K. 2011. Direct detection of free radicals and reactive oxygen species in thylakoids. *Methods Molecular Biology,* 684**,** 187-200.

HIDEG, E., KALAI, T., HIDEG, K. & VASS, I. 1998. Photoinhibition of photosynthesis in vivo results in singlet oxygen production detection via nitroxide-induced fluorescence quenching in broad bean leaves. *Biochemistry,* 37**,** 11405-11.

HIDEG, E., KOS, P. B. & VASS, I. 2007. Photosystem II damage induced by chemically generated singlet oxygen in tobacco leaves. *Physiol Plant,* 131**,** 33-40.

HRAC. 2020a. *Herbicide Resistance Action Committee* [Online]. Available: https://www.hracglobal.com/ [Accessed 10/03/2020].

HRAC. 2020b. *HRAC Mode of Action Classification 2020* [Online]. Available: https://hracglobal.com/files/HRAC_Revised_MOA_Classification_Herbicides_Poster.png [Accessed 08/03/2020].

HSU, B. D. & LEU, K. L. 2003. A possible origin of the middle phase of polyphasic chlorophyll fluorescence transient. *Functional Plant Biology,* 30**,** 571-576.

HUBBART, S., BIRD, S., LAKE, J. A. & MURCHIE, E. H. 2013. Does growth under elevated CO(2) moderate photoacclimation in rice? *Physiol Plant,* 148**,** 297-306.

HUESGEN, P. F., SCHUHMANN, H. & ADAMSKA, I. 2009. Deg/HtrA proteases as components of a network for photosystem II quality control in chloroplasts and cyanobacteria. *Res Microbiol,* 160**,** 726-32.

IAKIMOVA, E. T. & WOLTERING, E. J. 2018. The wound response in fresh-cut lettuce involves programmed cell death events. *Protoplasma,* 255**,** 1225-1238.

INOUE, S., EJIMA, K., IWAI, E., HAYASHI, H., APPEL, J., TYYSTJARVI, E., MURATA, N. & NISHIYAMA, Y. 2011. Protection by alpha-tocopherol of the repair of photosystem II during photoinhibition in Synechocystis sp PCC 6803. *Biochimica Et Biophysica Acta-Bioenergetics,* 1807**,** 236-241.

ISHIBASHI, M. & TERASHIMA, I. 1995. Effects of Continuous Leaf Wetness on Photosynthesis - Adverse Aspects of Rainfall. *Plant Cell and Environment,* 18**,** 431-438.

ISHIHARA, H., OBATA, T., SULPICE, R., FERNIE, A. R. & STITT, M. 2015. Quantifying protein synthesis and degradation in Arabidopsis by dynamic 13CO2 labeling and analysis of enrichment in individual amino acids in their free pools and in protein. *Plant Physiol,* 168**,** 74-93.

ISHIKITA, H., SAENGER, W., BIESIADKA, J., LOLL, B. & KNAPP, E. W. 2006. How photosynthetic reaction centers control oxidation power in chlorophyll pairs P680, P700, and P870. *Proceedings of the National Academy of Sciences of the United States of America,* 103**,** 9855-9860.

JAMBUNATHAN, N. 2010. Determination and detection of reactive oxygen species (ROS), lipid peroxidation, and electrolyte leakage in plants. *Methods Mol Biol,* 639**,** 292-8.

JOHNSON, D. R., WYSE, D. L. & JONES, K. J. 1996. Controlling weeds with phytopathogenic bacteria. *Weed Technology,* 10**,** 621-624.

JONES, K., KIM, D. W., PARK, J. S. & KHANG, C. H. 2016. Live-cell fluorescence imaging to investigate the dynamics of plant cell death during infection by the rice blast fungus Magnaporthe oryzae. *BMC Plant Biol,* 16**,** 69.

JONES, P. A. B., A.M. Mechanical damage to kill weeds. In: Proceedings Second International Weed Control Congress, 1996 Copenhagen, Denmark. 949-954.

KALAJI, H. M., BOSA, K., KOSCIELNIAK, J. & HOSSAIN, Z. 2011. Chlorophyll a fluorescence--A useful tool for the early detection of temperature stress in spring barley (Hordeum vulgare L.). *OMICS,* 15**,** 925-34.

KALAJI, H. M., JAJOO, A., OUKARROUM, A., BRESTIC, M., ZIVCAK, M., SAMBORSKA, I. A., CETNER, M. D., LUKASIK, I., GOLTSEV, V. & LADLE, R. J. 2016. Chlorophyll a fluorescence as a tool to monitor physiological status of plants under abiotic stress conditions. *Acta Physiologiae Plantarum,* 38.

KANEMATSU, S. & ASADA, K. 1990. Characteristic Amino-Acid-Sequences of Chloroplast and Cytosol Isozymes of Cuzn-Superoxide Dismutase in Spinach, Rice and Horsetail. *Plant and Cell Physiology,* 31**,** 99-112.

KATO, M. C., HIKOSAKA, K. & HIROSE, T. 2002. Leaf discs floated on water are different from intact leaves in photosynthesis and photoinhibition. *Photosynth Res,* 72**,** 65-70.

KAZINCZI, G., LUKACS, D., TAKACS, A., HORVATH, J., GABORJANYI, R., NADASY, M. & NADASY, E. 2006. Biological decline of Solanum nigrum due to virus infections. *Journal of Plant Diseases and Protection***,** 325-330.

KEPNER, R. A., BAINER, R. AND BARGER, E.L 1978. *Principles of Farm Machinery,* Westport, CT, USA, AVI.

KNOX, J. P. & DODGE, A. D. 1985. Singlet Oxygen and Plants. *Phytochemistry,* 24**,** 889-896.

KOH, E., CARMIELI, R., MOR, A. & FLUHR, R. 2016. Singlet Oxygen-Induced Membrane Disruption and Serpin-Protease Balance in Vacuolar-Driven Cell Death. *Plant Physiol,* 171**,** 1616-25.

KOLBERG, R. L. & WILES, L. J. 2002. Effect of steam application on cropland weeds. *Weed Technology,* 16**,** 43-49.

KONG, W. W., LIU, F., ZHANG, C., ZHANG, J. F. & FENG, H. L. 2016. Non-destructive determination of Malondialdehyde (MDA) distribution in oilseed rape leaves by laboratory scale NIR hyperspectral imaging. *Scientific Reports,* 6.

KOPSELL, D. A., ARMEL, G. R., MUELLER, T. C., SAMS, C. E., DEYTON, D. E., MCELROY, J. S. & KOPSELL, D. E. 2009. Increase in Nutritionally Important Sweet Corn Kernel Carotenoids following Mesotrione and Atrazine Applications. *Journal of Agricultural and Food Chemistry,* 57**,** 6362-6368.

KRIEGER-LISZKAY, A. 2005. Singlet oxygen production in photosynthesis. *Journal of Experimental Botany,* 56**,** 337-346.

KRIEGER-LISZKAY, A., FUFEZAN, C. & TREBST, A. 2008a. Singlet oxygen production in photosystem II and related protection mechanism. *Photosynthesis Research,* 98**,** 551-64.

KRIEGER-LISZKAY, A., FUFEZAN, C. & TREBST, A. 2008b. Singlet oxygen production in photosystem II and related protection mechanism. *Photosynth Res,* 98**,** 551-64.

KROEGER, J. H., ZERZOUR, R. & GEITMANN, A. 2011. Regulator or Driving Force? The Role of Turgor Pressure in Oscillatory Plant Cell Growth. *Plos One,* 6.

KRUK, J., HOLLANDER-CZYTKO, H., OETTMEIER, W. & TREBST, A. 2005. Tocopherol as singlet oxygen scavenger in photosystem II. *J Plant Physiol,* 162**,** 749-57.

KRUK, J. & TREBST, A. 2008. Plastoquinol as a singlet oxygen scavenger in photosystem II. *Biochim Biophys Acta,* 1777**,** 154-62.

KUME, A., AKITSU, T. & NASAHARA, K. N. 2018. Why is chlorophyll b only used in light-harvesting systems? *Journal of Plant Research,* 131**,** 961-972.

KUPPER, H., BENEDIKTY, Z., MORINA, F., ANDRESEN, E., MISHRA, A. & TRTILEK, M. 2019. Analysis of OJIP Chlorophyll Fluorescence Kinetics and QA Reoxidation Kinetics by Direct Fast Imaging. *Plant Physiol,* 179**,** 369-381.

LAGUE, E., GILL, J. AND PELOQUIN, G. 2001. Thermal control in plant protection. *In:* VINCENT, C., PANNETON, B. AND FLEURAT-LESSARD, F. (ed.) *Physical Control Methods in Plant Protection.* Berlin: Springer-Verlag.

LALOI, C., APEL, K. & DANON, A. 2004. Reactive oxygen signalling: the latest news. *Current Opinion in Plant Biology,* 7**,** 323-328.

LALOI, C. & HAVAUX, M. 2015. Key players of singlet oxygen-induced cell death in plants. *Front Plant Sci,* 6**,** 39.

LANGERHOLC, J. 1979. Moving Phase-Transitions in Laser-Irradiated Biological Tissue. *Applied Optics,* 18**,** 2286-2293.

LEE, B. H., LEE, H. J., XIONG, L. M. & ZHU, J. K. 2002. A mitochondrial complex I defect impairs cold-regulated nuclear gene expression. *Plant Cell,* 14**,** 1235-1251.

LEOPOLD, A. C., MUSGRAVE, M. E. & WILLIAMS, K. M. 1981. Solute leakage resulting from leaf desiccation. *Plant Physiol,* 68**,** 1222-5.

LEROUX, G. D., DOUHERET, J. AND LANOUETTE, M 2001. Flame Weeding in Corn. *In:* VINCENT, C., PANNETON, B. AND FLEURAT-LESSARD, F. (ed.) *Physical Control Methods in Plant Protection.* Berlin: Springer-Verlag.

LI, H., MELO, T. B., ARELLANO, J. B. & RAZI NAQVI, K. 2012. Temporal profile of the singlet oxygen emission endogenously produced by photosystem II reaction centre in an aqueous buffer. *Photosynth Res,* 112**,** 75-9.

LI, H., XIAO, J., GAO, Y. Q., TANG, J. J., ZHANG, A. L. & GAO, J. M. 2014. Chaetoglobosins from Chaetomium globosum, an Endophytic Fungus in Ginkgo biloba, and Their Phytotoxic and Cytotoxic Activities. *Journal of Agricultural and Food Chemistry,* 62**,** 3734-3741.

LI, S., ZHOU, M. & XU, X. 2018. Analysis of atomic beam collimation by laser cooling. *Sci Rep,* 8**,** 9971.

LIU, W., YUAN, G., DU, L., GUO, W., LI, L., BI, Y. & WANG, J. 2015. A novel Pro197Glu substitution in acetolactate synthase (ALS) confers broad-spectrum resistance across ALS inhibitors. *Pestic Biochem Physiol,* 117**,** 31-8.

LIU, X. Z. & HUANG, B. R. 2000. Heat stress injury in relation to membrane lipid peroxidation in creeping bentgrass. *Crop Science,* 40**,** 503-510.

LOLL, B., KERN, J., SAENGER, W., ZOUNI, A. & BIESIADKA, J. 2005. Towards complete cofactor arrangement in the 3.0 angstrom resolution structure of photosystem II. *Nature,* 438**,** 1040-1044.

LONG, S. P., HUMPHRIES, S. & FALKOWSKI, P. G. 1994. Photoinhibition of Photosynthesis in Nature. *Annual Review of Plant Physiology and Plant Molecular Biology,* 45**,** 633-662.

LONHIENNE, T., GARCIA, M. D., PIERENS, G., MOBLI, M., NOUWENS, A. & GUDDAT, L. W. 2018. Structural insights into the mechanism of inhibition of AHAS by herbicides. *Proc Natl Acad Sci U S A,* 115**,** E1945-E1954.

MAJDA, M. & ROBERT, S. 2018. The Role of Auxin in Cell Wall Expansion. *International Journal of Molecular Sciences,* 19.

MATHIASSEN, S. K., BAK, T., CHRISTENSEN, S. & KUDSK, P. 2006. The effect of laser treatment as a weed control method. *Biosystems Engineering,* 95**,** 497-505.

MATSUBARA, S., CHEN, Y. C., CALIANDRO, R., GOVINDJEE & CLEGG, R. M. 2011. Photosystem II fluorescence lifetime imaging in avocado leaves: Contributions of the lutein-epoxide and violaxanthin cycles to fluorescence quenching. *Journal of Photochemistry and Photobiology B-Biology,* 104**,** 271-284.

MATTILA, H., KHOROBRYKH, S., HAVURINNE, V. & TYYSTJARVI, E. 2015. Reactive oxygen species: Reactions and detection from photosynthetic tissues. *Journal of Photochemistry and Photobiology B:Biology,* 152**,** 176-214.

MAXWELL, C., GRIFFITHS, H. & YOUNG, A. J. 1994. Photosynthetic Acclimation to Light Regime and Water-Stress by the C-3-Cam Epiphyte Guzmania-Monostachia - Gas-Exchange Characteristics, Photochemical Efficiency and the Xanthophyll Cycle. *Functional Ecology,* 8**,** 746-754.

MAXWELL, K. & JOHNSON, G. N. 2000. Chlorophyll fluorescence--a practical guide. *J Exp Bot,* 51**,** 659-68.

MELANDER, B. & RASMUSSEN, G. 2001. Effects of cultural methods and physical weed control on intrarow weed numbers, manual weeding and marketable yield in direct-sown leek and bulb onion. *Weed Research,* 41**,** 491-508.

MELIS, A. 1999. Photosystem-II damage and repair cycle in chloroplasts: what modulates the rate of photodamage ? *Trends Plant Sci,* 4**,** 130-135.

MISHRA, S., JHA, A. B. & DUBEY, R. S. 2011. Arsenite treatment induces oxidative stress, upregulates antioxidant system, and causes phytochelatin synthesis in rice seedlings. *Protoplasma,* 248**,** 565-77.

MIYAMOTO, S., RONSEIN, G. E., PRADO, F. M., UEMI, M., CORREA, T. C., TOMA, I. N., BERTOLUCCI, A., OLIVEIRA, M. C., MOTTA, F. D., MEDEIROS, M. H. & MASCIO, P. D. 2007. Biological hydroperoxides and singlet molecular oxygen generation. *IUBMB Life,* 59**,** 322-31.

MIYAO, M., IKEUCHI, M., YAMAMOTO, N. & ONO, T. 1995. Specific degradation of the D1 protein of photosystem II by treatment with hydrogen peroxide in darkness: implications for the mechanism of degradation of the D1 protein under illumination. *Biochemistry,* 34**,** 10019-26.

MORKER, K. H. & ROBERTS, M. R. 2011. Light as both an input and an output of wound-induced reactive oxygen formation in Arabidopsis leaves. *Plant Signal Behav,* 6**,** 1087-9.

MORTENSEN, K. 1988. The Potential of an Endemic Fungus, Colletotrichum-Gloeosporioides, for Biological-Control of Round-Leaved Mallow (Malva-Pusilla) and Velvetleaf (Abutilon-Theophrasti). *Weed Science,* 36**,** 473-478.

MUELLER, M. J., MENE-SAFFRANE, L., GRUN, C., KARG, K. & FARMER, E. E. 2006. Oxylipin analysis methods. *Plant J,* 45**,** 472-89.

MULLIGAN, G. A. & BAILEY, L. G. 1975. Biology of Canadian Weeds .8. Sinapis-Arvensis L. *Canadian Journal of Plant Science,* 55**,** 171-183.

MULO, P., SIRPIO, S., SUORSA, M. & ARO, E. M. 2008. Auxiliary proteins involved in the assembly and sustenance of photosystem II. *Photosynth Res,* 98**,** 489-501.

MURATA, N., TAKAHASHI, S., NISHIYAMA, Y. & ALLAKHVERDIEV, S. I. 2007a. Photoinhibition of photosystem II under environmental stress. *Biochimica Et Biophysica Acta-Bioenergetics,* 1767**,** 414-421.

MURATA, N., TAKAHASHI, S., NISHIYAMA, Y. & ALLAKHVERDIEV, S. I. 2007b. Photoinhibition of photosystem II under environmental stress. *Biochim Biophys Acta,* 1767**,** 414-21.

MURCHIE, E. H. & LAWSON, T. 2013. Chlorophyll fluorescence analysis: a guide to good practice and understanding some new applications. *J Exp Bot,* 64**,** 3983-98.

MURCHIE, E. H. & NIYOGI, K. K. 2011. Manipulation of photoprotection to improve plant photosynthesis. *Plant Physiol,* 155**,** 86-92.

NAWROTH, P. A. E., M 1996. Mechanische Unkrautregulierung ohne Eingriff in das Bodengefuge - Geratetechnik, Prufstandsversuche, Ergebnisse. *Zeitschrift Fur Pflanzenkrankheiten Und Pflanzenschutz-Journal of Plant Diseases and Protection,* 15**,** 423-430.

NEILL, S. J., DESIKAN, R., CLARKE, A., HURST, R. D. & HANCOCK, J. T. 2002. Hydrogen peroxide and nitric oxide as signalling molecules in plants. *Journal of Experimental Botany,* 53**,** 1237-1247.

NELSON, N. & YOCUM, C. F. 2006. Structure and function of photosystems I and II. *Annu Rev Plant Biol,* 57**,** 521-65.

NISHIYAMA, Y., ALLAKHVERDIEV, S. I. & MURATA, N. 2005. Inhibition of the repair of photosystem II by oxidative stress in cyanobacteria. *Photosynthesis Research,* 84**,** 1-7.

NISHIYAMA, Y., ALLAKHVERDIEV, S. I., YAMAMOTO, H., HAYASHI, H. & MURATA, N. 2004. Singlet oxygen inhibits the repair of photosystem II by suppressing the translation elongation of the D1 protein in Synechocystis sp. PCC 6803. *Biochemistry,* 43**,** 11321-30.

NISHIYAMA, Y., YAMAMOTO, H., ALLAKHVERDIEV, S. I., INABA, M., YOKOTA, A. & MURATA, N. 2001. Oxidative stress inhibits the repair of photodamage to the photosynthetic machinery. *EMBO J,* 20**,** 5587-94.

NIXON, P. J., BARKER, M., BOEHM, M., DE VRIES, R. & KOMENDA, J. 2005. FtsH-mediated repair of the photosystem II complex in response to light stress. *J Exp Bot,* 56**,** 357-63.

NIXON, P. J., MICHOUX, F., YU, J., BOEHM, M. & KOMENDA, J. 2010. Recent advances in understanding the assembly and repair of photosystem II. *Ann Bot,* 106**,** 1-16.

NOCTOR, G., MHAMDI, A. & FOYER, C. H. 2016. Oxidative stress and antioxidative systems: recipes for successful data collection and interpretation. *Plant Cell and Environment,* 39**,** 1140-1160.

OCA. 2020. *Organic Comsumers Association* [Online]. Available: https://www.organicconsumers.org/news/demand-organic-food-growing-faster-domestic-supply [Accessed 12/03/2020].

OERKE, E.-C., DEHNE, H.-W., SCHONBECK, F., AND WEBER, A., 1999. *Crop Production and Crop Protection: Estimated Losses in Major Food and Cash Crops,* Amsterdam, The Netherlands, Elsevier, B.V.

OERKE, E. C. 2006. Crop losses to pests. *Journal of Agricultural Science,* 144**,** 31-43.

OHNISHI, N., ALLAKHVERDIEV, S. I., TAKAHASHI, S., HIGASHI, S., WATANABE, M., NISHIYAMA, Y. & MURATA, N. 2005. Two-step mechanism of photodamage to photosystem II: step 1 occurs at the oxygen-evolving complex and step 2 occurs at the photochemical reaction center. *Biochemistry,* 44**,** 8494-9.

OKADA, H., HONTSU, S., ASAKAWA, I., MIURA, S., TANIAMOTO, T., KATAYAMA, E., INOUE, K., IWASAKI, S., KICHIKAWA, K. & HASEGAWA, M. 2011. Changes Of Tumor Size And Tumor Contrast Enhancement During Radiotherapy For Non-small Cell Lung Cancer: Are These Changes Correlated With The Treatment Outcome? *International Journal of Radiation Oncology Biology Physics,* 81**,** S610-S610.

OKADA, K., IKEUCHI, M., YAMAMOTO, N., ONO, T. A. & MIYAO, M. 1996. Selective and specific cleavage of the D1 and D2 proteins of Photosystem II by exposure to singlet oxygen: Factors responsible for the susceptibility to cleavage of the proteins. *Biochimica Et Biophysica Acta-Bioenergetics,* 1274**,** 73-79.

ORT, D. R., AHRENS, W. H., MARTIN, B. & STOLLER, E. W. 1983. Comparison of photosynthetic perfomance in triazine resistant ans susceptible biotypes of Amaranthus hybridus. *Plant Physiology,* 72**,** 925-930.

PAPAGEORGIOU, G. C. & GOVINDJEE 2004. *Chlorophyll a fluorescence : a signature of photosynthesis,* Dordrecht, Kluwer Academic.

PAPAGEORGIOU, G. C. & GOVINDJEE 2011. Photosystem II fluorescence: slow changes--scaling from the past. *J Photochem Photobiol B,* 104**,** 258-70.

PARISH, S. 1990. A Review of Nonchemical Weed-Control Techniques. *Biological Agriculture & Horticulture,* 7**,** 117-137.

PERALES, M. & REDDY, G. V. 2012. Stem cell maintenance in shoot apical meristems. *Curr Opin Plant Biol,* 15**,** 10-6.

PERROT-RECHENMANN, C. 2010. Cellular Responses to Auxin: Division versus Expansion. *Cold Spring Harbor Perspectives in Biology,* 2.

PETERS, B. & STREK, H. J. 2018. Herbicide discovery in light of rapidly spreading resistance and ever-increasing regulatory hurdles. *Pest Manag Sci,* 74, 2211-2215.

PITZSCHKE, A., FORZANI, C. & HIRT, H. 2006. Reactive oxygen species signaling in plants. *Antioxidants & Redox Signaling,* 8**,** 1757-1764.

POSPISIL, P. 2016. Production of Reactive Oxygen Species by Photosystem II as a Response to Light and Temperature Stress. *Front Plant Sci,* 7**,** 1950.

POSPISIL, P., SNYRYCHOVA, I., KRUK, J., STRZALKA, K. & NAUS, J. 2006. Evidence that cytochrome b559 is involved in superoxide production in photosystem II: effect of synthetic short-chain plastoquinones in a cytochrome b559 tobacco mutant. *Biochem J,* 397**,** 321-7.

POWLES, S. B. 1984. Photoinhibition of Photosynthesis Induced by Visible-Light. *Annual Review of Plant Physiology and Plant Molecular Biology,* 35**,** 15-44.

PRASAD, A., SEDLAROVA, M., KALE, R. S. & POSPISIL, P. 2017. Lipoxygenase in singlet oxygen generation as a response to wounding: in vivo imaging in Arabidopsis thaliana. *Sci Rep,* 7**,** 9831.

RAFFAELLI, M., FONTANELLI, M., FRASCONI, C., SORELLI, F., GINANNI, M. & PERUZZI, A. 2011. Physical weed control in processing tomatoes in Central Italy. *Renewable Agriculture and Food Systems,* 26**,** 95-103.

RIFAI, M. N., ASTATKIE, T., LACKO-BARTOSOVA. & GADUS, J. 2002. Effect of two different thermal units and three types of mulch on weeds in apple orchards. *Journal of Environmental Engneering and Science,* 1**,** 331-338.

RILEY, B. 1995. Hot water: A 'cool' new weed control method. *Journal of Pestticide Reform,* 15.

RIZHSKY, L., LIANG, H. & MITTLER, R. 2003. The water-water cycle is essential for chloroplast protection in the absence of stress. *J Biol Chem,* 278**,** 38921-5.

ROACH, T., COLVILLE, L., BECKETT, R. P., MINIBAYEVA, F. V., HAVAUX, M. & KRANNER, I. 2015. A proposed interplay between peroxidase, amine oxidase and lipoxygenase in the wounding-induced oxidative burst in Pisum sativum seedlings. *Phytochemistry,* 112**,** 130-8.

ROACH, T. & KRIEGER-LISZKAY, A. 2014. Regulation of photosynthetic electron transport and photoinhibition. *Curr Protein Pept Sci,* 15**,** 351-62.

RYAN, G. F. 1970. Resistance of common grounsel to simazine and atrazine. *Weed Science,* 18**,** 614-616.

SAGE, R. F., SHARKEY, T. D. & PEARCY, R. W. 1990. The Effect of Leaf Nitrogen and Temperature on the Co2 Response of Photosynthesis in the C3 Dicot Chenopodium-Album L. *Australian Journal of Plant Physiology,* 17**,** 135-148.

SAHLHOF, K. & SONNENBURG, D. 2000. Aufbau und Untersuchungen am CO_2 laser. *In:* DIPLOMARBEIT TFH BERLIN, F. V. (ed.). Berlin.

SAVARY, S., WILLOCQUET, L., PETHYBRIDGE, S. J., ESKER, P., MCROBERTS, N. & NELSON, A. 2019. The global burden of pathogens and pests on major food crops. *Nat Ecol Evol,* 3**,** 430-439.

SAVATIN, D. V., GRAMEGNA, G., MODESTI, V. & CERVONE, F. 2014. Wounding in the plant tissue: the defense of a dangerous passage. *Front Plant Sci,* 5**,** 470.

SCHANSKER, G., SRIVASTAVA, A., GOVINDJEE & STRASSER, R. J. 2003. Characterization of the 820-nm transmission signal paralleling the chlorophyll a fluorescence rise (OJIP) in pea leaves. *Functional Plant Biology,* 30**,** 785-796.

SCHANSKER, G., TOTH, S. Z. & STRASSER, R. J. 2006. Dark recovery of the Chl a fluorescence transient (OJIP) after light adaptation: the qT-component of non-photochemical quenching is related to an activated photosystem I acceptor side. *Biochim Biophys Acta,* 1757**,** 787-97.

SCHELLER, H. V. & HALDRUP, A. 2005. Photoinhibition of photosystem I. *Planta,* 221**,** 5-8.

SCHREIBER, U., NEUBAUER, C. & KLUGHAMMER, C. 1989. Devices and Methods for Room-Temperature Fluorescence Analysis. *Philosophical Transactions of the Royal Society of London Series B-Biological Sciences,* 323**,** 241-251.

SEPPANEN, M. M., CARDI, T., BORG HYOKKI, M. & PEHU, E. 2000. Characterization and expression of cold-induced glutathione S-transferase in freezing tolerant Solanum commersonii, sensitive S. tuberosum and their interspecific somatic hybrids. *Plant Sci,* 153**,** 125-133.

SHABALA, S. 2011. Physiological and cellular aspects of phytotoxicity tolerance in plants: the role of membrane transporters and implications for crop breeding for waterlogging tolerance. *New Phytol,* 190**,** 289-98.

SHAO, J. Z., ZHANG, Y. B., YU, J. L., GUO, L. & DING, Y. 2011. Isolation of Thylakoid Membrane Complexes from Rice by a New Double-Strips BN/SDS-PAGE and Bioinformatics Prediction of Stromal Ridge Subunits Interaction. *Plos One,* 6.

SHARMA, P. & DUBEY, R. S. 2005. Drought induces oxidative stress and enhances the activities of antioxidant enzymes in growing rice seedlings. *Plant Growth Regulation,* 46**,** 209-221.

SHIBATA, Y., HOSHINO, Y., HARA, S., YAGASAKI, H., KOJIMA, S., NISHIYAMA, Y., MORISHIMA, T. & KIMURA, H. 2006. Clonality analysis by sequence variation of the latent membrane protein 1 gene in patients with chronic active Epstein-Barr virus infection. *J Med Virol,* 78**,** 770-9.

SHIRAI, T., DOGARIU, A. & WOLF, E. 2003. Directionality of Gaussian Schell-model beams propagating in atmospheric turbulence. *Opt Lett,* 28**,** 610-2.

SIRVYDAS, A., LAZAUSKAS, P., VASINAUSKIENE, R. & KERPAUSKAS, P. 2004. Weed control in onions by steam. *Zeitschrift Fur Pflanzenkrankheiten Und Pflanzenschutz-Journal of Plant Diseases and Protection***,** 581-587.

SMITH, M. W. & DOOLITTLE, R. F. 1992. A Comparison of Evolutionary Rates of the 2 Major Kinds of Superoxide-Dismutase. *Journal of Molecular Evolution,* 34**,** 175-184.

SOGAARD, H. T. 2005. Weed classification by active shape models. *Biosystems Engineering,* 91**,** 271-281.

SOKEFELD, M. G. R. K., W. . Site-specific weed control - from weed recording to herbicide application. Proceedings of the 20th German Conference on Weed Biology and Weed Control, 14-16 March, 2000 2000 Stuttgary-Hohenheim, Germany.

SONOIKE, K. 2011. Photoinhibition of photosystem I. *Physiol Plant,* 142**,** 56-64.

STRASSER, R. J., TSIMILLI-MICHAEL, M., QIANG, S. & GOLTSEV, V. 2010. Simultaneous in vivo recording of prompt and delayed fluorescence and 820-nm reflection changes during drying and after rehydration of the resurrection plant Haberlea rhodopensis. *Biochim Biophys Acta,* 1797**,** 1313-26.

STREUSAND, V. J. & PORTIS, A. R. 1987. Rubisco Activase Mediates ATP-Dependent Activation of Ribulose Bisphosphate Carboxylase. *Plant Physiol,* 85**,** 152-4.

STUMPP, M. T., MOTOHASHI, K. & HISABORI, T. 1999. Chloroplast thioredoxin mutants without active-site cysteines facilitate the reduction of the regulatory disulphide bridge on the gamma-subunit of chloroplast ATP synthase. *Biochem J,* 341 (Pt 1)**,** 157-63.

SUSILA, P., LAZAR, D., ILIK, P., TOMEK, P. & NAUS, J. 2004. The gradient of exciting radiation within a sample affects the relative height of steps in the fast chlorophyll a fluorescence rise. *Photosynthetica,* 42**,** 161-172.

SUTCLIFFE, J. 1977. *Plants and Temperature,* London, Edward Arnold.

TAKAHASHI, S. & BADGER, M. R. 2011. Photoprotection in plants: a new light on photosystem II damage. *Trends Plant Sci,* 16**,** 53-60.

TAKAHASHI, S., MILWARD, S. E., FAN, D. Y., CHOW, W. S. & BADGER, M. R. 2009. How does cyclic electron flow alleviate photoinhibition in Arabidopsis? *Plant Physiol,* 149**,** 1560-7.

TAKAHASHI, S. & MURATA, N. 2008. How do environmental stresses accelerate photoinhibition? *Trends Plant Sci,* 13**,** 178-82.

TELFER, A. 2014. Singlet oxygen production by PSII under light stress: mechanism, detection and the protective role of beta-carotene. *Plant Cell Physiol,* 55**,** 1216-23.

TIAN, Y., SACHARZ, J., WARE, M. A., ZHANG, H. & RUBAN, A. V. 2017. Effects of periodic photoinhibitory light exposure on physiology and productivity of Arabidopsis plants grown under low light. *J Exp Bot,* 68**,** 4249-4262.

TIDEMANN, B. D., HALL, L. M., HARKER, K. N., BECKIE, H. J., JOHNSON, E. N. & STEVENSON, F. C. 2017. Suitability of Wild Oat (*Avena fatua*), False Cleavers (*Galium spurium*), and Volunteer Canola (*Brassica napus*) for Harvest Weed Seed Control in Western Canada. *Weed Science,* 65**,** 769-777.

TIKKANEN, M., MEKALA, N. R. & ARO, E. M. 2014. Photosystem II photoinhibition-repair cycle protects Photosystem I from irreversible damage. *Biochimica Et Biophysica Acta-Bioenergetics,* 1837**,** 210-215.

TITTMANN, K., SCHRODER, K., GOLBIK, R., MCCOURT, J., KAPLUN, A., DUGGLEBY, R. G., BARAK, Z., CHIPMAN, D. M. & HUBNER, G. 2004. Electron transfer in acetohydroxy acid synthase as a side reaction of catalysis. Implications for the reactivity and partitioning of the carbanion/enamine form of (alpha-hydroxyethyl)thiamin diphosphate in a "nonredox" flavoenzyme. *Biochemistry,* 43**,** 8652-61.

TOOLE, E. H. 1946. Final results of the Duval buried seed experiment. *Journal of Agricultural Research,* 72**,** 201-210.

TREBST, A. 2003. Function of beta-carotene and tocopherol in photosystem II. *Z Naturforsch C J Biosci,* 58**,** 609-20.

TREBST, A. & DEPKA, B. 1997. Role of carotene in the rapid turnover and assembly of photosystem II in Chlamydomonas reinhardtii. *FEBS Lett,* 400**,** 359-62.

TREBST, A., DEPKA, B. & HOLLANDER-CZYTKO, H. 2002. A specific role for tocopherol and of chemical singlet oxygen quenchers in the maintenance of photosystem II structure and function in Chlamydomonas reinhardtii. *Febs Letters,* 516**,** 156-160.

TRIANTAPHYLIDES, C., KRISCHKE, M., HOEBERICHTS, F. A., KSAS, B., GRESSER, G., HAVAUX, M., VAN BREUSEGEM, F. & MUELLER, M. J. 2008. Singlet oxygen is the major reactive oxygen species involved in photooxidative damage to plants. *Plant Physiol,* 148**,** 960-8.

UMENA, Y., KAWAKAMI, K., SHEN, J. R. & KAMIYA, N. 2011. Crystal structure of oxygen-evolving photosystem II at a resolution of 1.9 angstrom. *Nature,* 473**,** 55-U65.

UNGERER, J., LIN, P. C., CHEN, H. Y. & PAKRASI, H. B. 2018. Adjustments to Photosystem Stoichiometry and Electron Transfer Proteins Are Key to the Remarkably Fast Growth of the Cyanobacterium Synechococcus elongatus UTEX 2973. *mBio,* 9.

VAN BREUSEGEM, F. & DAT, J. F. 2006. Reactive oxygen species in plant cell death. *Plant Physiol,* 141**,** 384-90.

VAN HEERDEN, P. D. R., SWANEPOEL, J. W. & KRUER, G. H. J. 2007. Modulation of photosynthesis by drought in two desert scrub species exhibiting C-3-mode CO2 assimilation. *Environmental and Experimental Botany,* 61**,** 124-136.

VAN ITTERSUM, M. K., AND RABBINGE, R., 1997. Concepts in production ecology for analysis and quantification of agricultural input–output combinations. *Field Crops Research,* 52**,** 197-208.

VARELLA, M, 2011 Do light and alfalfa responses to cloth and slatted shade represent those measures under an agroforestry system? *Agroforestry Systems* 81:157–173

VASS, I. & CSER, K. 2009. Janus-faced charge recombinations in photosystem II photoinhibition. *Trends Plant Sci,* 14**,** 200-5.

VASS, I., CSER, K. & CHEREGI, O. 2007. Molecular mechanisms of light stress of photosynthesis. *Ann N Y Acad Sci,* 1113**,** 114-22.

VASS, I., STYRING, S., HUNDAL, T., KOIVUNIEMI, A., ARO, E. M. & ANDERSSON, B. 1992. Reversible and Irreversible Intermediates during Photoinhibition of Photosystem .2. Stable Reduced Qa Species Promote Chlorophyll Triplet Formation. *Proceedings of the National Academy of Sciences of the United States of America,* 89**,** 1408-1412.

VEIT, B. 2004. Determination of cell fate in apical meristems. *Curr Opin Plant Biol,* 7**,** 57-64.

WALSH, M. J., BROSTER, J. C., SCHWARTZ-LAZARO, L. M., NORSWORTHY, J. K., DAVIS, A. S., TIDEMANN, B. D., BECKIE, H. J., LYON, D. J., SONI, N., NEVE, P. & BAGAVATHIANNAN, M. V. 2018. Opportunities and challenges for harvest weed seed control in global cropping systems. *Pest Manag Sci,* 74**,** 2235-2245.

WANG, F., LIU, J., CHEN, M., ZHOU, L., LI, Z., ZHAO, Q., PAN, G., ZAIDI, S. H. & CHENG, F. 2016. Involvement of Abscisic Acid in PSII Photodamage and D1 Protein Turnover for Light-Induced Premature Senescence of Rice Flag Leaves. *PLoS One,* 11**,** e0161203.

WANG, Z., LI, G., SUN, H., MA, L., GUO, Y., ZHAO, Z., GAO, H. & MEI, L. 2018. Effects of drought stress on photosynthesis and photosynthetic electron transport chain in young apple tree leaves. *Biol Open,* 7.

WARWICK, S. I., BECKIE, H. J., THOMAS, A. G. & MCDONALD, T. 2000. The biology of Canadian weeds. 8. Sinapis arvensis L. (updated). *Canadian Journal of Plant Science,* 80**,** 939-961.

WEI, C. F. & LINTILHAC, P. M. 2007. Loss of stability: A new look at the physics of cell wall behavior during plant cell growth. *Plant Physiology,* 145**,** 763-772.

WILLIAMS, T. J. 1963. Biological Flora of the British Isles No. 87 Chenopodium album L. *The Journal of Ecology,* 51**,** 711-725.

WILSON, K. E. & HUNER, N. P. 2000. The role of growth rate, redox-state of the plastoquinone pool and the trans-thylakoid deltapH in photoacclimation of Chlorella vulgaris to growth irradiance and temperature. *Planta,* 212**,** 93-102.

WOLTJEN, C., HAFERKAMP, H., RATH, T. & HERZOG, D. 2008. Plant growth depression by selective irradiation of the meristem with CO2 and diode lasers. *Biosystems Engineering,* 101**,** 316-324.

XU, H., VAVILIN, D. & VERMAAS, W. 2001. Chlorophyll b can serve as the major pigment in functional photosystem II complexes of cyanobacteria. *Proceedings of the National Academy of Sciences of the United States of America,* 98**,** 14168-14173.

YADAV, D. K., KRUK, J., SINHA, R. K. & POSPISIL, P. 2010. Singlet oxygen scavenging activity of plastoquinol in photosystem II of higher plants: electron paramagnetic resonance spin-trapping study. *Biochim Biophys Acta,* 1797**,** 1807-11.

YAMAMOTO, Y., KOBAYASHI, Y. & MATSUMOTO, H. 2001. Lipid peroxidation is an early symptom triggered by aluminum, but not the primary cause of elongation inhibition in pea roots. *Plant Physiol,* 125**,** 199-208.

ZHU. P, Y. S., MA, J, LI. SX, CHEN. Y 2008. Effect of Shading on the Photosynthetic Characteristics and Yield at Later Growth Stage of Hybrid Rice Combination. *Acta Agronomica Sinica,* 34.

ZOLLA, L. & RINALDUCCI, S. 2002. Involvement of active oxygen species in degradation of light-harvesting proteins under light stresses. *Biochemistry,* 41**,** 14391-402.